NASA CONTRACTOR REPORT

NASA CR-1949

NASA CR-1949

FABRICATION AND TEST OF A SPACE POWER BOILER FEED ELECTROMAGNETIC PUMP

I - Design and Manufacture of Pump

by J. W. Gahan, A. H. Powell, P. T. Pileggi, and S. R. Thompson

Prepared by
GENERAL ELECTRIC COMPANY
Cincinnati, Ohio 45215
for Lewis Research Center

NATIONAL AERONAUTICS AND SPACE ADMINISTRATION • WASHINGTON, D. C. • APRIL 1972

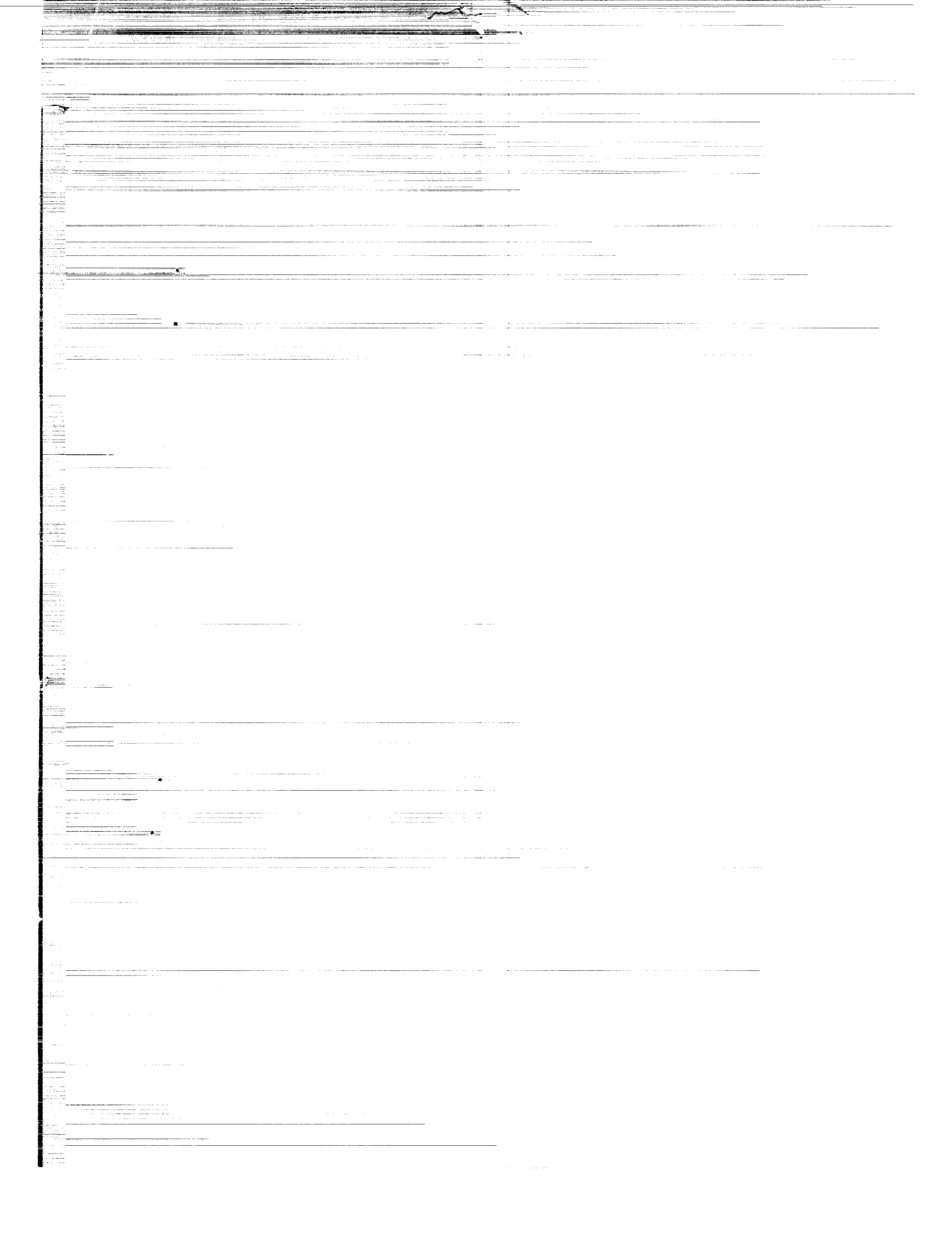

1. Report No. CR-1949	2. Government Accession No.	3. Recipient's Catalog No.
4. Title and Subtitle FABRICATION AND TEST OF A SPACE POWER BOILER FEED ELECTROMAGNETIC PUMP I - DESIGN AND MANUFACTURE OF PUMP		5. Report Date March 1972 6. Performing Organization Code
7. Author(s) J. W. Gahan, A. H. Powell, P. T. Pileggi, and S. R. Thompson		8. Performing Organization Report No. GESP-459, Part I 10. Work Unit No.
9. Performing Organization Name and Address General Electric Company Cincinnati, Ohio 45215		11. Contract or Grant No. NAS 3-9422 13. Type of Report and Period Covered Contractor Report
12. Sponsoring Agency Name and Address National Aeronautics and Space Administration Washington, D.C. 20546		14. Sponsoring Agency Code
15. Supplementary Notes Project Manager, James P. Couch, Power Systems Division, NASA Lewis Research Center, Cleveland, Ohio		

16. Abstract

A three-phase helical induction electromagnetic (EM) pump has been designed and built. This pump was designed for use as the boiler-feed pump of a potassium Rankine-cycle space electric power system. The pump is constructed of high temperature materials including a T-111 duct, Hiperco 27 magnetic material, nickel clad silver conductor wire, and a completely inorganic insulation system. The pump is designed to deliver 3.25 lb/sec potassium at 1000° F with a developed head of 240 psi while being cooled by 800° F NaK. At these conditions, the overall pump efficiency is expected to be 18%.

17. Key Words (Suggested by Author(s)) Space power system Pump Liquid metal Electromagnetic pump	18. Distribution Statement Unclassified - unlimited		
19. Security Classif. (of this report) Unclassified	20. Security Classif. (of this page) Unclassified	21. No. of Pages 228	22. Price* $3.00

* For sale by the National Technical Information Service, Springfield, Virginia 22151

TABLE OF CONTENTS

		Page No.
I.	SUMMARY	1
II.	INTRODUCTION	3
III.	OVERALL DESIGN	5
	A. General Description	5
	B. Stator Assembly	7
	C. Duct Assembly	10
	D. Design Considerations	11
IV.	MODEL STATOR	15
	A. Scope	15
	B. Materials	15
	C. Fabrication	16
	D. Evaluation and Conclusions	18
V.	CONDUCTOR SEALING	22
	A. General	22
	B. Seal Welding	22
	C. Nickel Plating	26
VI.	JOINT BRAZING	31
	A. Initial Considerations	31
	B. Induction Brazing - Focusing Coil	35
	C. Braze Alloy Development	41
	D. Brazing with Peripheral Coil	48
	E. Final Brazing Procedure	50
VII.	MANUFACTURE OF FINAL STATOR	53
	A. Unwound Stator	53
	B. Wound Stator	54
	C. Miscellaneous Components	57
	D. Final Stator Assembly	60
VIII.	MANUFACTURE OF DUCT	63
	A. Material Selection and Procurement	63
	B. Fabrication of Duct Parts	69
	C. Fabrication of Helix and Shroud Assembly	78

TABLE OF CONTENTS (Continued)

		Page No.
VIII.	MANUFACTURE OF DUCT (Cont'd)	
	D. Insulation of the Duct	90
	E. Final Check-Out	91
IX.	ASSEMBLY OF PUMP	92
	A. Duct and Shroud Final Assembly	92
	B. Duct Welded Into Stator	94
	C. Final Assembly, Argon Fill and Check-Out	94
X.	DISCUSSION OF RESULTS	97
XI.	CONCLUSIONS	101
XII.	REFERENCES	102
XIII.	APPENDIX	104
	FIGURES	109
	TABLES	191

LIST OF ILLUSTRATIONS

Figure No.		Page No.
1A	Conceptual Sketch of EM Boiler Feed Pump	109
1B	Layout Arrangement of EM Boiler Feed Pump	110
2	Equivalent Electric Circuit for Helical EM Pump	111
3	Calculated Performance Curves - Pressure vs Flow - 1000°F K	112
4	Calculated Performance Curves - Efficiency and PF vs Flow - 1000°F K	113
5	Calculated Performance Curves - Power Input vs Flow - 1000°F K	114
6	Trial Coils for Evaluating Feasibility of Full Coils	115
7	Model Stator for Pump Showing End-Turn Connections	116
8	Model Stator for Pump Showing Connections for Lead End	117
9	Arrangement of Slot Insulation in Pump Stator	118
10	Coil Turns After Disassembly from Model Stator	119
11	Partially Disassembled Model Stator	120
12	Section of Ni Clad Ag Wire with Nickel Plug	121
13	Section of Group of Ni Clad Ag Wire, Plugged and GTA Welded	122
14	Facility Set-Up for Nickel Plating Ni Clad Ag Wire	123
15	Quality Control Samples of Plated Ni Clad Ag Wire	124
16	Microphotograph of Nickel Plated End of Outside Strand	125
17	Microphotograph of Nickel Plated End on Inside Strand	126

LIST OF ILLUSTRATIONS (Cont'd)

Figure No.		Page No.
18	Section (at 8X) of Sample F4, Brazed with Au-Cu Alloy	127
19	Microphotograph of Sample F2, Brazed with Au-Cu Alloy	128
20	Sample Joint Prepared for Test Brazing	129
21	Microphotograph of Sample F11, Brazed with Au-Ni-Ge Alloy	130
22	Microphotograph of Sample F13, Brazed with Au-Ni-In Alloy	131
23	Microphotograph of Sample F13 (Middle Strands)	132
24	Microphotograph of Sample F14 with Plug Welded in Place	133
25	Microphotograph of Sample F19, Brazed with Au-Ni-In Alloy	134
26	Microphotograph of Sample F21, Brazed with Au-Ni-Ge Alloy	135
27	Sections of Sample F23, Brazed with Au-Ni-In Alloy	136
28	Sections of Sample F25, Plugged, Brazed with Au-Ni-In	137
29	Microphotograph of Sample F25 Showing Grain Boundary Attack	138
30	Test to Check Strength of Joint Braze Material	139
31	Samples of Braze Alloy Erosion Test on Thin Nickel	140
32	Test Set-Up for Au-Ni-In Braze Alloy Evaporation Test	141
33	Enclosure and Coil for Development Brazing of Joint Samples	142
34	Production Joint Brazing Equipment	143

LIST OF ILLUSTRATIONS (Cont'd)

Figure No.		Page No.
35	Section of Brazed Joint Sample with Plating Defects	144
36	Section of Improved Brazed Joint Sample	145
37	Record of Joint Thermocouple Output During Braze Cycle	146
38	Microphotograph of Section of Final Joint Sample	147
39	Unwound Stator with Trial Coil Bar in Laminated Core	148
40	Coil Bar Being Formed for End Connections	149
41	Coil Bar Completely Formed for Connection Layup	150
42	Inserting Bars, or Coil Sides, in Stator Core	151
43	All Coils (Bars) Assembled in Stator, Ready for Brazing Joints	152
44	Stator (Connection End) With Half of Joints Brazed and Others Ready	153
45	Stator in Braze Tank Support Ready for Joint Brazing	154
46	Coil Joint Ready for Induction Brazing Cycle	155
47	Outer Row of Coil Joints After Brazing	156
48	Coil Joints (Opposite Connection End) After Brazing and Taping	157
49	Coil Joints (Connection End) After Brazing and Taping	158
50	Assembled Stator (Connection End) Prior to End Shield Attachment	159
51	Duct End of Finished Stator Before Final Assembly	160

LIST OF ILLUSTRATIONS (Cont'd)

Figure No.		Page No.
52	Lead End of Finished Stator with Lead Seals and Pressure Switch	161
53	T-111 Alloy Tubes for Duct Wrapper and Extension	162
54	T-111 Alloy Tubes for Duct Helix and Extension	162
55	Parts for Duct Made of T-111, etc.	163
56	Helix for Duct After Final Machining with Extension	164
57	Inlet Pipe Transition Design Configuration	165
58	Trial Sample Brazed Bimetallic Pipe Joint	166
59	Load-Deflection Curve for Tensile Test of Trial Joint	167
60	Microstructures of "As Brazed" Trial Joint	168
61	Microstructures of Brazed Joint After Thermal Exposures	169
62	Duct Inlet Pipe Transition (Bimetallic) Assembly	170
63	Duct Outlet Pipe Transition (Bimetallic) Assembly	170
64	Assembly of Helix and Center Return Pipe for Duct	171
65	Helix Extension and Center Return Pipe for Duct	171
66	Assembled Duct (Without Transition Pipes) After Welding and Before Machining	172
67	Assembled Pump Duct After Machining of Wrapper	173
68	Pump Duct with Part of Wrapper Removed to Expose Leak Area	174

LIST OF ILLUSTRATIONS (Cont'd)

Figure No.		Page No.
69	Close-Up of Leak Area at T-111 Duct Helix Extension Weld	175
70	Enlarged View of Suspected Leak Area in T-111 Duct	176
71	Duct Assembly Leak Area Repaired by Welding	177
72	Duct Assembly After Repair and Replacement of Wrapper	177
73	Duct Wrapper Welded Areas Showing Areas of Surface Defects	178
74	Inlet End of Assembled Duct with Core in Place	178
75	Completely Assembled Duct Prior to Adding Insulation	179
76	Foil Insulation Being Applied to T-111 Duct	180
77	Connection End of Duct After Insulation	181
78	Duct with Heat Insulation Complete	182
79	Layout of Assembled Pump with Instrumentation Items	183
80	"Trial" Mating of Insulated Duct Into Stator Bore Can	184
81	Duct with Shroud and Instrumentation Tacked in Place	185
82	Close-Up of Inside of Duct Shroud at Fit-Up	186
83	Schematic Diagram of Leak Check and Argon Filling Set-Up	187
84	Overall View of Completely Assembled Pump with Instrumentation	188
85	Duct Inlet/Outlet End of Assembled EM Pump	189
86	Power Lead Connection End of Assembled EM Pump	190

LIST OF TABLES

Table No.		Page No.
1	Pump Calculated Characteristics at Design Point	191
2	Detailed Electrical Design Characteristics	192
3	Detailed Hydraulic Design Characteristics	193
4	Detailed Thermal Design Characteristics	194
5	Calculated NPSH Requirements	195
6	Nickel Plated Sample Strands - Samples S1-S11	196
7	Nickel Plated Sample Strands - Samples S12-S21	199
8	Nickel Plated Sample Strands - Samples S22-S33	200
9	Brazed Joint Samples - #1 through #13	201
10	Brazed Joint Samples - #14 through #18	202
11	Brazed Joint Samples - #F1 through #F8	203
12	Brazed Joint Samples - #F11 through #F17	204
13	Brazed Joint Samples - #F19 through #F25	205
14	Braze Erosion Tests on Nickel Foil	206
15	Critical Temperatures for Au-Ni Braze Alloys with In and Ge	207
16	Braze Erosion Tests with Au-Ni-In or Ge Alloys	208
17	Initial Braze Samples with Ni Plate Ends	209
18	Brazed with Various Plating Methods - Samples P3-P5	210
19	Brazed Joints - Conductors Plated in Groups - Samples P6 to P11	211
20	Refractory Materials for EM Pump Duct	212

LIST OF TABLES (Cont'd)

Figure No.		Page No.
21	Effect of Percent Reduction on T-111 Grain Size	213
22	List of Quality Assurance Tests for T-111 Products	214
23	Chemical Composition of T-111 Ingots	215
24	Mechanical Properties of T-111 Items	216
25	Quality Assurance Results on T-111 Items	217
26	Quality Assurance Results on Cb-1Zr Foil	218

I. SUMMARY

The General Electric Company, under NASA Contract NAS3-9422, has completed the building of a 3-phase, helical induction electromagnetic (EM) pump for use as a boiler feed pump in a Rankine cycle space electric power system. The preliminary design was developed under NASA Contract NAS3-8500 (Reference 1). The rating of this pump is 3.25 lb/sec flow rate at a developed head of 240 psi, when pumping 1000°F potassium.

The contract also required the building of a suitable test facility, the installation of the pump in the test loop, a performance test series to explore the full pump capability, and finally a 10,000 hour endurance test at rated conditions.

This report (Part I of three parts) describes the final pump design and fabrication, which included the building of a model (trial) stator, the final stator, the T-111 duct, and the overall assembly of the pump. Subsequent reports will cover the test facility design and construction, the performance tests through all "off-design" conditions, and the 10,000 hour endurance test.

The fabrication of the EM pump stator also involved the building of a model stator to check out construction details, extensive development of conductor end sealing methods, and joint brazing techniques using a new alloy to permit the pump winding temperature to go as high as 1200°F. The pump has windings made of nickel clad silver wire, high purity alumina slot insulation, and "S" glass tape winding insulation.

The pump duct, made of T-111 refractory metal, required new fabricating techniques, especially in machining the helix, and the establishment of T-111 joining procedures involving careful control of the welding atmosphere and post-weld annealing.

Final assembly of the pump involved welding the duct into the stator, evacuation of both the stator cavity and the duct cavity (which are separated by a thin-walled Inconel can in the stator bore) and then back-filling with argon to approximately 8 psia. Electrical checks during stator assembly and after installation of the duct provided assurance of the winding integrity.

The assembled pump, with an outside diameter of 11 inches and total length of 35 inches, weighing 430 lb with attached pressure transducers and gages, was then prepared for installation in the pump test loop for the performance and endurance test programs.

II. INTRODUCTION

An electromagnetic pump design study program, conducted under NASA Contract NAS3-8500 with a final report (Reference 1), provided the basic guidelines for building a flight type boiler feed (potassium) pump for full scale testing under this program. The pump which has now been built has the following design specifications:

	Design Point	Off-Design Range
Potassium Temperature, °F	1000	900 - 1400
K Flow Rate, lb/sec	3.25	0.75 - 4.25
Pressure Rise, psi	240	35 - 300
Net Positive Suction Head, psi	7	1 - 22
NaK Coolant Temperature, °F	800	700 - 900
Voltage, V	135	30 - 165

Major materials specified for use in the pump included:

Duct	-	T-111 Alloy
Magnetic Structures	-	Hiperco 27
Conductors	-	Nickel clad silver (20% Ni area)
Electrical Ground Insulation	-	High purity 99.5% alumina and "S" glass tape
Interlaminar Insulation	-	Plasma sprayed alumina

The design has taken advantage of materials and techniques to obtain a higher efficiency than has been previously obtained from the wide variety of EM pumps now in successful operation. It is also expected to provide long trouble-free operation in a space environment.

The first part of this report describes the design of the EM Boiler Feed Pump in detail, and the construction and test of a "model" (or trial) stator is described. The test results led to the final details needed for the stator insulation and the coil winding and insertion techniques. During this time, means for sealing the ends of the special nickel clad silver conductor and brazing the joints to withstand high temperatures were developed as explained in the report.

The duct, made of T-111, involved many special problems of material procurement, fabrication, and joining which are described in the report. After final assembly the EM pump was installed in the test facility for the extensive performance tests that will be covered by Part II of this final report. Part III of the report will be issued after the programmed 10,000 hour endurance test has been completed.

III. OVERALL DESIGN

A. General Description

In all electromagnetic (EM) pumps, a body force is produced on a conducting fluid by the interaction of an electric current induced in the fluid, and the surrounding magnetic field. This body force results in a pressure rise in the fluid as it passes from the inlet to the outlet of the EM pump. The force is analogous to the familiar fundamental principle of force on a current carrying conductor in a magnetic field which is the operating principle of many common electromagnetic devices.

The polyphase helical induction EM pump employs this principle in the same manner as a polyphase induction motor. The pump contains an electromagnetic stator assembly and a duct assembly in the stator bore. When power is applied to the three phase stator winding, a revolving magnetic field is produced in the stator bore. This magnetic field induces voltage in the conducting fluid contained in the duct, and as a result of this induced voltage, currents will flow in the fluid. These currents interact with the magnetic field to produce a body force on the fluid causing it to move through the duct and also develop pressure. The pressure gradient at any point in the fluid is proportional to the product of magnetic field strength and the component of current density perpendicular to magnetic field strength. The total pressure rise developed by the pump is the integral of this pressure gradient over the total developed length of the helical flow passage in the pump duct.

The general configuration for the specific helical induction EM pump built on this contract for a Boiler Feed (potassium) Pump applica-

tion is shown in Figure 1A. The basic design was developed on prior government contracts as reported in References 1 and 2. The pump consists of a stator assembly including the frame, heat exchanger and wound stator, plus a duct assembly consisting of a duct, center iron core and thermal insulation. Figure 1B shows the basic pump dimensions.

In the configuration shown in Figure 1, the potassium being pumped enters the pump duct tangentially through the inlet pipe into a short annular region, then into and through the helical passage where pressure is developed by the electromagnetic body force on the fluid. After leaving the helical passage, the fluid flows back through the center return leaving the pump through an outlet pipe at the same end it entered.

In order to permit operation at relatively low net positive suction head (NPSH), the first two turns of the helical flow passage were designed with a larger cross-section than the remaining turns. In this way, low fluid velocity is maintained near the pump entrance where the NPSH is low. As pressure is developed in the helical passage, the velocity is increased. After the second turn of the helix, the velocity is maintained at a relatively high value for the remainder of the pumping section to permit more efficient pumping.

The pump is cooled by a heat exchanger built around the outer surface of the pump frame. The heat exchanger consists of a machined helical passage with an inlet pipe at each end and an outlet pipe at the center. Most of the heat is conducted from the windings through the stator core to the frame where the heat is removed by circulation of an alkali metal coolant (NaK) through the heat exchanger.

The stator core and windings are completely enclosed and sealed by the frame, end shields, and a thin "can" inside the stator bore. This enclosed stator region is filled with argon to 7-9 psia (at room temperature) to facilitate heat transfer between the windings and the stator laminations (and thus the heat exchanger). Electrical power is transmitted to the stator windings through hermetic lead seals in the pump frame. The thin bore can, besides sealing the stator cavity region, acts as a protective shield to prevent outgassing products from the stator from reaching the duct.

The region between the duct and the stator can contains thermal insulation consisting of multiple layers of dimpled metallic (Nb-1%Zr) foil. This region is sealed from the outside environment by a shroud at the inlet/outlet end, welded between the end shield and the inlet/outlet pipes. The space between the duct and stator can is also filled with argon to the same pressure as the gas in the stator region.

B. Stator Assembly

The stator consists of a laminated punching stack and coils arranged to form a two pole magnetic field revolving at 60 revolutions per second (when supplied with 60 Hz three phase power). Selection and evaluation of the specific electrical, magnetic and insulating materials for the stator assembly were based primarily on prior development work done under government contracts. The results of this work and the data generated are contained in References 3 through 5.

The punching stack, or unwound stator core, consists of magnetic laminations which provide a low reluctance path for the magnetic flux

as in a conventional induction motor stator. The material for these laminations is Hiperco 27, 0.025 inch thick. For the conditions of operation with this lamination thickness, Hiperco 27 has excellent magnetic characteristics, good thermal conductivity and reasonably low loss. Each lamination contains 24 slots for the stator winding.

Interlaminar insulation is provided by a plasma sprayed alumina coating on one side of each lamination. This coating is approximately 0.001 to 0.002 inches thick.

The important dimensions for the unwound stator core are as follows:

Core length	10 inch
Bore diameter (punching)	1.4 inch
Outside diameter (punching)	10 inch
Slot width	0.386 inch
Slot depth	2.12 inch

The stator laminations are held together by 8 bars of rectangular cross-section, spaced uniformly around the outer periphery of the punching stack and welded at each end to a stiff ring to form a tightly compressed stack of laminations. The stator core has an interference fit at its outer periphery with the pump frame thereby insuring good heat transfer from the stator to the heat exchanger. In addition, two dowel pins are inserted through the frame into one of the welding rings after assembly to properly position the stator core.

The slot insulation, coil layer separators, turn separators and top wedges are high purity (99.5 percent or greater) alumina which has been solid molded and then ground to size. The slot insulation consists

of three pieces; a bottom piece and two side sheets and is described more fully in Section IV. The slot insulation side sheets are 0.038 inch thick, the bottom piece, coil layer separator and top wedge are 0.052 inch thick, and the turn separators are 0.025 inch thick.

The complete two pole stator winding consists of 24 coils, each coil spanning eight teeth, thereby giving a 2/3 pitch. The winding has 32 turns in series per phase, and is connected in a one circuit, 3 phase, Y-connection with a floating neutral. Each coil consists of four turns, six strands of wire in hand per turn; each strand is bare rectangular nickel-clad silver wire, 0.073 inch x 0.149 inch in cross-section. The stator is fabricated using so-called "half-coil" construction. A bar, consisting of four groups of six wires each, is formed and cut to the proper shape and length. Forty-eight of these bars are made and inserted into the slots. The ends of the groups of six wires are joined together in the proper arrangement to form the 24 complete coils and the one circuit, 3 phase, Y-connected winding. All the coils are insulated in the end turn region with S-glass tape, which contains no organic materials. The ends of the conductors, prior to insertion, are carefully cleaned and nickel-plated to seal the silver in the nickel sheath. After insertion, joining is accomplished by a special induction brazing process using a gold-nickel-indium braze alloy. The special winding and insulating procedure, nickel plating process, brazing procedure and brazing alloy were all developed on this contract and are described in more detail in Sections V and VI of this report.

Surrounding the wound stator is the pump heat exchanger and frame. The NaK coolant is circulated through the helical passage in the heat

exchanger to remove heat conducted from the windings through the stator core.

The material for the pump frame and heat exchanger is Hastelloy B. This material is a satisfactory containment material for the liquid coolant (NaK) in the heat exchanger and comes very close to matching the thermal coefficient of expansion of the Hiperco 27 stator core. Thus, the interference fit between the heat exchanger and the core is properly maintained, and good heat transfer between the core and heat exchanger is assured at operating temperature. Beyond the ends of the heat exchanger, the pump frame material is Inconel. The end shields and stator can in the stator bore are also Inconel.

The heat exchanger, frame, end shields and stator can provide all welded construction and form a completely sealed envelope around the stator assembly. The only penetrations through this envelope are the hermetic lead seals to transmit power to the stator windings, thermocouple wells to provide means of monitoring temperature, a pressure tap to detect stator cavity pressure and an evacuation plug to provide a means of leak testing the unit, evacuating the stator region, and filling with argon. All these penetrations are completely sealed by brazed or welded joints.

C. Duct Assembly

The helical duct for this boiler feed pump (refer to Figure 1) is made of T-111 alloy. Its outside diameter is 4.1 inches, axial length of helix is 13.88 inches and overall length is 28 inches.

The first turn of the helical flow passage in the duct has a rather large cross-sectional area to permit low fluid velocity at entrance and hence operation at lowest possible NPSH. The cross-sectional area of the second turn gradually changes from this relatively large area to a smaller area which is maintained for the remaining turns of the helical passage. During this second turn, the velocity increases to the final (relatively high) value for more efficient pumping during the remainder of the duct. This variable fluid velocity is accomplished in the duct by employing a dual pitch for the helix with a pitch of 0.85 inch for the first two turns and 0.57 inch for the remaining turns.

Enclosed between the helical flow passage and the center return pipe is a center iron core. This core consists of magnetic laminations (washers) of Hiperco 27 having the same thickness and same interlaminar insulation as the stator core laminations. These laminations are held together in a tight stack and positioned by a key and ring at each end.

The thermal insulation between the duct and stator can consists of 10 layers of laminated strips of dimpled Nb-1%Zr foil. These strips are 0.5 inch wide by 0.002 inch thick with the dimples being 0.010 inch deep. The thermal insulation is attached directly to the duct by a limited number of spot welds.

The thermal insulation region is sealed by the shroud welded between the end shield and inlet/outlet pipes. After assembly this region is evacuated and filled with argon to 7-9 psia.

D. Design Considerations

The operating performance of the pump is calculated by using data and the equivalent circuit shown in Figure 2, the solution of which

has been programmed for a digital computer. Performance curves, shown in Figures 3, 4 and 5 for 1000°F potassium, and tabulated values in Table 1, show the overall rating and calculated performance characteristics for the final design. Additional calculated results and design characteristics are presented in detail in Tables 2, 3, 4 and 5.

In addition to these results, certain operational limits and conditions are necessary to insure satisfactory performance throughout the pump's life. The principal operational limits are as follows:

1) Duct and fluid temperature	1400°F maximum
2) Winding temperature (hot spot)	1300°F maximum
3) Duct pressure	350 psia maximum
4) Stator cavity pressure at Room Temperature	7 psia minimum 9 psia maximum
5) Net positive suction head	See Table 5

The limitation on duct and fluid temperature and pressure is primarily one of strength. The duct was originally designed mechanically to safely withstand pressures up to 300 psi at 1300°F maximum. Due to manufacturing limitations with T-111 alloy, the T-111 ducts actually have somewhat thicker walls than necessary from purely a stress standpoint. Therefore, although the maximum recommended pressure is 300 psi, the T-111 ducts are capable of withstanding 350 psi for short periods of time at 1400°F. From an operational standpoint, the pump is designed for continuous operation at 1000°F with the rated flow and developed pressure.

The maximum for hot spot winding temperature is a reasonable limit consistant with good performance and life for the winding and insulation

system. All performance calculations are based on an electrical resistivity of the conductor material at an average temperature of 1050°F. Average temperatures above this, although allowable, will cause increased winding resistance and losses and lower efficiency. At an average winding temperature of 1050°F, the hot spot temperature should not exceed 1200°F.

The limitation on stator cavity pressure depends on both mechanical and electrical considerations. The maximum pressure of 9 psi at room temperature is a mechanical limitation. At operating temperature, the pressure in the winding cavity increases by a factor of about 2.5. To minimize weight, the frame structure has been mechanically designed for maximum internal pressures of about 25 psia. Hence, at room temperature, internal winding cavity pressure must be limited to about 9 psia. The lower limit of 7 psia is based on electrical considerations. Because of reduced arc-over voltage of the winding and insulation system at pressure below about 7 psia, it is recommended that this be the minimum winding cavity pressure at room temperature so the pressure is just slightly greater than atmospheric at operating temperature.

The limitation on net positive suction head is based on cavitation considerations, using the criterion of requiring an NPSH of at least two velocity heads at entrance to the pumping section. This criterion is explored in Reference 2 and appeared to be reasonably conservative. Maximum flow rates in Table 5 for several values of NPSH are based on this criterion.

At the design point of 1000°F, 3.25 lb/sec flow rate, 240 psi developed pressure and 7 psi NPSH, the pump can operate continuously.

The pump can operate for limited period of time at 1000°F at developed pressure up to 300 psi over a flow rate range of 0.75 lb/sec to 4.25 lb/sec. With the potassium at 1300°F, the pump can also operate for limited periods of time up to 300 psi developed pressure over the same flow rate range. The principal limitation on time of operation is winding temperature and duct temperature. These temperatures should not be allowed to exceed the recommended limits. By appropriate increases in NaK coolant flow rate or decreases in NaK coolant temperature, it may be possible to operate continuously at some of these other points.

Performance calculations are based on 800°F NaK coolant inlet temperature and 50°F NaK coolant temperature rise. These are the recommended normal operating values and preferred for continuous operation. For shorter periods of time, such as during performance testing, the NaK coolant inlet temperature can be allowed to go as high as 900°F with the 50°F rise, and the NaK coolant temperature rise can be allowed to go as high as 100°F with the 800°F inlet temperature.

IV. MODEL STATOR

A. Scope

A model, or full size, sample stator was built early in the program, after detailed drawings were completed, to identify any potential problems in stator design and construction. Of particular interest was the overall stator design philosophy or approach, including the winding configuration and dimensions and the ceramic insulation dimensions and handling characteristics.

B. Materials

The materials used in the construction of the model stator were generally the same as those planned for the production stator except for such differences as: (1) Stator laminations made from carbon steel with oxide interlaminar insulation coating in lieu of Hiperco 27 with an alumina plasma sprayed coating. (A separate early trial for the processing of Hiperco 27 was conducted). (2) Alumina slot insulation nominal thicknesses were 0.025 inch for the side sheet and 0.075 inch for the bottom piece, coil separator, and wedge, except that some turns were insulated with a BN (boron nitride) felt paper. (3) The winding conductor was electrolytic tough pitch copper with the same dimensions as the planned 0.071 inch x 0.164 inch nickel clad silver. (4) Heat cleaned "E" glass was used for taping the individual turns, coil ends, and connections in the coil end turn region since specified "S" glass material was not available in time for the model stator work.

C. Fabrication

1. Stator Core

The fabrication of the model stator core (unwound stator) was the same as for the production stator core discussed in detail under Section III-B except that oxide coated carbon steel was used for the lamination material.

2. Stator Windings

a. Full Coil Construction

The initial effort during the model stator phase was to try and use the full coil construction to eliminate the cost and time delay associated with making the multiplicity of joints necessary for half coil or bar construction to maintain the same degree of reliability as for full coil construction. The full coil geometry used for this trial is shown by Figure 6. The investigation demonstrated that the use of full coils was not feasible because of insufficient space in the bore to accommodate the upper coil sides of the "jump" or "throw" coils and insert the remaining lower coil sides under the raised "jump".

b. Half Coil Construction

Based on the results noted above, the choice of half coil construction was mandatory. Implementing the use of half coil construction involved refining the upper and lower coil side geometries, selecting suitable turn and coil connection configurations, and developing the winding assembly procedure.

Calculated dimensions for the upper and lower coil sides or bars were made. Several sample coil sides were fabricated to these calculated dimensions, and the coil end forming and coil lengths refined.

Several configurations were developed for connecting the end (opposite to the lead end) groups of six strands or conductors of the bottom coil side to the appropriate ones of the top coil side. Two of the most promising turn to turn connection arrangements are shown in Figure 7. The connection arrangement selected for use in the production stator was the lower left group of Figure 7 except that the connections for the inner turn closest to the stator bore surface was arranged "over-under" instead of "side by side".

Figure 8 shows the related connection arrangements for the lead connection end. The connection arrangement selected for the lead connection end corresponds to that selected for the end opposite to the lead end, Figure 7.

c. Winding Assembly Procedure

The side insulation sheets were assembled in place as shown in Figure 9A, Item 1, followed by the bottom insulator, Item 2. The bottom half turn was assembled in place and the ends were taped with one layer of "E" glass using a half lap. The taping was started at the edge of the ceramic and continued on to within one inch of the joint edge. Separator, Item 3, was made of boron nitride felt for 12 of the 24 top bars. All other bars used the alumina. This procedure was repeated for the next three half turns in the slot. The four half turns were then end taped together into a coil side or bar and tied onto an insulated bracing ring to restrain the coil ends. All of the foregoing was repeated for the remaining 23 slots.

The half turns for the top coil sides were assembled following the same procedures as for the bottom coil sides except that these coil sides were not tied to the bracing ring.

Insulating fibre blocks were assembled into place at the top of each slot and a fixture assembled in place to moderately press the windings compactly in each slot. A hipotential test of 1000 volts RMS was successfully applied for one minute between all of the assembled and unconnected windings and ground.

The turn, coil series, and pole-phase connections were made and brazed and the connections were individually wrapped with three layers of "E" glass. A hipotential test of 800 volts RMS and a surge test of 800 volts peak were successfully applied to the completely connected stator windings.

A high temperature relaxation bake was applied to the completed wound stator to eliminate approximately 75 mils of radial looseness in the slot resulting from the accumulated waviness of approximately 1 1/2 mils for each of 48 vertically oriented strands. To perform this relaxation bake out, the insulating fibre blocks were replaced with carbon steel blocks. The wound stator assembly was baked at 900°F for 1/2 hour and cooled to room temperature in a nitrogen atmosphere.

D. Evaluation and Conclusions

A considerable amount of core iron and winding copper oxidation occurred during the relaxation bake. This corrosion was caused by a leaky furnace door and contamination of the nitrogen atmosphere.

When attempting to apply a hipotential test of 800 volts RMS, arcing to ground occurred at 700 volts. Subsequently, it was determined that the windings could withstand at least a 300 volt RMS test voltage to ground without arcing, so the coil vibration measurements proceeded.

Coil vibration measurements were carried out in three cycles by applying the calculated full load current of 160 amperes over a frequency range of 15 to 60 Hz. Coil end vibration and sag or deflection was measured by means of a calibrated transit. No observable coil end vibration was observed.

Summarizing the results of the three test cycles showed:

Cycle	Time (Hours)	Temperature (°F)	Coil Vibration (Mils)	Coil Sag (Mils-approx.)
1	4 1/2	400-485	None	4.5
2	6	738-780	None	20
3	3 1/2	625-959	None	98

Toward the latter part of the third cycle, a shorted turn was noted as evidenced by a red color in the turn in question.

The stator windings were systematically disassembled to establish the cause for the low level of ground insulation noted prior to running the coil vibration tests and the shorted turn encountered during this test. This was accomplished by numbering each of the slots and corresponding wedges (numbers 1 through 24) and numbering each turn as it was removed with the slot number and a turn number (1 through 8) in the order removed. A sampling of megger readings were taken and recorded for turn-turn and turn-ground insulation. Slot liners were placed with respective turns and separators between respective turns as they were removed. Some of the parts are shown in Figure 10, while the partially disassembled stator is shown in Figure 11. The systematic disassembly and examination disclosed the following:

1. The E glass taped end turns appeared to be in very good condition. No evidence of scuffing or fraying.

2. The E glass insulated support rings appeared to be in very good condition. The complete absence of scuffing or fraying substantiates the conclusions based on visual observations, that no relative motion occurred between the coil ends and the bracing rings during the vibration tests.

3. The low level of ground insulation was caused primarily by iron and copper oxides which formed initially during the high temperature relaxation bake. Cracked or broken ceramic slot liners, particularly at the edge of the slots, also contributed to the low level of ground insulation observed. The 0.025 inch ceramic slot liners appeared to be too fragile for the high reliability desired.

4. The shorted turn was due to the omission of a separator between the turn in question during the course of manufacture.

5. The 0.075 inch thick spacers or separators fared quite well since only one of 72 pieces was broken prior to removing from the stator.

6. 36 of 144 pieces of the 0.025 inch turn separators were examined after removal. 64% of these 36 pieces were found to be broken or cracked.

7. The boron nitride felt stayed in place. No electrical failure occurred where the felt was used, although it had "frayed" some.

8. The general method of half coil assembly and end turn connections appeared to be satisfactory for the production stator.

Based on the test evaluations, several changes were made for the production stator. The side sheet thickness was changed from a nominal thickness of 0.025 to 0.038 inch; the bottom piece, coil separator, and wedge were changed from a nominal thickness of 0.075 to 0.052 inch; and the conductor dimensions were changed from 0.071 x 0.164 inch to 0.073 x 0.149 inch as dictated by the dimensional changes in the ceramic insulation. Refer to Figure 9B for the final slot details.

Nickel Clad Silver Conductor

The conductors (wires) are made from a round configuration by rolling to the required cross sectional dimensions. The round wire was specified to have a 20% (by cross section) pure nickel sheath with a core of pure silver.

Overall coil resistance in the production stator was heavily dependent on the wire resistance. An investigation to determine the actual resistance of the wire used for the stator coils was conducted at the NASA-Lewis Research Center. The procedure and results are given in Appendix A, and indicate an actual wire resistance at 68°F of 1.944 micro ohm-centimeters with a 21% Ni sheath.

V. CONDUCTOR SEALING

A. General

To preclude the possibility of any silver migration from the conductor ends, it was necessary to develop a technique to seal the ends of the nickel-clad silver wire with nickel or an equivalent material prior to making the brazed connections. Each of the 24 stator slots contain 8 conductors of 6 strands each, thereby giving a total of 1152 strands of wire which had to be sealed at each end. Several techniques for sealing these ends were considered and evaluated. These techniques fell into two basic approaches:

(1) Seal welding the ends of the nickel-clad silver wire, either singly or in groups of 6 strands.

(2) Nickel plating over the ends of the individual nickel-clad silver wires.

Both of these approaches were explored in detail on this contract and are interrelated with the brazing technique so cannot be completely separated from a discussion of brazing. However, a brief review of the basic conductor sealing investigation is included in this section. Additional detail, where appropriate, is included in Section VI, Joint Brazing.

B. Seal Welding

Several seal welding techniques and approaches were considered, tried and evaluated. The first attempt was to GTA weld directly over the end of a single nickel-clad silver strand of wire with nickel filler. A sample was made and examined. The sample gave complete fusion and ex-

cellent appearance but contained appreciable silver in the seal weld and hence was unacceptable.

A second technique using palladium filler was made and produced a good seal consisting of a palladium-silver alloy. Although the seal still contained silver, the melting point of the Pd-Ag alloy which formed the seal is 300°F (or more) higher than the melting point of silver. Hence, this appeared at first to be a promising means of sealing prior to induction brazing so that the silver would not run out the ends of the strands and mix with the braze alloy during brazing. The Pd-Ag alloy would be completely sealed by the braze alloy during induction brazing of all conductors together, eliminating exposed silver.

The major concern was whether or not the silver in the palladium alloy would migrate to the surface of the subsequent braze. This was investigated and although it was felt that the silver concentration at the braze alloy surface due to migration would be negligible, it was decided to seek a method which would seal the end of the wire with nickel and completely preclude the possibility of any exposed silver prior to brazing.

An investigation was initiated to develop a method of completely sealing the conductors by welding the nickel sheath closed, and thus prevent exposure of any silver to the final braze when joining the conductors. Initial effort was devoted to removing silver from the conductor ends thus permitting insertion of a nickel "plug" for GTA seal welding over the wire end and to the nickel sheath. It was soon determined that the silver could not be effectively removed by mechanical means.

Various chemical solutions were tried for silver removal, and only an acid (95% H_2SO_4 - 5% HNO_3 by volume) was effective in removing the silver. However, it also attacked, to a limited extent, the nickel sheath. Finally, electrochemical removal using a sodium cyanide electrolyte with a stainless steel cathode and the nickel-clad silver as the anode, was successful. A number of samples were prepared in which 1/8 inch of silver was removed from the wire ends, without any effect on the nickel. This method is applicable to the cut and formed stator conductors, so reels of nickel-clad silver wire could be rolled to the correct size, annealed, cut, and formed, prior to sealing.

Using sample pieces of wire with the silver removed electrochemically, attempts were made to establish the best technique for sealing the ends as follows:

a. Seal the samples using various forms of nickel powder as a filler. Result: The powder "balled-up" and was difficult to keep in position; thus was not satisfactory.

b. Use a piece of round nickel filler wire. Result: Careful and precise fitting of the plug was found to be essential, and gave only fair results.

c. Prepare (by rolling and forming) nickel filler wire which had the precise dimensions of the inside of the nickel sheath (the silver cross-section). Result: Short lengths were cut (by careful sawing) to form plugs, several of which were successfully inserted and the conductor group welded to the sheath by the GTA process.

Figures 12 and 13 show etched cross-sections of the best samples (one single strand and one bundle of six strands) which were prepared.

The photographs at 15x magnification show that the nickel plug was not melted all the way to the bottom. This assures that no silver boiled up and entered the nickel seal weld. The data also indicates that a good seal was obtained over the edges and corners of the nickel sheath. The outside edges of the nickel sheath appear thin in the illustrations only because of light reflection from the edges during photographing. These edges were slightly beveled during polishing operations after mounting the sample.

The silver is indistinct (black) in the photographs due to the nickel etchant used to produce the desired detail in the nickel portion of the mounted sample. The sample looked very good, indicating that this approach was quite promising, although somewhat involved for production use. The samples demonstrate satisfactory removal of silver and feasible use of nickel plugs and GTA welding to seal the ends of the wire without melting any silver.

In general, practically all the stator winding brazed connections consist of brazing together two groups of six strands each. Hence it is desirable to be able to seal the strand ends in groups of six or twelve. The basic plan that was selected for making samples consisted of preparing a group of twelve strands of wire; six representing one conductor and six representing the other. This simulated the conditions in the production stator. These samples would be sealed and brazed and then evaluated to develop and establish a final procedure. Sealing with nickel plugs was accomplished by removing silver for approximately

1/8 inch from the end of each strand of wire, inserting a 1/8 inch long nickel plug into the end and GTA welding over the ends of a bundle of six strands clamped tightly together. Then a nickel cup was placed over the sealed ends of two bundles of six, and this sample assembly was induction brazed (as discussed in detail in Section VI).

It was very quickly determined that for proper brazing the fit of the nickel cups is very critical. Considerable difficulty was experienced in assembling the cups on the sealed ends of the nickel-clad silver wire due to weld build-up around the edges of the bundles of strands. To overcome this difficulty, the approach was modified to use a nickel ferrule (a band, open at both ends). This ferrule was assembled over a bundle of twelve wires with pre-placed nickel plugs in the ends after the silver had been removed. Then the end of the entire bundle was GTA welded (ferrule-cladding-plugs) to form a complete seal. In this way, it was possible to get a snug fit of ferrule to wire strands, eliminate the voids that existed at the bottom of the nickel cup, and obtain a better seal weld at the strand edges. While this approach apparently provided a satisfactory seal for the silver, it was very complicated, and had some small risk in that a perfect seal weld might not always be achieved. In addition, the electrochemical removal of the silver at the end of the wire was very critical and some concern was expressed that it might cause some attack on the nickel sheath.

C. Nickel Plating

Nickel plating the ends of the nickel-clad silver wire was considered as a means of sealing, instead of removing silver and plug

seal welding, primarily because of its simplified procedure. It was desired to develop a plating procedure that provided a tightly adhering nickel plate, about 0.004 inch thick, over the end of the strand, which would not peel off, blister or leak silver from the strand, when it was heated and held at 1750°F to 1800°F for five minutes. Initial attempts consisted of plating just the ends of a bundle of six strands with nickel approximately 3-6 mils thick and also plating the ends plus the exposed sides of a tightly held bundle of six strands. Neither of these approaches with standard plating procedures were satisfactory due to poor bonding, blisters and contamination.

As a result, an investigation was undertaken to plate individual strands, trying out various refinements and modifications in the basic plating procedures. After plating, the strands were evaluated by heating (to simulate brazing temperatures), and examined. Plating the ends only resulted in a very poor plating bond. Because of the extreme difficulty in achieving a good plating bond and seal across the ends only of the nickel-clad silver wire, it was decided to concentrate on plating the ends plus the sides. The first set of individual strand samples (S1 through S11) made this way are tabulated in Table 6. These were not completely satisfactory primarily because of blistering, which appeared to be due to a combination of (1) entrapped gases (probably H_2) and fluids behind the plating or in small (light) surface scratches on the nickel-cladding and (2) a poor plating bond in certain regions, no doubt enhanced by the entrapped gases and fluid. To improve this situation, four specific modifications to the basic procedure were tried and evaluated. These were:

(1) Electrolytic polishing of wire surface to remove scratches and better prepare the surface for plating.

(2) Ultrasonic cleaning of the wire surface in methyl chloroform solution both before and after the electrolytic polishing.

(3) Activation of H_2SO_4 without power and elimination of any strike to minimize H_2 gas charging.

(4) Special vacuum outgassing at 1300-1400°F by very slowly raising temperature to this value (say over 6-8 hour period) and then holding for 1-2 hours to better remove entrapped H_2 gas.

In addition, a rhenium plating solution (proprietary) was obtained and used to provide a rhenium flash plate over the nickel plate on some samples to eliminate the possibility of corrosion during brazing. These various samples (S12 through S21) are described and the results tabulated in Table 7. All told, a total of 18 plating processes and techniques were tried and evaluated.

A detailed review of all the samples resulted in a conclusion that samples S14, S16, and S19 appeared to be best. The results pointed to a plating procedure that was selected for final evaluation with three minor alternatives:

1. Use of a special nickel strike.

2. No "outgas" after plating.

3. Use of a rhenium overplate.

To evaluate the three alternatives and make certain of the final plating procedure, additional individual strands were plated and heated. These samples, (S22 through S33) are listed in Table 8. Referring to

the results in Table 8 it was concluded that samples numbers S26, S27, and S33 with a special sulphate type of nickel strike, and no outgassing after plating, were very good.

Additional minor refinements such as brushing the ends during the rinse were made in the plating procedure to further improve the quality of nickel plate and seal, prior to plating the conductors to be used in the production stator. Also, white (lint-free) gloves were required for all handling of the conductors and clean wooden boxes with plastic separators were prepared for storage and transportation.

On the basis of all the tests, the preferred procedure for plating the strands in bundles of six was established and is shown in the table on the next page. The extensive testing showed that every step was very important and must be included in the production plating.

Figure 14 shows the special set-up used for the nickel plating. Careful daily checks of all solutions were required to be sure the solutions were within specifications. Furthermore, a quality control group of short conductors was plated with the first production group each day. These were visually inspected and frequently sectioned for examination to make sure the plating was of uniform quality.

Details of the nickel plate on a typical facility quality control sample (#3) are included at 4X magnification in Figure 15. Figures 16 and 17 are photomicrographs (100X) of two of the strands shown in Figure 15. Note especially the good build-up of nickel plate over the end of the exposed silver, and then up the sides of the wire, over the nickel sheath.

TABLE SHOWING STEPS IN APPROVED NICKEL PLATING PROCESS

Note: Handle all conductors using white (lint-free) gloves.

(1) Prepare ends of bundles of six strands by trimming the wire off square.

(2) Separate strands 1/16 to 3/32 inch, and bevel all edges of nickel sheath (0.015 to 0.030 inch radius), with a clean, fine file.

(3) Ultrasonic clean in methyl chloroform for minimum length of 1 1/8 inch.

(4) Rinse in acetone and then cold water, proceeding while wet to (5).

(5) Anodic etch in 50% H_2SO_4 with 450 A/ft^2 for 2 minutes.

(6) Rinse in running distilled cold water, brushing ends of strands with medium bristle toothbrush and while wet go to (7).

(7) Nickel strike in 32 oz/gal nickel sulphate and 16 oz/gal H_2SO_4 at 1900 A/ft^2 for 30 seconds, brushing ends for first few seconds of immersion.

(8) Plate in Sulphamate bath with anti-pitting agent at 40 $amps/ft^2$ for approximately one hour to obtain 0.004-0.005 inch plating thickness (1/16 inch from end).

(9) Rinse in cold distilled water, hot water, and air dry.

VI. BRAZING ELECTRICAL CONNECTIONS

A. Initial Considerations

The use of the high temperature NaK coolant (800-900°F) which results in winding hot spot temperatures of 1200°F, required the development of a special joining method for the conductor end connections. The goal was to provide for reliable long-time operation (up to 30,000 hours) at 1200°F, in argon, with no adverse effect on nearby materials, especially the electrical insulation. The procedure developed had to be suitable for practical application to the production stator, using the rectangular nickel clad silver wire in bar wound (half coil) construction, and involving about 200 joints.

Important factors considered in developing and selecting the joining process included:

Space limitations

Low electrical resistance of joint

Reliability (joint quality)

Repeatability of process

Number of joints required

No exposed silver in the final joint

Initial work consisted of reviewing all the possible joining methods including welding, mechanical clamping, and brazing. All were rejected except for brazing.

Then a number of braze alloys were considered and several trial brazes were made using both induction and gas tungsten arc (GTA) methods of heating. Data on various braze alloys considered is listed below:

	Chemical Composition			Freezing/Melting Point	
	AU (%)	Cu (%)	Ni (%)	Solidus (°F)	Liquidus (°F)
	35	65		1814	1850
	50	50		1751	1778
	40	60		1796	1832
	35	62	3	1787	1877
	80	20		1635	1635
	82		18	1740	1740
	81.5	15.5	3	1652	1670
(Nicoro 80)	81.5	16.5	2	1670	1697

Of the alloys listed (none of which include silver), Nicoro 80 appeared to be the most promising and was selected for initial consideration in this development. It has excellent wetting and flowing characteristics, is readily available in various forms and was developed for high temperature brazed connections. One possible alternative was the 80-20 gold-copper eutectic.

Preliminary brazing trial sample work is summarized below:

1. GTA Welding/Brazing Coil Ends (Bundle of 12 strands) in Nickel Ferrule

One sample was made using 0.045 inch diameter Nicoro 80 as braze (filler) metal with the ferrule positioned 1/16 inch above ends of the Ni clad Ag wires. Two layers of braze were deposited with argon shielding as provided by GTA heating torch. When sectioned, adherence to the wire ends and the ferrule was found to be complete. The first braze layer melted the silver core of the wires approximately 1/16 inch below original surface without melting of the Ni cladding. Chemistry was not

checked, but it is estimated that the first braze layer contained 30 to 50 percent Ag. As expected, the second layer contained much less Ag. Braze flow between strands during the initial application, from capillary action,was slight. The second application of braze did not improve this condition.

This was a very simple joint and relatively easy to make. However, there was exposed silver in the braze and between some wire strands. It was felt, furthermore, that repeatability and reliability for the production stator would be very hard to obtain. Hence, no further work was conducted using a GTA weld torch for heating and joint environment conditions.

2. Induction Brazing with "Face" Coil - Conductors in Nickel Cup

a. No Sealed Ends

Initial induction brazing experiments were conducted using a pancake-type induction heating coil consisting of a single turn of 5/16 inch square copper tubing with added magnetic laminations on one side of the coil for flux concentration purposes. A glass tape was used to insulate the coil from the end of the nickel cap; the cap was placed on top of the coil with the conductor strands pointing up.

One sample was made using a nickel cup and 0.045 inch filler wire of Nicoro 80 in an argon atmosphere chamber. Heating was accomplished in 12 to 15 seconds. It was observed that the nickel stayed in a clean, bright condition. Filler metal flowed readily and wetted the nickel easily. Some overheating occurred on the end of the assembly. It is assumed that this occurred in the second heating cycle during an attempt to fill the last small voids in the assembly by the use of the powdered filler metal (AuNi). Difficulty was encountered in filling the cup,

but filler alloy went up between strands far beyond the cup, due to better capillary conditions.

The sample was sectioned and polished for viewing. The ends of the conductors lost some silver (approximately 1/8 inch from end max.) due to overheating the end of the assembly. A sound braze was observed between all nickel surfaces in the cup and up to 1-1/8 inch above the cup.

Additional samples were made; one with preplaced filler, and one with the bottom of the connection clip loaded approximately half full with filler. The results were similar to the above. This could be a good repeatable process, but it required very careful fixturing. Furthermore, the braze alloy would tend to dissolve Ag, even without overheating; thus, Ag could become exposed.

b. Sealed Ends of Conductors

Exposed silver could only be eliminated by sealing the ends of the conductors, and an investigation was undertaken to produce a suitable seal.

Initial work was concentrated on sealing the wires by GTA welding the nickel. A complete joint was also made with the ends of the group of conductors held in a nickel ferrule and then sealed with palladium filler using the GTA torch, forming a Pd-Ag alloy seal. Then this sample was induction brazed with a face coil, feeding Nicoro 80 filler wire in each side, in an argon atmosphere chamber. The sample was sectioned and indicated that the Pd-Ag alloy seal did not melt during subsequent brazing, and the brazed joint appearance was good (gold in color) with only a few voids. The major concern, as indicated previously in Section V, was

whether or not the percentage of silver in the first palladium alloy layer would migrate through the next braze layer.

As a result of this preliminary work and because of the strong desire to have the ends of the conductor completely sealed, it was decided to pursue induction brazing with Nicoro 80 and Au-Cu brazing alloys of fully sealed conductors. The development of the conductor sealing method has been covered in Section V.

B. Induction Brazing with Focusing Inductor

An experimental set-up was prepared in the laboratory using an argon filled metal enclosure and induction heating equipment. After determining procedures, a series of joint assemblies were made. Table 9 lists these samples, various parameters which were investigated, and the results. Each brazed sample consisted of 12 short ($\approx$ 4 inch) strands of nickel-clad silver wire, six representing one bar conductor and six representing another bar conductor, with the ends sealed by welding as noted. This simulates the conditions in the production stator of the EM pump. This first set of samples (13 complete assemblies) were made using a focusing inductor ("face" coil) for induction heating. Based on these results, a second set of five samples was made. These are tabulated in Table 10. All of these samples had the conductor ends sealed, the second set using the "nickel plugs-ferrule-GTA weld" type seal which at this point was considered the best sealing approach.

As a result of the sample work shown in Table 10, the 80/20 Au/Cu braze alloy appeared to be the more promising and another set of samples (Nos. F1-F8) as tabulated in Table 11 was made. In general, these joints looked quite good; electrically and mechanically the joints were excellent.

However, on very careful metallographic examination, they showed considerable erosion of the nickel sheath. Figures 18 and 19 show the microphotograph of a section through sample F4 and illustrate the joint and associated nickel sheath erosion. This indicated that the rate and method of induction heating and the specific braze alloy all required further investigation for reliable results.

Most of these samples had been made with fairly rapid heating and high heat input. High-heat inputs produce superheating of the braze and (very likely) melting and superheating of the silver conductor. The available superheat provides the heat source to permit flow of the braze for a relatively long distance away from the braze joint, and the method tends toward release of silver to various exposed parts of the joint. It is inferred that slower heating (1) establishes a more gradual temperature gradient along the conductors, (2) results in some possible overheating in the glass-tape-covered area of the conductors with the possibility of outgassing reactions there (and adverse effect on the brazing atmosphere), (3) provides some slight superheat of the brazing alloy for good braze flow without exceeding the melting point of the silver, (4) provides a more gradual thermal gradient in the braze area itself, thus assuring sufficient temperature for braze flow through the joint area, and (5) offers a better range of total heat input control because of the longer time duration. It was obvious that very careful and accurate control of the joint temperature was essential.

To obtain a better understanding of the temperature gradients existing throughout the sample joint assembly during induction heating, two special samples (Nos. F9 and F10) were assembled, instrumented with thermo-

couples, and heated. A typical assembly is shown in Figure 20. In parallel with this, a separate program was initiated to develop a more suitable braze alloy and obtain more basic data on erosion of the nickel sheath by the braze alloy. This separate program is described in Section VI-C.

During and after completing these studies, two additional sets of samples (F11-F17 and F19-F25) were made and results are tabulated in Tables 12 and 13. These samples made use of the improved techniques of induction heating, and also used the improved braze alloys. In fact, two samples F24 and F25 were made with peripheral induction heating coil rather than the face coil to evaluate further that technique of heating. Figures 21 through 29 show photomicrograph cross-sections of several sample brazed joints in these two additional sets of samples.

From the first three joints (F11, 12 and 13), it was quite obvious that the braze alloy containing germanium was definitely erosive. The indium alloy (Refer to Figure 23 for sample F-13) was more promising, so the other samples were made predominantly with the indium braze alloy. Some interesting and significant observations and conclusions can be made from these samples.

It can be noted that the joint which had the indium braze "preplaced" (F15) showed poor flow and did not fill the areas between the conductors. The braze cycle involved raising the joint ferrule temperature (as measured by the attached thermocouple) to 1450°F and holding for five minutes to stabilize, then raising the temperature to 1700°F to obtain braze melting and flow. Sluggish braze flow and poor wetting were observed.

Sample F16 was made using hand feeding of the indium alloy braze. Temperature was raised to 1600°F; the braze started to flow sluggishly;

the temperature was raised to 1700°F, and the braze went up in all the conductors satisfactorily.

Subsequent sectioning of samples F16 and 17 showed that the silver in the conductors had not melted and only minor erosion of the nickel sheath had occurred. However, while there were no visible holes through the sheath, braze alloy was present near the plugs (in the ends of the conductors) of 2 or 3 strands indicating some kind of pinhole leak. It was suspected that the holes may be at the corners of the conductors and plugs, or in the sheath itself.

A joint brazed with indium alloy (F16) was checked electrically and found to be as good as earlier joints made with Au-Cu braze. It also had a lower resistance than required for the design temperature rise limits.

Sample F14 (Refer Figure 24) was not brazed but was sectioned after plug seal welding the strands and ferrule together. Grain boundary attack observed in brazed samples, from the inside of the strands, was also found in one section of this welded (but not yet brazed) sample. The plug weld seal between conductor sheaths, plugs, and ferrule appeared to be satisfactory. No voids were detected.

Significant observations on some of the other brazed samples were as follows:

Sample No. F19 (Refer Figure 25)

a. Brazed with 5% In alloy at 1700°F; no silver melting observed.

b. Slight erosion (1 mil) of the 5-mil nickel sheathing by the braze alloy near the entrance fillet side, toward the end of the stranding. No erosion detected in other areas.

c. Braze alloy penetration through nickel sheathing grain boundaries into interior strand areas. The grain boundary openings could have resulted from leaching action taking place during desilvering and/or subsequent welding operations, since attack appeared to take place from inside the sheathing. Similar attack evidenced in other samples, although to not as great an extent (Refer to Samples No. F2, F21, F14).

d. Presence of a large weld fault which did not apparently contribute to any of the above described phenomena.

e. No braze alloy was present between four inner conductors (two pairs of adjacent conductors).

f. Some microshrinkage within interstrand capillary areas had occurred.

Sample No. F21 (Refer Figure 26)

a. Brazed with 3.2% Ge alloy at 1780-1800°F. Some melting of the silver conductor materials had occurred.

b. Extensive erosion (4 mils) of the 5-mil nickel sheath directly below entrance fillet. No significant erosion in other areas.

c. Generally excellent braze flow between strands was observed; all interstrand areas were filled with braze material.

d. Some nickel grain boundary penetration from the inside of the strands (not a braze alloy by-product).

e. Braze material was found on the inside of two conductors.

Sample No. F23 (Refer Figure 27)

NOTE: Conductor ends were not sealed in any way on this one sample, as a check on braze temperature control and silver solubility.

a. Brazed with Au 17.1 Ni-5 In at 1700-1760°F. Very slight melting of Ag at ends of two conductors.

b. No erosion, good braze flow to end of conductors.

c. Some braze alloy shrinkage in middle strands, but good fillets and braze flow above nickel cup.

Sample No. F25 (Refer Figures 28 and 29)

a. Brazed with Au-17.1 Ni-5 In at 1720-1750°F using two-turn peripheral coil and 450 k Hz induction heating equipment.

b. Good braze fill between some conductors (refer Figure 28) but not between several at center of the group.

c. At least two conductors showed extensive grain boundary attack inside sheath and on nickel plug (refer Figure 29). No external sheath erosion.

At this point, it appeared more desireable to employ nickel plating the ends of the conductors as the preferred sealing technique (see Section V for details) and to further explore the use of the 450 k Hz power supply and peripheral coil induction heating. Hence brazing development effort followed this path.

A test was also made to qualitatively determine the strength of brazed lap samples prepared with Au-Ni-7 In, Au-20 Cu, Au-Ni-5 In, and Au-Ni-3.2 Ge alloys. Sample joints were made with nickel sheet and

mounted on a stand (as shown in Figure 30) in a vacuum-furnace. Temperature was raised from 1200°F in 25°F increments, holding for five minutes at each temperature. One indium alloy sample (7% In) failed at 1475°F, and the other (5% In) at 1500°F. The sample joint made with the germanium alloy and a gold-copper alloy did not fail at 1600°F, although the nickel softened and bent from the weights at the ends, as shown in Figure 30. The indium alloy appears to have adequate high temperature strength (375°F to 400°F above normal service operating temperatures) although not quite as good as the Ge and Cu bearing alloys).

C. Braze Alloy Development and Erosion Tests

Because of the initial difficulty experienced in developing a satisfactory brazing procedure and in utilizing available brazing alloys, it was concluded that more basic data was needed concerning the erosion of the nickel sheath by the braze alloy, while also determining how to better control the heating to the brazing temperature. Therefore a series of experimental samples for special investigation were prepared using a recess, or dimple, in a piece of 0.002 inch thick nickel foil. Each sample held a small piece of the braze alloy under investigation, and a thermocouple was attached close to the recess to accurately check the temperature. Various times and temperatures were used to evaluate the braze alloys. The results are shown in Table 14. Figure 31 shows the front and back sides of a foil sample with three alloys, after 15 seconds at 1780°F.

Several facts are obtained from the results shown in Table 14.

1. Initial melting of all three alloys (Au-18Ni, Au-20Cu, and Au-16.5Cu-2Ni) was 40 to 80°F above published values. The value shown for Au-18Ni is above the melting point of silver.

2. At only 50°F above melting of the alloys containing copper, erosion of the nickel took place quite rapidly (1 minute).

3. The Au-18Ni produced no erosion of nickel at 100°F above melting, in 15 minutes.

4. The gold-nickel resulted in lowest erosion but its very high melting point makes the joint brazing a potentially dangerous procedure because the silver in the conductors will be molten and flow easily out of any small fracture in the sheath.

It was concluded that the Au-18Ni was the most promising alloy but further investigation was initiated to determine if there was available (or could be developed) another braze alloy that would have a little lower melting temperature, without copper being present.

An extensive review of high temperature braze alloys and various metals that could be added to adjust melting temperatures, along with a study of phase diagrams for different combinations, was made. Based on the lower erosion of thin nickel with a gold-nickel (82 - 18) braze, the work was concentrated on this alloy as the basis for a new tertiary alloy system. For development of the best braze alloy, several specific requirements were established. These included:

1. Flow at a temperature above 1600°F and below 1760°F.

2. Be non-erosive on nickel at the brazing temperatures.

3. Wet and flow between adjacent nickel surfaces for good interstrand braze fill.

4. Produce joints having adequate strength and stability at a 1200°F service temperature.

5. Have a low electrical resistivity, so that resultant joints have low losses.

Several elements, including silicon, boron, carbon, germanium, and indium, were considered as potential additives to an Au-Ni base alloy to act as melting point depressants. (An Au-Cu base was rejected because of Cu erosion on Ni). The preferred elements should adequately lower the melting temperature of the basic material without adding excessive quantities, in order that the inherent properties of the original alloy remain unaffected. Further, it was desirable that the additive exhibit good substitutional solid solubility with the components of the original alloy to avoid formation of low melting phases and possible reduction in braze ductility as a result of intermetallic phase formation.

Boron, carbon, and similar elements were quickly rejected as candidate additives. Their small atom sizes indicated that they would interstitially combine with the braze alloy and on subsequent application to a braze joint would only increase the inherent erosive tendencies because of similar reactions with the nickel parent metal.

Indium additions appeared to have several attractive features; e.g., (1) relatively equivalent atom sizes, i.e., Au-Ni-In, (2) good individual solubility with both gold and nickel, and (3) large reductions in liquidus temperatures of the Au/In and Ni/In binary systems with small increases in In content. Indium has a low elemental melting point

(approximately 300°F) and a high vapor pressure, but because of the excellent solid solubility characteristics and the fact that the new alloy would have a low In concentration, these adverse characteristics were not expected to produce difficulties, so this alloy was considered for joint testing.

Germanium and Silicon additions to the Au-Ni alloy were considered simultaneously in view of the known similarity between these elements. A new brazing material containing these melting temperature depressants appeared promising because it would contain no components with objectionable vapor pressure properties. However, examination of the Au-Ge/Si and Ni-Ge/Si binary phase diagrams revealed the following:

1. Satisfactory solid solubility of both Ge and Si in Ni, but only minor temperature depressant effects.

2. Small quantities of both Ge and Si in Au rapidly depress the liquidus temperatures in those systems.

3. A low melting (<660°F) eutectic phase can be formed in both the Ge/Au and Si/Au systems which could lead to possible incipient melting in a braze alloy containing these elements during exposure at the expected 1200°F service temperature.

4. No solid solubility of Si in Au; thus, if the solubility of Si in Ni were exceeded in an Au-Ni-Si ternary alloy, the maximum possible use temperature becomes 660°F to avoid incipient melting. Ge, on the other hand, exhibits a limited solid solubility with Au (maximum of 1.2% Ge at 660°F). Ge additions were considered superior to Si.

Therefore, silicon additions were rejected, and further study of the Au-Ge phase diagram, showed the maximum solubility of Ge in Au at 1200°F is 0.8%. Projection of this composition to the liquidus line indicated insufficient melting temperature depressant effects, since essentially no reduction would occur in the Ni-Ge system. To achieve the desired depressant effects (reduce melting point of the tertiary alloy to approximately 1700°F) an initial concentration of 1.6% Ge, added to the basic Au-18Ni alloy was selected for evaluations. While that concentration exceeded the allowable limits in the Au-Ge binary system, the presence of approximately 18% Ni in the ternary alloy indicated that such Ge additions could possibly be tolerated.

The initial quantities of the In and Ge containing alloys were prepared on a laboratory scale basis by (1) accurately weighing the necessary amounts of Au-18Ni, and Ge or In constituents, (2) cutting individual pieces of the material into small segments and placing them in an alumina crucible, (3) heating the crucible in vacuum (partial He pressure (15 in. Hg) above the melt for the In alloys to avoid evaporation) to temperatures necessary to completely liquify all braze components, and (4) holding the braze alloy thus formed at temperatures above its melting point for a sufficient time to allow homogenization of the melt before cooling to room temperature.

Table 15 presents the solidus and liquidus temperature for the various braze alloys determined during these tests. Small portions of each braze ingot, produced by the above technique, were applied to 0.002 inch thick nickel foil samples, and tested in vacuum to established braze flow and erosion characteristics. The results are listed in Table 16.

Based on the results of the tests shown in Table 16, a quantity (about 200 grams with indium and 100 grams with germanium) of the alloys used for samples numbers 1 and 7 was prepared. The metals were melted in a water cooled copper cup, by button arc melting, heat treated at 1200°F for 16 hours in argon, forged, and hot rolled at 1000°F to a final sheet thickness of 0.030 inch using multiple 10% passes. The sheets were then sheared to provide strips about 0.080 inch wide and 3 inch long. Using this material, sample joints were brazed and examined as described in Section VI-B (see also Table 12).

Samples were taken from each of the finished braze alloy strips and checked for melting and erosion using the basic test previously described. The results were as follows:

Composition	Heating Cycle	Results
Au-17 Ni-7 In (est.)	1700°F/5 min.	No erosion. However, initial melting occurred at 1500°F, full melting at 1650°F; indicating higher indium (est. 7%) than preferred 5%.
Au-17.4 Ni-3.2 Ge	1700°F/2 min.	Eroded through nickel. Rechecked with another piece; same results.

The above data indicates there had been some change in the germanium filler alloy as compared with the first small laboratory (melted in vacuum) samples, the results of which were indicated by samples 7 and 8 of Table 16.

Meanwhile, other batches of the germanium filled alloy were made, in both large and small quantities. The larger quantity (made in a chilled copper cup with GTA torch heating, processed in inert gas) exhibited the same erosive action as the previous batch. The small

quantity (melted in vacuum) caused no erosion and duplicated the first small laboratory sample results shown in Table 16, samples 7 and 8. A metallographic check of the braze materials indicated a two phase structure (the second phase possibly higher in germanium).

However, in view of the problems with the germanium containing braze alloy and need for further investigation, it was decided to concentrate on the indium filler alloy. Therefore, a quantity of braze alloy was obtained for the final brazed joint development samples and production brazing. Braze alloy wire, 0.035 inch square, to the above composition was purchased to specifications. The quantitative analysis of the wire, compared with the specified composition, was as follows:

		Specified	Actual
Indium	-	4.8 to 5.2%	4.31%
Nickel	-	16.6 to 17.6%	17.36%
Gold	-	Balance	Balance

Two samples of the wire were placed in "dimples" in a 0.002 inch thick nickel sheet about 1/2 inch apart, a thermocouple placed between them, and the assembly heated in a vacuum furnace. This was the same procedure as was followed during development of this special braze alloy. The results from two series of tests of samples from the same wire showed:

Initial melting observed at 1580°F

Material fully molten at 1660°F

Holding the samples at 1700°F for five minutes did not produce any visible indication of erosion or damage to the thin nickel that was

holding the molten sample. The melting point was very close to the value obtained with samples during the braze alloy development.

Finally, to check for possible contamination in the stator due to indium evaporation, a 12.5 gm sample made from the same ingot as used for the braze wire was mounted in a test fixture and the temperature kept at 1200°F in a 15 psi argon atmosphere for 100 hours. The set-up is shown in Figure 32.

Accurate determination of the sample weight before and after the test showed a measured loss in weight of 0.0001%. The evaporation would be less in the actual stator because the surrounding argon gas pressure would be about 20 psia. Also, the exposed surfaces of braze alloy are very small (conservatively estimated at 60 mm^2 per joint) compared with the large area (500 mm^2) for the sample. Thus it was concluded that the quantity of indium which would be evaporated during pump operation will be negligible. A similar test performed in a high vacuum (about 1×10^{-7} torr) showed a measureable weight loss after 350 hours of only 0.001%.

D. Induction Brazing with Peripheral Coil and Nickel Plate Conductor Sealing

All the investigation activity indicated that a peripheral type induction heating coil, operating from a 450 k Hz supply, was more suitable for uniform heating than the focusing inductor with the 3 k Hz supply. To accommodate the unique geometric configuration and arrangement of the production stator winding, a modified peripheral coil (so called "hairpin" shape) was developed. Figure 33 shows the experimental brazing chamber, set-up with the "hairpin" coil.

Because of the strong desire to employ nickel plating as the sealing technique for the production stator, a final series of brazed samples were made to check this approach. Previous brazed samples were made in the small experimental argon purged chamber, shown in Figure 33. In order to braze the production stator in a suitable argon environment, a special vacuum purged dry box, connected to an argon supply, was set-up for all the final stator production brazing but used initially for the final joint samples with full length coils. This dry box was equipped with an oxygen analyzer to monitor atmosphere and an instrumentation feedthru for thermocouple leads to control brazing temperature. The chamber was capable of being pumped down to less than 10 microns before backfilling with argon. It is shown in Figure 34.

The first two sets of brazed sample joints with nickel plate sealing are described in Tables 17 and 18. These were brazed in the chamber shown in Figure 33 with the specially developed Au-17% Ni-5% In braze alloy using "1725°F for three minutes" brazing cycle. Figure 35 shows a cross-section of sample P5. After these were brazed and evaluated, changes and refinements were incorporated into the set-up and brazing technique to improve future brazed joint assemblies.

The next set of brazed samples are tabulated in Table 19, while Figure 36 shows a cross-section of one of those samples, number P9. This sample was brazed in an argon atmosphere, using the set-up and induction coil with the 450 k Hz machine, shown in Figure 34. This general coil design, and specific induction machine, were later used for the production brazing work, with the thermocouple output on each joint arranged so as to control the power applied.

All of the brazed joint samples made during the development work used short length (approx. 4 inch) strands of the nickel-clad silver wire. As mentioned previously, each sample joint consisted of 12 of these short length strands with the ends nickel plated and inserted in a nickel cup to simulate the actual production joints. The nickel cup is about 1/4 inch deep and the braze alloy flow between the strands extends for as much as 1 inch above the cup, providing a strong, high quality electrical joint.

Based on these samples, the basic plating procedure, and the brazing method with Au-Ni-5% In braze alloy using the "hairpin" heating coil and the 450 k Hz power supply, were selected for production. Brazed joints comparable to samples P6, P9 and P11 are typical of what is expected in the production stator. These joints were completely acceptable mechanically and electrically, so full-sized coil samples, which would serve as the brazing procedure qualification samples, were made.

E. Final Brazing Procedure

Before production brazing could be done, several "full-sized" brazed joint qualification samples were made using the final brazing procedure, the final "hairpin" induction heating coil design, and the complete vacuum-purged argon environment dry box set-up that would be used for production. This included all the instrumentation, monitoring and control equipment.

A complete pair (upper and lower) of full size nickel clad silver bars were made for these final brazing qualification trials. Each bar consisted of four conductors of six strands each of 0.073 inch x 0.149

inch wire cross-section. The ends were nickel plated as described in Section V, and then inserted into the "model" stator core. The sample brazes were made in the actual production set-up, shown in Figure 34. Fourteen sample brazed joints (#1 to 14) of full-size trial bars were made. The last seven of these were made on trial bars having exactly the same size and shape of actual production bars and under simulated production conditions. All seven joints were made using the proportioning control equipment to regulate and maintain the brazing temperature below 1750°F, with the production braze alloy. These joints represented the brazing procedure qualification samples and were electrically and thermally checked with satisfactory results.

However, metallographic examination showed some slight amount of nickel plate cracking and silver melting. It was concluded that brazing was done at a slightly higher than necessary temperature and that an initial power surge from the induction heating power supply caused too abrupt an initial temperature rise. Modifications to the power supply were made to suppress this surge and experiments were conducted with 3 short samples (#15, 16, 17) to establish the lowest possible brazing temperature as recorded by the thermocouple attached to the bottom of the nickel cup which was over the ends of the plated wires. The original seven joints were made at temperatures as high as 1735°F as recorded from the thermocouple whereas it was finally determined that a maximum temperature of only 1720°F was required.

Four more representative qualification braze samples with long conductors (#18, 19, 20 and 21) were made under the improved conditions. Finally, two samples (called B1 and B2) were satisfactorily made using

the wire configuration used for the small number of joints on the inside row of the stator on the end opposite the lead seal connections. A copy of one of the temperature recorders/controller charts is included as Figure 37 to indicate a typical cycle and the close temperature control. All these samples were sectioned for metallographic examination. These were satisfactory; no nickel plate fracture and no silver melting, thereby establishing the final brazing procedure. A microphotograph of one of the final samples is included as Figure 38. Significant steps in the brazing procedure and technique are given below:

1. All handling of parts done with white lint-free gloves.
2. All tools, fixtures, clips, and braze wire cleaned.
3. Assemble nickel clips over the ends of a group of coils. Place chromel-alumel T/C on bottom of cup - connect to control.
4. Stator mounted in dry box support, box closed, evacuated to <20 microns, back-filled with pure argon, evacuated and back-filled a second time.
5. Gas purity tester started, along with brazing, and as many joints made as possible with argon purity remaining below 100 ppm.
6. Brazing temperature controlled by proportional control - temperature kept below 1730°F. Preferable total braze time of five minutes.
7. Data on time/temperature of every joint documented. Joints carefully inspected for good fill in cup and at least 1/2 inch up the wire capillaries.

VII. MANUFACTURE OF FINAL STATOR ASSEMBLY

A. Unwound Stator

The unwound stator core consists of a tightly compressed stack of precisely punched magnetic laminations to provide a low reluctance path for the magnetic flux. Each lamination is 0.025 inch thick and contains 24 slots for the stator winding, as shown in Figure 39, an end view of the lamination stack with a trial coil in place. The magnetic material is Hiperco 27 which has a relatively high Curie point (approximately 1600°F) and hence is capable of operation at the temperatures required for the Boiler Feed Pump. Each lamination, after it is punched to closely controlled dimensions and orientation, is de-burred, annealed, and given a plasma sprayed alumina coating, 0.001 inch to 0.002 inch thick, on one side only, to provide interlaminar electrical insulation when the laminations are stacked to form the stator core.

The laminations are stacked to the required stator core length of 10-inch with all winding slots carefully aligned. The two end laminations are special, having 24 steel fingers spot welded to the teeth between the slots, to provide mechanical rigidity and prevent flare when the stator core is stacked and tightly compressed. The compressed stack of laminations are held together by eight carbon steel bars. These bars are rectangular in cross-section and are inserted in shallow grooves spaced uniformly around the outer periphery of the punching stack. The bars were welded at each end to a welding ring which bears on the 24 steel fingers (while the laminations were held compressed under a two ton load) to form a tightly compressed stack of laminations as is

obvious from Figure 39. The O.D. of the assembled stator core was machined to fit in the heat exchanger with 0.004 inch to 0.008 inch diametral interference to provide good heat transfer, the I.D. was machined to 4.402 to 4.400 inch, and each of the 24 slots were filed and completely cleaned to remove all burrs and dirt.

The unwound stator core was then wrapped in a polyethylene covering to keep it in a clean condition until used for the actual stator winding operations.

B. Wound Stator

The wound stator consists of the lamination stack (unwound stator) with slot insulation, and half coils mounted in the slots with their ends brazed together to form the full coils and provision for connection to the power lead seals.

Coil Preparation

Initial effort for the coils involved purchase of nickel clad (20% by area) silver wire in round shape, which was then rolled to the final rectangular shape (0.072 to 0.074 inch x 0.148 to 0.150 inch), annealed in a vacuum furnace and cleaned (vapor degreased). The final wire was placed on 12 inch diameter reels, from which it was removed, straightened, and then formed over hard plastic form blocks in bundles of six wires. Each strand was wiped with a lint-free cloth, moistened with toluene, and the operator used sulphur-free neoprene gloves.

Figure 40 shows the bars (wrapped in mylar sacrifice tape) being formed. Figure 41 shows a completely formed set of four bars (conductors) assembled to provide a half slot of coil sides. Each set of formed

bars was carefully numbered and identified as to position in the slot and stator, and temporarily stored in plastic bags.

The bars (six wires) were then separated at the ends (the center was left taped) with a mechanical spacer, the ends carefully cut square and then beveled slightly with a fine file, ready for plating. The bars were then nickel plated in a preplanned sequence with suitable quality control and inspection, as described in Section V.

After plating, the conductor ends (groups of 6 wires) were taped with "S" 994 glass tape, using a half lap layer arrangement. The taping extended from the point where the ceramic slot insulation would end, to within 1.5 inch of the end of the wires (to allow for the joint brazing). Then four conductors were taped to form a coil side or bar, with one-half lap layer of "S" glass tape.

Coil Assembly

The ceramic slot insulation was then put in place in the unwound stator, and the taped coil sides were carefully inserted. Figure 42 shows the partially assembled wound stator, with most of the bottom coil sides in place. Insulating blocks simulating the upper coil side layer were inserted successively into opposite slots and an expanding fixture was used to moderately press the coil sides to the bottom of the slots. The expanding fixture is also visible in Figure 42.

Insulating blocks were put in all the slots after all the lower coil sides were in place, and an expanding fixture used to press the blocks in all 24 slots. A hipotential test of 1000 V rms was applied between the windings and ground. A turn test using a 500 V DC megger was applied between turns 1-2, 2-3, and 3-4. All tests were satisfactory.

The top coil sides were then assembled in the slots after inserting a ceramic spacer. These coil sides were then pressed into the slots using the expanding fixture and with fiber strips over the assembled coil sides. The same hipotential and megger test (as for the lower coils) was successfully completed. Figure 43 shows the completely assembled wound stator just prior to installing the clips for the end joint brazing. The trial fiber strips were then replaced with carbon steel strips and the expanding fixture used to hold all coil sides in place for the brazing work.

End Joint Brazing

Connection clips, made of high purity nickel, were assembled over the conductor ends for the brazing. The work was done in steps, i.e., inner row, center row, etc., at the rate of about 6 joints per day. Each joint had a thermocouple attached prior to set-up of the wound stator in the support fixture and braze tank. Figure 44 shows the connection end of the stator with half of the joint ends brazed, and the clips applied to the other half of the inner row of joints (before the T/C's were attached).

The stator with the prepared joint clips was placed in the braze tank as shown in Figure 45 before the tank cover was put on the tank base. The argon gas analyzer element is in the rectangular box on the stator support while the braze coil and water lines are in the center under the stator. A close-up view of the set-up with the braze coil ready to be placed around a joint clip (cup) is shown in Figure 46. A close-up of several brazed joints is shown in Figure 47. Note how the braze alloy flows well up in the capillary area between the conductors to provide a very low resistant joint.

Following completion of the coil brazed joints, all joints were insulated with two half-lap layers of "S" 994 glass tape. Figure 48 shows the completed "opposite connection end". Figure 49 shows the connection end after the coil joints were taped and the pole-phase and Y-neutral connections had been brazed but not yet taped.

The completed wound stator was checked finally by replacing the steel strips in the slots with fiber strips and making several electrical check tests. The resistance was measured for all three terminal combinations, a hipotential test of 600 V rms was successfully applied between the windings and ground (frame) and a 800 V peak surge test was applied without any problem. The stator was now ready for final assembly.

C. Miscellaneous Components

Heat Exchanger

The heat exchanger is an integral part of the pump frame and surrounds the stator core. It contains a machined helical passage in the frame, with a wrapper shrunk over the helical passage and welded circumferentially at the ends to the frame, as shown in Figure 1. This provides a hermetically sealed heat exchanger for containing the liquid metal coolant, NaK, which is circulated thru the helical passage to remove the heat conducted from the windings through the stator core. It is designed for NaK to flow in thru a nozzle at each end and discharge thru one nozzle at the center. This provides uniform cooling of the stator winding. The heat exchanger is made of Hastelloy B and is assembled with a shrink fit over the laminated stator core to provide good heat transfer. Its thermal expansion comes close to matching

that of the Hiperco 27 stator core, thereby assuring good thermal contact at all temperatures.

Special GTA welding procedures, using Hastelloy B filler metal, were developed to weld the nozzles to the wrapper, and the wrapper to the frame. The ends of the heat exchanger are butt welded to an end shield and lead seal support ring. The material for these parts is Inconel so a special GTA welding procedure was prepared for making these bimetallic, full penetration butt joints. These welds were made with Inconel filler material. For the production stator these welds were visually inspected, liquid penetrant inspected, and mass spectrometer leak tested. Where practical and meaningful, they were also given a radiographic inspection.

Lead Seals

Each of the three power lead seals or feed-throughs are a hermetically sealed assembly consisting of a 5/8 inch diameter nickel stud thru the center of a ceramic insulator which isolates the current carrying stud, with an Inconel flange to attach the lead seal to the frame. The stud is held by a brazed attachment to a metal flange on one end of the ceramic insulator. The other end of the insulator is brazed thru a connecting adapter to the Inconel flange. This lead seal sub-assembly was a modification of an available standard line of seals and is designed for operation at temperatures up to 750°F with 40 psi differential pressure across it. It was mass spectrometer leak tested and high potential tested to assure its mechanical and electrical integrity.

The lead seal flange is welded to the Inconel lead seal support ring as can be seen in Figure 50, a view of the stator during final assembly. The bottom of each nickel stud has a specially prepared square hole for brazing the nickel-clad silver power extension leads from the stator winding to the stud. This was accomplished by brazing a bundle of nickel-clad silver strands to each stud to provide the transition connection to the windings. The brazing was done using "clam shell" heaters in a vacuum environment with the Au-17Ni-5 In braze alloy. The bundles of nickel-clad silver strands were cut to size, properly formed and shaped, and nickel plated on the ends prior to brazing. After assembling the lead seals in place on the lead seal support ring, the free ends of the bundles of strands were induction brazed to the power leads of the stator winding during the final stator assembly operations. This brazing was done in the vacuum purged dry box with an argon environment, using the Au-17Ni-5 In special braze alloy.

Stator Can and End Shields

The stator can and end shields are made of Inconel. The end shields contain penetrations for thermocouple wells and evacuation tubes. These TC wells are Inconel, furnace brazed with a Au-Ni alloy to the end shields to provide hermetic sealing. The evacuation tubes are soft, pure nickel tubing, TIG welded to the end shields to provide hermetic sealing. These evacuation tubes have a two-fold purpose: (1) to provide a means of mass spectrometer leak testing the complete stator assembly and (2) to provide a means of evacuating the stator cavity and back-filling with argon to the proper pressure.

The Inconel end shields are butt-welded at the outer diameter (using GTA process) to the heat exchanger and lead seal support ring. One end shield has an opening at the stator bore diameter for the stator can. The stator can is 0.018 inch thick and is made from rolled Inconel sheet, which is then fastened with a longitudinal butt seam weld that is done by an automated process. This seam weld was liquid penetrant inspected, radiographically inspected and mass spectrometer leak tested to assure its integrity. The stator can was sized to fit in the stator bore with a slight (0.005 inch to 0.012 inch) clearance at room temperature. The stator can provides radial support for the ceramic insulating wedges in each of the stator slots.

One end of the stator can is sealed by an edge weld to a solid plate at the can I.D. This is made as a sub-assembly. The other end is edge welded at the can O.D. to the end shield I.D. at final assembly to complete the sealed envelope around the wound stator assembly.

D. Final Stator Assembly, Inspection and Testing

After completing the wound stator and preparing the other component parts, the principal steps remaining to assemble the complete stator included the following:

1. Shrink wound stator into heat exchanger.
2. Weld segment of lead seal support ring to heat exchanger.
3. Assemble lead seals in place, hold by tack weld and braze three power leads to lead seal "pigtails". Refer to Figure 50 for a view at this assembly point.
4. Check electrical characteristics.

5. Assemble ceramic wedges above the coil sides and slide the stator can into place in the stator bore.

6. Electrical check.

7. Weld end shield, with stator can opening to heat exchanger, and edge weld can to end shield I.D. A view of this assembly is included as Figure 51.

8. Complete assembly and welding of lead seal support ring.

9. Assemble and weld end shield to lead seal support ring.

10. Complete welding of lead seal flange to lead seal support ring. The lead end of the completed stator is shown in Figure 52.

11. Electrical check.

12. Mass spectrometer leak test complete assembly.

13. Back fill with argon to 7-9 psia.

14. Electrical check.

15. Seal evacuation tubes and prepare for shipment.

The electrical checks and tests above consisted of cold resistance measurement, insulation resistance measurement (megger), high potential testing and surge testing.

In addition to the above, an excitation test to measure winding reactance was attempted. However, this turned out to be meaningless due to the magnetic characteristics of the nickel sheath on the nickel clad silver wire. Nickel is magnetic up to its Curie point of approxi-

mately 675°F. Hence any reactance measurements at room temperature are meaningless and cannot be predicted reliably. The stator winding reactance could not be checked until the unit was placed in operation and brought up to temperatures greater than 675°F. All other electrical checks were satisfactory.

The mass spectrometer leak test verified that the stator cavity was hermetically sealed. The complete stator assembly was properly boxed and braced for shipment to the final assembly area.

VIII. MANUFACTURE OF DUCT

The duct for the Boiler Feed EM Pump was fabricated of T-111 refractory alloy. It has bi-metal joints attached to the inlet and outlet pipes to permit exposed (to atmosphere) connections to the stainless steel facility piping. The work involved careful specification and procurement of the various sizes of T-111 alloy, machining of the helix, development and assembly of the bimetal joints (T-111 to Nb-1Zr to type 321 stainless steel), welded assembly of the duct parts, and application of Nb-1Zr foil for thermal insulation.

The material selection, fabrication, assembly, thermal insulation, and final check-out, will be covered in this section of the report.

A. Material Selection and Procurement

The major material procurement effort involved the T-111 alloy, due to the large sizes and difficult manufacturing processes. Therefore, this item will receive major attention in this part of the report. The other materials used in the duct (Nb-1Zr and stainless steel) were readily available, but procured under careful control.

1. T-111 Alloy Procurement and Quality Control

A summary of the T-111 alloy mill products required for the Electromagnetic Pump Development Program is shown in Table 20. The three groups of alloy items indicate the way the material was obtained from three different vendors. It was originally intended to use 1.5-inch diameter bar for the Group II, T-111 alloy items, but tubes with a 0.100-inch wall tube were successfully obtained.

To assure high quality T-111 alloy products, all items were ordered to NASA approved specifications, developed on another NASA program (Reference 9) and covered by the GE-NSP specification shown in Table 20. Then, vendor processing procedures were reviewed and monitored, and "in-house" quality assurance was performed on samples from each lot of T-111 alloy. Each of these phases of quality control, procurement, and test are discussed below.

a. T-111 Alloy Material Specifications

All T-111 alloy mill forms were ordered to the specifications listed in Table 20. The vendors had agreed to produce T-111 alloy products according to all the stipulations of the appropriate specifications except as noted below.

Table 20 - Group I (Hollows: >3-inch-diameter bar)

Exception was taken to hydrostatic and flare test requirements and the total mechanical percent reduction of 75 percent. The hydrostatic and flare tests were waived because relatively low stresses are expected in the intended application for these large diameter hollows and because ultrasonic inspection was deemed sufficient for insuring material integrity. The 75 percent total mechanical reduction requirement is specified to insure proper final product grain size. However, the vendor guaranteed that the grain size of the final product would meet the specifications, and they demonstrated that they could produce the required grain sizes using lower total reductions; therefore, the 75 percent reduction requirement was waived.

Table 20 - Group II (1.5-inch OD x 0.1-inch wall tube)

The vendor agreed to supply the tube in accordance with the

applicable specification 01-0035-01D except in the following requirements: Annealing, ingot chemistry, hydrostatic and flare tests, stress rupture, surface condition, ultrasonic defects, and method of inspection.

Approval was given for the tubes to be annealed at a maximum pressure of 3×10^{-5} torr with the condition (as stated in the specification) that the tubes be completely wrapped in Nb-1Zr foil with no surfaces exposed to the vacuum furnace environment. The vendor would only report on analysis per ingot and guarantee maximum hydrogen content of 15 ppm, while taking exception to all the final product interstitial elements.

Also, they would not guarantee stress rupture requirements. The stress rupture requirements were waived because, based on previous experience, T-111 alloy tube processed in accordance with the specifications would meet the required minimum rupture life. GE-NSP quality assurance detailed testing confirmed that the tubing met the conditions for both minimum rupture life and external and internal surface integrity.

b. Material Processing

T-111 refractory alloy has adequate properties and corrosion resistance to satisfy all the EM pump duct design requirements. It was mandatory, however, that adequate control be exercised over the production of T-111 alloy to assure that the necessary quality requirements were met. Because of the lack of extensive commerical experience in the production of T-111 alloy, a thorough knowledge of its processing history was

important. The influence of processing history on the properties of refractory alloys has been described (Reference 10) and demonstrated.

The control and documentation of material histories for this program required close cooperation with the producers. All critical processing parameters and procedures, such as percent of reduction between the final anneal and the previous recrystallization anneal; percent total reduction; final annealing temperature; conditioning procedures prior to final anneal; and annealing environment were checked and approved. This information was reported along with the certificates of test, and this type of information was an important aid in assuring maximum reproducibility of the products.

There was considerable variation among vendors regarding the nonproprietary T-111 alloy processing information that each vendor was willing to furnish. Furthermore, because of the sizes involved (such as the large tubes), new techniques had to be developed to obtain the proper reductions (mechanical working), ultimate required grain sizes, etc. The data in Table 21 gives an indication of one phase of the problem, involving the large tube.

c. Quality Assurance and Internal Documentation

Gaining the maximum utilization of the data obtained from this program demanded that the quality assurance procedures be reliable and strictly enforced. This insured documentation of the history and integrity of the pretest materials. The quality assurance tests conducted on T-111 alloy by the primary producer and/or by GE-NSP are listed in Table 22. Test certificates for all the T-111 alloy items were submitted by the vendors. As a further control on the quality of

incoming T-111 alloy material, a quality control check was made of the chemical composition of the interstitial elements, O, C, H, and N and the metallurgical structure of samples from each lot of material.

d. T-111 Alloy Procurement History and Problems

As part of the purchase specifications, the T-111 vendors were required to submit production milestone schedules for all items, shortly after receiving the orders. The schedules were updated periodically, and a close check of the quality and delivery of T-111 items was maintained through numerous phone contacts and periodic visits to both vendors' and their subcontractors' facilities. Some delays were encountered during inspection of materials, such as the large diameter (>4 inches) T-111 alloy items, as they had never been ultrasonically inspected before to the specifications, and development effort was required to master the techniques necessary to adequately inspect these items.

Other problems involved the "debugging" of new melting and annealing facilities for the bars, and difficulty in qualifying one vendor's new vacuum annealing facilities. For this qualifying, GE-NSP furnished T-111 alloy coupons (0.040 inch thick sheet) bare (unwrapped) and wrapped with refractory metal foil for trial annealing. Both wrapped and unwrapped coupons showed a low level of contamination resulting from the annealing treatment. However, because the furnace pressure exceeded the 1×10^{-5} torr minimum pressure allowed by the specification for annealing T-111 alloy bar, the vendor was required to wrap all items for final anneals.

e. T-111 Alloy Quality Assurance Test Results

All T-111 alloy materials used on this program passed vendor testing and "in-house" quality assurance.

Photographs of the as-received tube hollows used for the pump wrapper and wrapper extension are shown in Figure 53, photographs of the hollows used for the helix and helix extension are shown in Figure 54. Vendor analysis of major T-111 alloy ingots are shown in Table 23. Analyses of all elements except for C, O, H, and N are considered the final product contents. Except as noted in Table 23, all ingots met the composition requirements.

The final product mechanical properties of the major T-111 alloy mill forms satisfied all vital specification requirements, and are listed in Table 24. "In-house" chemical and metallographic results for the items that were used are shown in Table 25. Except as noted, the items met all NASA approved specifications.

2. Nb-1Zr Foil for Thermal Insulation

The duct thermal insulation was made from Nb-1Zr alloy foil 1/2-inch wide by 0.002 inch thick, dimpled and applied like tape to form a series of layers.

A summary of the Nb-1Zr alloy foil needed for this program is also shown in Table 20. Because Nb-1Zr alloy foil can be processed conventionally and its processing practices are relatively well established, no significant procurement problems were encountered, and all material was purchased to the NASA approved material specifications.

The first Nb-1Zr alloy foil material ordered for the program was rejected because of extremely high interstitial content in the final

product. The second shipment of Nb-1Zr alloy foil was within specification and suitable for the intended application. The results of the chemical analysis of the rejected material, and the material subsequently used, are summarized in Table 26.

B. Fabrication of Duct Parts

General

All parts, except the T-111 pump duct, were made with normal machining techniques, i.e., turning, boring, drilling, honing, milling, etc. The T-111 pump duct, however, has a variable pitch helix and this required special planning and machining techniques. All machine work was done in accordance with best shop practices and inspected. Final dimensions, surface finish, etc. were checked and the results documented. Various finished parts are shown in Figure 55.

1. T-111 Duct Helix

The initial phase involved machining the duct blank from the forged bar, the duct extensions from tubing, welding the extensions to the duct blank, and then finish machining of the I.D. to specified dimensions.

The spiral fin on the pump duct was produced on a "die sinking" lathe. This machine differs from a conventional tracing lathe by using a cylindrical rotating master rather than a flat template master. The master was made by accurately drilling a series of holes, in an aluminum tube, 90° apart along the path of the spiral, inserting pins in the holes, laying a 3/16 inch aluminum wire coil against the pins and dip brazing the assembly. The pins were then removed and the master was complete.

The duct blank and extension assembly was mounted on a "relieved step" arbor and the cavity filled with cerrolow matrix to provide a solid back-up to reduce chatter. The compound was set at 90° to the cross slide to provide longitudinal feed with hydraulic tracer. Since the length of travel on the tracer feed was only 4 inches this had to be combined with mechanical feed. The feed box was set at two threads per inch which provided 0.500 feed and the tracer provided the remainder, as well as the change in pitch and the smooth transition between the two pitches. In order to provide better control and reduce operator fatigue the decision was made to mill the spiral rather than "chase" it. A precision heavy duty flexible shaft was mounted on the compound. The other end was fastened to a speed reducer which was driven by a 1 hp motor.

The cutter was set to turn at 494 rpm (18 SFPM) and the lathe spindle was turning 1 rpm giving a tooth chip load of about 0.006 inch. The increased power input due to the low speed of the flexible shaft caused the bearings to deteriorate and excessive vibration developed.

Before resuming the machining, the milling set-up was further modified. A precision cartridge quill was mounted on the lathe and the speed reducer was mounted above it. The spindle of the quill was driven by a posidrive belt from the speed reducer and the flexible shaft drove the speed reducer from the motor. This set-up was virtually vibration-less and vibration occurred only when the cutter dulled. This was some-what desirable since it provided a warning that tool sharpening was required.

The cutting fluid used for the machining of the spiral was Chloronol. It was not possible to obtain a smooth surface finish in the machining operation since cutting was done by the side of the end mill. This left a slightly "corrugated" finish which was "benched" out after machining was completed, with a fine file and abrasive cloth. The finished T 111 duct helix is shown in Figure 56.

2. Other Duct Parts

The balance of the parts required for the duct involved well known machining techniques. However, special care was taken to obtain a suitable set of spring washers to provide the pressure to keep the duct core securely in place, even at the maximum off-design temperature of 1400°F potassium.

The wavy washers were made of Rene' 41, annealed, formed, and solution heat treated at 1950°F for 30 minutes. The resulting spring washers were 0.015 inch thick. A total stack of 6 washers provided the required initial force of 25 pounds (room temperature) and a maximum deflection of 0.060 inch, with a maximum of 10% relaxation at 1000°F, over the planned test period of 10,000 hours.

3. Duct Inlet and Outlet Transition Pipes

The boiler feed EM pump duct was constructed of T-111 alloy, whereas Type 321 stainless steel was utilized for the test loop piping material. Tubular transition joints between those materials were required in the inlet and outlet pipes external to the basic pump duct. The method selected for fabricating those transitions involved the usage of intermediate Nb-1Zr members to provide assemblies having optimum reliability characteristics. The general assembly technique entailed (1) the joining

by GTA welding, of T-111 tube segments to one end of the intermediate members, using Nb-1Zr filler metal, and (2) the vacuum brazing of the opposite Nb-1Zr component ends to Type 321 stainless steel pipe segments, using the cobalt base braze alloy designated J-8400.*

This technique was chosen because of considerable experience in the brazing of Nb-1Zr to stainless steel tubular joints for elevated temperature/alkali metal applications (Reference 11). Such brazed joints were shown to be structurally sound and metallurgically stable after various cyclic and long term elevated temperature exposures (to 1800°F and times up to 5000 hours) in the presence of alkali metals. Further, welding of Nb-1Zr to T-111 with Nb-1Zr filler metal has been demonstrated to produce thermally stable weldments after 2400°F/1 hour postweld annealing treatments (Reference 12) and that overaging heat treatment produced T-111/Nb-1Zr welds which were ductile at temperatures to -100°F, even after exposure to time/temperature conditions which tend to cause embrittlement in unannealed Nb-1Zr welded structures (1500°F/50 hours).

A tongue-in-groove design was selected for the Nb-1Zr/Type 321 stainless steel EM pump transitions, since that basic configuration had been successfully used in the construction of previous bimetallic joints. Before actual fabrication of the inlet and outlet pipes was initiated, several evaluation tests were conducted on representative tongue-in-groove sample brazed assemblies. These laboratory controlled tests were used to confirm the stability and load capability of the

*J-8400 Braze Composition: 21Cr-21Ni-3.5W-8.0Si-0.8B-0.04C-Bal. Co

sample brazements at the temperature levels expected at the inlet and outlet pipes during operation of the Boiler Feed EM Pump. The design and fabrication of the inlet and outlet transition assemblies, and descriptions of the supporting evaluation tests and results obtained, will be further indicated in ensuing paragraphs.

Design of Bimetallic Joints

The tongue-in-groove design configurations of the Nb-1Zr/Type 321 stainless steel transition (bimetallic) joint for the inlet pipe (the outlet pipe is of similar design) is depicted in Figure 57. As indicated previously, bimetallic tube joints of various sizes between Nb-1Zr and stainless steels have been successfully fabricated for use in alkali metal containment systems. In these earlier assemblies, the refractory and nonrefractory alloys had generally equivalent wall thicknesses, and tongue-in-groove designs were used in their construction. The tongue members were usually stainless steel, whereas those in the EM pump joints were machined from Nb-1Zr alloy. This reversal in design was initiated to (1) most readily accommodate the large differences in wall thickness between the stainless steel loop piping and the T-111 alloy duct piping, (2) provide joints having optimum braze flow and fill characteristics, and (3) provide a joint which could be most readily machined; i.e., the groove in stainless steel is less difficult to machine than a similar operation in Nb-1Zr alloy.

The outside diameters of the tongue and groove components were selected to produce an interference fit in that area during assembly for brazing; conversely, the inside diameters were set to diametrically separate the components approximately 0.02 inch at room temperature

assembly. These dimensions were required because the coefficient of thermal expansion for stainless steel is considerably greater than that for Nb-1Zr (α = 11 x 10^{-6} in/in/°F vs. α = 5 x 10^{-6} in/in/°F.) Therefore, the initially tight fitting outside diameters were desireable to minimize spacing in that area when assemblies were heated to the brazing temperature (2160°F). Further, the inner annular spacing was required to allow the relative motion of the refractory and nonrefractory metal components to take place during heating to the brazing temperature. Allowances were also made in the calculated initial inside diameters to produce the desired annular brazing gap (0.001 to 0.002 inch) at the 2160°F brazing temperature.

Bimetallic Joint Evaluation Testing

Two Nb-1Zr to Type 321 stainless steel trial joints, having dimensions in the tongue and groove area as shown in Figure 57, were brazed at 2160°F for 5 minutes in vacuum with the J-8400 braze alloy. Postbraze helium mass spectrometric leak testing, visual examination, and radiographic inspection of both joints indicated excellent joint characteristics; i.e., leak tight and good braze flow through the filleting. The first of these sample joints was fabricated to assist in evaluating the assembly procedures of the Nb-1Zr/stainless steel brazed joint. The second specimen was prepared to confirm the elevated temperature load carrying capability of the tongue-in-groove brazed joints. This tensile specimen after brazing is shown in Figure 58.

The initial sample joint was cut into four segments, one of which was prepared for microstructural examination in the "as-brazed" conditions. The second segment of the initial sample and the bimetallic tensile

specimen was exposed to the following thermal treatments:

1. Thermal stability test - heat to 1500°F in vacuum and hold for 100 hours;
2. Thermal cycling test - cycle between 1000°F and 1500°F ten times, one cycle every 40 minutes.

The third segment of the first specimen was exposed only to the thermal stability test, whereas the fourth segment was thermal cycled only. The effects of the thermal exposure, on the metallurgical stability of Nb-1Zr/Type 321 stainless steel brazements, were determined by microstructural examination and comparison of the four segments of the first sample.

Excess braze alloy on the outside Nb-1Zr surfaces of the bimetallic tensile specimen, immediately adjacent to the braze fillet, was removed before the joint was exposed to the above heat cycles. The OD of the Nb-1Zr component was machined to remove 0.005 inch of material (radial measurement) from the edge of the braze fillet to the end of the specimen. This action was taken because (1) the major quantity of plastic deformation under axial stressing was expected to occur in the Nb-1Zr component, (2) the coefficient of thermal expansion for the J-8400 braze alloy is approximately three times that of Nb-1Zr, and (3) of the basic hard, non-yielding nature of the solidified braze alloy. Therefore, as deformation of the Nb-1Zr member occurred, either on axial loading or thermal cycling, the unsupported braze alloy on the specimen surfaces would also have to yield or craze locally to relieve the induced stresses. Such surface crazing would be undesirable in a tensile test specimen.

Examination of the thermally cycled tensile test sample by helium mass spectrometric leak testing, radiographic and ultrasonic inspection, and visual examination (10X), prior to tensile testing revealed no failure or joint degradation. The specimen was then instrumented with Pt/Pt-13Rh thermocouples for the tensile test.

The bimetallic tensile specimen was axially stressed in a vacuum capsule rupture test stand. The specimen was heated to 1500°F in six hours and the temperature stabilized before application of load. This time/temperature cycle was necessary to maintain pressures within the vacuum capsule at less than 5×10^{-5} torr. Load was subsequently applied in 400-pound increments, every 30 seconds, until yielding occurred. Deflections were measured by a dial indicator guage (0.0001 inch scale graduations) in contact with the specimen load train. The resultant load versus deflection curve for the test is presented in Figure 59. Maximum applied load was 6120 pounds, corresponding to a stress of 19,000 psi, based on the original Nb-1Zr wall thickness. The total quantity of plastic deflection produced by this load was 0.060 inch. Measurement of the test specimen, after removal from the vacuum capsule, indicated a 0.004 inch reduction in the Nb-1Zr outside diameter next to a brazed joint. However, the sample was still leak tight, as shown by helium mass spectrometry leak testing, and no visible evidence of braze fillet cracking was present.

A requirement of the pipe transitions in this EM pump service is that they withstand an internal pressure of 350 psi at 1500°F. Assuming sound, complete flow-through, brazed assemblies, the hoop stresses present at the brazed joints are no greater than the circumferential stresses

associated with the individual Nb-1Zr and Type 321 stainless steel components; thus, no joint failures under the action of this type of stress would be anticipated. The 350 psi internal pressure converts to an axial load of 500 pounds, based on the cross sectional area of the inlet pipe stainless steel component. This load will produce an axial stress in the Nb-1Zr components (1.5 inch OD x 0.1 inch wall) of 1140 psi. A comparison of this value with the 19,000 psi, necessary to cause yielding of the tensile specimen, demonstrates the wide design margin and inherent reliability of the braze joint design from the standpoint of axial strength.

Typical microstructures of the "as-brazed" segment of the initial braze sample are shown in Figure 60; representative microstructures of the thermally exposed segments are presented in Figure 61. As shown in these figures, there was an intermetallic phase formed at the braze/Nb-1Zr interface during brazing, which was unaffected by subsequent thermal treatments. As a result, no evidence of change was found in the Nb-1Zr base metal. Further, some penetration of the stainless steel by brazing alloy constituents also occurred during brazing, but the temperatures and time used in thermal stability testing were not sufficient to promote additional reactions. From the results of the post-thermal exposure testing of the tensile specimen, it is apparent that the occurrence of the indicated metallurgical reactions, during brazing, did not reduce the resistance to failure of the tongue-in-groove joints when exposed in the 1000-1500°F temperature range.

Fabrication of Transition Pipes

The T-111/Nb-1Zr/type 321 stainless steel inlet and outlet pipe transition parts were fabricated and inspected to assure compliance

with important diameter tolerances. The T-111 alloy tube was GTA welded to the Nb-1Zr transition pieces, using Nb-1Zr filler metal. The inside and outside diameters of the transition pieces were undersize and oversize, respectively, to allow for machining after welding to produce the required brazing fit-up dimensions, thus avoiding any weld distortion problems.

Radiographic and visual inspection was made of each weld, they were vacuum annealed at 2400°F/1 hour, and then the Nb-1Zr ends of the welded assemblies were machined to the configurations. The type 321 stainless steel tubing was machined to provide matched sets for brazing.

The components for a transition joint were assembled and vacuum brazed. Nondestructive inspection was made to determine the integrity of the brazed assemblies, using ultrasonic inspection, radiographic inspection, dye penetrant inspection, helium mass spectrometer leak testing, and binocular visual examination.

Both transition assemblies for the pump were fabricated and inspected, as described, and found satisfactory. The completed inlet and outlet pipe transition joints are shown in Figures 62 and 63. The T-111 ends of each assembly were subsequently GTA welded to their respective locations on the EM pump duct and the welds locally annealed at 2400°F for one hour in vacuum.

C. Fabrication of the Duct and Shroud Assembly

The duct and shroud assembly consists of the T-111 alloy EM pump duct, transition pipes and a stainless steel protective shroud for

joining to the stator. Transition from T-111 alloy tubing of the duct to the stainless steel tubing of the facility is accomplished with the brazed stainless steel to Nb-1Zr alloy tube joints in the inlet and exit lines. A laminated Hiperco 27 core is located in the annulus between the helical duct and center return tube, held in place by a spring loaded retaining sleeve held in by a snap ring that engaged with the T-111 duct.

Design and Manufacturing Considerations

Prior to the manufacture of the T-111 EM pump duct, GE-NSP had built a number of Nb-1Zr and T-111 ducts, but with relatively thick walls, and with the inlet and exit pipes parallel to the helical duct axis. In contrast, this pump duct had the inlet pipe at 90° to the axis, and a much longer inlet annulus, so the overall length of the helical duct was 24 7/16 inches. Therefore, the duct helix and duct wrapper had to be fabricated from two tube blanks, because of limitations in available ingots.

The diameter of the helical duct extension was made larger than that of the duct to avoid interference of weld metal with the iron core and retainer sleeve. Because of possible distortion from welding of final machined parts, the helical duct blank was welded to the duct extension blank prior to final machining.

Manufacturing Planning

Before starting fabrication, operational steps in fabrication of the T-111 pump duct assembly were defined in detailed manufacturing instruction. To insure minimum leakage across the helical fins, it was standard practice to "interference fit" the duct wrapper onto the helix.

For T-111 and Nb-1Zr alloy ducts an interference of 0.001 to 0.002 inch is desirable. The finished wrapper wall thickness of this EM pump duct was 0.06 to 0.07 inch. Therefore, to obtain such a thin wall, 0.35 inch was added to the wrapper OD and duct end cap diameters to add rigidity for internal machining and then the final OD (and wall thickness) was obtained by machining after the shrink-fit procedure.

Process drawings were prepared to manufacture all the sub-assembly parts in a carefully planned sequence. The order of assembly for the T-111 duct was as follows:

1. Weld helical duct blank to the duct extension blank.
2. Weld center core retainer and duct cap to the center return tube.
3. Weld inlet tube to wrapper extension on ID.
4. Insert center tube through helical duct and welded duct cap to the duct with a centering ring at the opposite end.
5. Slip wrapper extension over the duct extension and weld duct outer cap to duct extension.
6. Tack weld duct extension to duct outer cap.
7. Shrink fit wrapper on the helical duct.
8. Weld duct end cap, wrapper, wrapper extension, and duct outer cap together.
9. Machine duct OD to size.

Cleaning and Inspection of Parts

All machined parts were dimensionally inspected to drawing

requirements by both the machining vendor and GE-NSP quality control. There were no significant deviations from the drawings. Critical dimensions were the diameters, roundness and straightness of the duct wrapper and helical duct to provide for a good interference fit.

After machining and dimensional inspection, all T-111 parts for the duct were vapor degreased with trichlorethylyne and then fluorescent penetrant inspected for surface flaws. All indications were considered revelant and the areas "benched" with very fine files. No cracks, tears, or other defects were found. Indications of defects were proved to be machining marks and scratches.

After liquid penetrant inspection, the parts were again vapor degreased to remove inspection residue. Finally all parts were chemically cleaned in a solution of 1 part hydrofluoric acid, 4 parts nitric acid, 1 part sulfuric acid, and 2 parts water by volume. After cleaning, the parts were stored in clean polyethylene bags until ready for loading in to the welding chamber.

Welding Procedures and Process Control

The T-111 pump duct was completely welded by the GTA process in a vacuum-purged, helium-filled, stainless steel chamber evacuated by a mechanical vacuum pump, a vacuum blower, and an oil diffusion pump to 1×10^{-5} torr. Leak rate was less than 5 microns per hour. Welding was done with a water-cooled torch.

Helium gas was analyzed for oxygen, nitrogen and hydrocarbons by gas chromatography and for water vapor using an electrolytic hygrometer. Inlet helium passes through a purification train to remove residual oxygen and water vapor. During a welding cycle, chamber helium is

continuously monitored for water vapor, and for oxygen and nitrogen at the start, finish, and at one hour intervals.

Welding of the duct was done to the strict requirements of NASA approved specifications for welding of Niobium, Tantalum, and Their Alloys by the Inert Gas Tungsten Arc Process. Chamber atmosphere was monitored to specification requirements. Prior to and after the welding cycle, T-111 quality control sheet specimens were welded. Process control records were completed for each welding cycle and the quality control specimens retained for future reference. Approved T-111 alloy wire was added to the joints as required.

In-Process Inspection

During assembly of the T-111 duct, three types of inspection were utilized. Visual inspection was made of welded joints and machined surfaces using magnification up to 50X. Containment welds were radiographically inspected, using an Ir-192 gamma source, and the radiographic films were examined for weld quality.

Containment welded subassemblies were checked for leaks using a helium mass spectrometer leak detector, and completed assemblies were similarly checked. No detectable leakage at maximum sensitivity of the leak detector (1×10^{-10} std cc/sec of air) was permitted.

Helical Duct Blank

The helical duct tube blank and the duct extension blank were joined together so that the entire helical duct could be machined as one piece as described in Section VIII-B. A boss was machined on one end of the helical duct tube blank to match the duct extension blank (0.13 inch wall). The mating edges were beveled to provide a 90° single V-groove joint.

The two pieces were GTA welded together to specifications. After welding and minor straightening the concentricity and straightness of the assembly was concentric with the duct blank within 0.010 inch, which was acceptable for machining.

The weld was dye penetrant inspected, helium leak checked, and radiographed for soundness. No defects were detected.

Assembly of the Duct

Machined parts for the duct are shown in Figure 55. They include the duct end cap, duct wrapper, wrapper extension, duct outer cap, helical duct, duct cap, and retainer on the center return pipe. The inlet and outlet transition pipes are not shown.

The first assembly was the core retainer ring and duct cap to the center return pipe. The retainer ring was fillet welded in its correct location. Then the duct cap was welded to the end of the center pipe. After welding, the total runout of the cap was 0.022 inch and squareness with the pipe was satisfactory. The subassembly was helium leak checked and the welds were checked by radiography for soundness. The subassembly met specification requirements.

The next subassembly was the inlet transition pipe to the duct wrapper extension. The pipe had to be tangential to the wrapper extension. The two machined parts did not mate exactly and hand fitting was done to obtain desired relative position. The two parts were welded together around the ID junction only at this time. (Later a weld pass was placed around the outside). The weld was visually inspected and benched smooth.

The center return pipe was inserted through the ID of the helical duct, and the duct cap was aligned with the helical duct. A plug was used in the opposite end of the duct to center the pipe. Then the cap was welded to the duct, the weld radiographed, and the subassembly helium leak checked. It was sound and no leak could be detected.

The helical duct with center pipe is shown in Figure 64. Close-up of the duct extension with the center return pipe is shown in Figure 65.

The next step involved the installation of the duct outer cap and wrapper extension. The wrapper extension was slipped over the duct extension against the helix. Then the duct outer cap was welded to the helical duct extension and radiographed. The wrapper extension was aligned with, and tack welded to, the outer cap in four places to hold it while shrink fitting the wrapper on the helix. Concentricity of the wrapper extension and cap was satisfactory.

The duct wrapper and helical duct had been machined with approximately 0.002 inch interference, except for a 3/4 inch long relief on the wrapper ID. This relief allowed greater clearance between the parts at the start of the shrink fit operation. The helix was carefully deburred and the corners on the wrapper ID were beveled. Both parts were chemically cleaned.

For the assembly, the helical duct was submerged in a thermos of liquid nitrogen (-320°F) for about 2 hours. The change in temperature (about 390°F) reduced the helix diameter about 0.005 inch. The helix was withdrawn from the liquid nitrogen and the wrapper (at room temperature) was dropped over the helix against the wrapper extension.

After tack welds between the wrapper extension and outer duct cap were broken, the wrapper extension was aligned so as to be concentric with both the wrapper and cap. The assembly was placed in the welding chamber and three girth welds were made between wrapper, wrapper extension, and both end caps. First, the wrapper extension was welded to the wrapper. Second, the wrapper extension was welded to the outer cap. Third, the end cap was aligned with the wrapper and welded to it. Finally, the inlet tube was welded to the wrapper extension on the outside. The assembled T-111 pump duct is shown in Figure 66.

Final Machining of the Duct

The OD of the helix had been left oversize to provide thicker walls for machining and assembly. A projection had been provided on the end cap to accept a lathe center for machining the duct OD. Indicating from the wrapper OD, a center was machined in the end cap projection.

The pump duct OD was then machined to drawing dimensions across the duct cap and wrapper, and the cap projection was then cut off, completing the T-111 duct assembly. It is shown in Figure 67, ready for final inspection and the anneal operation prior to insulation and attachment of the transition joints.

Quality Insurance Inspection

After final machining, the pump duct was visually inspected. It was also thoroughly and carefully checked for any leakage, internal and external, using a calibrated helium mass spectrometer leak detector. The leak detector was attached to one tube and a calibrated leak placed in the other tube. The duct was evacuated of air. Time delay for helium introduced through the leak to reach the leak detector was

recorded. With the calibrated leak capped, the entire duct was enclosed in a helium filled plastic bag. No leaks were detected. Then the leak detector attachment and calibrated leak were switched on the duct tubes and the leak detection procedure repeated. Again no leaks were detected.

Post-Weld Vacuum Anneal of Duct

The T-111 duct was wrapped in Nb-1Zr foil with a 0.040 inch T-111 sheet quality control specimen under the foil. Foil spot tacking was done with a molybdenum tipped electrode. The duct was vacuum annealed at 2400°F for one hour in a qualified refractory element vacuum furnace. After annealing, the Nb-1Zr foil was removed, and the T-111 quality control sample was made a part of the process control records. The duct was again checked for leaks with the helium mass spectrometer leak detector as described previously. A leak was now indicated in the center cavity of the helical duct. The leak rate was about 5 x 10^{-7} std cc/sec of air indicating that the leak was very small.

Repair of Internal Leak

It was then necessary to determine the location of the leak. First, the T-111 center return pipe was shielded from helium by placing another tube over it with an alcohol seal at the bottom of the cavity. The leak was still present when helium was directed into the cavity showing that it was in the machined helical duct section.

To determine accurately the leak location, the duct was placed in a vertical position and the interior was attached to the leak detector. With helium directed into the cavity, the leakage was indicated on the leak detector. Alcohol was then slowly added to the cavity until the

level rose to the point where it covered the leak as indicated by a sudden decrease in leakage reading. The leak was thus determined to be somewhere on the circumference of the duct in the vicinity of the weld originally made between the helical duct and duct extension tube blanks at a distance of 9.02 inches from the face of the duct outer cap. The leak was not in the helix zone and was thus repairable without disturbing the interference fit, but the wrapper extension had to be removed in order to uncover the leak.

The pump duct was mounted in a lathe and the wrapper was parted 9 5/8 inches from the outer cap face. Then the outer cap was cut through from its face on a 3 5/8 inch diameter. A V-shaped "parting" tool was used to produce a weld groove for the subsequent re-assembly. This freed the wrapper extension which was slipped off the end, exposing the duct extension. Figure 68 shows the duct assembly after the wrapper extension was removed. Suitable marks were used to simplify repositioning the wrapper extension in the original location after the leak was corrected.

A leak check fixture was made to fit over the center return pipe and seal against the end of the duct with an O-ring. This provided means for evacuating the interior of the duct, and leak checking again, but it failed to now reveal any indication of leakage. (Similar behavior had been observed in other T-111 parts. Apparently there existed a minute intergranular defect causing leakage, and relief of residual stress or application of local stress would permit the leak to close).

In order to make the leak reappear, the duct extension area was heated to 1000°F in the vacuum purged welding chamber at 10^{-5} torr pressure. An all refractory metal, clam shell type heater was used. Subsequent leak checking revealed leakage, and careful probing with a helium stream pinpointed the location as shown in Figure 69. Figure 70 shows an enlargement (about 40X) of the circular scribed area indicated in Figure 69. There appeared to be a grain boundary separation, covered during welding and/or machining, that propagated through the wall during vacuum annealing of the completed duct.

The defective area was carefully "benched out" by filing a circumferential groove about 0.05 inch deep by 1 inch long in the duct wall. A full penetration weld was made across the grooved area as shown in Figure 71. The repaired area was then "benched" flush with the duct OD. It was carefully examined visually and radiographically for soundness, and the duct thoroughly helium leak checked. It was completely tight.

The T-111 duct wrapper extension, which had been removed, was repositioned on the duct. It was welded to the wrapper on the OD. Then the end cap was welded back in place. Overall views of the repaired T-111 duct assembly are shown in Figures 72 and 73. The wrapper weld was radiographed for soundness. The duct assembly was again helium leak checked and proved to be leak tight.

Close visual inspection of the new welds, and surfaces near them, at 30X with binoculars showed several grain boundary separations and checks in the machined areas. The locations are indicated in Figure 73 as A, B, and C. There appeared to be machining tears and microcracks

in some parts of the welds, or in the heat affected zone between the two welds. These imperfections were carefully benched out using a fine grinding wheel. Machined surfaces were hand filed and polished with 400 grit emery cloth until the checks were no longer visible with 30X binoculars. They were actually very shallow, perhaps one or two grains deep. Similar conditions have been observed in other machined T-111 alloy parts adjacent to fusion welds.

The repaired T-111 pump duct was wrapped in Nb-1Zr foil and again post weld vacuum annealed at 2400°F for one hour in the same equipment used for the first anneal. Great care was exercised to control heating rate to insure uniform temperature throughout the part. The annealed pump duct was then carefully and thoroughly helium leak checked, and it was completely tight.

Installation of Core and Bimetal Joints

The core, springs, retainer sleeve, and snap rings were successively installed in the center area of the duct after removing a slight oversize area on the core and shortening the retainer to compensate for changes due to the rework on the duct wrapper. A check of the stack of six wavy washers, each 0.017 inch to 0.018 inch thick, made of Rene' 41, showed the following compression force as a function of deflection.

Deflection (inches)	Force (lb)
0.015	2
0.020	5
0.036	15
0.050	25
0.090	60
Solid at 0.100	--

Based on the above data, and the fact that the differential expansion between the core/retainer sleeve assembly and the T-111 duct would be 0.060 inch, the sleeve length was modified to provide an initial load of 10 lbs (0.030 inch deflection) and a clearance from "solid" of 0.010 inch at maximum temperature. The double snap ring was installed without difficulty to hold the core assembly in place, and then was tack welded to the retainer sleeve at four places to prevent it from slipping during operation, as shown in Figure 74.

Brazed bimetal joints (T-111 to Nb-1Zr to type 321 stainless steel) were welded to the duct inlet and outlet pipes using T-111 alloy filler wire. The welded joints were radiographed and helium leak checked. They were sound and leak free. Both welded joints were locally vacuum annealed at 2400°F for one hour in the welding chamber using clam shell furnaces. The welded and brazed joints again passed helium leak check. Figure 75 is an overall view of the T-111 duct with bimetal joints attached.

D. Insulation of the Duct

To reduce heat transfer between the duct and the stator bore can, foil layer insulation was applied to all surfaces of the duct. The material specified for the insulation was 0.002 inch thick Nb-1Zr (Refer to Part A-2 of this section).

The duct wrapper (tube over the helix), the inlet, and the outlet pipes, were covered with 10 layers of the foil. Each layer consisted of a spiral wrapping of the 1/2 inch wide foil which had been slightly "dimpled" to provide separation of the layers. Figure 76 shows the insulation being applied. The final (outside) layer over the helix area was made with plain foil. All the material was thoroughly cleaned before application by ultrasonic wash and rinse in freon.

The ends of the duct were insulated with 10 round washers of the Nb-1Zr foil, with Nb-1Zr wire separators. The end insulation was attached to the axial layers by spot welding several pieces of plain foil to both top layers. Figure 77 is a closeup of the end of the duct with the foil over the bimetal joint attachment welds. Figure 78 shows the completely insulated duct, ready for installation into the stator.

E. Final Check-Out of Duct

Following the completion of the thermal insulation, the duct was again checked for leaks using a mass spectrometer leak detector. It was then inspected and all overall dimensions checked to be sure it would fit into the stator.

The duct was finally wrapped in plastic which was sealed around the inlet and outlet pipes to prevent contamination. The shroud (refer to Figure 1) was not yet assembled to the duct, but was prepared for assembly when the duct was "trial" inserted into the stator. However, the pressure transducer, pressure switch, and potassium leak detector were sub-assembled to the shroud cover so that all was in readiness for the final assembly.

IX. ASSEMBLY OF PUMP

General

The stator and duct, manufactured in different plants, were brought together for check and final assembly. This section of the report will described preparation of the duct and stator for assembly, the assembly, evacuation and filling with argon, ready for installation in the test facility. A layout drawing of the assembled pump is shown in Figure 79.

A. Duct and Shroud Final Assembly

In this pump the T-111 duct is encased in an Inconel "bore" can that was evacuated and back-filled with high purity argon to provide a suitable atmosphere. The pump stator section is also filled with argon for proper winding protection and performance. Instrumentation was provided to monitor argon pressure in both cavities, and to detect any potassium leakage into the duct cavity.

Pressure switches were mounted on stator and duct cavities for "low pressure" alarm signaling. A pressure transducer for actual pressure data, and potassium leak detector were attached to the duct cavity. Pressure switches and transducer were made of stainless steel as were the duct shroud components.

One pressure switch, the pressure transducer, and the metal leak detector were interconnected with stainless steel tubing and fittings for mounting on the duct cavity. The duct shroud consisted of a shroud ring, a cap, and the inlet and outlet pipe sleeves. The shroud cap also contained a thermocouple well, and a duct cavity evacuation tube. The second pressure switch was connected to the stator cavity by a

single-turn stainless steel tubing coil attached to the stator cover at the lead seal end.

All parts and instruments were thoroughly cleaned and degreased prior to assembly. Welding was done by the gas tungsten arc process. The stator pressure switch and connecting tube was assembled, leak checked, and mounted on the stator cavity during final assembly of the part of the pump. The duct pressure switch, pressure transducer, and potassium leak detector were subassembled and leak checked, prior to final assembly of the duct into the stator.

After receipt of the stator, the insulated duct was "trial" assembled into the stator can to make sure there were no fit-up problems. Figure 80 shows this operation in process just prior to the shroud subassembly work.

The duct shroud and pipe sleeves were prepared for subassembly including cutting a section from the edge of the shroud ring, which was retained and welded back in place during the shroud installation. The thermocouple well was welded into the duct cap. A nickel evacuation tube was inserted through a hole in the shroud cap and seal welded to it. Then the Inconel 600 collar was placed over the nickel tube and welded to the cap using Inconel 62 filler wire. The instrumentation bracket was tack welded to the cap. This completed the preparation of all the parts prior to final assembly.

All the shroud components were again mounted on the stator and duct. After an argon purge in the duct cavity, all the shroud parts were tack welded together and to the stator, but yet not to the inlet and outlet tubes of the duct. Small tack welds to the stator were then

broken and the duct and shroud removed from the stator. Internal configuration was checked for clearances. Figures 81 and 82 show the duct and shroud assembly before final welding.

B. Duct Welded into Stator

The duct and shroud were then remated with the stator, and the shroud assembly was again tack welded to the stator, completing the shroud "fit-up". The cap was welded to the shroud ring and the ring to the stator. At the same time, a section cut from the ring to clear the inlet tube was welded in place and the inlet and outlet tubes were welded to the shroud.

Final welding involved the joining of the inlet and outlet sleeves to the stainless steel sections of the bimetal joints on the duct. This procedure minimized mechanical loading on the bimetal joints by completing all other welding first. The last weld was made to join the outlet sleeve to the outlet tube. Stainless steel welds were made using Type 321 stainless steel filler wire. The weld between the stainless steel shroud and the Inconel end shield was made with Inconel 62 filler wire. All welds were visually inspected at 10X magnification for soundness.

C. Final Assembly and Argon Filling of the Pump

After the duct was installed in the stator, the duct cavity was helium leak checked and proved to be tight. Finally, the duct and stator cavities were evacuated and back-filled to 8 psia high purity (2.3 ppm O_2 and 5.4 ppm H_2O) argon.

Arrangement for evacuation, overall leak checking, and argon filling of the pump is shown schematically in Figure 83. The stator

had nickel tubes on both ends and the duct had one nickel tube on the shroud cap. Nickel tubing, 3/8 inch OD by 0.035 inch wall, was used because pure nickel can be sealed (cold welded) leak tight by pinching it in until it separates, by using a hydraulic hand tool with special jaws. The helium leak detector and argon fill set-up was connected to both the pump cavities so that they could be evacuated, leak checked, and filled with argon simultaneously. The argon line was vented to atmosphere through a flow meter to purge the line of air and to insure positive pressure on the argon line during filling of the pump cavities.

Both cavities were helium leak tight. Initial evacuation of the cavities, prior to filling, was slow when the pressure was below 50 microns, apparently because of adsorbed moisture in the stator cavity. The pump stator was therefore heated to about 220°F by passing 120 A DC (from a welding machine) through the windings for three hours. The system then evacuated to 4 microns at room temperature. The fill line was purged of air and the pump cavities filled to 8 psia high purity argon. All vacuum valves were closed and the rubber connecting tubing pinched tight with C-clamps. Then the nickel tubes were pinched and sealed with the hydraulic tool.

The helium leak detector was adjusted to detect argon and the sealed nickel tubes leak checked by sliding a rubber tube over the seal and evacuating that area. All three seals were leak tight. No indication of argon leakage was detected.

The next step was to install the secondary seal caps over the sealed nickel tubes. Holes, 1/16 inch diameter, were drilled in the end of the caps for purging and final seal. Each cap was placed over

the nickel tube against a collar. The interior was purged with argon using a small hypodermic needle through the 1/16 inch hole. Then the caps were welded to the collar.

Helium leak check of cap to collar welds revealed a leak in the nickel tube seal on the stator cavity (duct end). The leak detector could not evacuate the cap cavity low enough to leak check. The cap was then carefully cut through at the weld. Close examination showed that the argon purge hypodermic needle had nicked the edge of the pinch off. Reevacuation of the stator cavity, argon filling and final pinch-off was necessary. It was successfully completed. The cap was rewelded to the collar and the weld helium leak checked. The duct cavity pressure transducer showed no pressure change during these operations. The duct can was completely leak tight.

Final operation involved filling each nickel tube sealing cap with high purity argon and seal welding the 1/16 inch diameter holes. Each cap was evacuated to less than 100 microns and back-filled with argon. The evacuation tube was removed and the hole immediately plug welded by the GTA method using argon shielding. The plug welds were checked for leak tightness by visual inspection. The completed pump, just before welding the 1/16 inch holes in the caps, is shown in Figures 84, 85 and 86.

Final Electrical Check

A resistance check of the windings (line-line) showed they were within the design limits of 0.039 to 0.046 Ω. The windings (coils) to ground checked (with megger) above the design minimum of 10 meg ohms when new. All tests at room temperature.

X. DISCUSSION OF RESULTS

Fabrication and assembly of an EM Boiler Feed Pump was successfully completed and then sent to the test facility. During construction of the pump, several major problems were encountered and solved. These will be discussed here as indicative of the satisfactory results obtained on this part of the program.

T-111 Duct

A duct helix was machined out of a tube of T-111 with more length and turns, and with thinner walls, than had ever previously been fabricated. Problems encountered in welding and machining thin sections were satisfactorily solved. A very fine intergranular leak which developed near the weld between the helix and extension tube had to be located and repaired. It was successfully welded shut and the weld annealed without further problems.

Machining of the thin (0.050 inch thick) helix walls required low cutting speeds with adequate lubrication and "back-up" with a low temperature casting alloy.

The helix wrapper was shrink fitted into place successfully while it had a thicker wall by cooling the helix to -390°F. After the assembly, the outer wrapper wall was machined to the final 0.060 inch thickness without difficulty.

Inlet/Outlet Transition Pipes

A new design of transition pipes (bimetal joints) to connect the T-111 duct to the 321 stainless steel test loop piping was successfully developed. The tongue and groove design, in which the T-111 was welded

to a short length of Nb-1Zr that was then brazed to the stainless steel section, proved very satisfactory. A cobalt base braze alloy was used and the brazing was in vacuum at 2160°F for 5 minutes, providing complete joint filling.

Preliminary sample bimetal joints were cycled over wide temperature ranges, while under tension, without failure. Final parts for production were X-ray, ultrasonic, and helium leak checked without any sign of problem areas.

Stator Coil End Seals

The nickel clad silver wire used for the stator coils had to be brazed in such a way that the silver would not be exposed for migration or deposition during long time operation at up to 1200°F in argon at 20 psia. Initial designs of brazed joints without sealing the wires were rejected, and an extensive investigation and development program was undertaken to design a suitable seal.

Welding was tried but finally rejected and a very high quality nickel plating procedure was developed to provide a 0.005 inch thick layer over the wire ends that would not crack and fail at the 1720°F brazing temperature. Careful process control was necessary for consistently good results, but many tests showed that the final design met all requirements.

Stator Coil Joint Brazing

The 800°F coolant temperature resulted in an estimated hot spot temperature of 1200°F so a new braze alloy and joint design were required. Extensive investigations of available alloys, both by trial

brazes and study of technical data, led to a decision to develop a new braze alloy. The specification for the alloy included a melting/brazing temperature as high as possible but below the melting point of the silver in the wire.

The resulting braze material was a new alloy of 5 In, 18 Ni, and Balance Au. It had a useful brazing range of 1650 to 1735°F. To go with the limited range alloy, a very good argon atmosphere was needed and the induction heating at 450 k Hz had to be precisely controlled from a thermocouple mounted on each joint. A total of over 200 joints were successfully made to complete the stator.

Stator Coil Insulation

The nickel clad silver conductors are wrapped with "S" 994 glass tape where they are outside the stator iron slots. In the iron, the bare conductors are set in the slots with 99.4% alumina ceramic liners to provide the insulation. Minimum thickness is along the sides of the slots where the alumina is 0.036 to 0.040 inch thick. All the insulation is arranged to extend 1/16 inch beyond the iron on each end, if the alumina is perfectly centered in the iron.

During assembly it was found to be very difficult to keep all the alumina liners perfectly centered, and if any of the liners move 1/16 inch or a little more, the bare conductor is separated from the iron by a surface that is only 0.036 inch wide. This is a relatively short creepage path if any contamination takes place on the surface. Furthermore, the extensive ceramic insulation area (both sides of 24 slots) with the minimum thickness noted, means that actual resistance to ground at the operating temperature (1000°F) will be relatively low (less than

1 meg-ohm). Both the surface creepage and actual resistance of the insulation at temperature may warrant further consideration.

Overall Assembly

Final assembly of the stator and the duct took place without any major problems. The stator bore can was successfully slid into place and all final welding of end covers, etc., completed satisfactorily. Final leak checks and electrical checks were all successful.

Duct insulation was applied as designed, and the required 10 layers did not cause an excessive outside diameter.

The duct was easily installed in the stator, and after welding of the duct shroud to the stator end shield, final evacuation and back-fill with high purity argon was accomplished with only limited delay due to considerable outgassing in the stator. Some improvement in this last assembly step would be possible by arranging for greater heating of the pump using the stator coils, during the evacuation.

XI. CONCLUSIONS

The electro-magnetic (EM) pump which was designed for pumping 1000°F potassium at high pressure for boiler feed applications in Rankine cycle space power systems has been successfully built and placed on test. The pump has a design point rating of:

Fluid Pumped	-	Potassium @ 1000°F
Flow	-	3.25 lb/sec
Pressure	-	240 psi
Coolant	-	NaK @ 800°F
Voltage	-	135 V, 3 phase
Frequency	-	60 Hz

Physical dimensions of the pump include:

Overall length	-	35 inch (not including instrumentation)
Diameter	-	11 inch
Weight	-	431 lbs (with instrumentation)

The pump which has been developed and built is the highest efficiency EM type unit which has ever been constructed and placed on test in this range of ratings. Weight has also been considerably reduced, compared with previous EM pumps which have been built.

To accomplish the advance in EM pump design, new techniques were developed for winding, insulating, sealing and brazing the stator coils, fabrication problems were solved in building the helical duct using T-111 refractory alloy, and core, etc., sizes were greatly reduced. However, the pump was satisfactorily assembled and delivered to test, and appears to meet all design goals.

XII. REFERENCES

1. Diedrich, G.E. and Gahan, J.W., "Design of Two Electromagnetic Pumps", Report NASA CR-911, General Electric Company, November 1967.

2. Verkamp, J.P. and Rhudy, R.G., "Electromagnetic Alkali Metal Pump Research Program", Report NASA CR-380, General Electric Company, February 1966.

3. Pendleton, W.W., "Radiation-Resistant Magnet Wire for Use in Air and Vacuum at 805°C", Technical Documentary Report ASD-TDR-63-164, Anaconda Wire and Cable Company, July 1963.

4. Kueser, P.E., et. al., "Magnetic Materials Topical Report", Report NASA CR-54091, Westinghouse Electric Corporation, September 1964.

5. Kueser, P.E., et. al., "Electrical Conductors and Electrical Insulation Materials Topical Report", Report NASA CR-54092, Westinghouse Electric Corporation, October 1964.

6. Blake, L.R., "Conduction and Induction Pumps for Liquid Metals", Proc. IEE, Part A, Vol. 104, No. 13, February 1957.

7. Watt, D.A., "The Design of Electromagnetic Pumps for Liquid Metals", Paper No. 2763, IEE, December 1958.

8. Alger, P.L., "The Nature of Polyphase Induction Machines", John Wiley and Sons, Inc., 1951.

9. Miketta, D.N. and Frank, R.G., "Material Specifications for Advanced Refractory Alloys", Report NASA CR-54761, General Electric Co., October 1965.

10. Thomas, D.E., Harms, W.O., and Huntoon, R.T., "Proceedings of Symposium on Materials for Radio-Isotope Heat Sources", AIME Nuclear Metallurgy, Volume 14, 1969, Page 203.

11. Thompson, S.R., "Brazed Transition Joints for Liquid and Alkali Metal Systems", Technical Document GESP-160, General Electric Company, NSP, February 17, 1969.

12. Harrison, R.W. and Hoffman, E.E., "Advanced Refractory Alloy Corrosion Loop Program", Quarterly Progress Report No. 4, Period Ending April 15, 1966, Report NASA CR-72029, General Electric Company.

XIII. APPENDIX A

RESISTIVITY OF Ni CLAD Ag WIRE

Information Prepared by:

J. P. Couch and J. C. Sturman, NASA-LeRC.

Wire Specification:

20% (by Area) Nickel Clad Silver; refer to Figure A-1. Dimensions are: 0.073 ± 0.001 inch by 0.149 ± 0.001 inch.

Description of Test:

Resistance of 4 feet of wire was measured in argon, over a temperature range from room temperature to 1500°F. Two separate tests were run. The first included 14 data points between 73° and 1501°F taken over an 8 hour period. The second test was run the next day and included 10 data points between 73° and 1525°F taken over an 8 hour period.

Resistance measurements were taken at both increasing and decreasing temperatures. A third test was run five days after the second series, in which the wire was held at about 1230°F for a period of 29 hours to determine whether the resistance changed with time.

Results of Tests:

The data from all experiments are plotted in Figure A-2. Resistances determined in the second test are slightly higher than those from the first. The data from the third test are in close agreement with the second. There was no conclusive change in resistance with time at 1230°F. The nickel clad showed progressively greater surface oxidation at the

conclusion of each test indicating that the argon environment was not as pure as desired.

Data from the first test can be fitted to the following equation:

$$\Omega/ft = 7.9803 \times 10^{-4} + 1.6538 \times 10^{-6}\ t + 3.0294 \times 10^{-10}\ t^2 \qquad (A\text{-}1)$$

(Standard deviation = $\pm$ 0.0056 x 10^{-3} Ω/ft)

Data from the second test fits the following equation:

$$\Omega/ft = 8.0449 \times 10^{-4} + 1.7191 \times 10^{-6}\ t + 2.7432 \times 10^{-10}\ t^2 \qquad (A\text{-}2)$$

(Standard deviation = $\pm$ 0.0050 x 10^{-3} Ω/ft)

Data from the third test is essentially the same as from the second test.

When all data are combined, they fit the following equation:

$$\Omega/ft = 8.0342 \times 10^{-4} + 1.6722 \times 10^{-6}\ t + 2.9501 \times 10^{-10}\ t^2 \qquad (A\text{-}3)$$

(Standard deviation = $\pm$ 0.0184 x 10^{-3} Ω/ft)

In all equations "t" is in °F.

The second equation (A-2) is recommended for use in calculating the wire resistance.

Determination of Resistance:

To convert the data to resistivity, it is necessary to multiply the resistance per foot (above equations) by the cross-sectional area of the wire. This area was determined by sectioning the wire, preparing a photomicrograph of the cross-section, and measuring the area on the photo with a planimeter. Three areas were measured: the outside area of the wire; the area occupied by silver; and the area of a rectangle whose sides are flush with width and breath of the wire. Figure A-1 is a copy of the photomicrograph. The measured areas are: rectangle, 7.44

in^2; outside of wire, 6.81 in^2; and silver area, 5.38 in^2, each with a standard deviation of ± 0.005 in^2. Since the wire is 0.073 inch ± 0.001 inch by 0.149 inch ± 0.001 inch, its rectangular area is 0.010877 in^2 with a standard deviation of ± 0.000096 in^2. The actual cross-sectional area of the wire is then found by multiplying the rectangular area by the ratio (6.81 ± 0.005)/(7.44 ± 0.005) giving:

$$0.009956 \pm 0.000052 \text{ in}^2$$

Multiplying the resistance equation (A-2) by this area then gives the resistivity of the Ni-clad Ag wire:

$$\rho = 0.6675 + 1.426 \times 10^{-3}\, t + 2.276 \times 10^{-7}\, t^2$$

where ρ is in μ ohm-in and t in °F. Also

$$\rho = 10.20 + 2.179 \times 10^{-2}\, t + 3.477 \times 10^{-6}\, t^2$$

where ρ is in $\frac{\text{ohm-cir. mil}}{\text{ft.}}$ and t is in °F.

Conclusions:

The uncertainty in these equations, taking into account the uncertainty in the area, temperature and resistance measurements, is probably less than ± 3%. Comparison of the resistivity from this test with the resistivity of 23% Ni-clad Ag from reference 3 shows very good agreement.

From the area data, it is also possible to determine the relative areas between Ni and Ag in the wire, viz.

$$5.38/6.81 = 0.790 \text{ area fraction Ag}$$

Thus, the wire tested, and used in the boiler feed pump, was 21% by area of Ni.

Appendix A

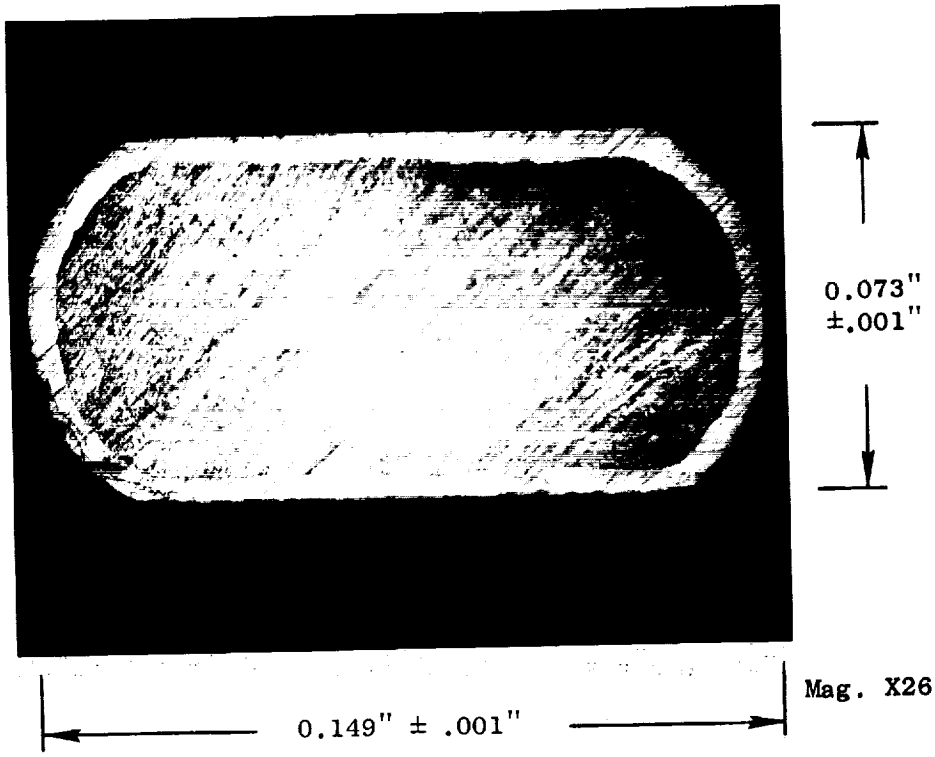

Figure A-1. Cross Section of Nickel Clad Silver Wire Used for EM Boiler Feed Pump. (459-A1)

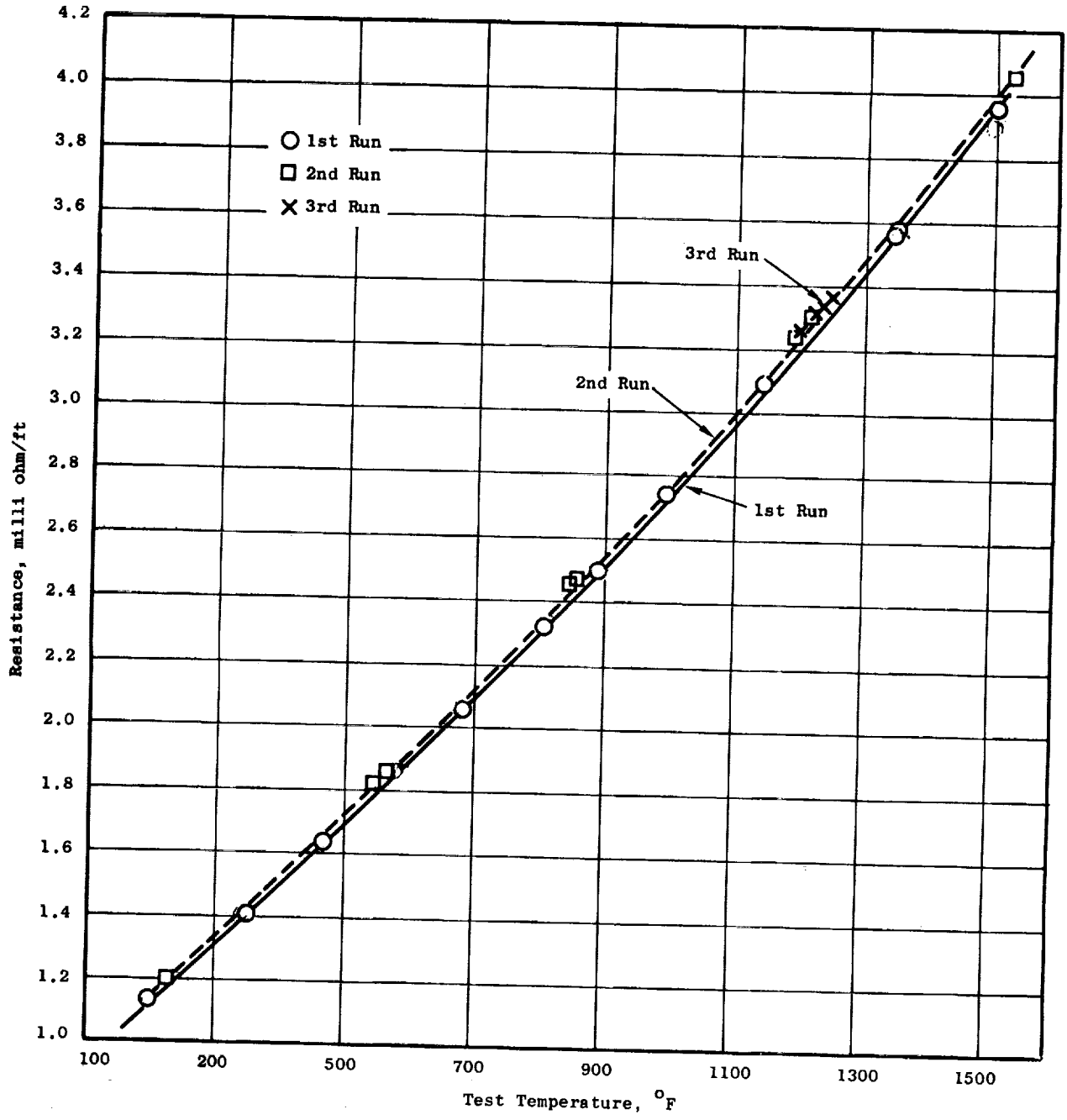

Figure A-2. Plot of Data Points from Three Test Runs on Nickel Clad Silver Wire Used in EM Boiler Feed Pump.

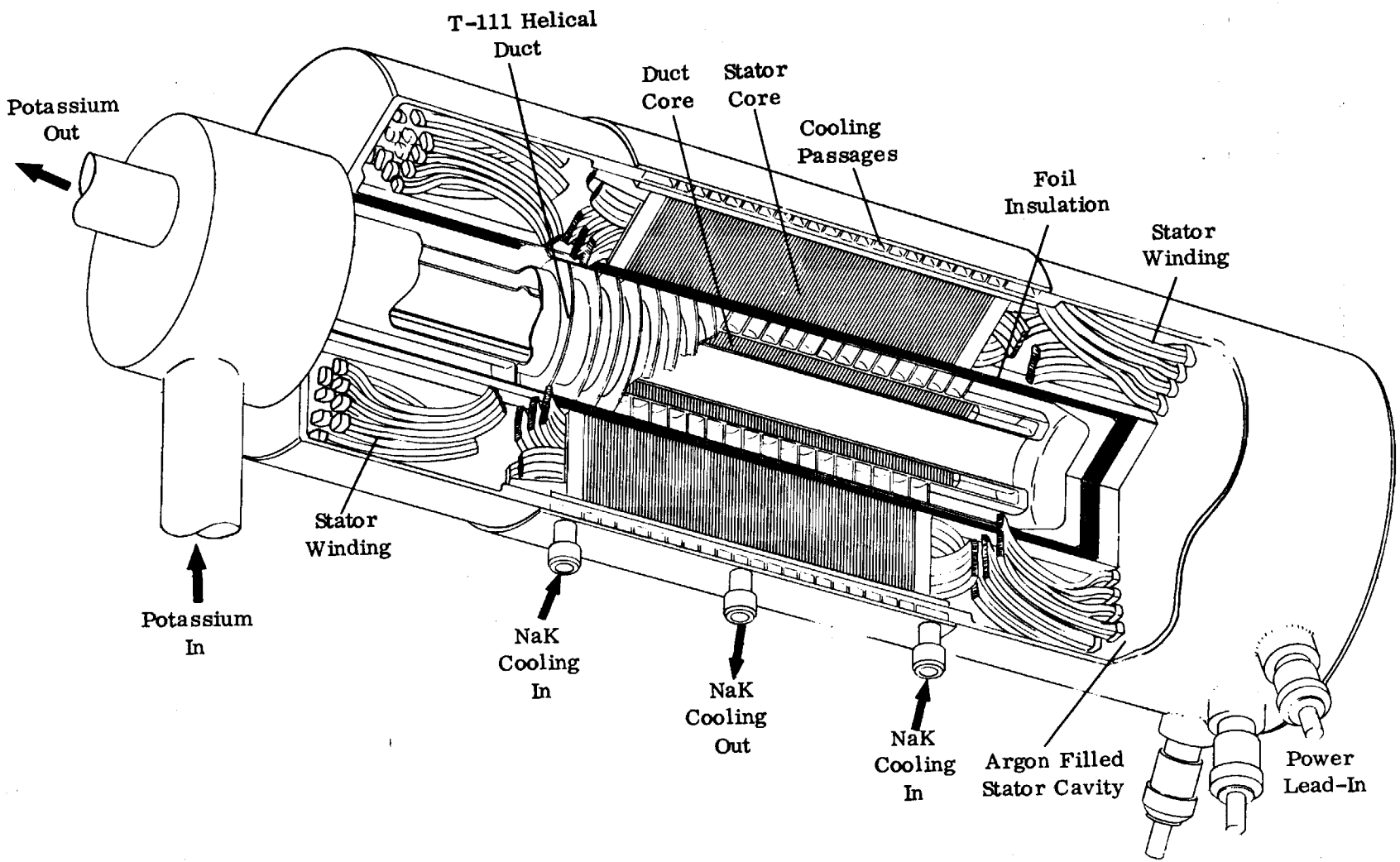

Figure 1A. Conceptual Design Sketch of EM Boiler Feed Pump, having Design Rating of 3.25 lb/sec Flow, and 240 psi Developed Head, with 1000°F Potassium.

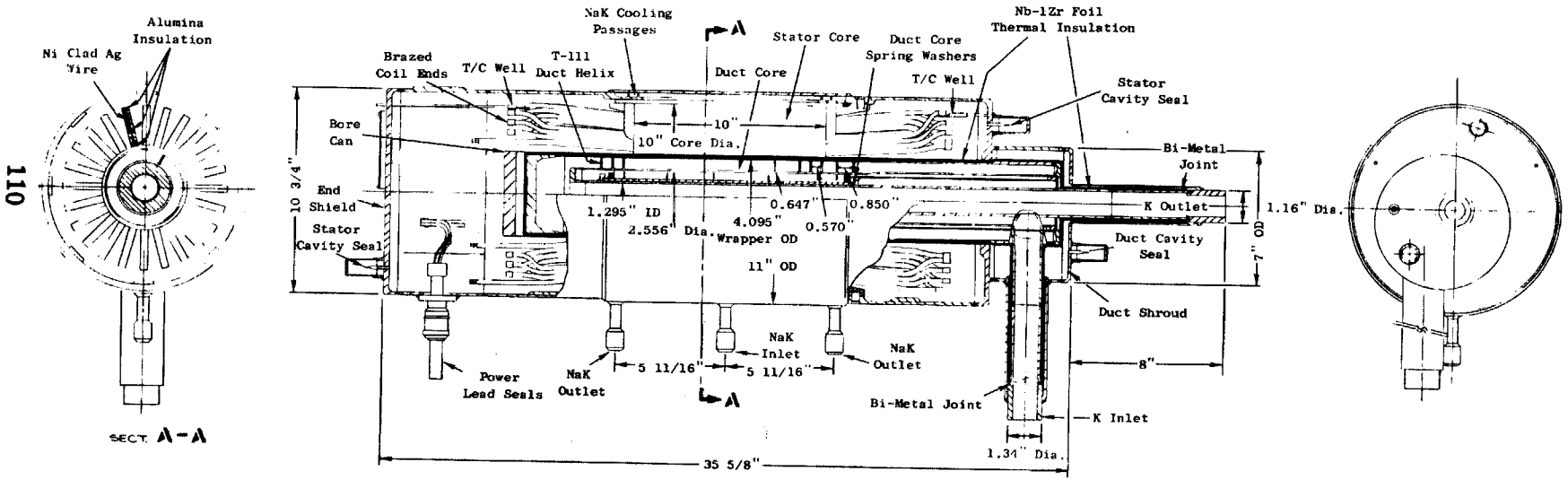

Figure 1B. EM Boiler Feed Pump.

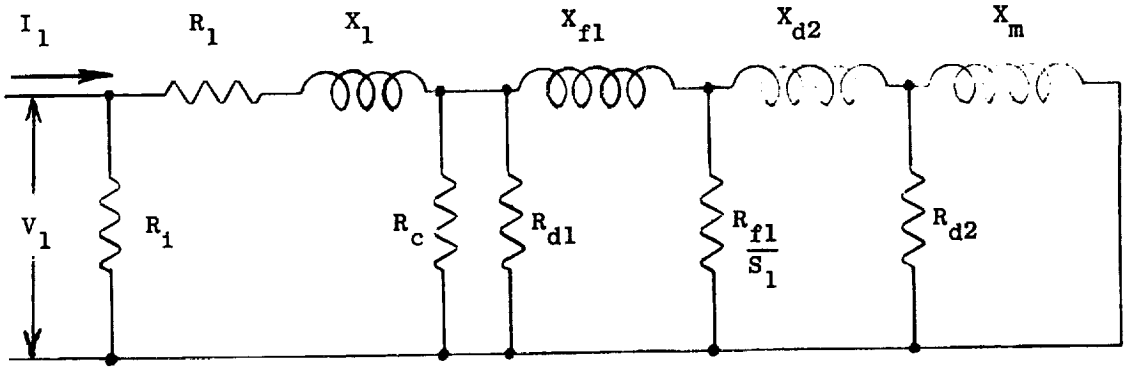

Definition of Terms	Final Pump Design Values
R_i = Effective Iron (Stator) Loss Resist.	R_i = 14.9 Ω
R_1 = Stator Resistance	R_1 = 0.059 Ω
R_c = Effective Resist. of Stator Can	R_c = 20.8 Ω
R_{d1} = Effective Resist. of Duct Wrapper	R_{d1} = 2.7 Ω
R_{d2} = Effective Resist. of Inner Duct Cyl.	R_{d2} = 3.99 Ω
R_{f1} = Effective Resist. of Fluid	R_{f1} = 0.32 Ω
S_1 = Effective Slip	S_1 = 0.46
X_1 = Leakage Reactance	X_1 = 0.19 Ω
X_{f1} = Reactance Asso. with Fluid	X_{f1} = 0.023 Ω
X_{d2} = Reactance Asso. with Inner Duct Cyl.	X_{d2} = 0.011 Ω
X_m = Mutual Reactance	X_m = 0.32 Ω
I_1 = Phase Current	I_1 = 164A
V_1 = Phase Voltage	V_1 = 78V

Figure 2. Equivalent Electric Circuit for Helical Type EM Pump Design Calculations.

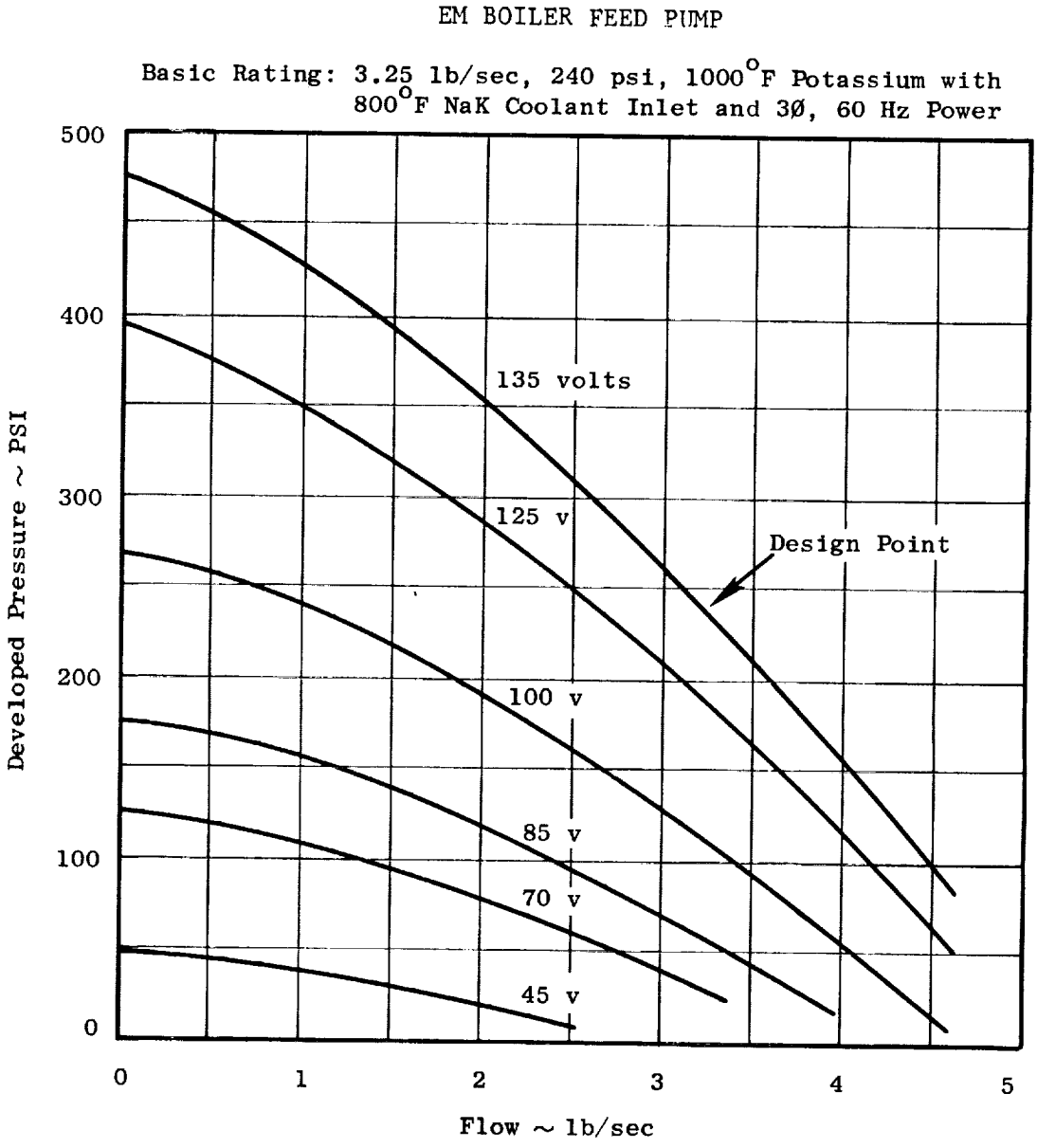

Figure 3. Calculated Performance Curves Showing Pressure Developed Versus Potassium Flow at Various Line Voltages.

EM BOILER FEED PUMP

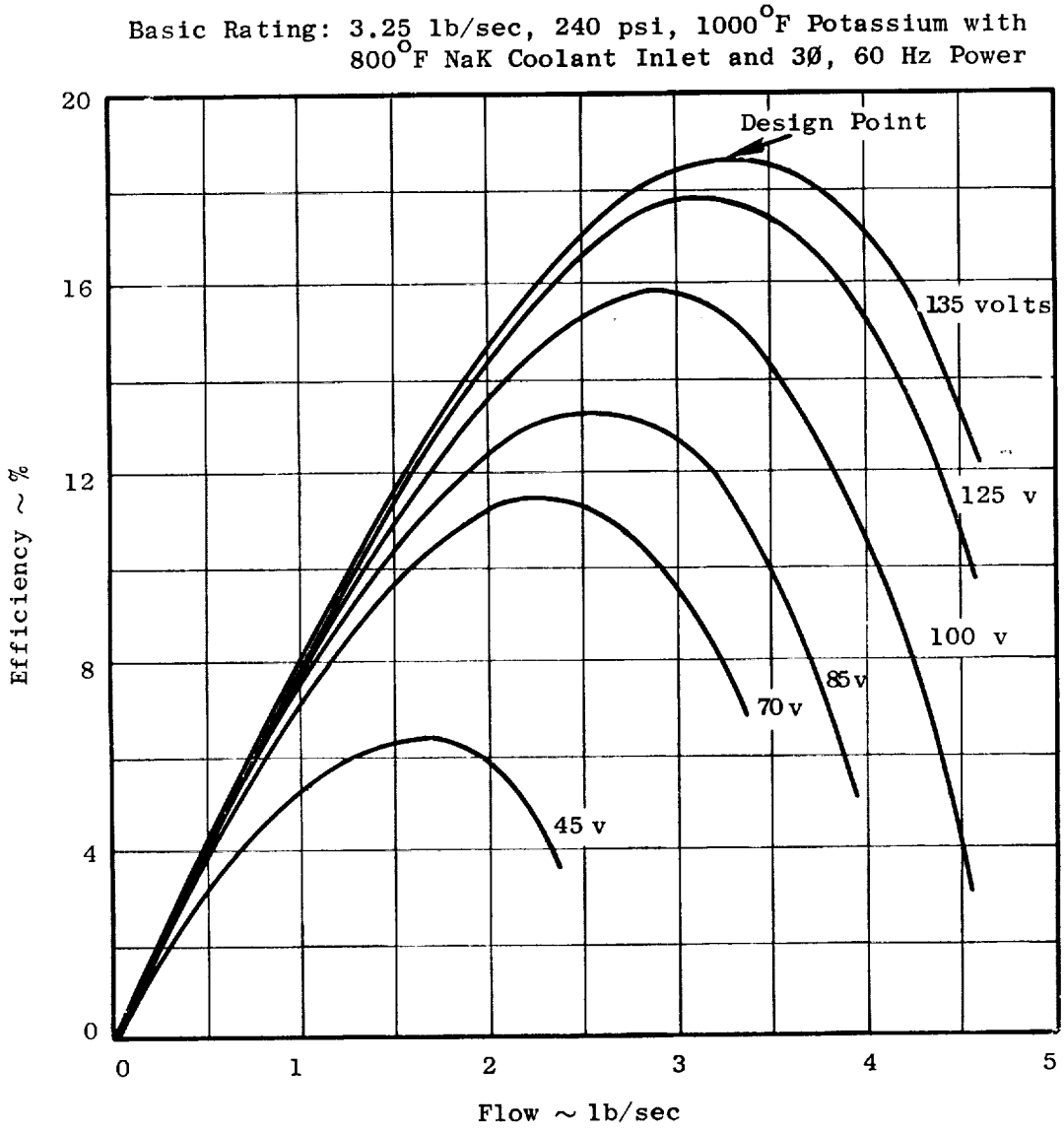

Figure 4. Calculated Performance Curves Showing Efficiency Versus Potassium Flow at Various Line Voltages.

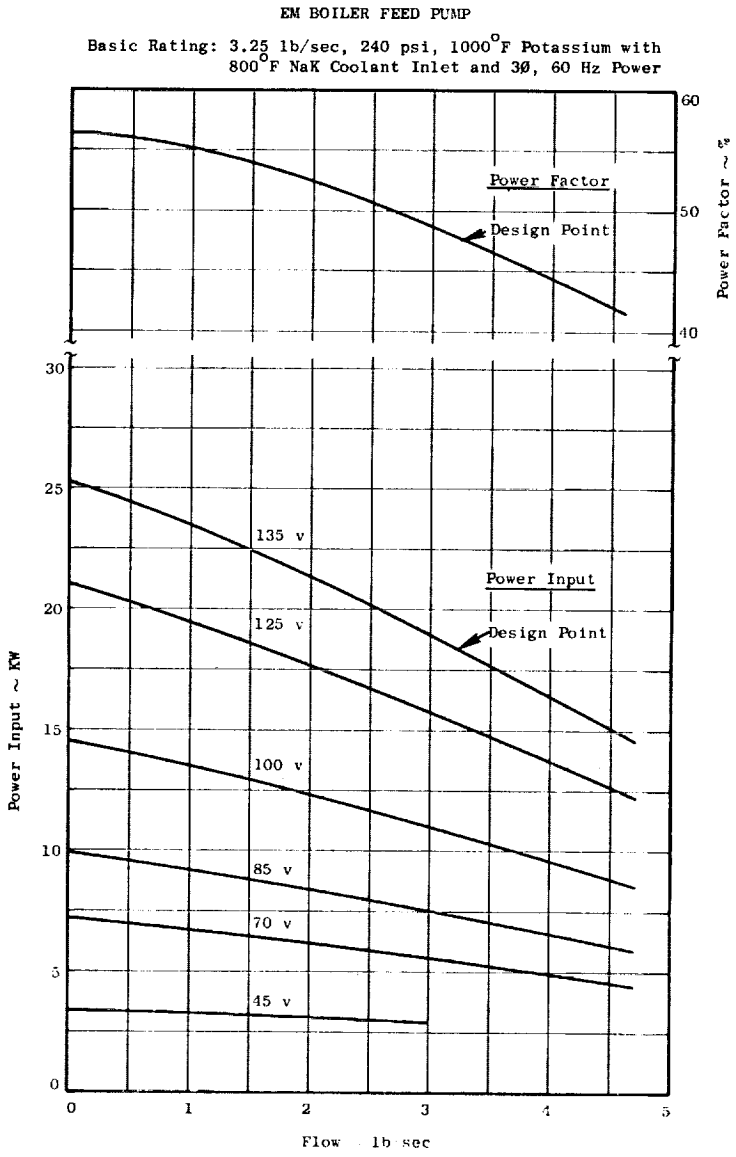

Figure 5. Calculated Performance Curves Showing Power Input and Power Factor Versus Potassium Flow at Various Line Voltages.

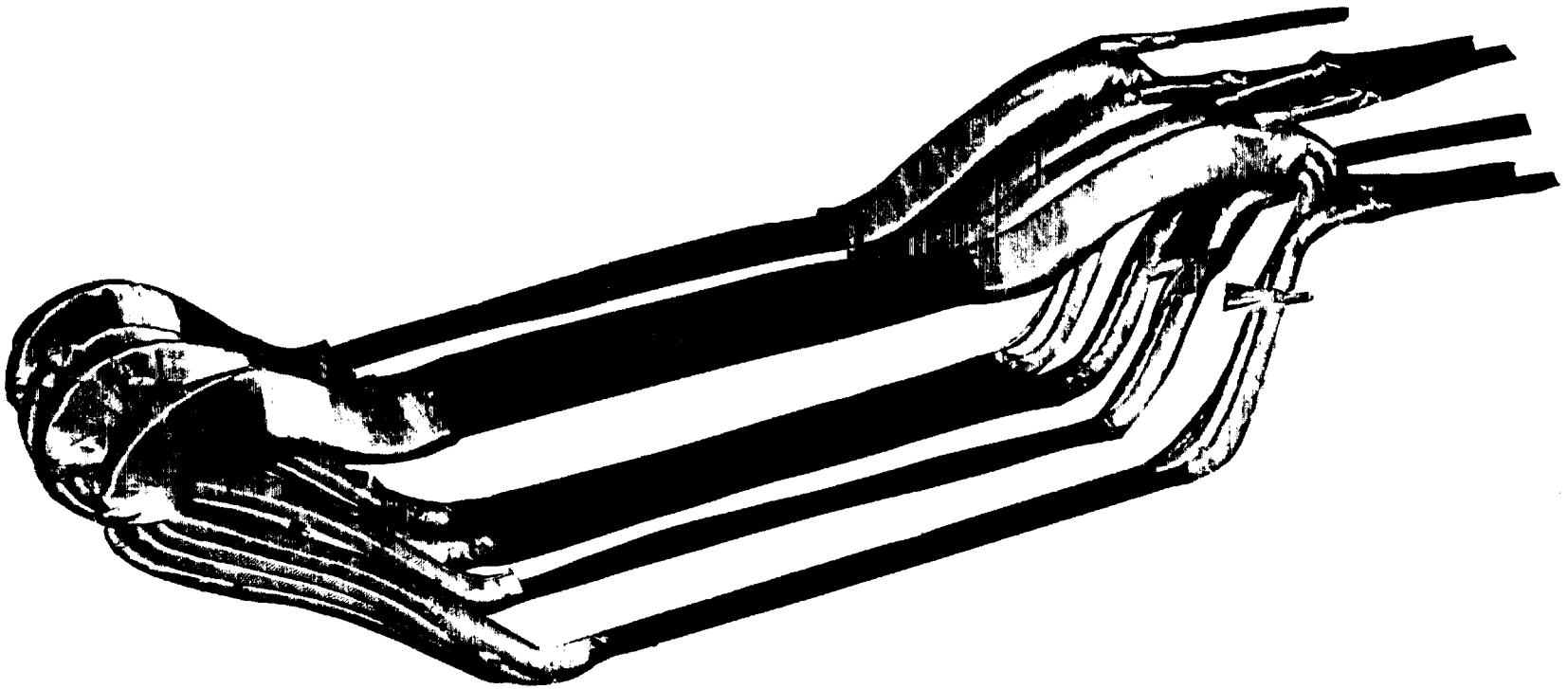

Figure 6. Trial Stator Coils, Made of Copper, Used for Evaluating the Feasibility of Using Full Coils in the Pump.

Figure 7. Model Stator for EM Pump with Trial Bar Windings and End Connections, on End Opposite Leads.

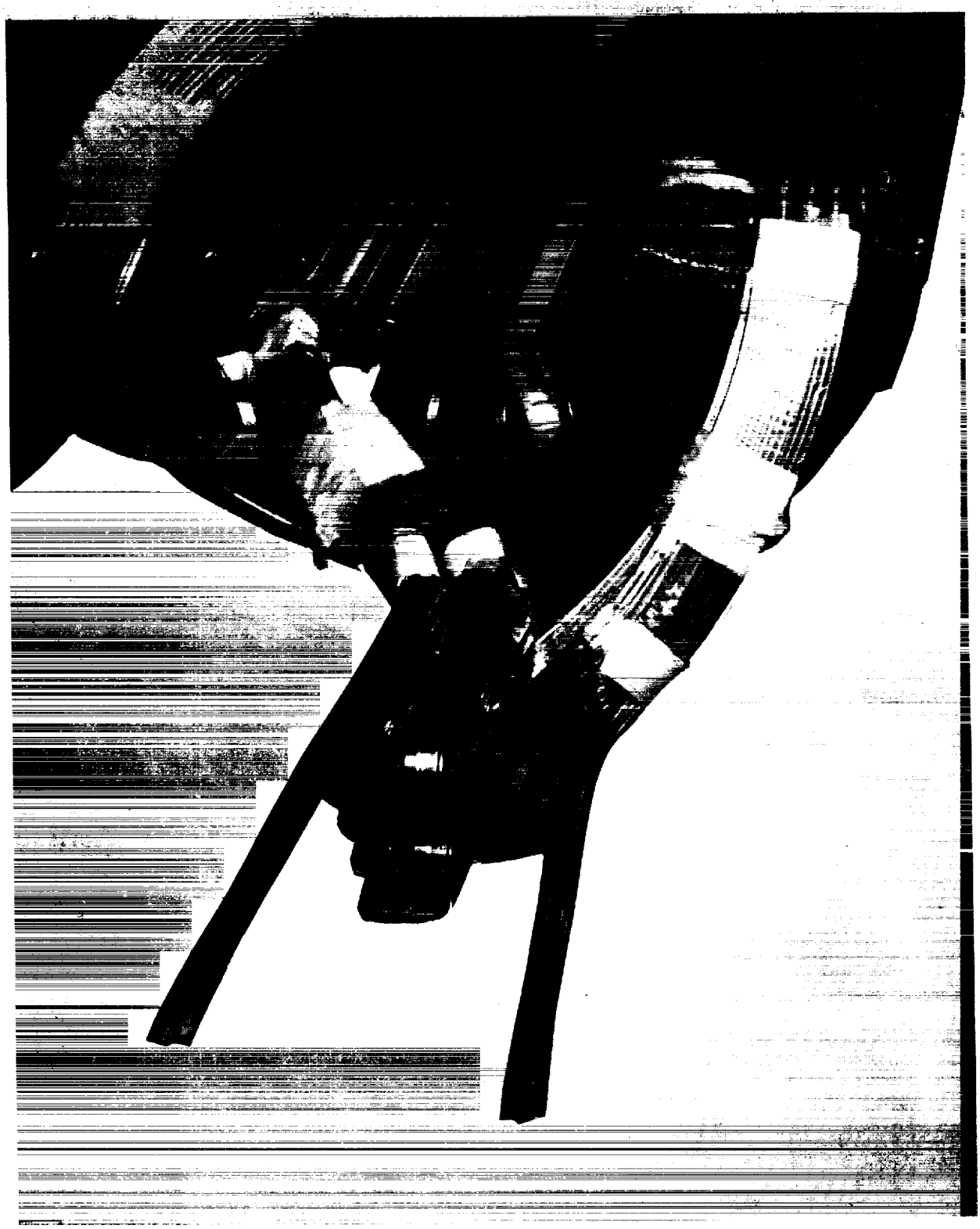

Figure 8. Model Stator for EM Pump Showing One of Two Proposed Types of Bar Winding End Connections, on Lead End.

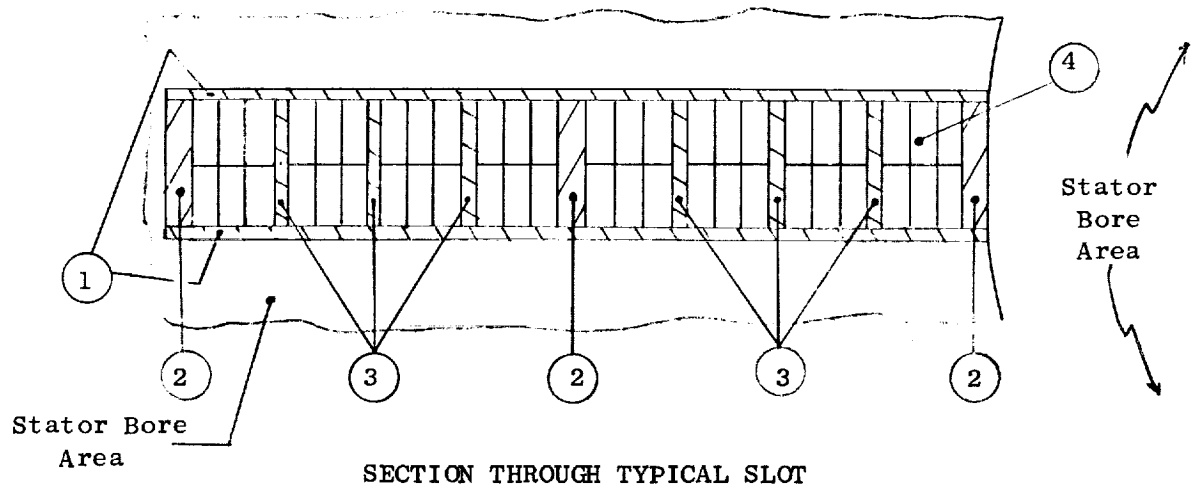

SECTION THROUGH TYPICAL SLOT

Item	Part A Model Stator	Part B Final Design
1. Side Sheet		
Material	99.5% Alumina	99.5% Alumina
Width	2.10"	2.10"
Length	10.13"	10.13"
Thickness	0.025"	0.038"
2. Bottom, Coil Wedge		
Material	1/2 of 99.5% Alumina 1/2 of BN felt	All 99.5% Alumina
Width	0.30"	0.30"
Length	10.13"	10.13"
Thickness	0.075"	0.052"
3. Turn Separators		
Material	99.5% Alumina	99.5% Alumina
Width	0.30"	0.30"
Length	10.13"	10.13"
Thickness	0.025"	0.025"
4. Conductors		
Material	Copper	Ni Clad (20%) Ag
Width	0.164"	0.149"
Thickness	0.071"	0.073"

Figure 9. Arrangement of Slot Insulation and Coil Wires in EM Boiler Feed Pump Stator Iron. (459-9)

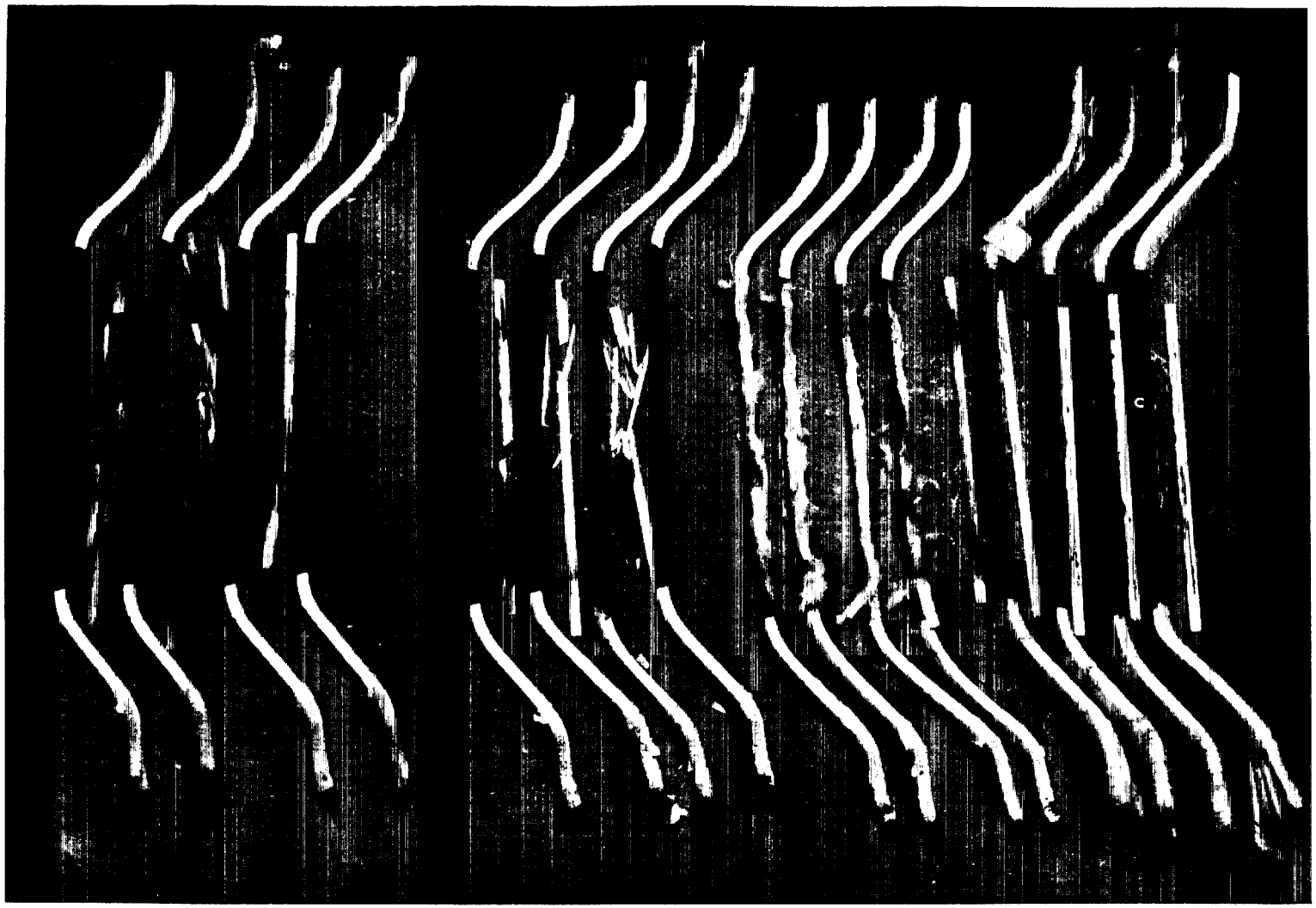

Figure 10. Half Coils (Bars) from Model Stator After Tests and Dismantling, Showing Ceramic and Boron Nitride Turn Insulation.

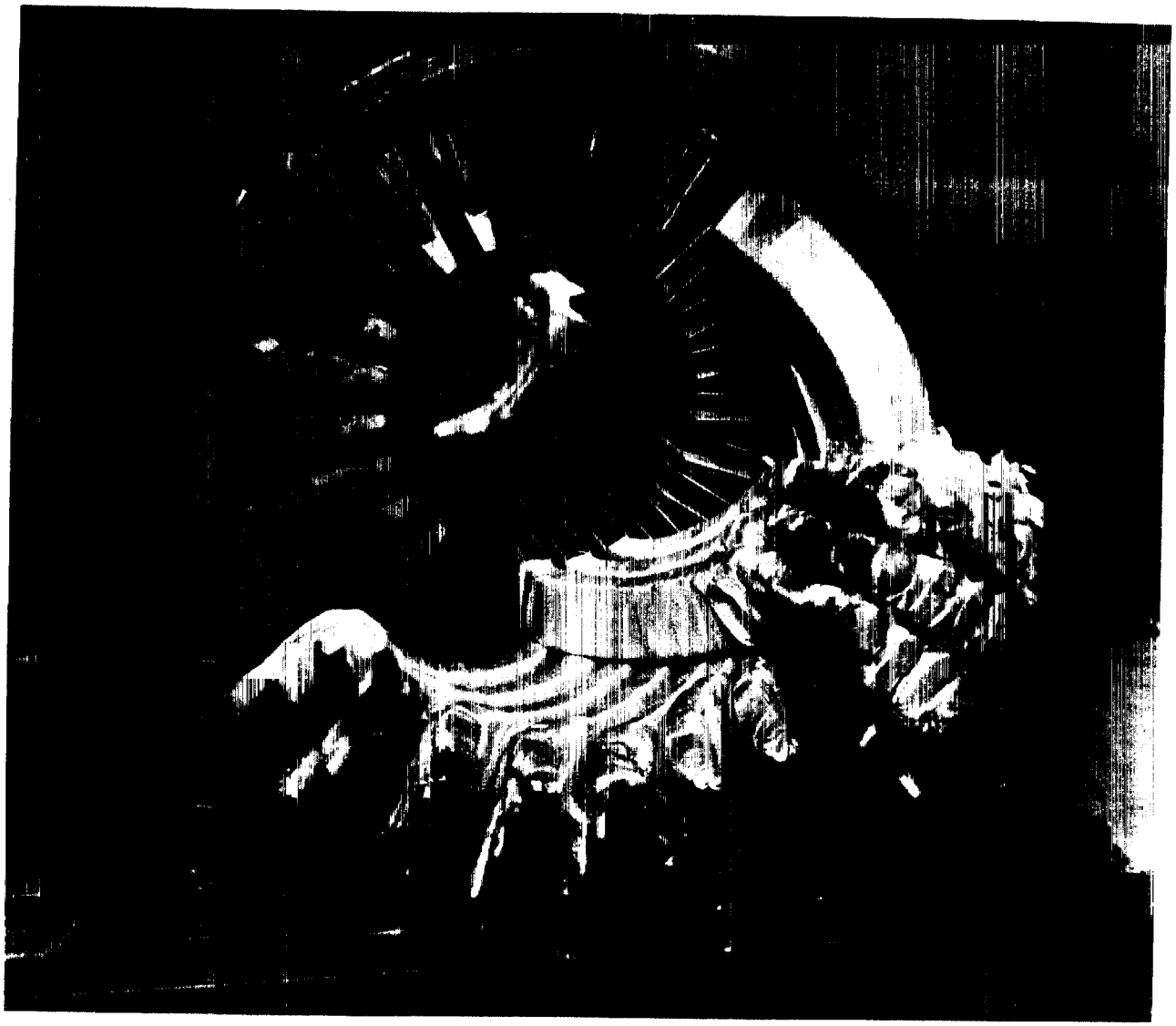

Figure 11. Part of Coils Remaining in Model Stator After Tests and Partial Dismantling for Inspection.

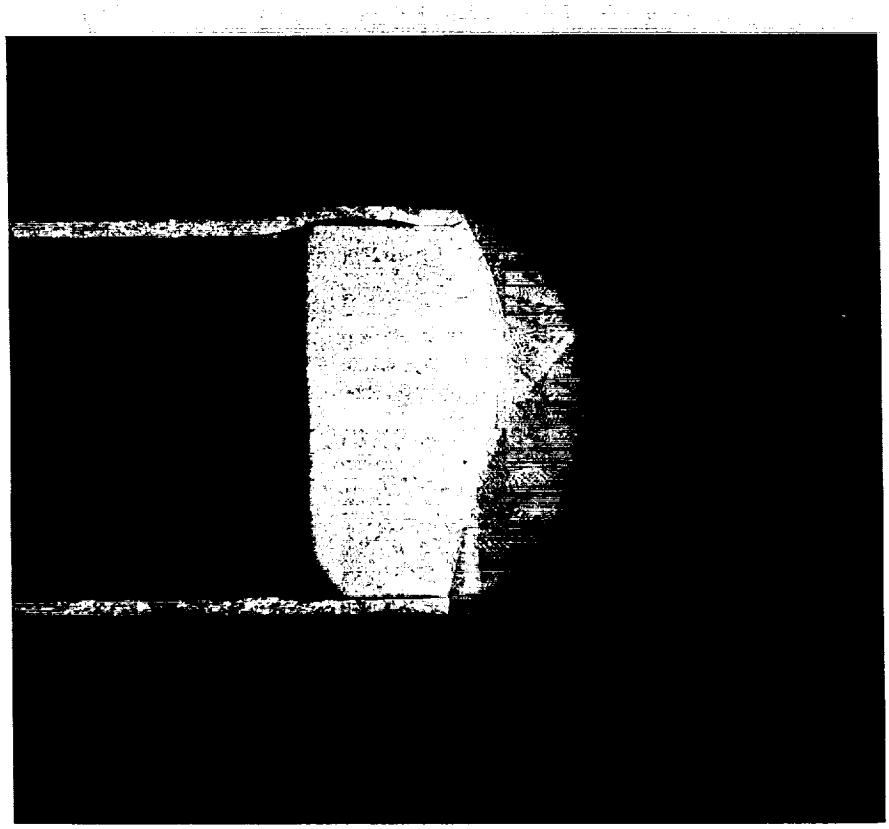

Figure 12. Etched Section (15X) of Nickel Clad Silver Wire with Nickel Plug TIG Welded in End Where Silver was Removed.

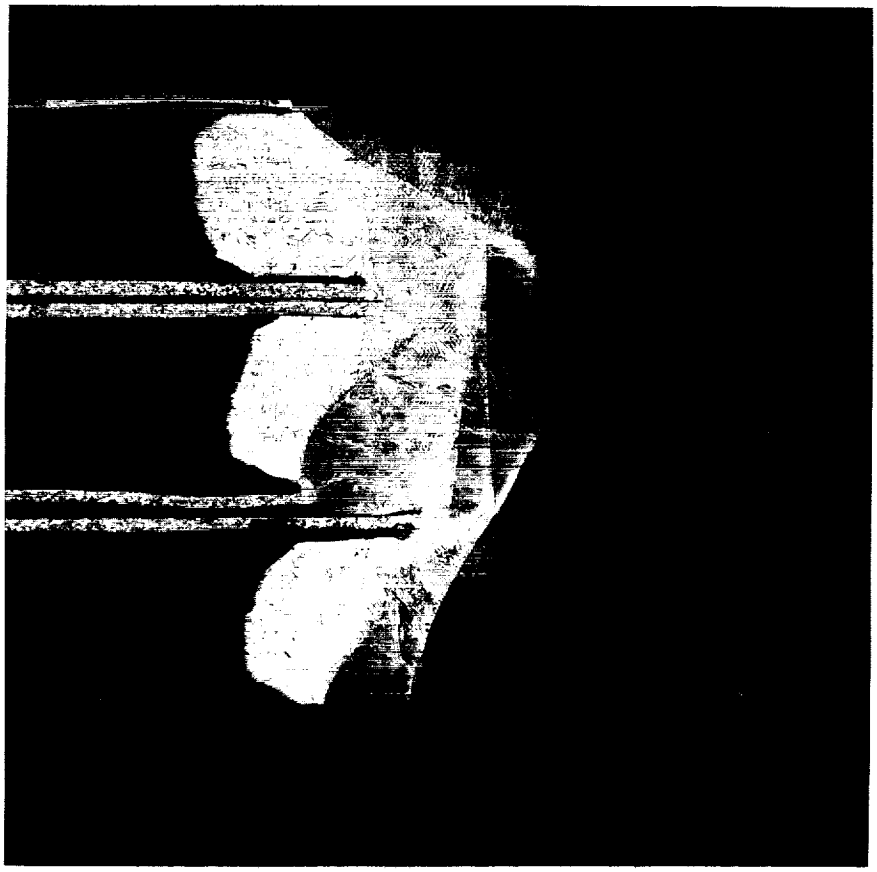

Figure 13. Etched Cross Section (15X) at Center of Group of Nickel Clad Silver Conductors with Nickel Plugs TIG Welded in Ends After Silver was Removed.

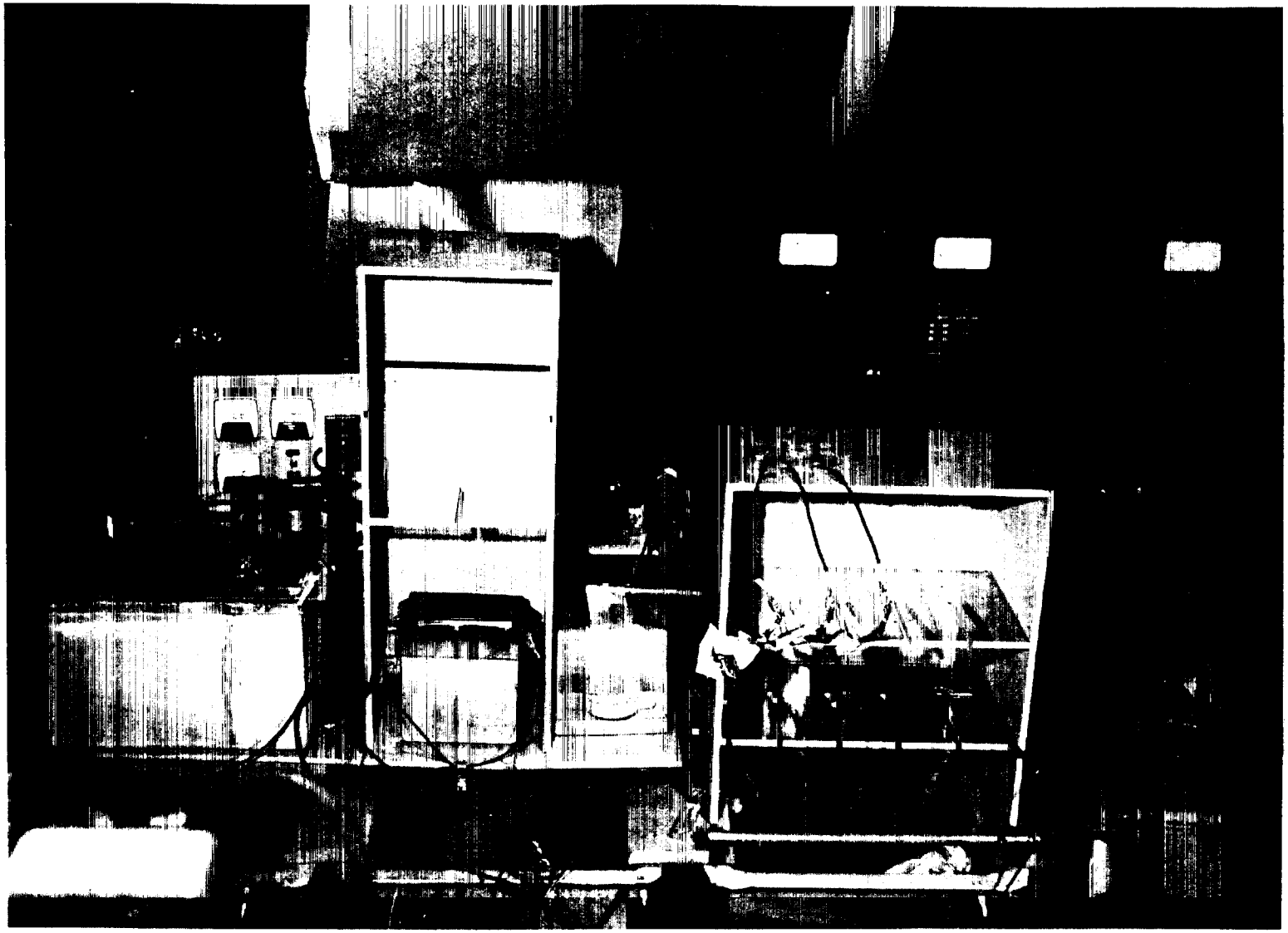

Figure 14. Special Set-up for Nickel Plating the Ends of Nickel Clad Silver Conductors for EM Pump Stator, Showing Anodic Etch Solution in the Center, Nickel Strike at Left, and Nickel Sulfamate Bath at Right, with Rack Holding Three Groups of Conductors and a QC Sample.

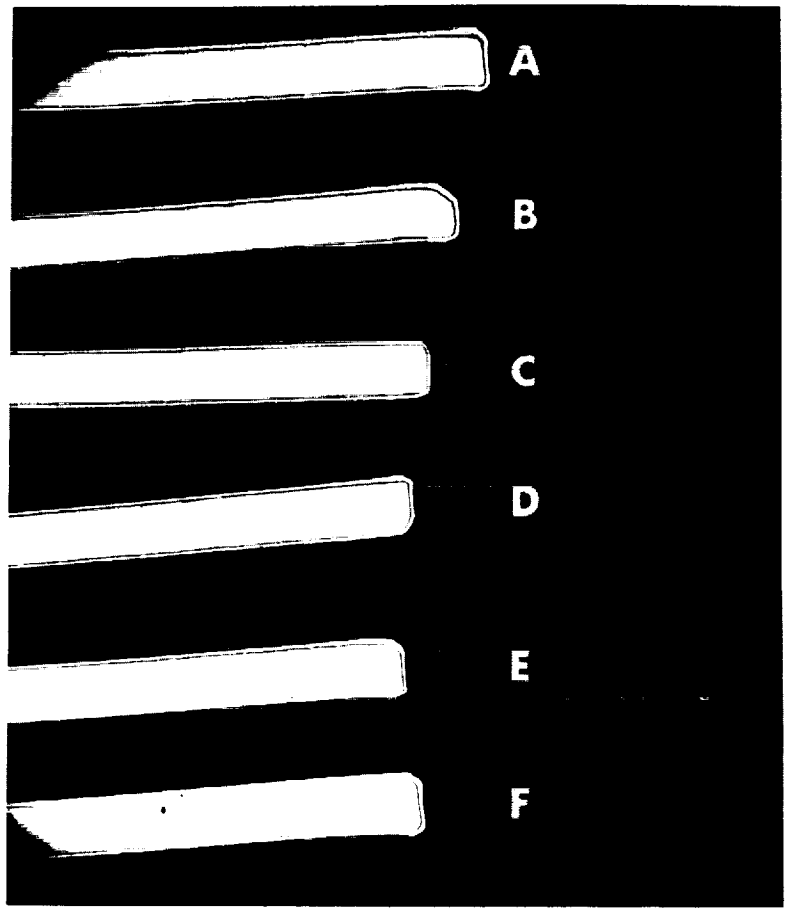

Figure 15. Section at 4X Magnification, Through Narrow Width of Six Nickel Clad Silver Wires Comprising Quality Control Sample #3, After Application of Nickel Plate to Seal Ends.

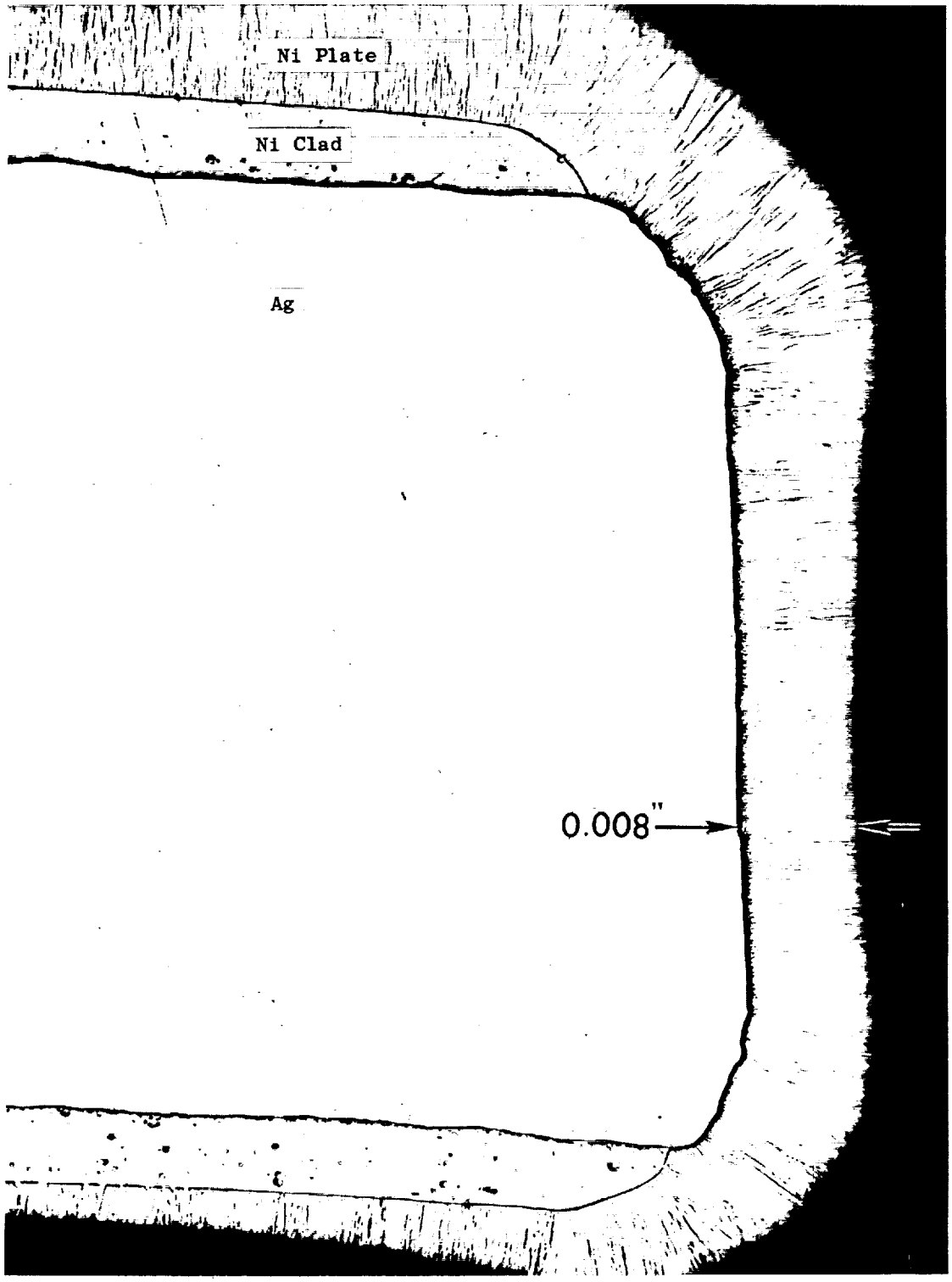

Figure 16. Photomicrograph (100X) of Outside Strand (A) of Quality Control Sample #3, After Nickel Plating Over the End of the Nickel Clad Silver Wire.

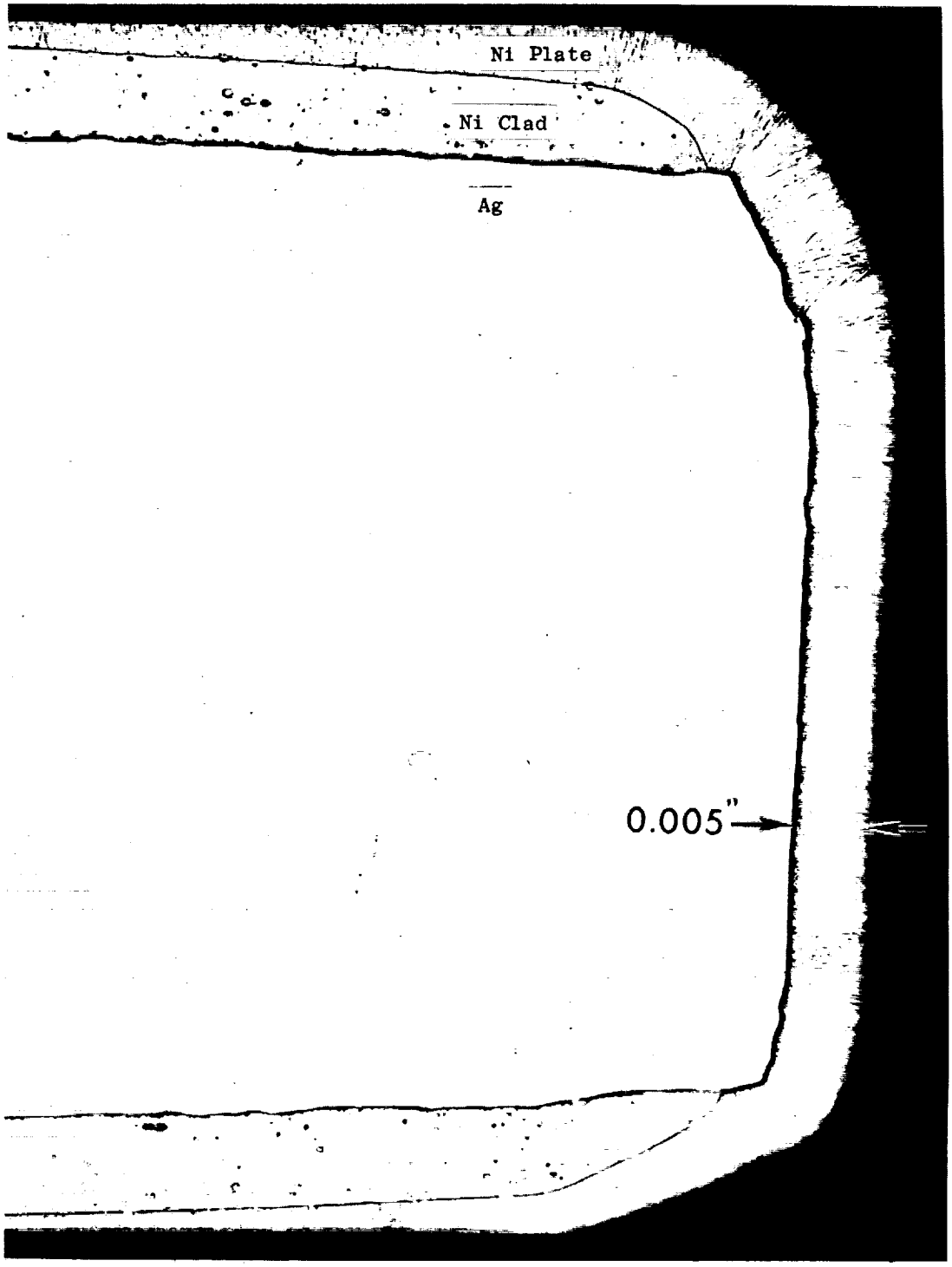

Figure 17. Photomicrograph (100X) of Inside Strand (C) of Quality Control Sample #3, After Nickel Plating Over the End of the Nickel Clad Silver Wire.

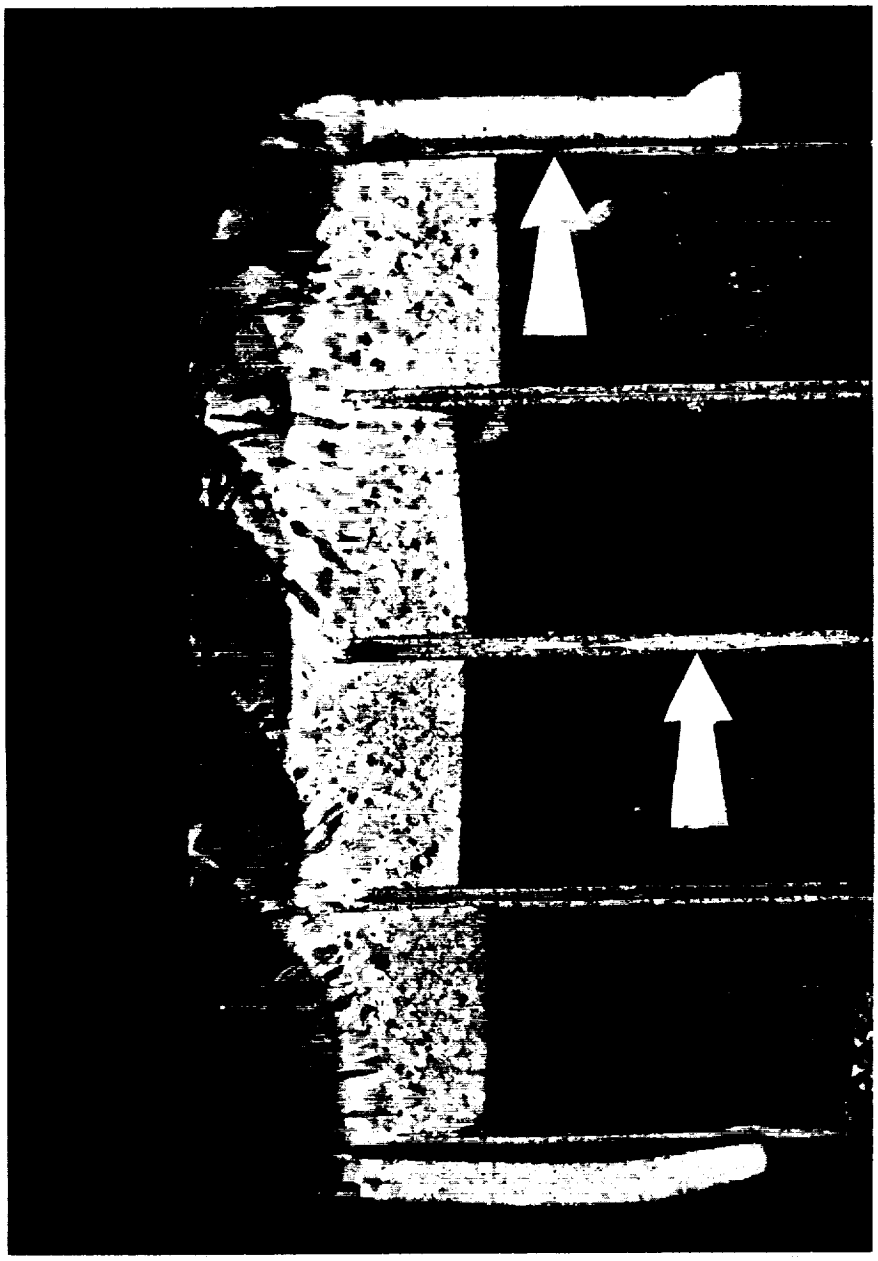

Figure 18. Section (8X) Through First Layer of Sample Joint #F4, Brazed with Gold-Copper (80-20) Alloy with Nickel Plugs TIG Welded to Ends of Conductors, Showing Sheath Erosion at Arrows.

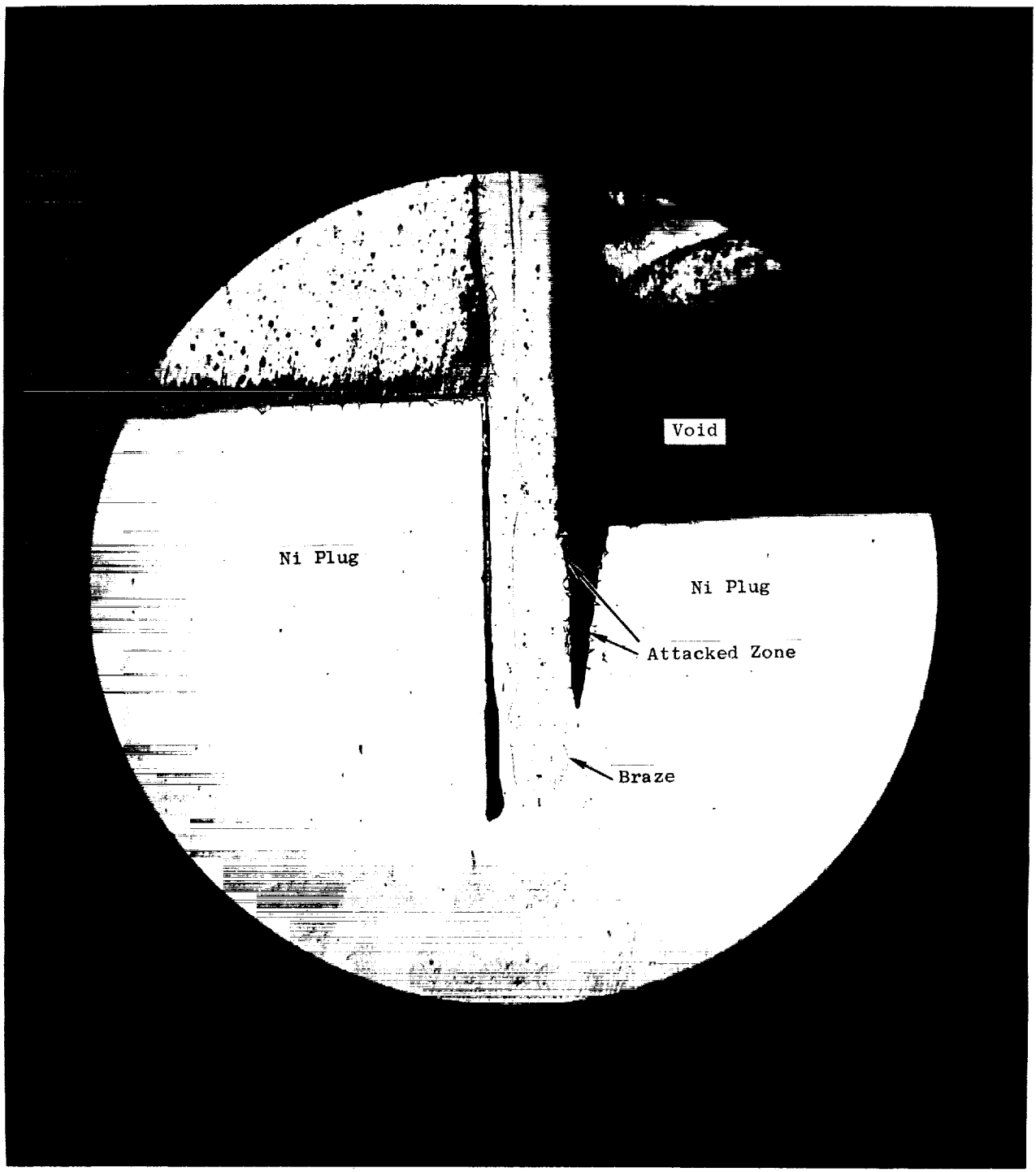

Figure 19. Microphotograph (50X) of Joint Sample #F4 Showing Grain Boundary Attack on Side of Nickel Plug, and Braze Erosion of Nickel Sheath on Conductor.

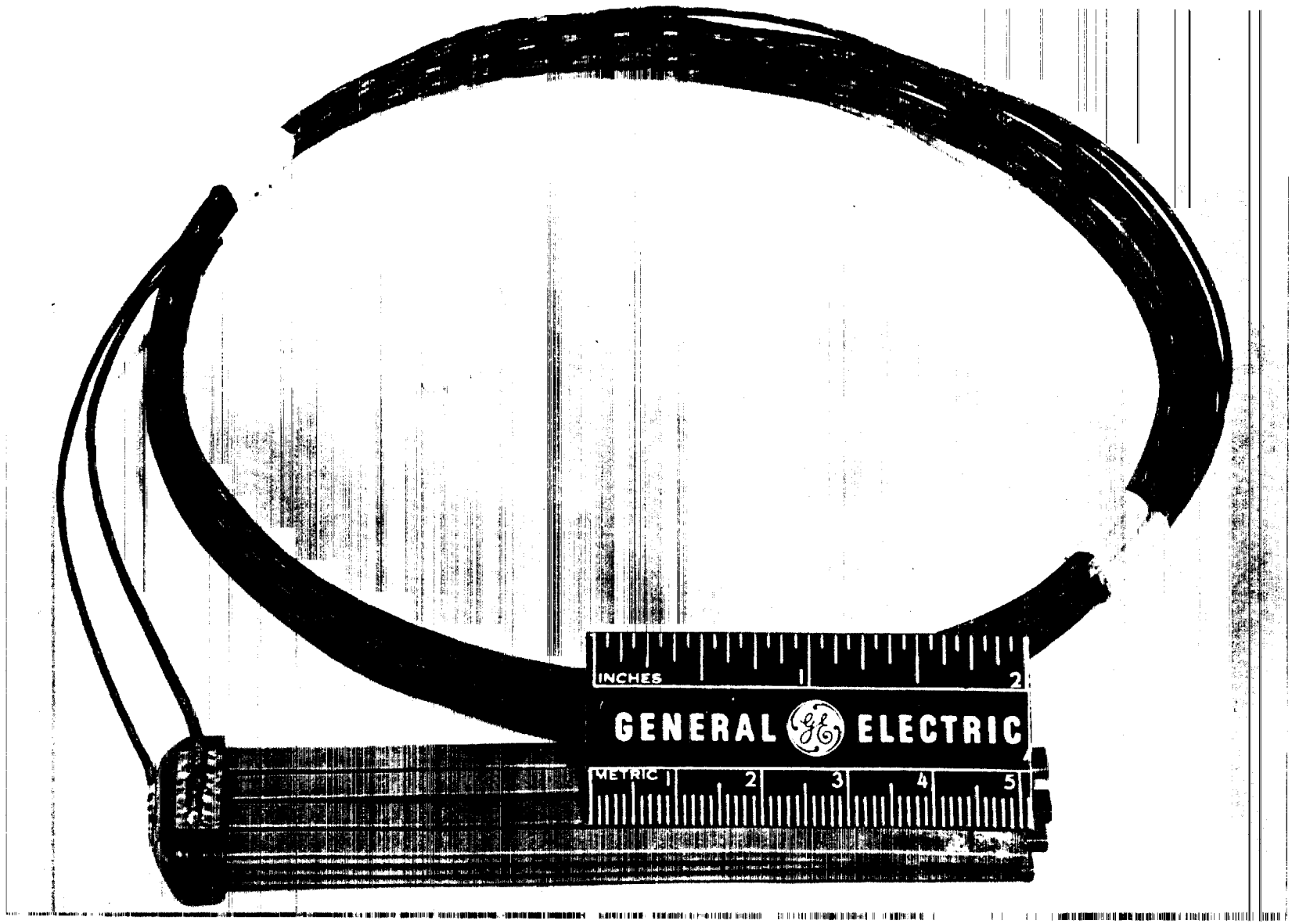

Figure 20. Sample Joint Prepared for Test Brazing, with Two Thermocouples Attached to Nickel Ferrule Which was TIG Welded to Nickel Plugs in Ends of Conductors.

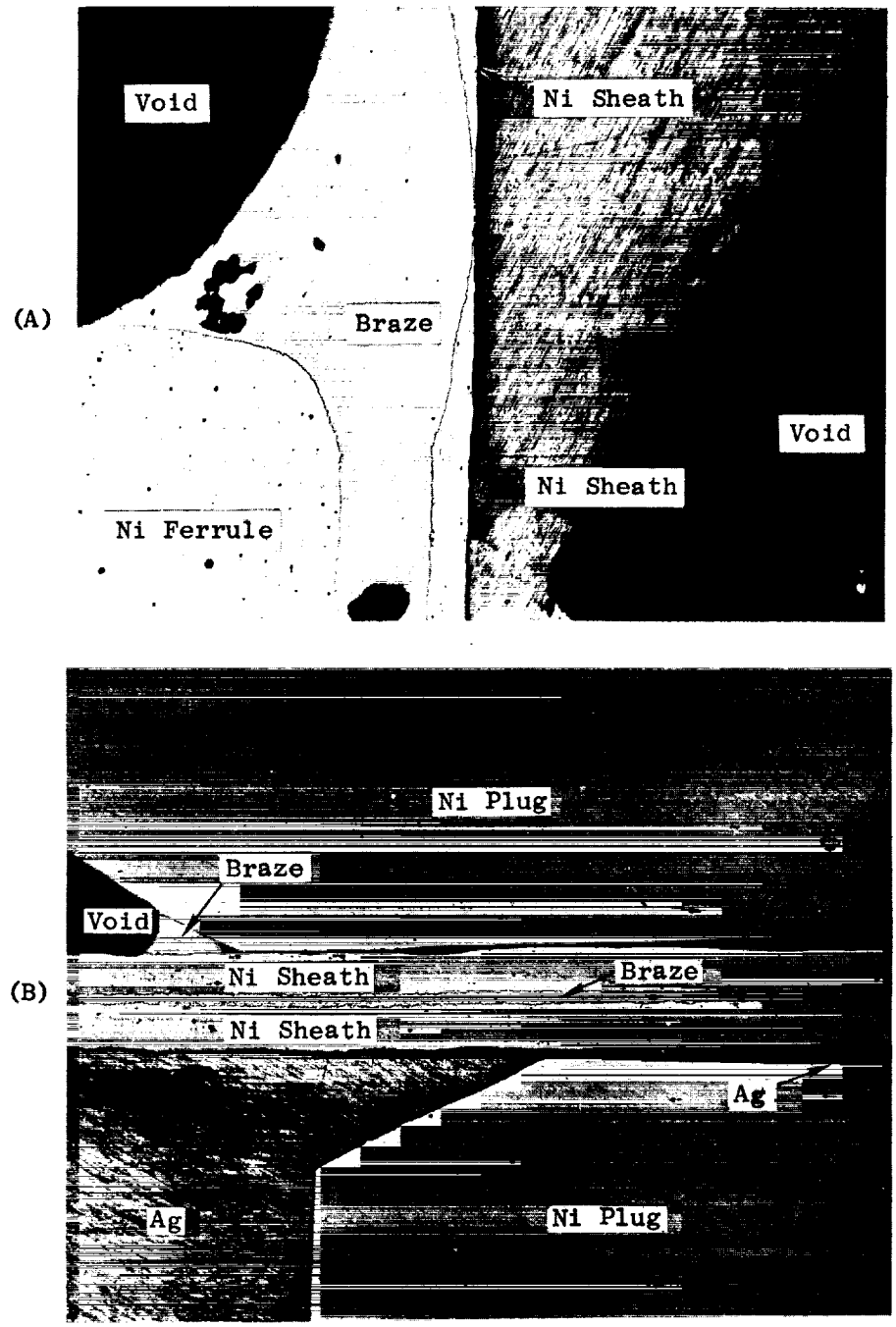

Figure 21. Microphotograph (50X) of Joint Sample #F11, Shown in (A) the Entrance Fillet Sheath Erosion, and (B) a Mid-Bundle Area with Good Braze Flow without Erosion but Braze Alloy on Plug Side of Sheath.

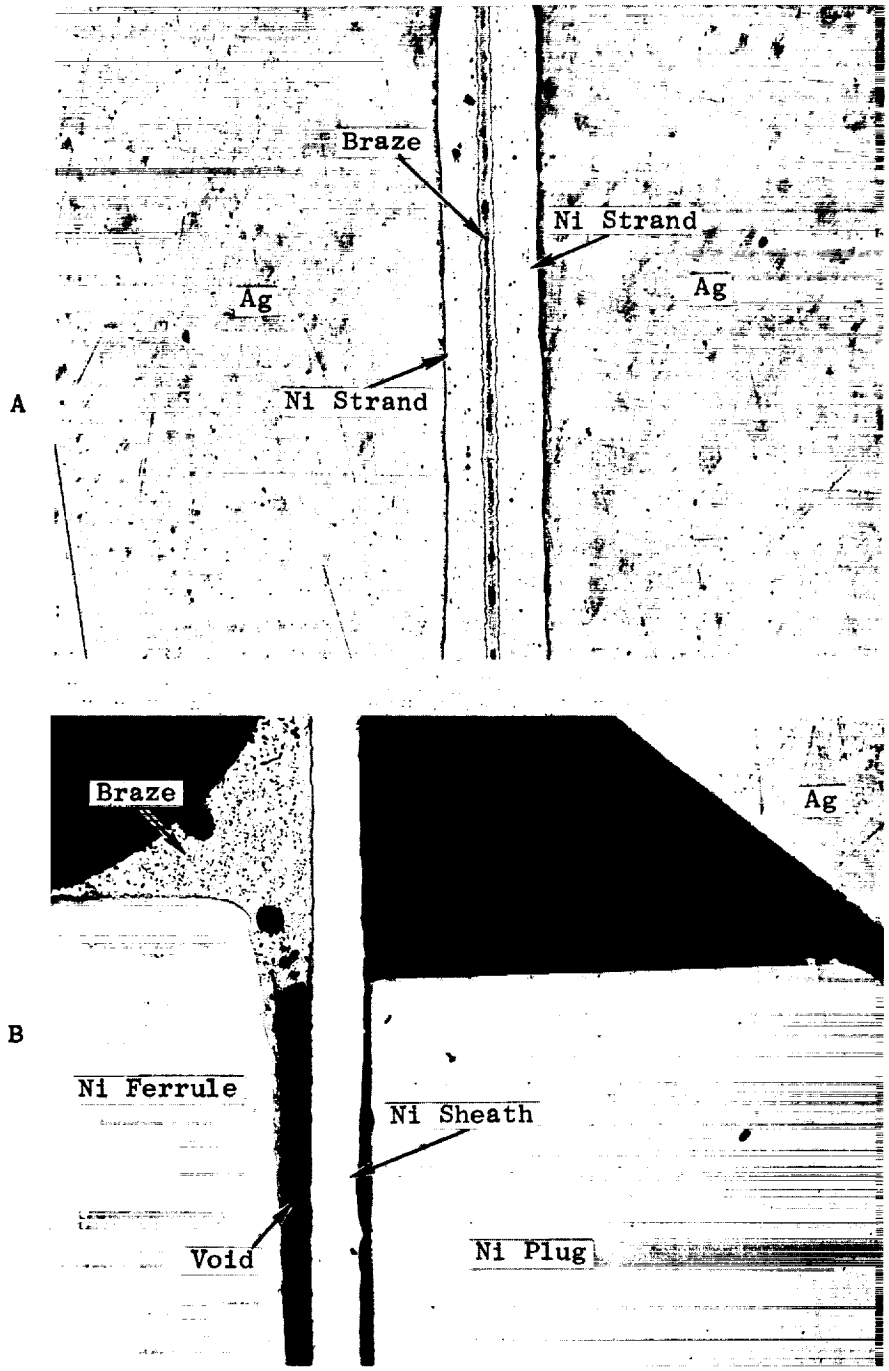

Figure 22. Microphotographs (50X) of Joint Sample #F13 (Outside Strand), Showing (A) Typical Microstructures with Inter-strand Capillary Microshrinkage, and (B), Bridging Tendencies of 7% In Braze Alloy.

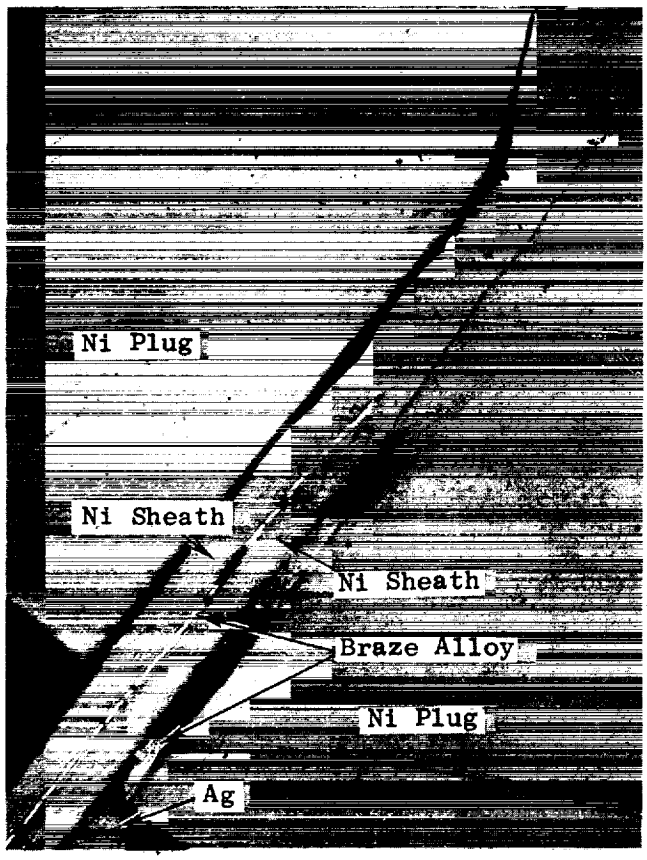

Figure 23. Microphotograph (50X) of Joint Sample #F13 (Middle Strand), Showing Braze Alloy on Plug Side of Sheath Although no Sheath Erosion or Hole is Visible.

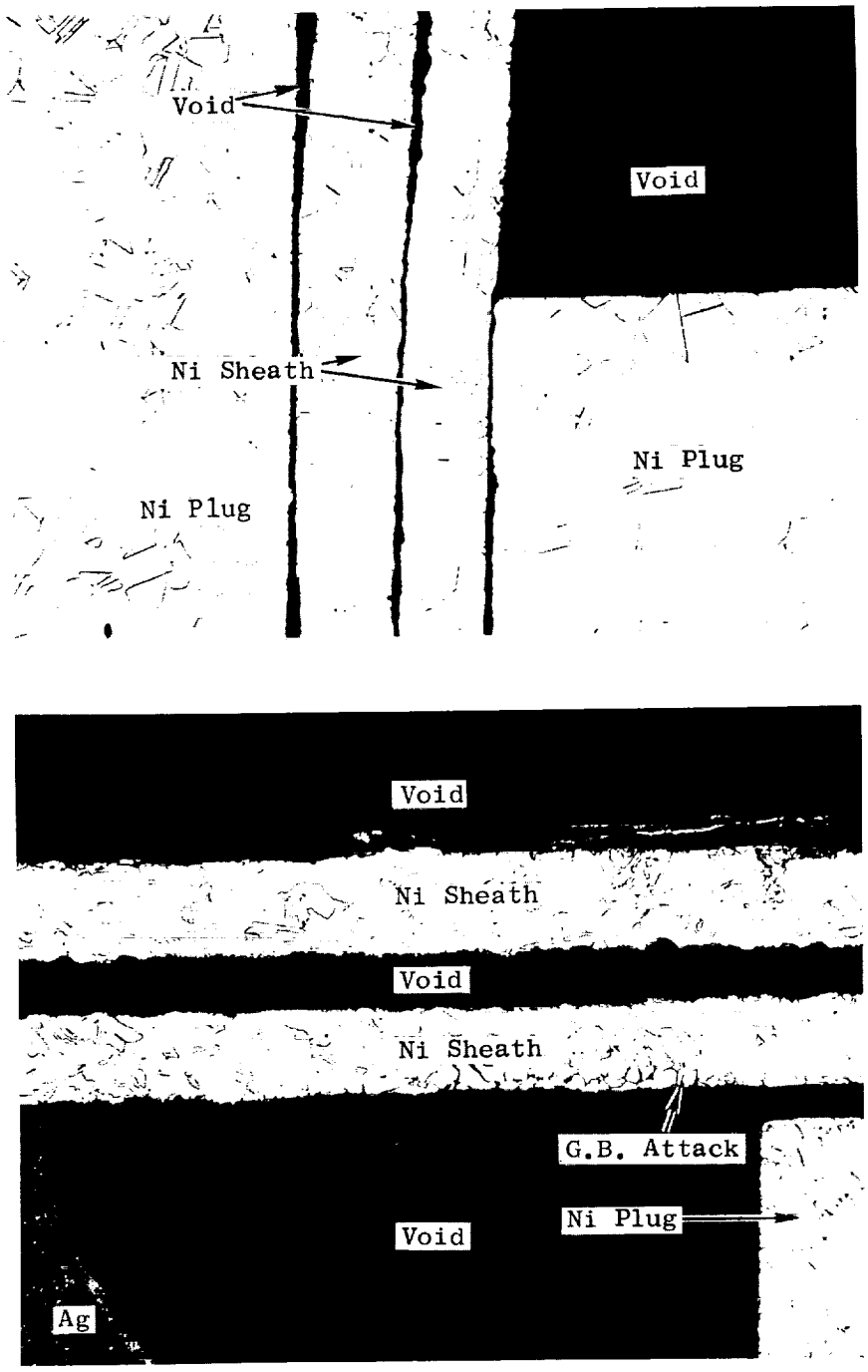

Figure 24. Microphotographs (100X) of Joint Sample #F14, as Welded and not Brazed, Showing (A) A Typical Condition for Most Conductors, but (B) Noticeable Grain Boundary Attach Inside Ni Sheath.

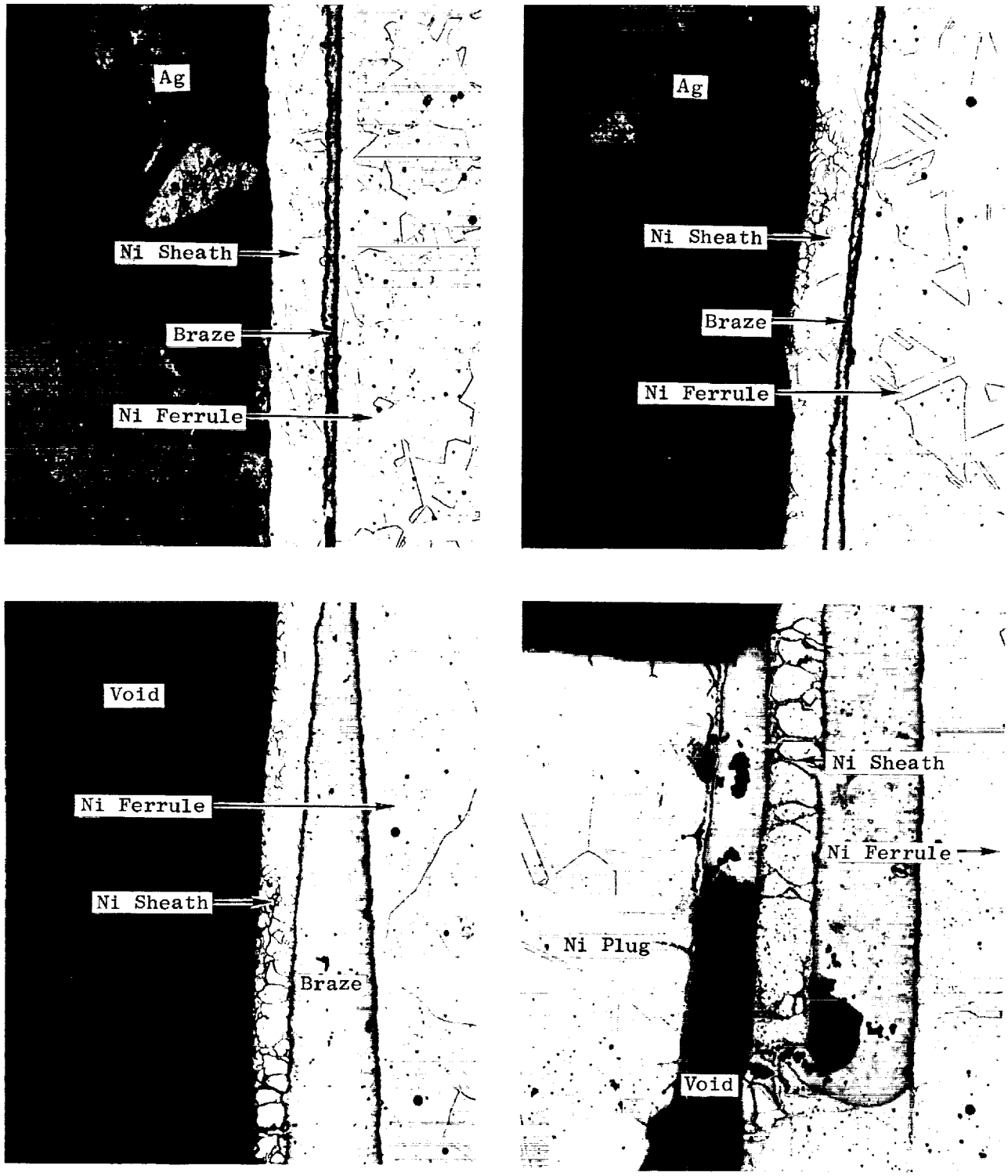

Figure 25. Microphotographs (100X) of Joint Sample #F19, After Brazing, Showing (A,B,&C) Grain Boundary Attack in Nickel Sheath, and (D) Braze Alloy Penetration Through Sheath.

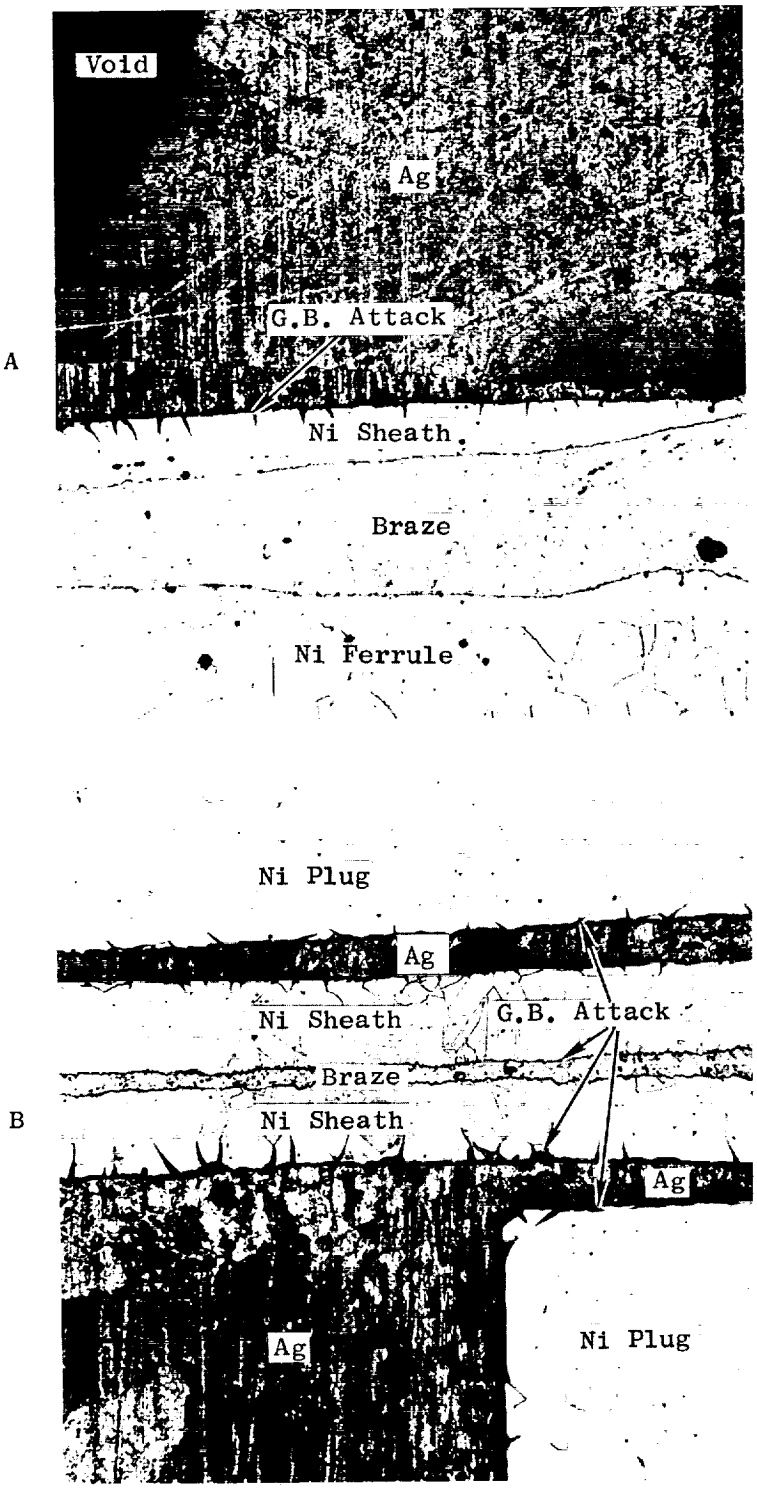

Figure 26. Microphotographs (100X) of Joint Sample #F21, After Brazing with Ge Alloy Showing (A) Sheath Erosion by Braze Plug Grain Boundary Attack (On Inside) and (B) No Erosion by Braze but Again Grain Boundary Attack.

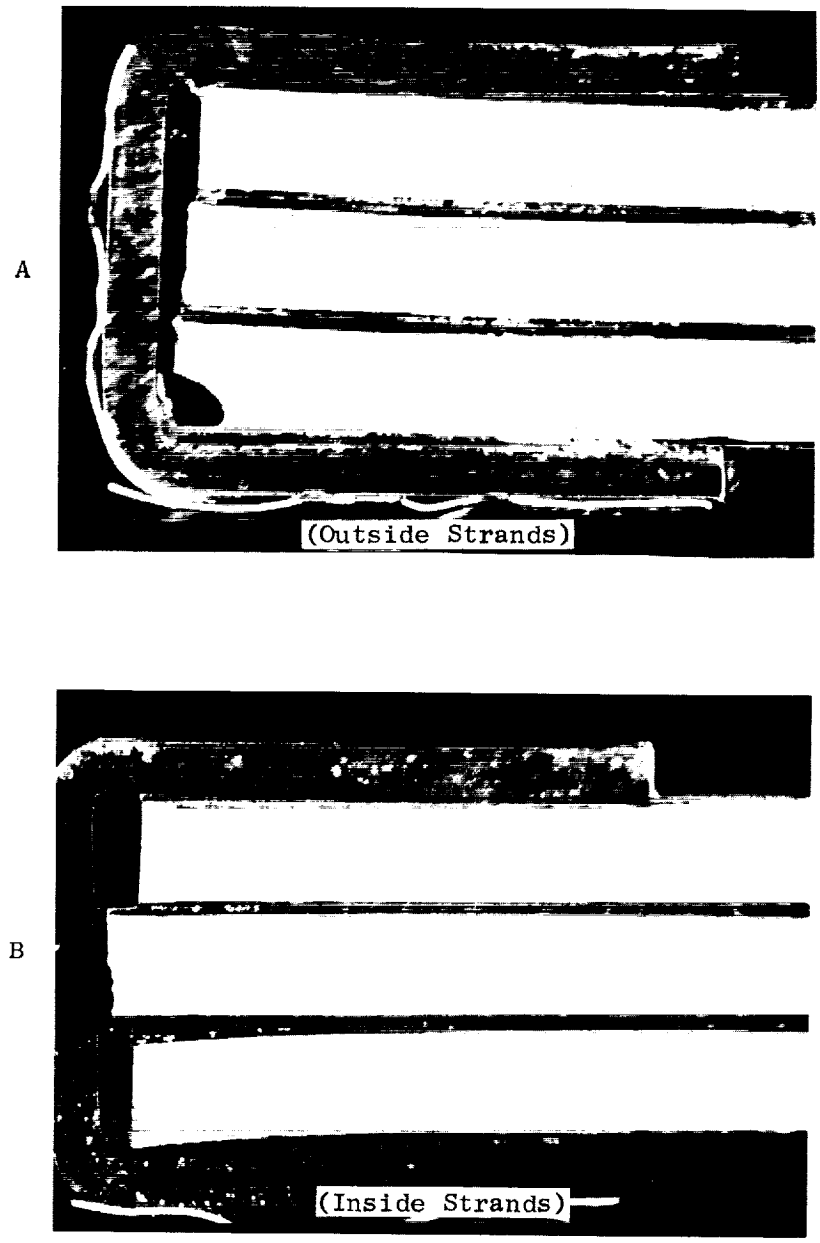

Figure 27. Sections (8.5X) of Joint Sample #F23, Brazed with 5% In Alloy, Below Melting Point of Silver, and with no Sealing of Ends of Strands or Silver Melting.

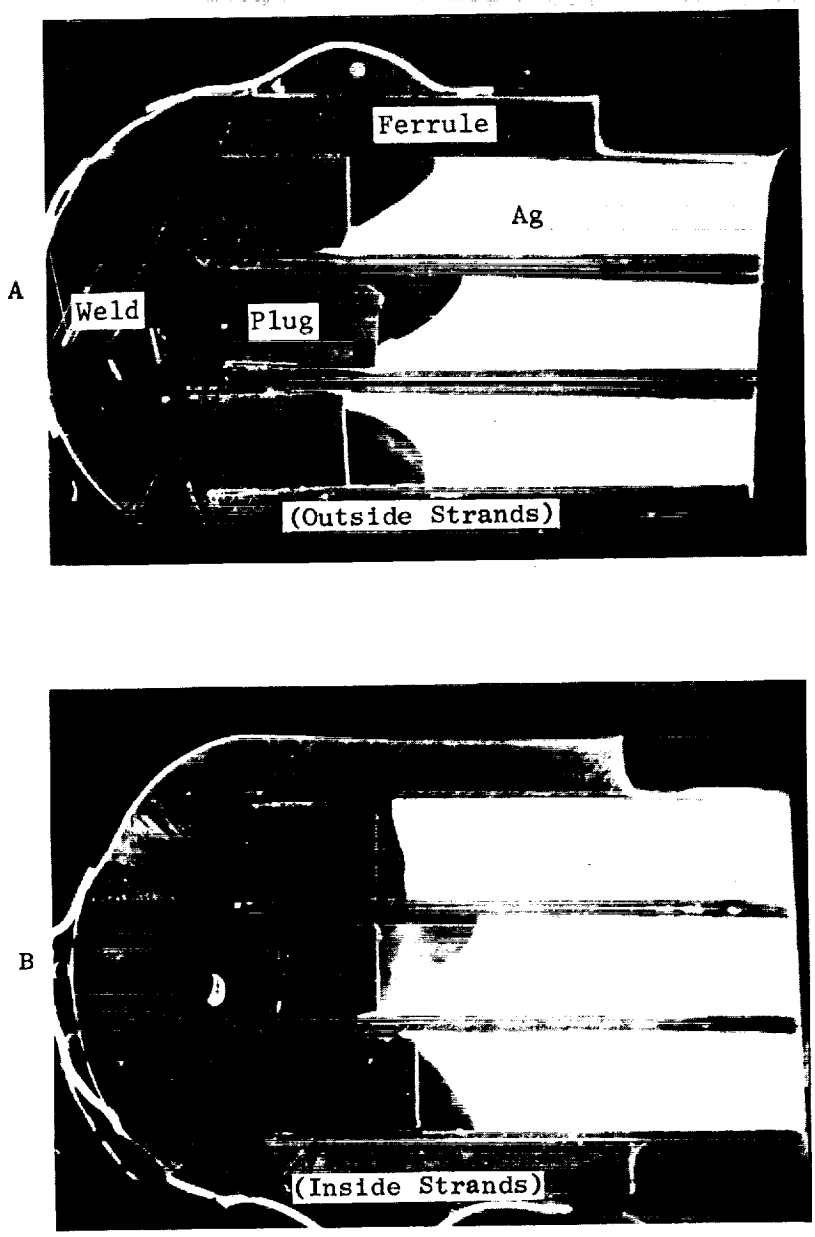

Figure 28. Sections (8.5X) of Joint Sample #F25, Brazed with 5% In Alloy, Showing Full Cross Sections with Conductor Ends Sealed with Nickel Plugs and Some Silver Melting.

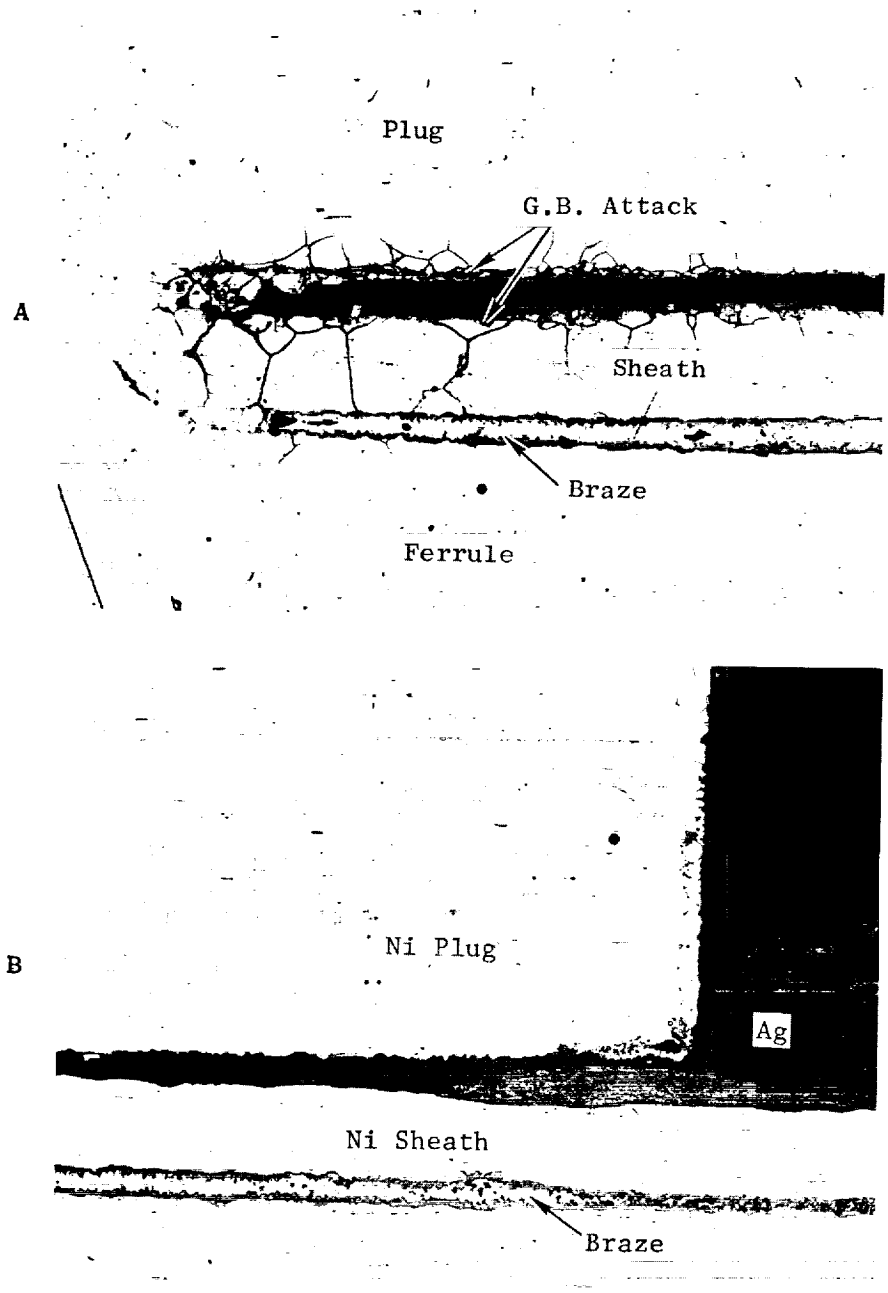

Figure 29. Microphotographs (100X) of Sample #F25, Brazed with 5% In Alloy, Showing (A) Grain Boundary Separation but (B) Good Braze Flow without Nickel Erosion or Silver Melting.

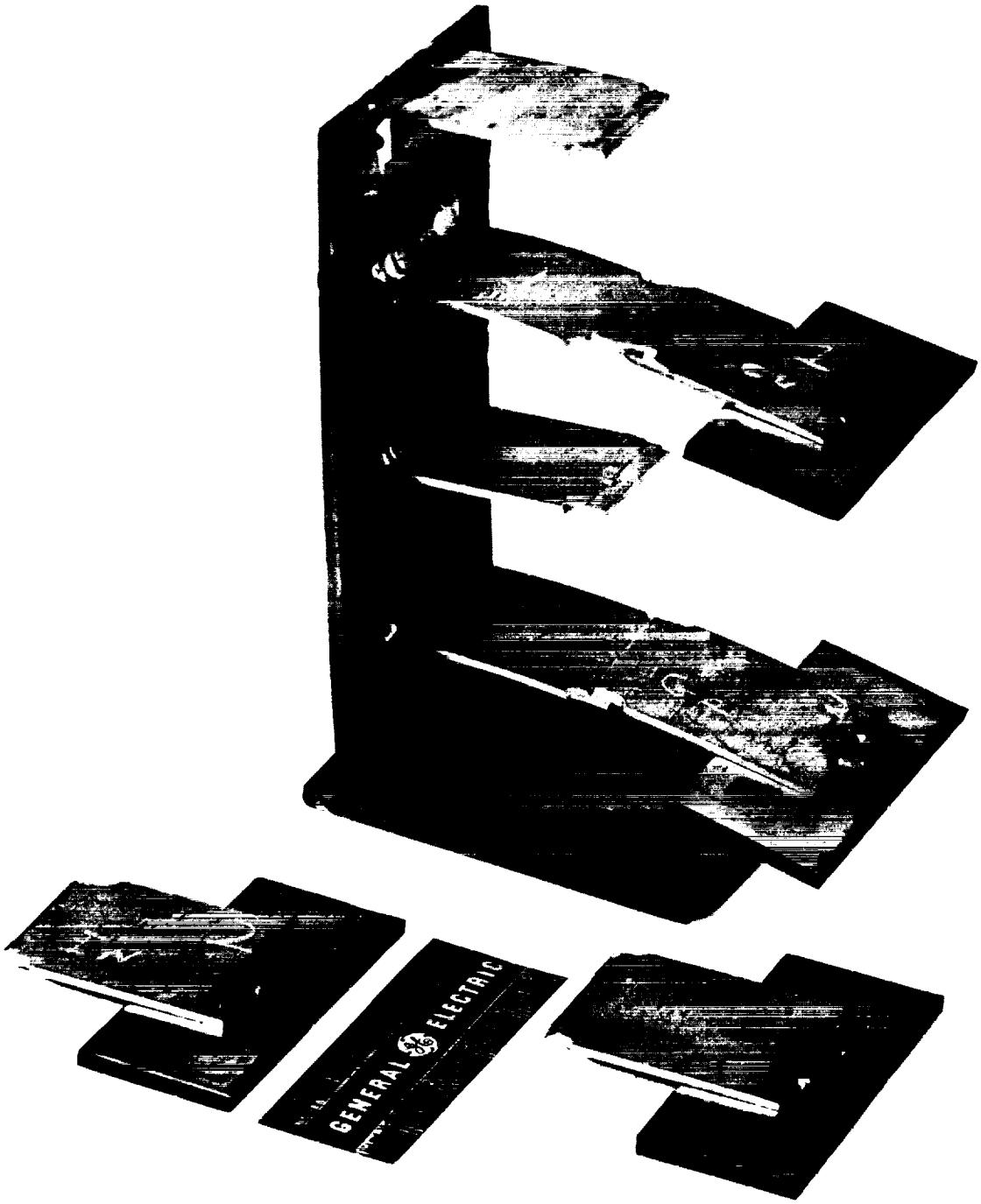

Figure 30. Results from Test to Check Strength of Joints Brazed with Different Alloys, with those of In Alloy Having Failed Between 1475°F and 1500°F.

Figure 31. Front (A) and Back (B) Sides of Sample Braze Alloy Tests Using 0.002 Inch Thick Nickel, After 15 Seconds at 1780°F, with Center Sample (Au-20Cu) Having Eroded Through the Nickel but Others Okay.

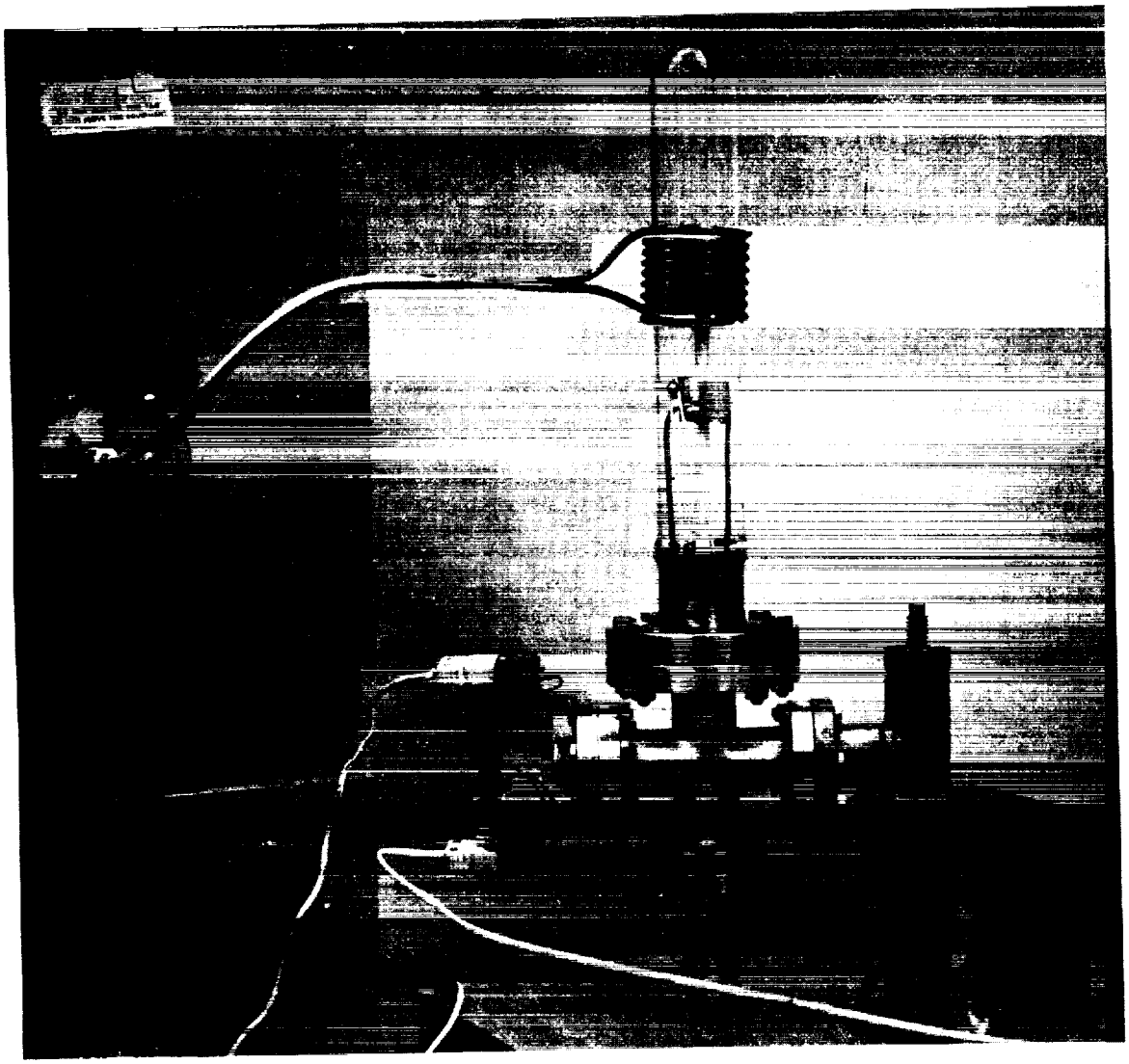

Figure 32. Test Equipment and Test Set-up for Au-Ni-In Braze Alloy Sample Evaporation Test Showing Induction Heating Coil Around Evacuated and Argon Filled Test Chamber.

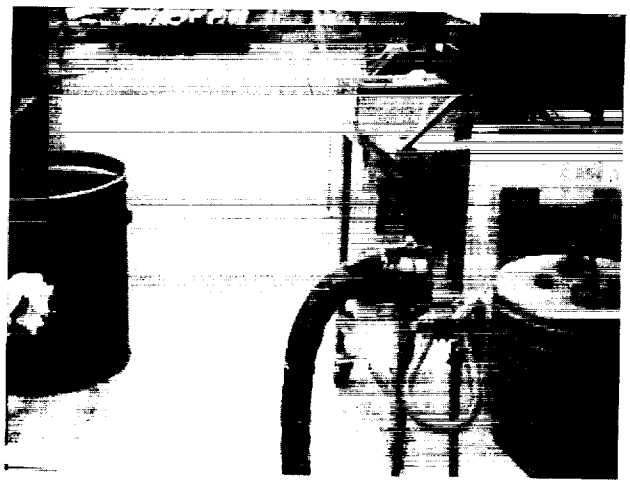

A - 450 Kc output transformer at right, with water and power leads connecting to test chamber and coil.

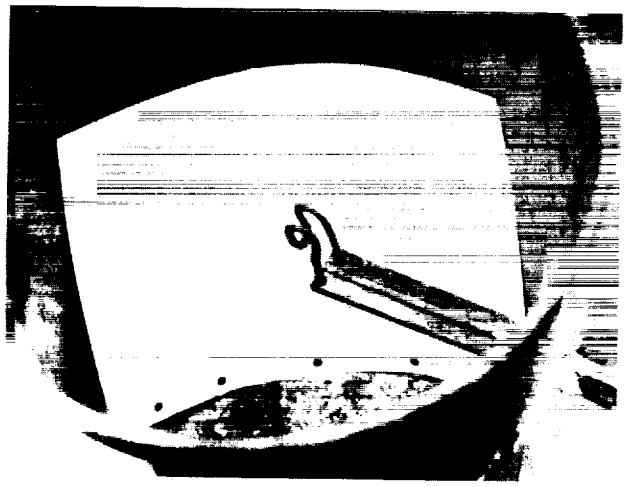

B - Initial "hairpin" peripheral coil.

C - Modified "hairpin" coil with extra turn under main coil, sealed into test chamber with silicon rubber.

Figure 33. Preliminary Enclosure and Trial Coils for Development Brazing of Joint Samples using 450 KC Induction Heating Equipment.

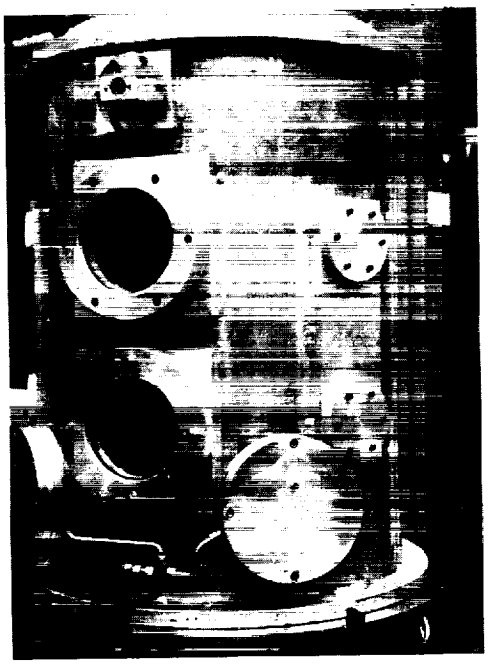

Braze Tank in Place with Viewing Ports (Center) and Glove Ports Each Side Cover Center.

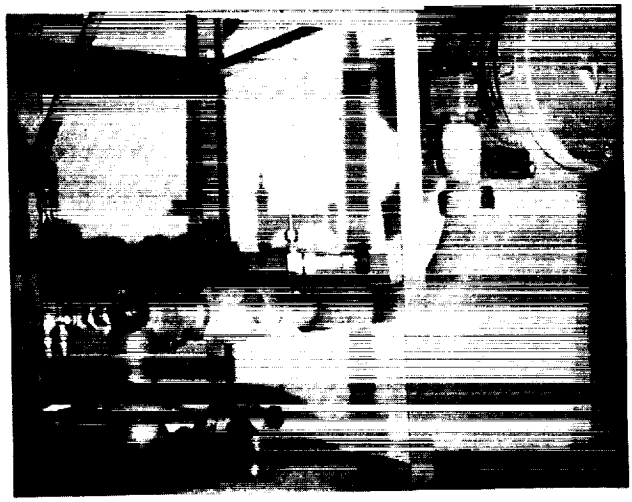

Vacuum Pump Attached to Braze Tank Through Large Manifold and Vacuum Valve, with Thermocouple Gage Mounted at Right and Power Leads Behind.

Close-up View of Induction Heating Coil and Adjustable Support, with Power Leads from Potted Feed-Thru, O_2 Analyzer Detector at Right, and T/C Switch in Rear.

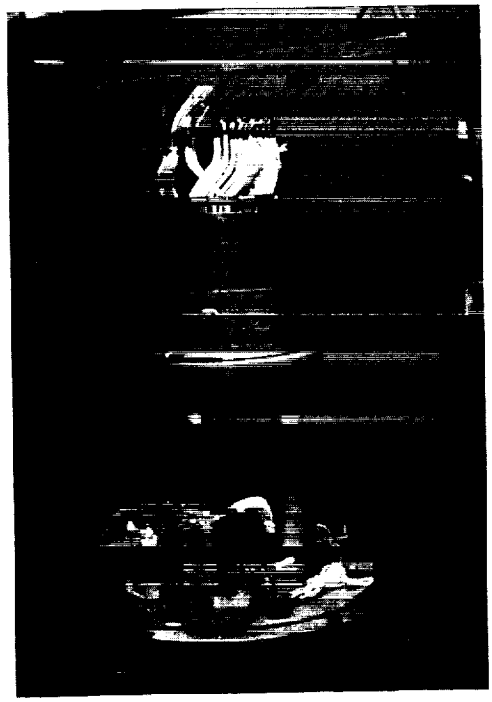

Tank Cover Removed to Show Stator with Trial Coils in Fixture During Set-up for Brazing Operation.

Figure 34. Set-up of Production JointBrazing Equipment with Vacuum Purged Braze Tank, Heating Coil, and Stator Support Fixture, for Brazing Coil Joints.

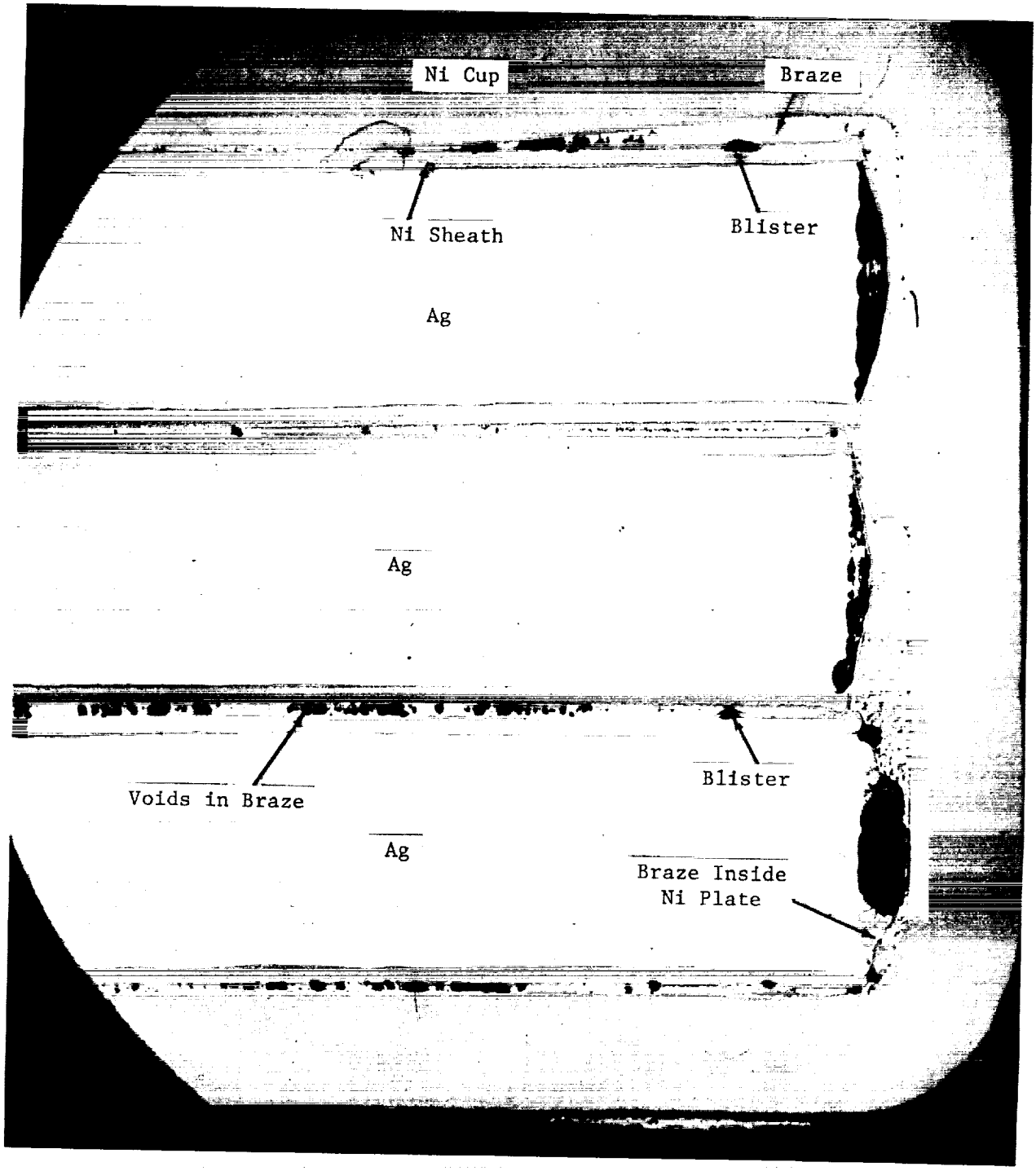

Figure 35. Section (25X) of Brazed Joint Sample #P5, Showing Nickel Plating Blister Defects, and Leaking of Braze Into Conductors.

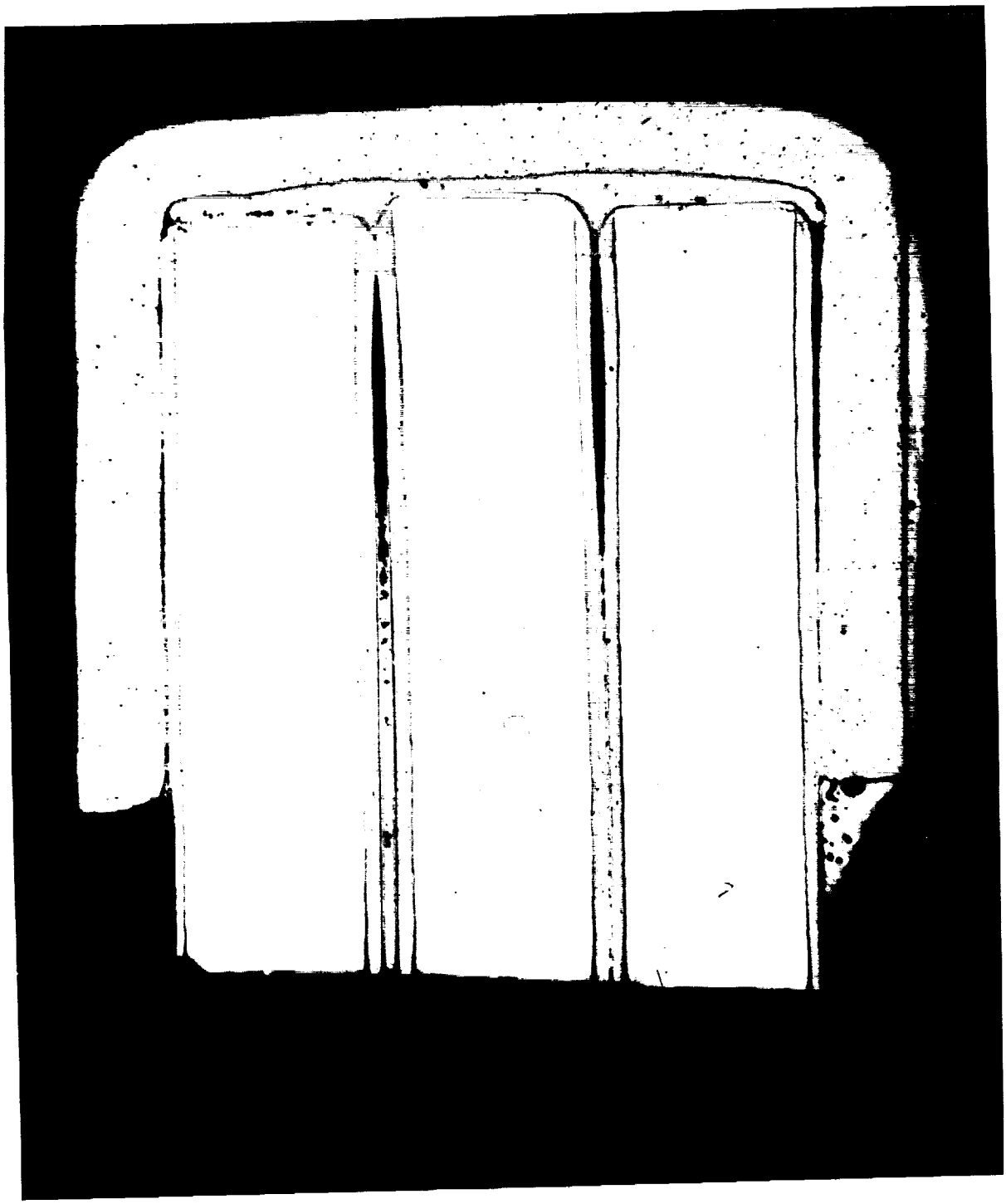

Figure 36. Section (20X) of Brazed Joint Sample #9 with Good Nickel Plate Over Conductor Ends, and Generally Good Braze Alloy Flow Into Nickel Cup and Up Between Strands.

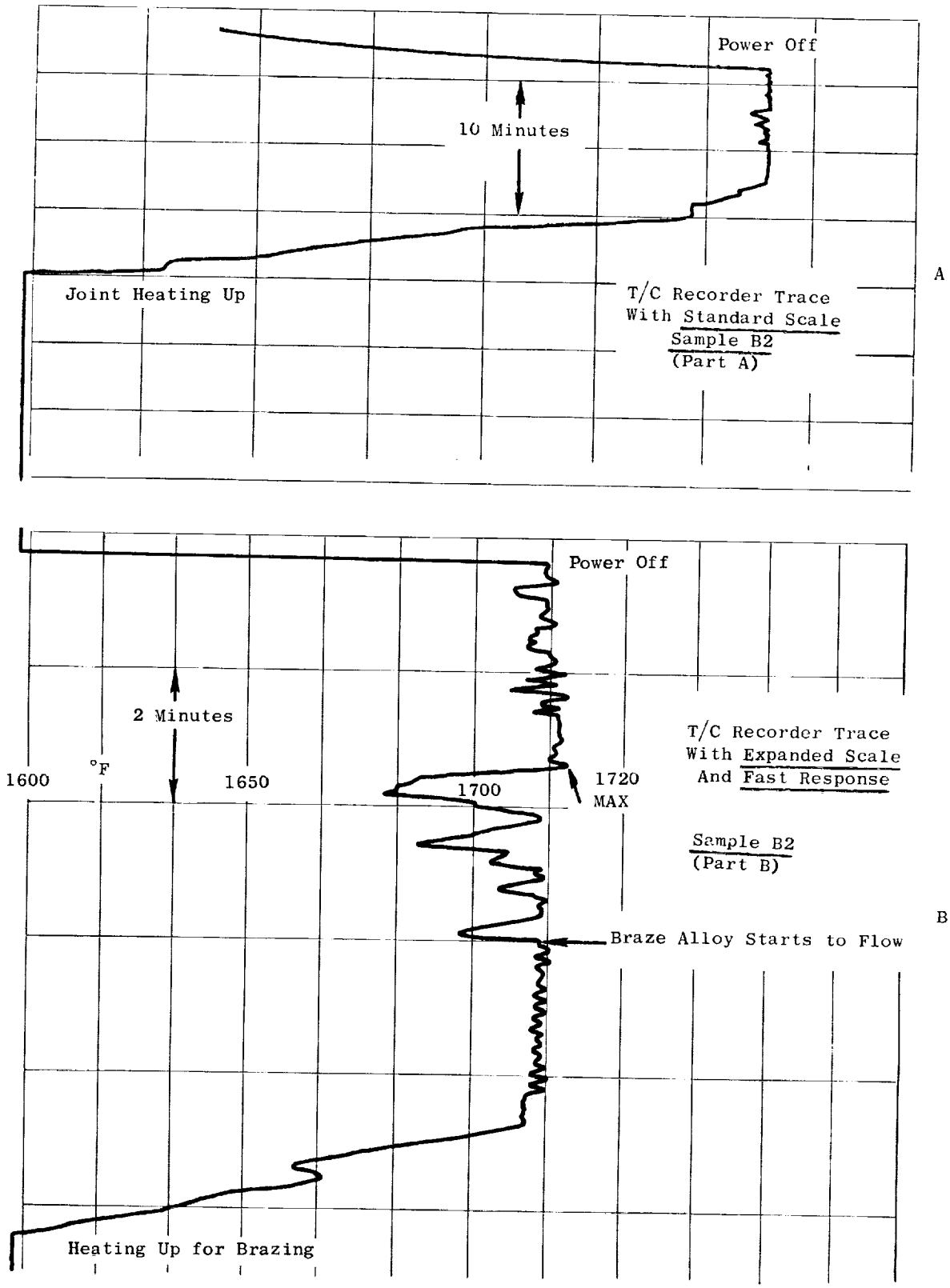

Figure 37. Records of Sample Joint Thermocouple Output During Braze Cycle for Sample #B2, With the Chart (A) Showing the Complete Temperature Cycle and (B) The Amplified Trace From the Fast Response Controller.

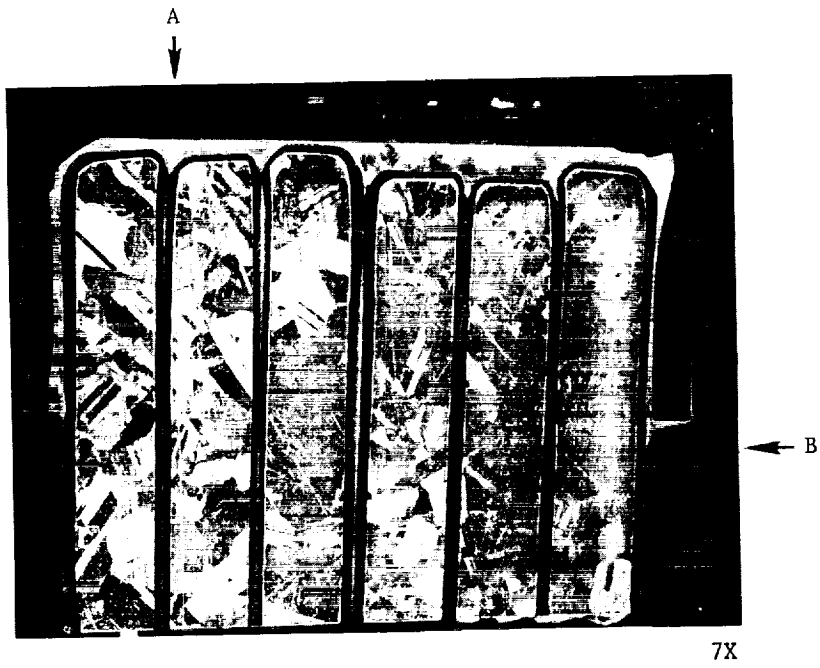

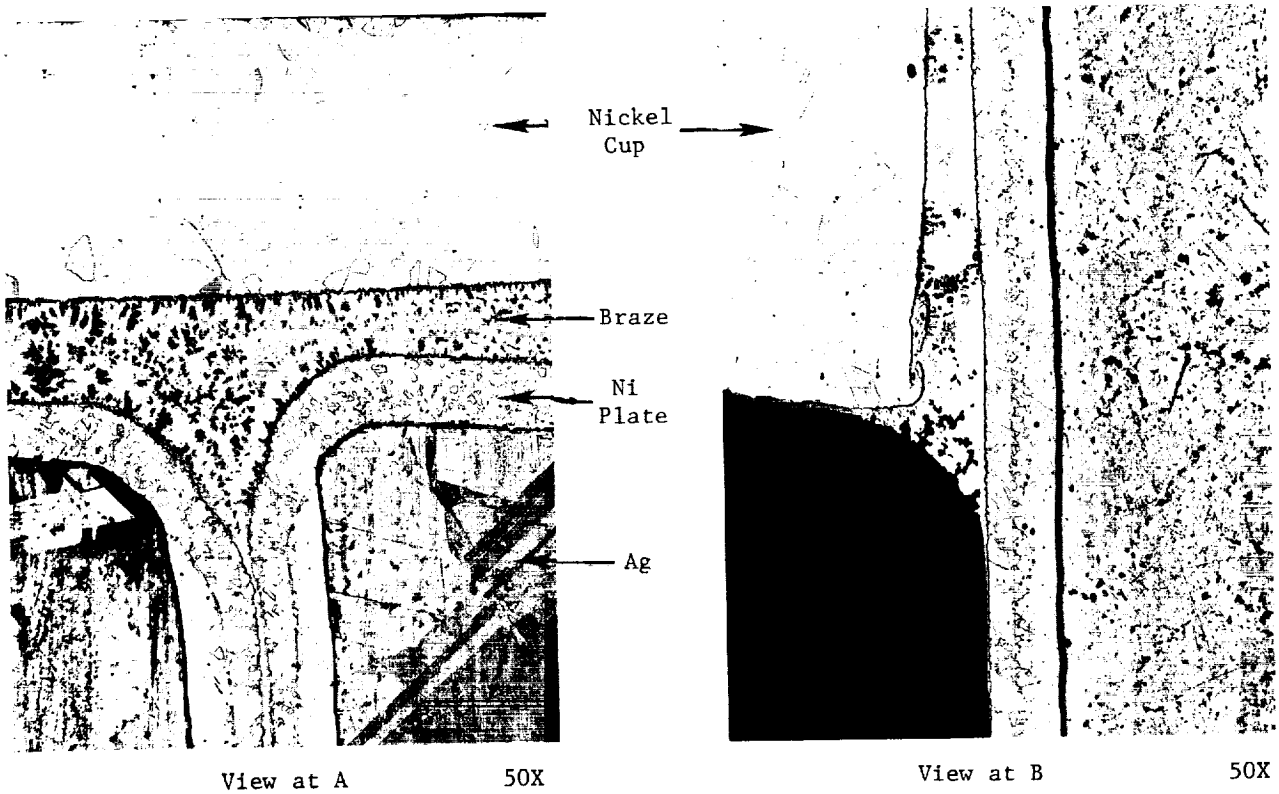

Figure 38. Sections of Joint Sample B2, Showing Six of the Strands After Brazing, at 7X, and 50X Microphotos of the Joint at Point A (End of Strand) and B (Entrance of Braze).

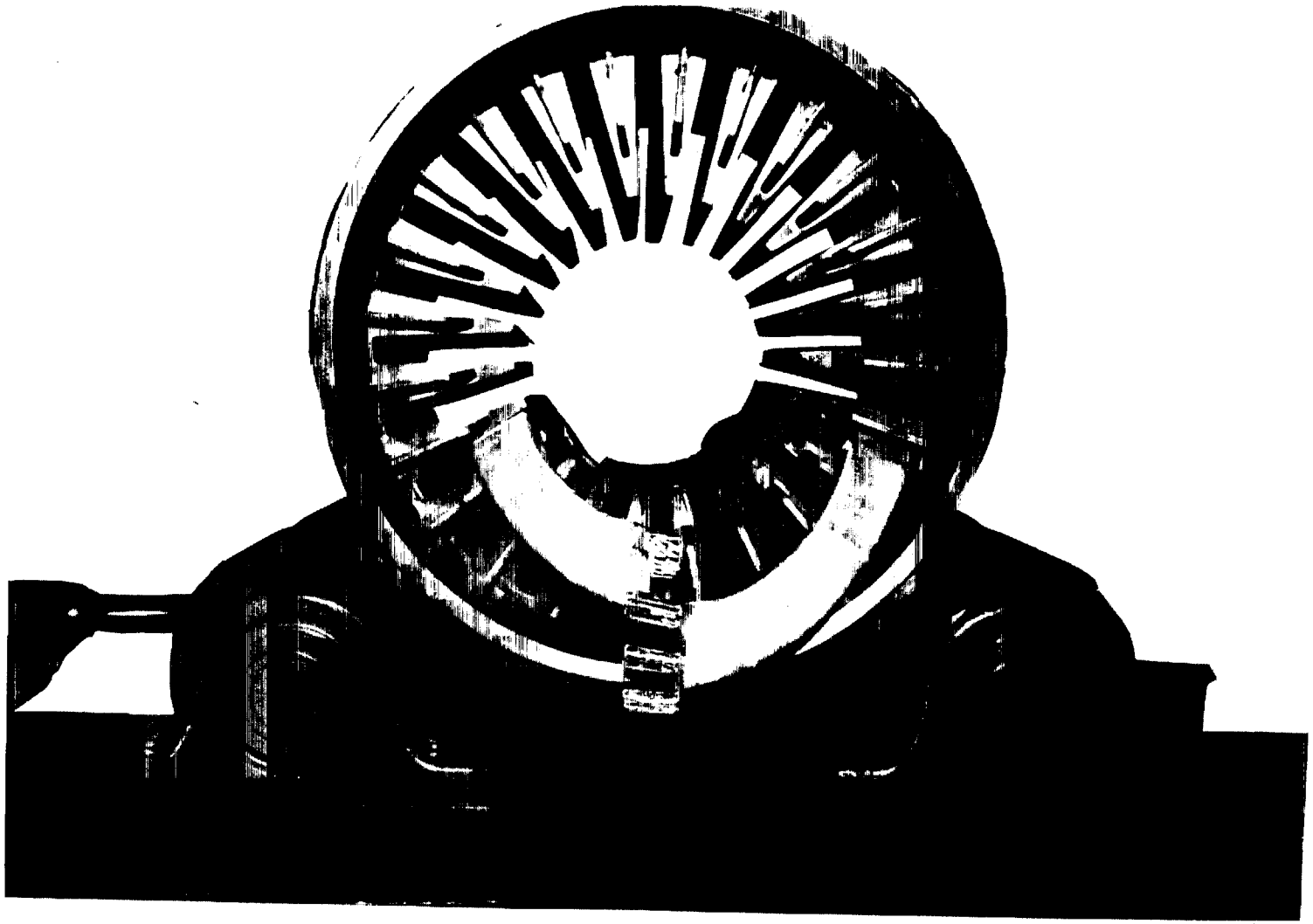

Figure 39. EM Pump Unwound Stator with Trial Bars Inserted in Laminated Core Slot to Check Winding Connection Arrangement.

Figure 40. End of Coil Bar Consisting of Four Conductors (Each with Six Wires) Being Formed for the End Winding Connecting While Temporarily Held Together with Mylar (Sacrifice) Tape.

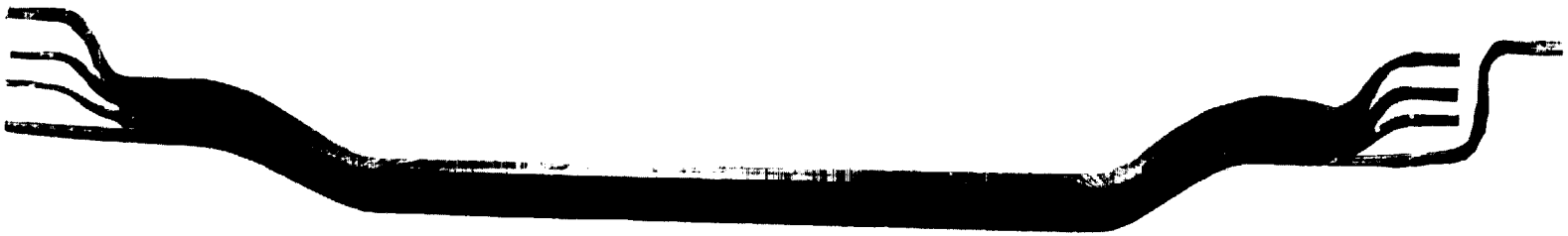

Figure 41. A Typical Upper Bar or Coil Side, with Conductor Ends Formed While Wires are Held by Sacrifice Tape, Prior to Nickel Plating (Sealing) of the Ends.

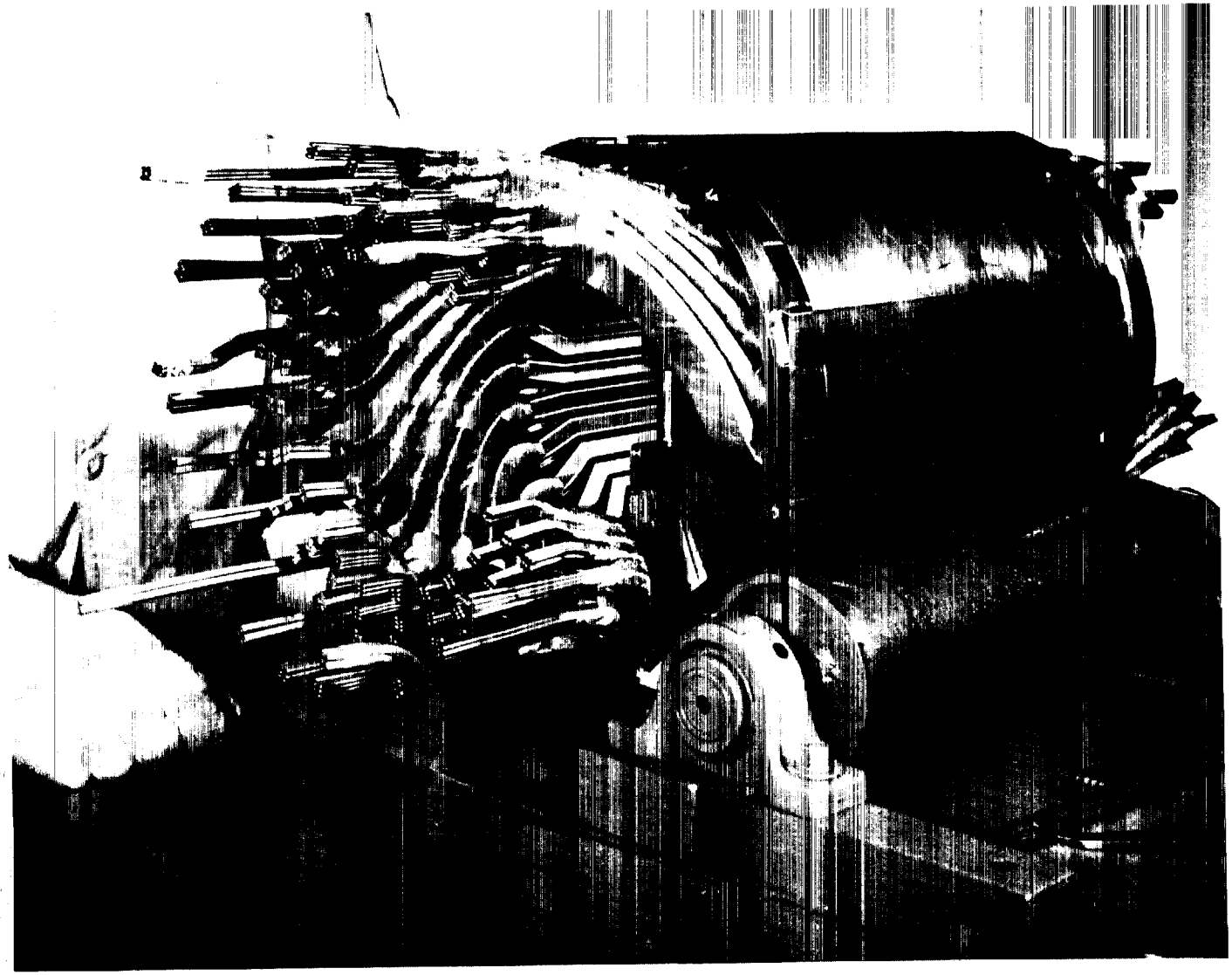

Figure 42. Coil Bars, or Sides, Being Inserted in Stator Iron Core, with Alumina Liners Visible in the Slots, and Coil Ends Covered with "S" Glass Tape.

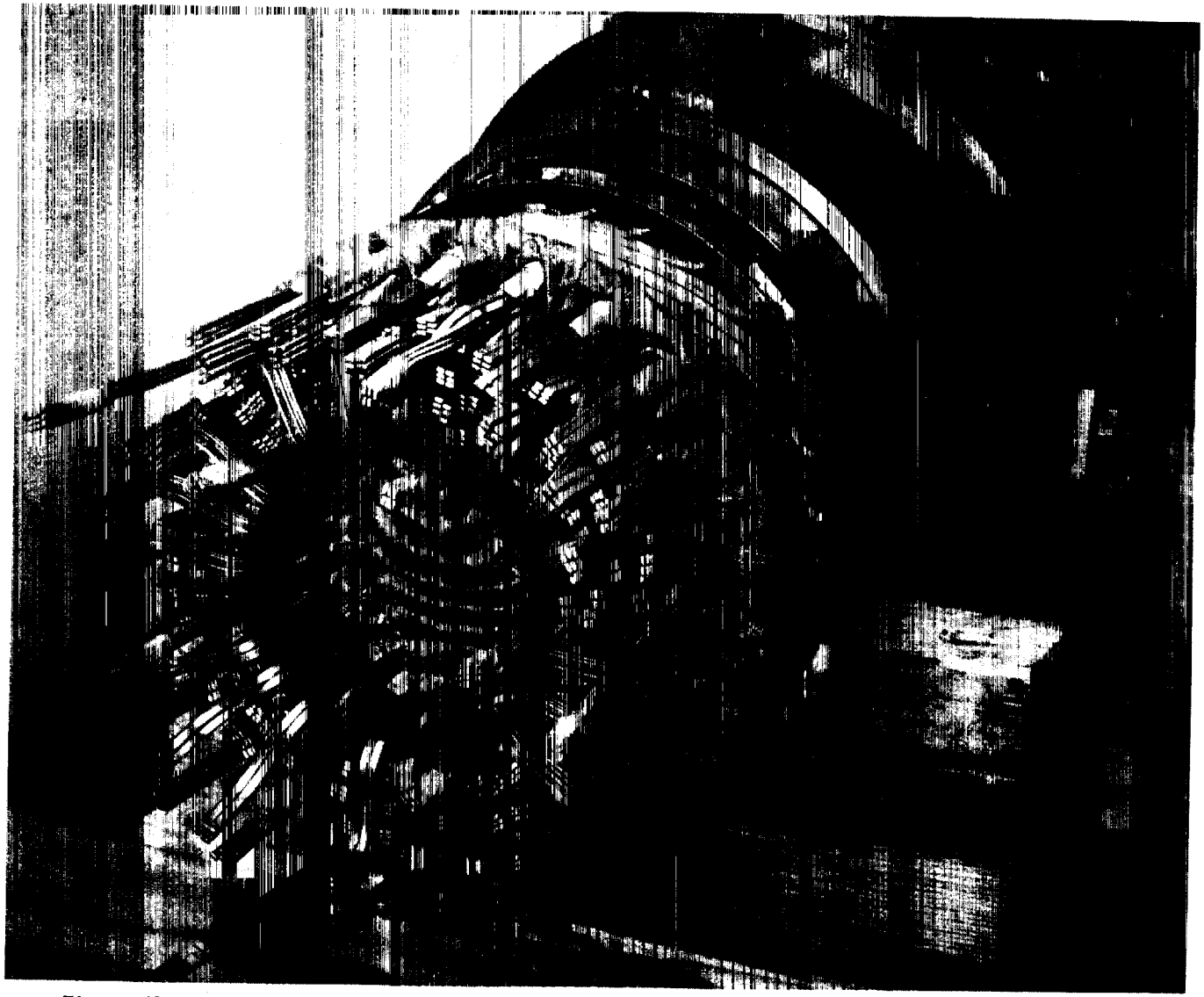

Figure 43. All Coil Bars, or Sides, Assembled in Stator Core with Holding Fixture Attached, Ready for Placement in Brazing Tank and Start of End Joint Brazing.

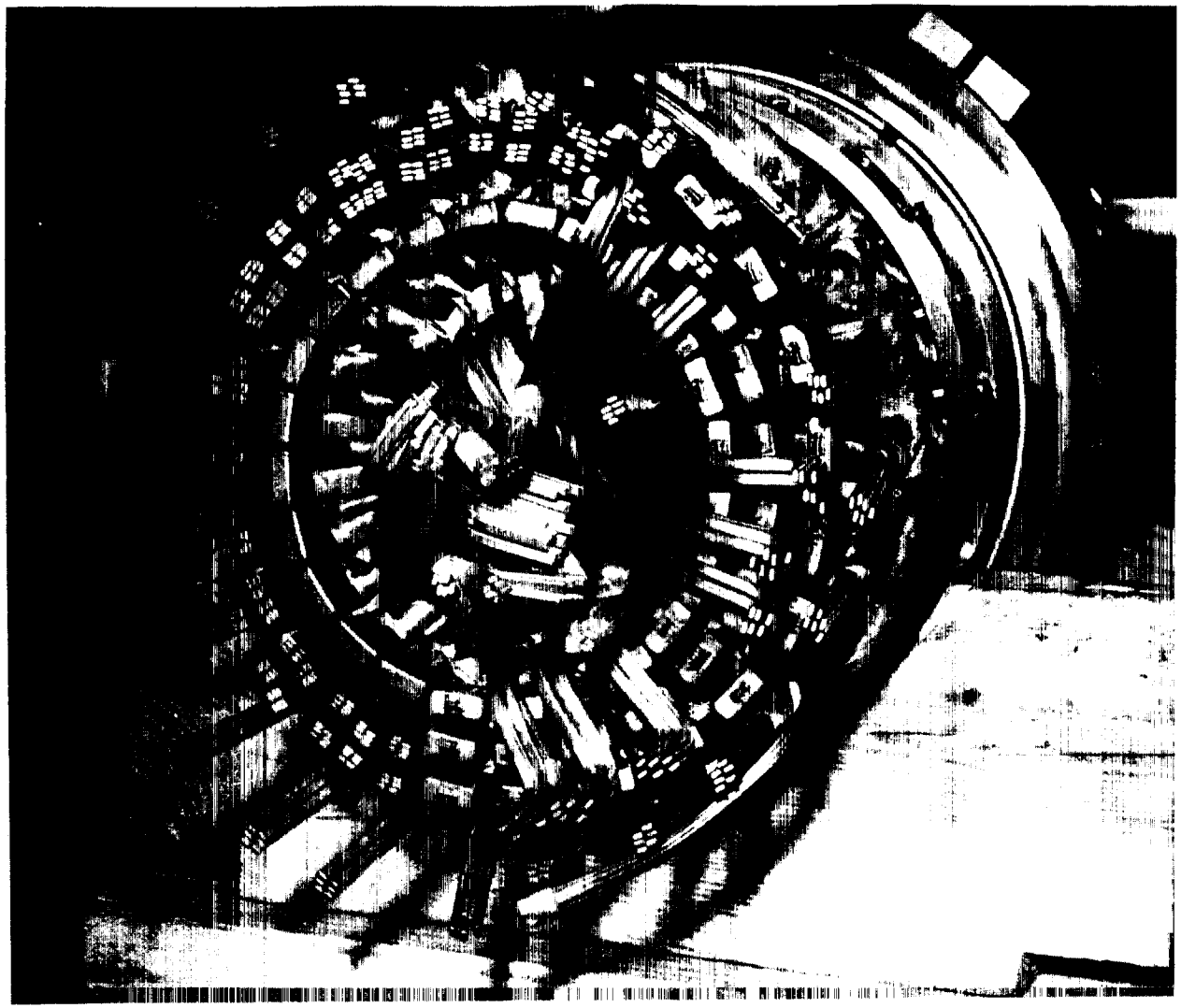

Figure 44. Stator, Viewed from Connection End, with Half of End Joints Brazed and the Balance of the Inner Row with Nickel Cups in Place Ready for T/C Attachment and Brazing.

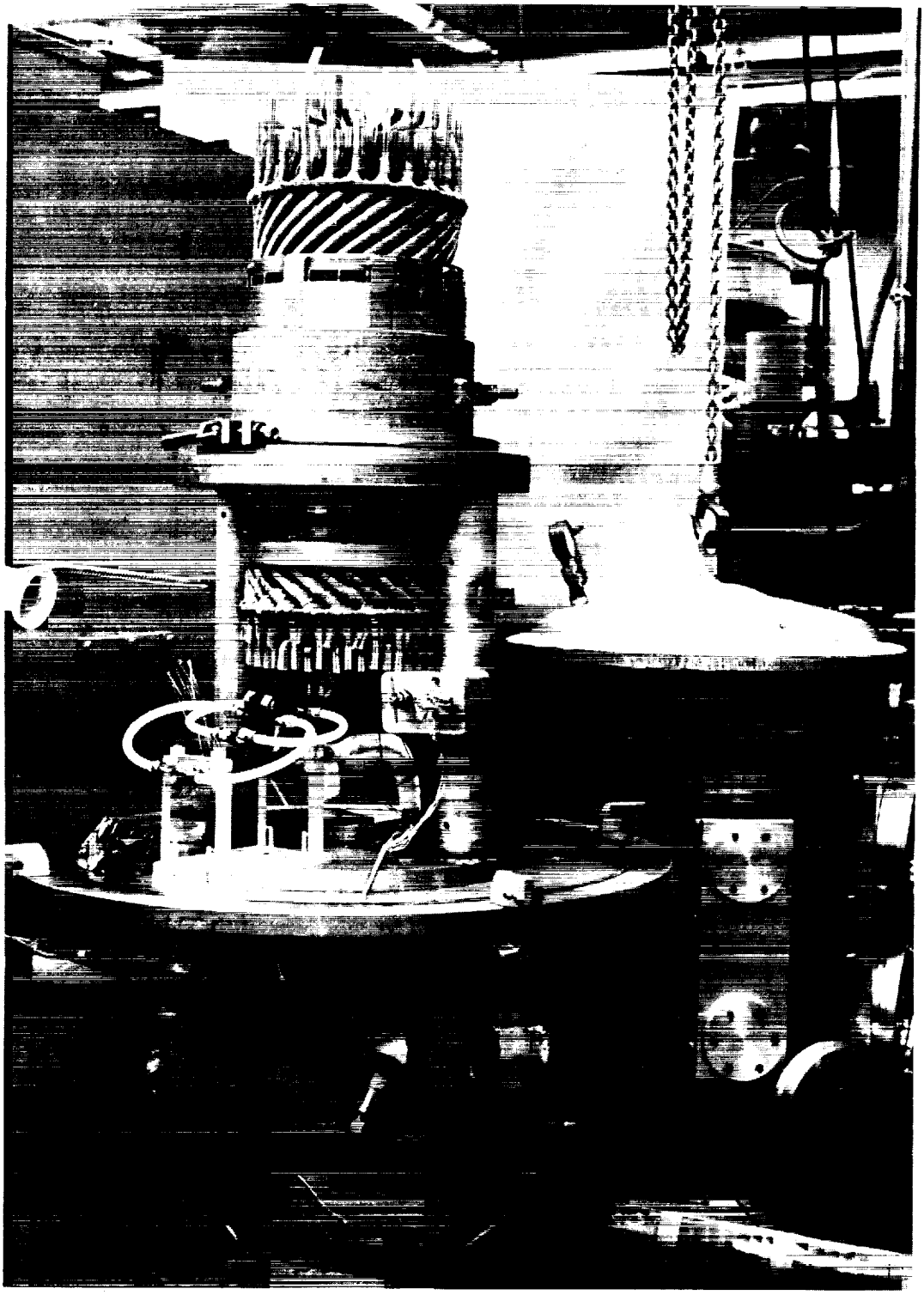

Figure 45. Wound Stator Mounted in Braze Tank Supporting Fixture and Induction Coil Being Positioned for Making a Brazed Joint, Just Prior to Placing the Tank Top on the Base.

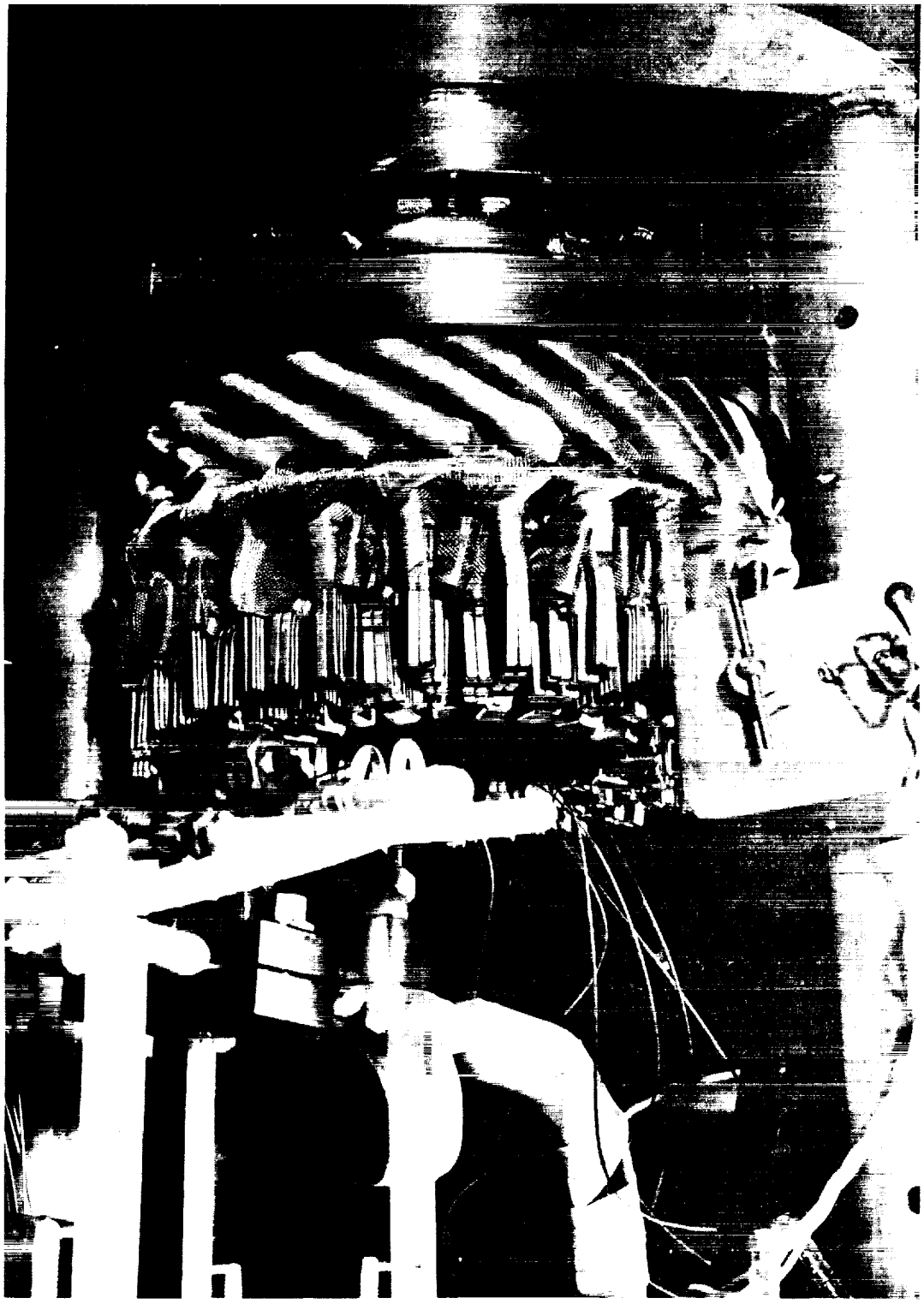

Figure 46. Coil End Joint with Nickel Cup in Place, and Induction Heating Coil Ready for Final Positioning for Brazing Cycle.

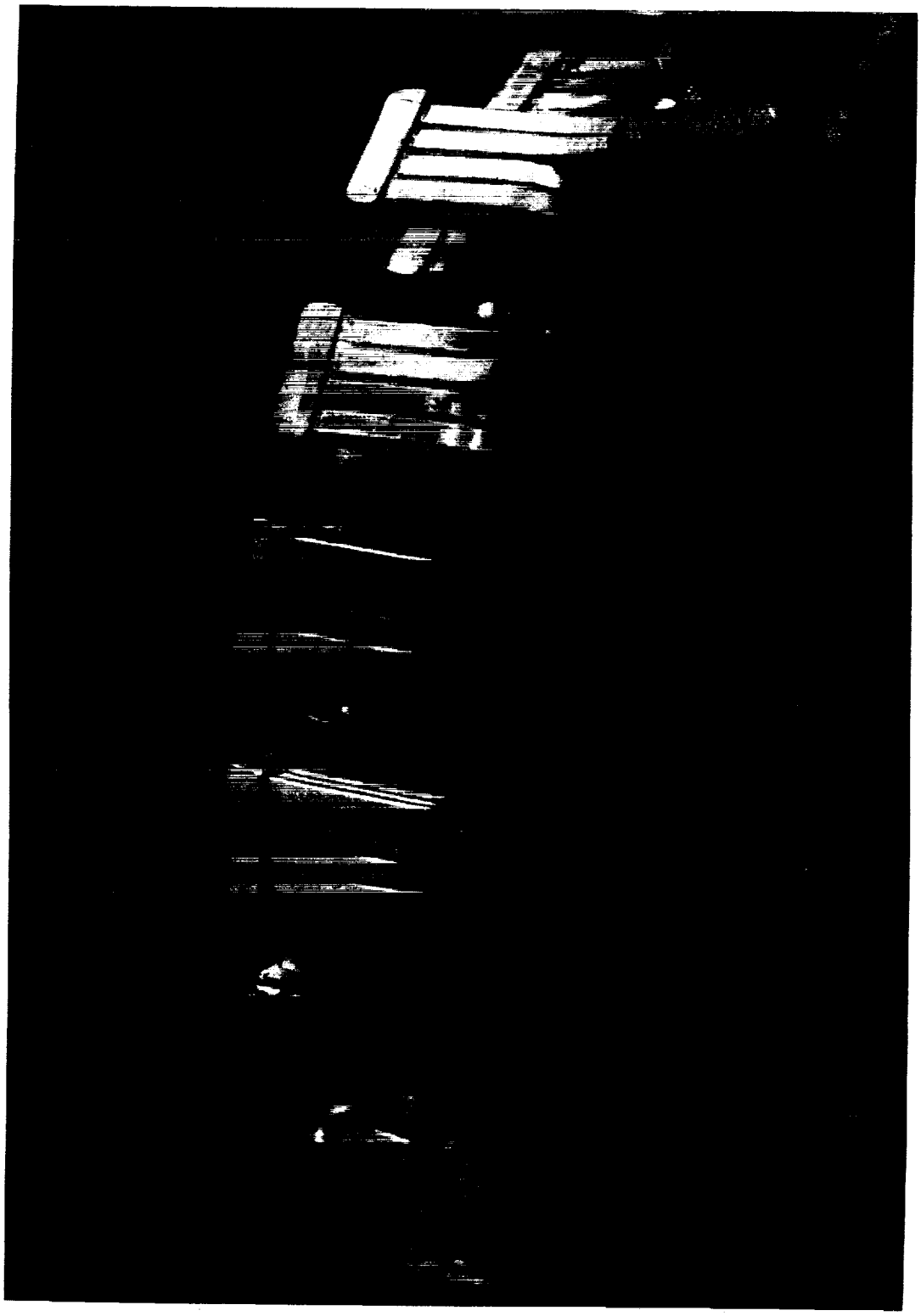

Figure 47. Outer Row of Coil Joints on the Stator Opposite Connection End, After Brazing and Removal of Thermocouples, with Braze Alloy Well up Between the Wires.

Figure 48. Coil (Bar) Joints (Opposite Connection End of Stator) After Brazing and Final Insulation with "S" Glass Tape.

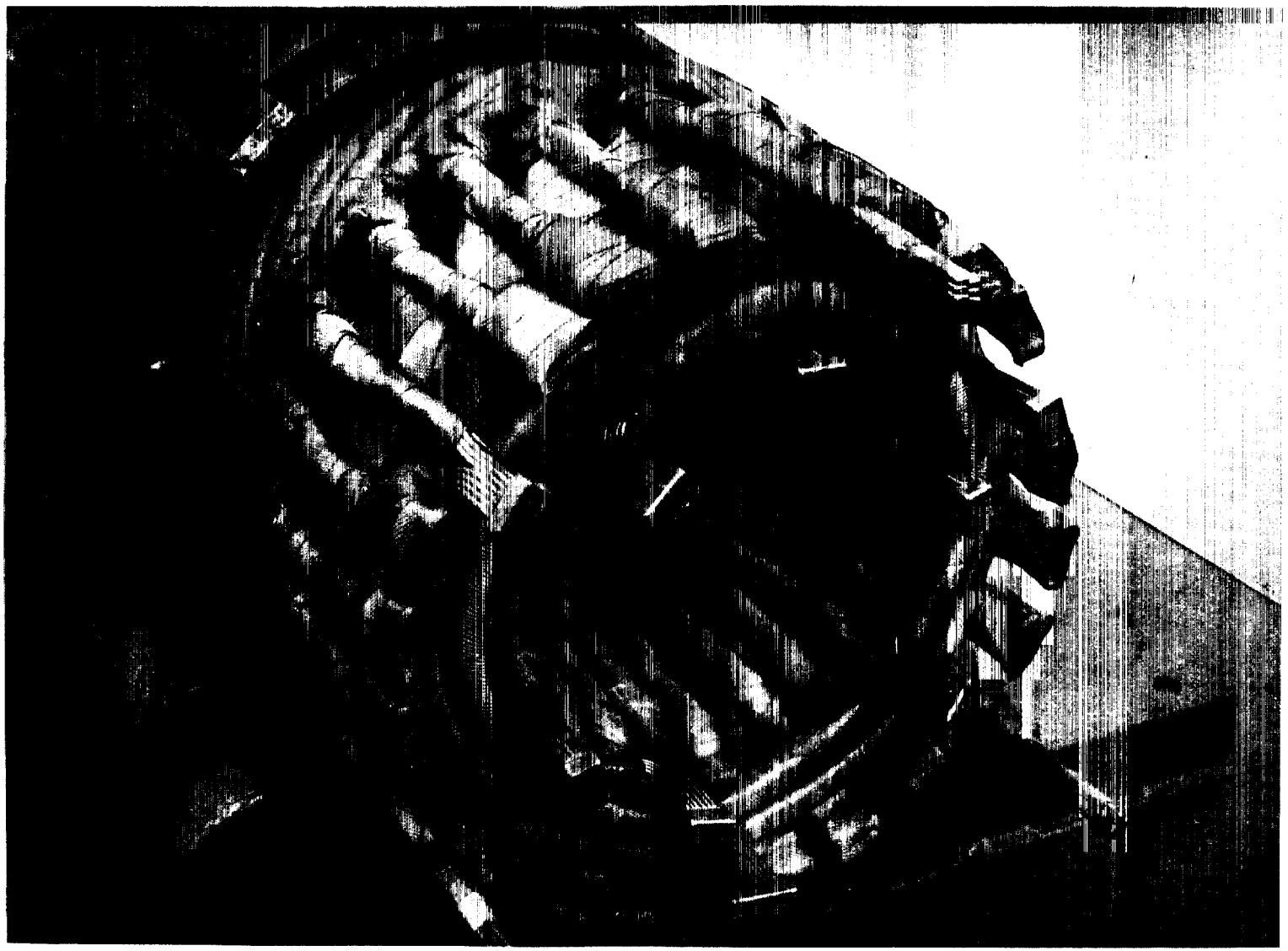

Figure 49. Coil Joints (Connection End of Stator) After Brazing and Final Insulation of Bar and Series Connections, with Pole-Phase and Wye Neutral Connections Brazed but not Insulated, and Line Connections Ready for Attachment to Lead Seal Jumpers in Final Assembly.

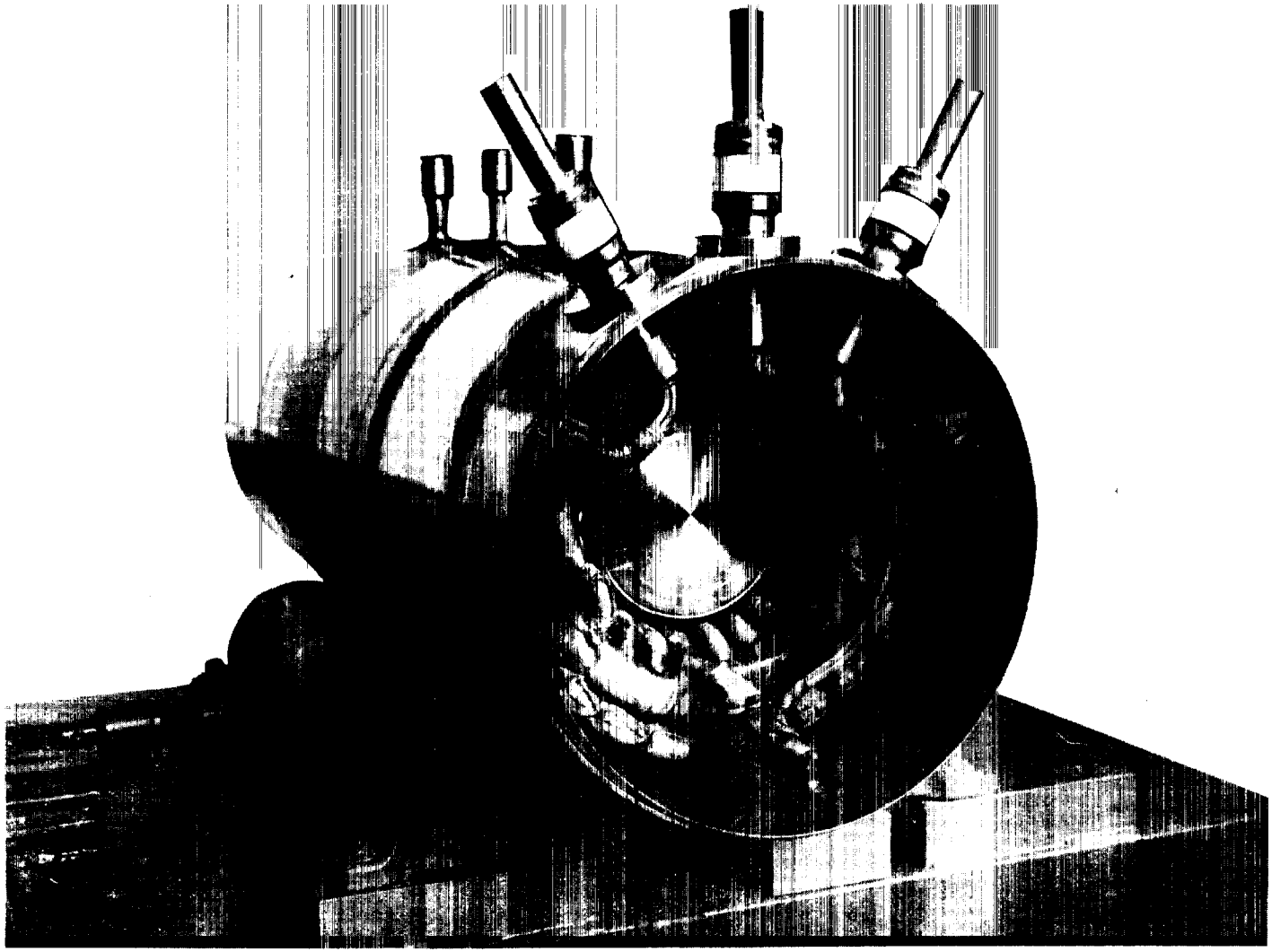

Figure 50. Assembled Stator Viewed from Connection End Prior to End Shield Attachment, Showing Lead Seal Jumpers Brazed to Coils and Joints Taped.

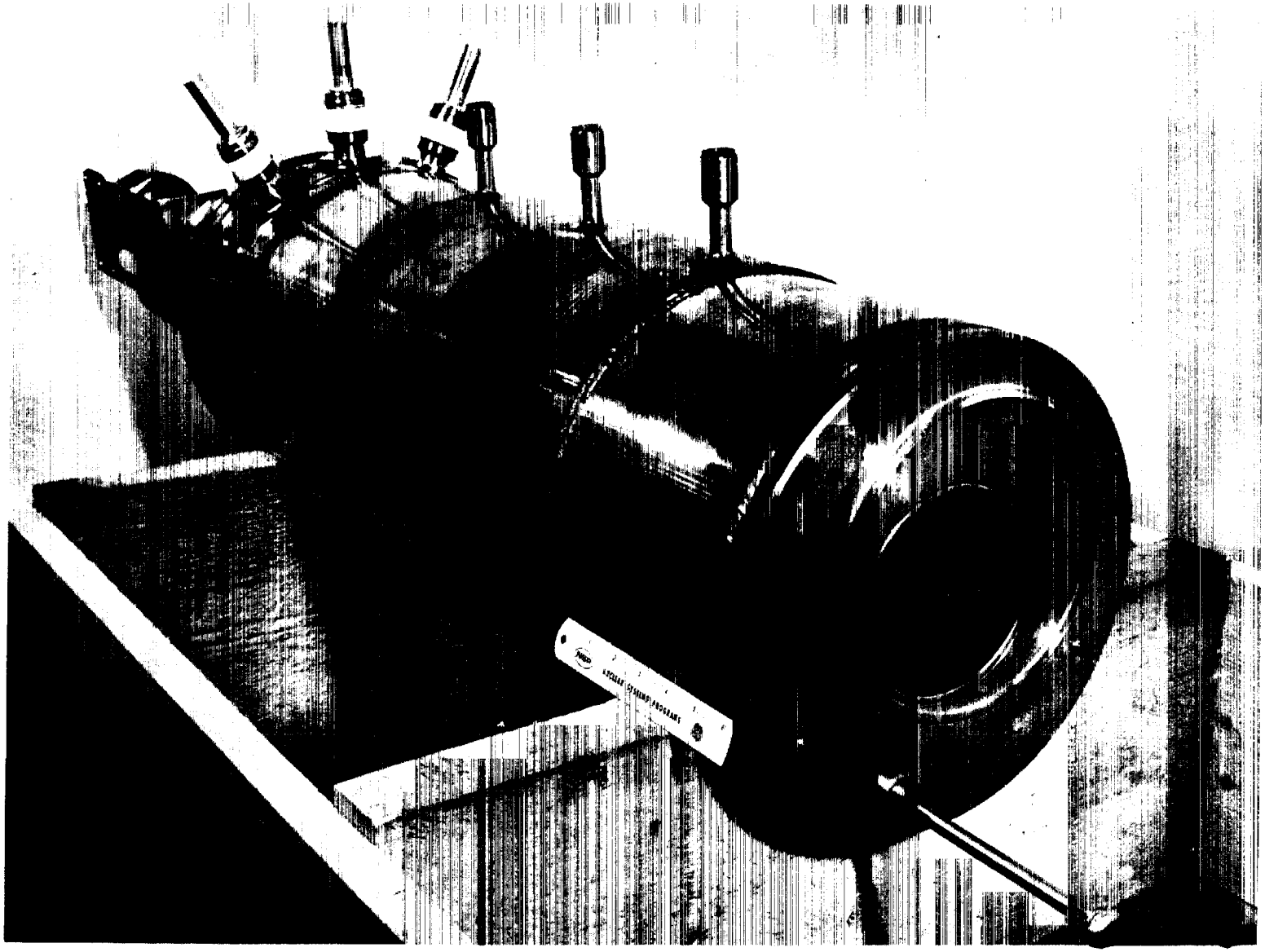

Figure 51. Duct (Opening) End of Finished Stator with Bore Can Visible, Just Before Final Assembly of the Duct in the Stator.

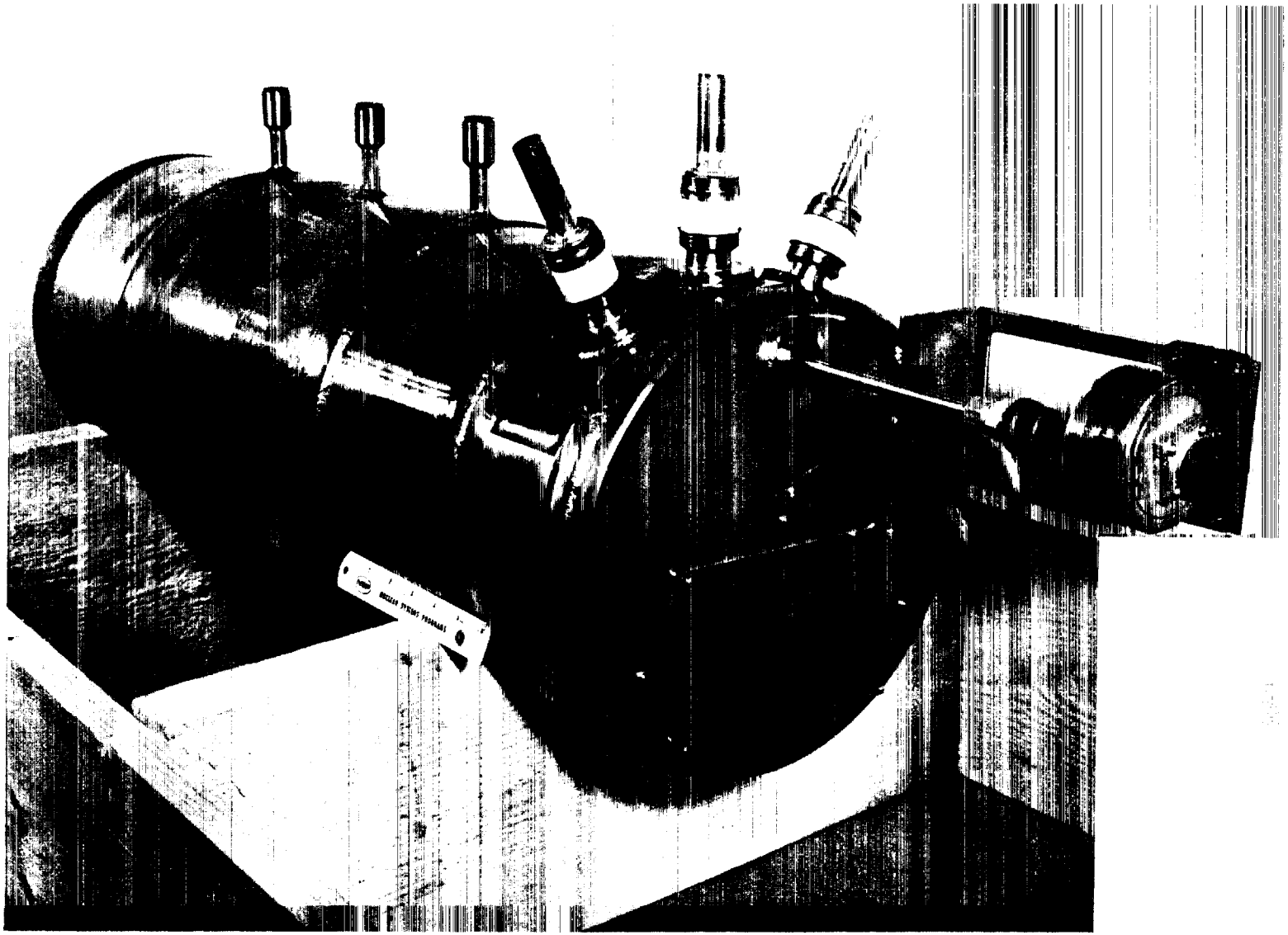

Figure 52. Lead Connection End of Finished Stator with Power Feed-Throughs and Stator Cavity Pressure Switch Attached, and Seal-Off Tube Temporarily Capped to Maintain Argon Gas in Cavity During Shipping.

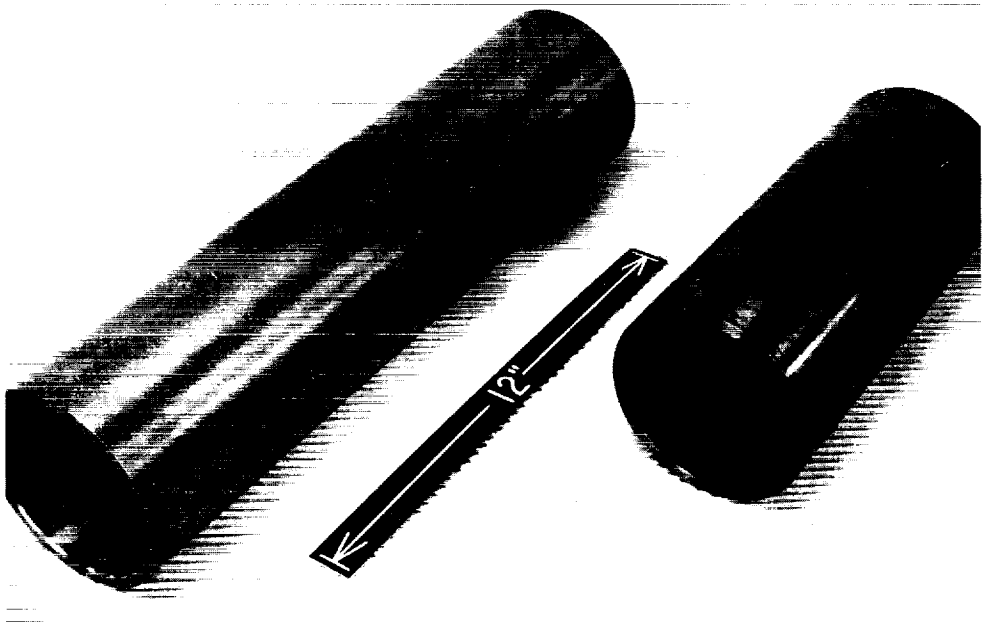

Figure 53. T-111 Alloy Tubes as Received from Vendor for use in Fabricating the Duct Wrapper and Wrapper Extension.

Figure 54. T-111 Alloy Tubes as Received from Vendor for use in Fabricating the Duct Helix (Left Hand Thick Walled Piece) and the Duct Extension.

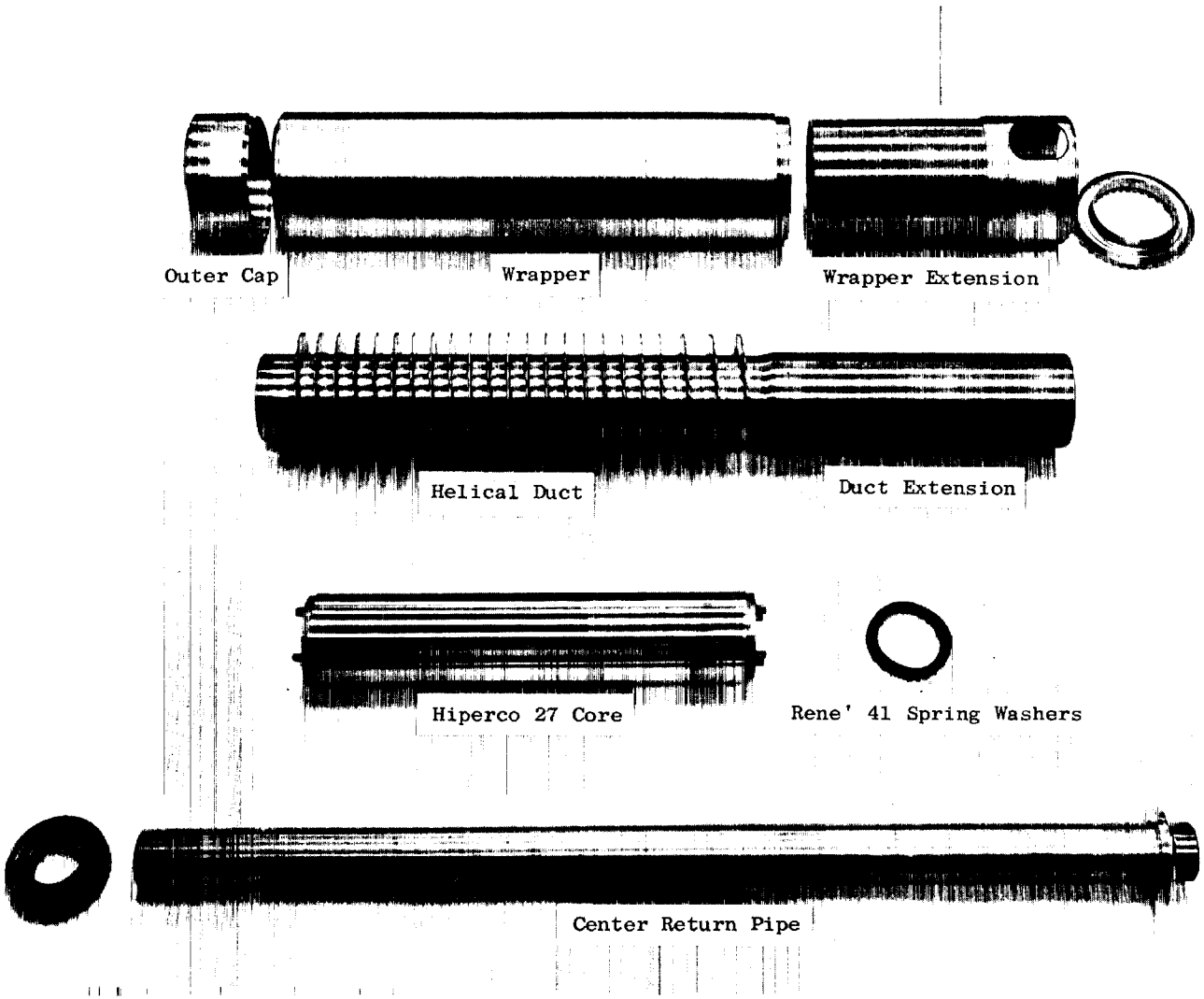

Figure 55. Machined Parts for the EM Pump Duct Assembly, all Made of T-111 Except the Hyperco Core (Directly Below the Helix) and the Rene' 41 Wavy Spring Washers.

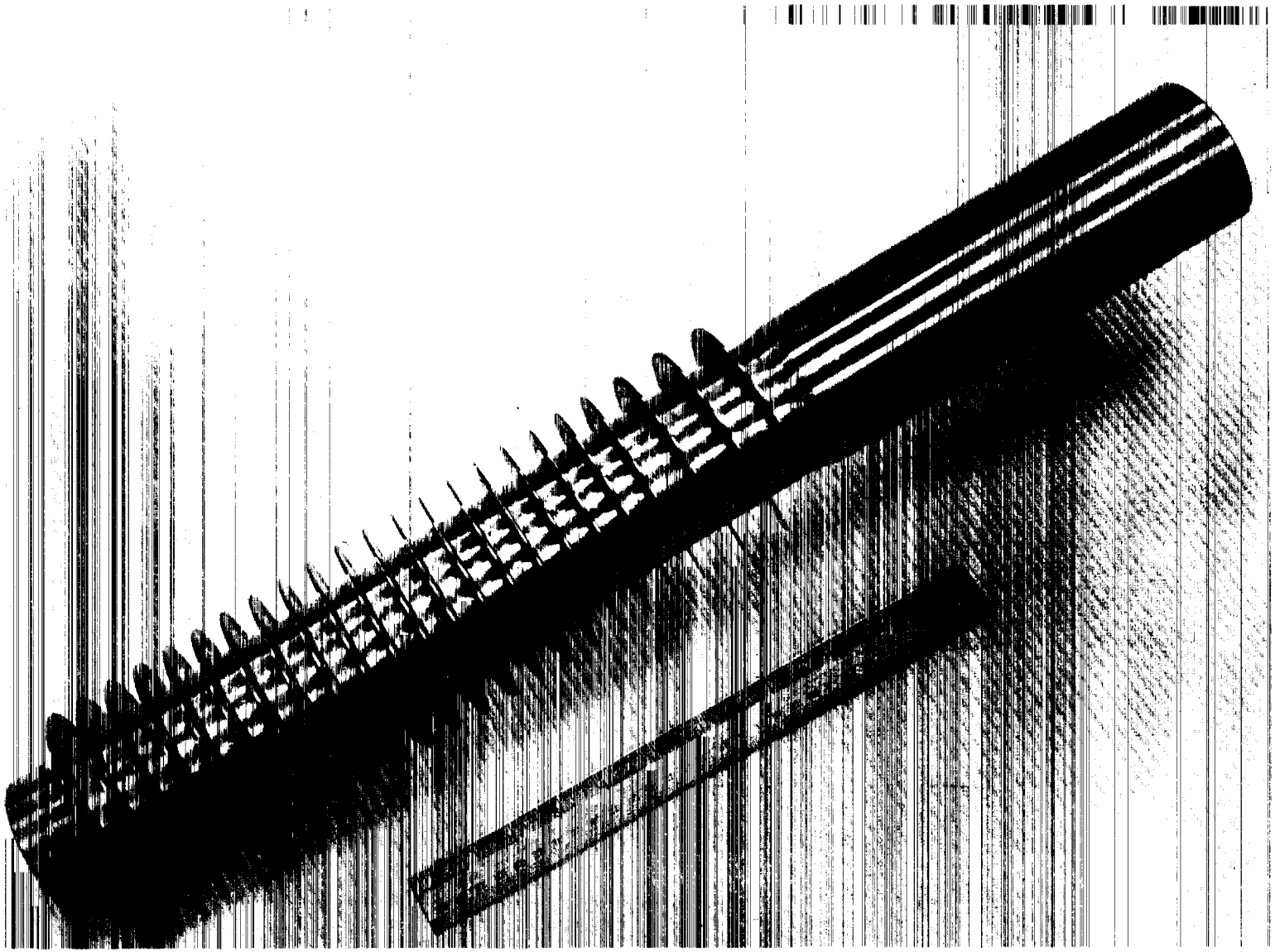

Figure 56. Helix for EM Pump Duct After Final Machining with Helix Extension Welded to the Helix Section.

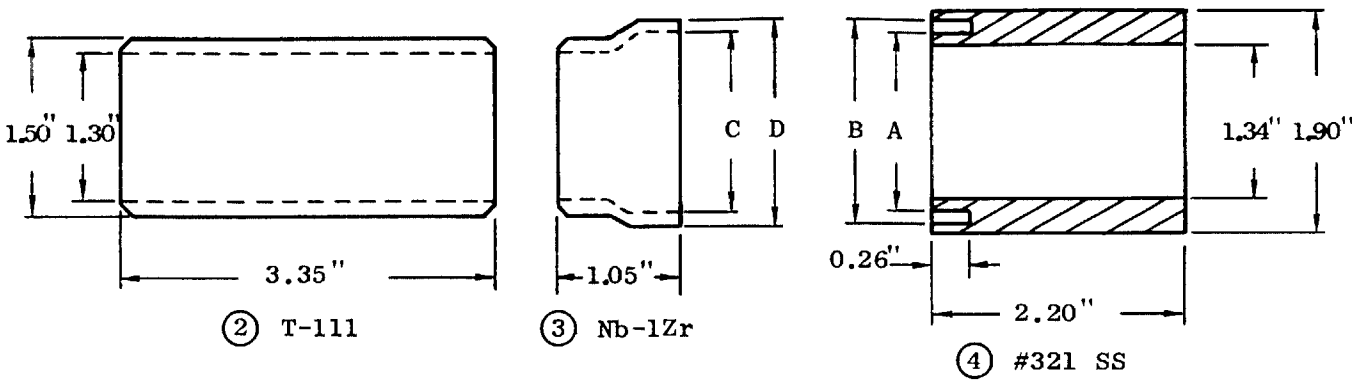

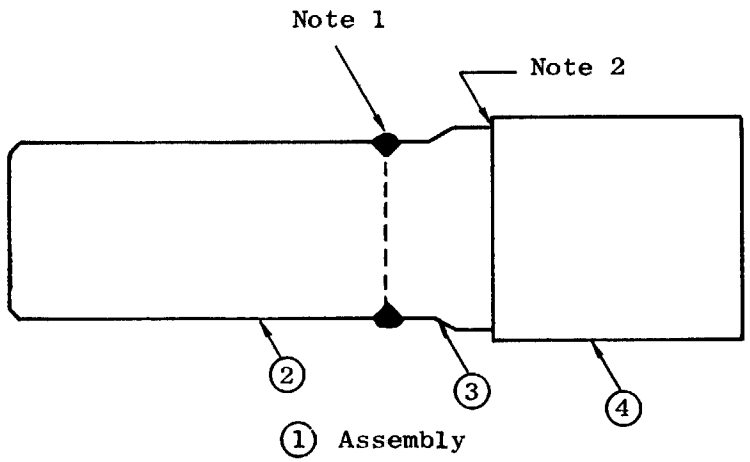

Dimensions
A = 1.539-1.541"
B = 1.766-1.767"
C = 1.564-1.566"
D = 1.765-1.766"

Notes:
1. Weld with TIG Process Using Nb-1Zr Filler Metal
2. Braze at 2160°F, in Vacuum Furnace, with Cobalt Base Alloy

Figure 57. Layout of Inlet Pipe (Bi-Metallic) Transition Design Configuration Showing Important Braze Joint Details Which are also Similar in the Outlet Pipe Design.

Figure 58. Trial Sample Transition (Bi-Metallic) Brazed Pipe Joint in Which Smaller Diameter Part is Nb-1Zr and Larger Diameter (Lower) Part is Type 321 Stainless Steel.

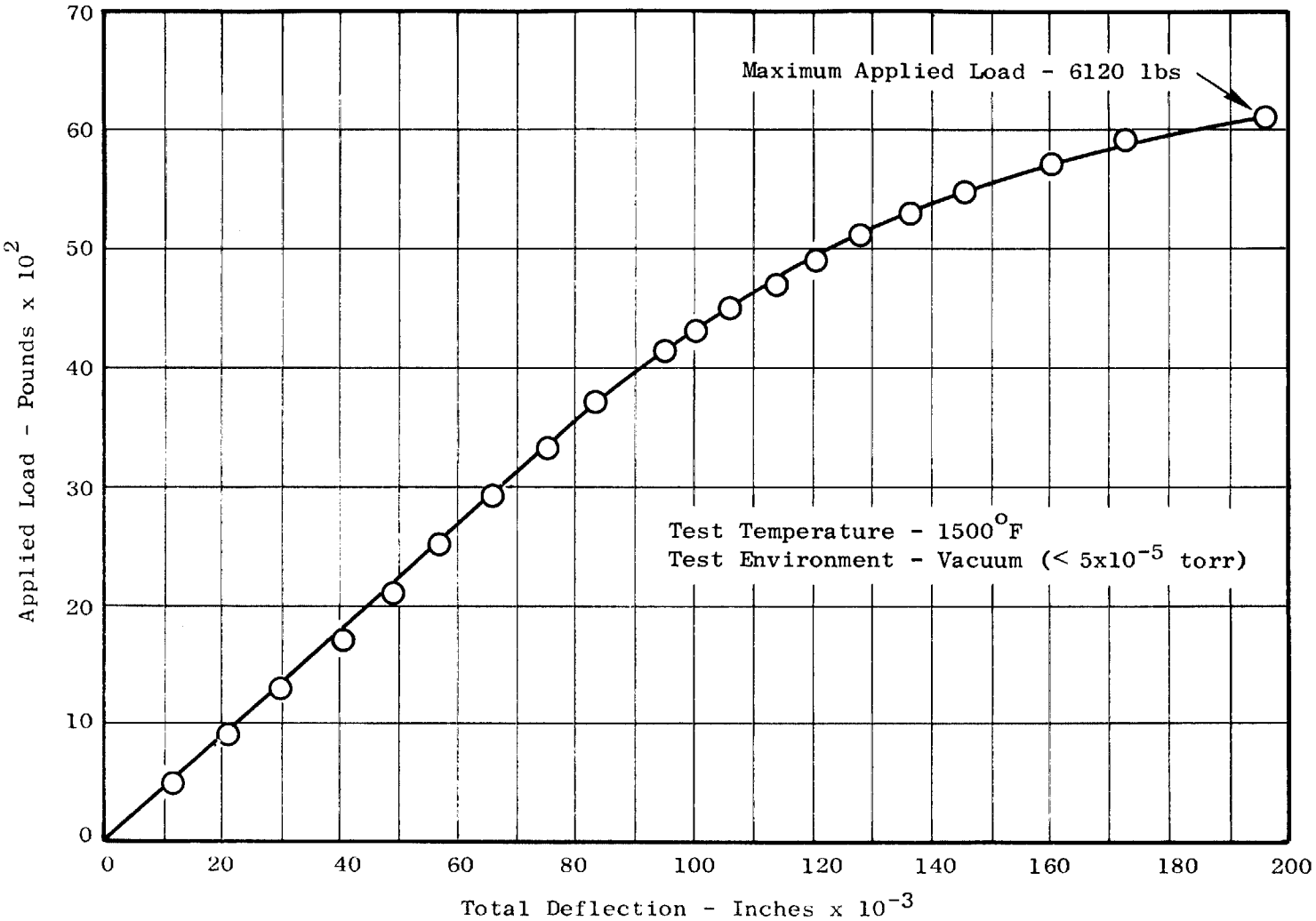

Figure 59. Load-Deflection Curve From Tensile Test Data for Test on Trial Brazed Bi-Metallic Sample Joint.

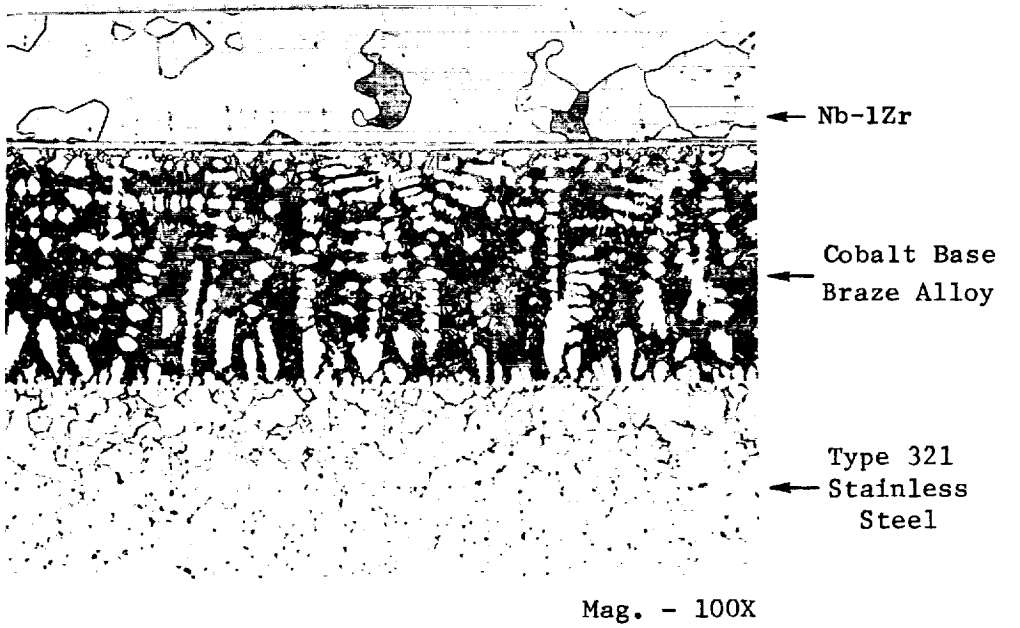

A. Overall View of Braze Area

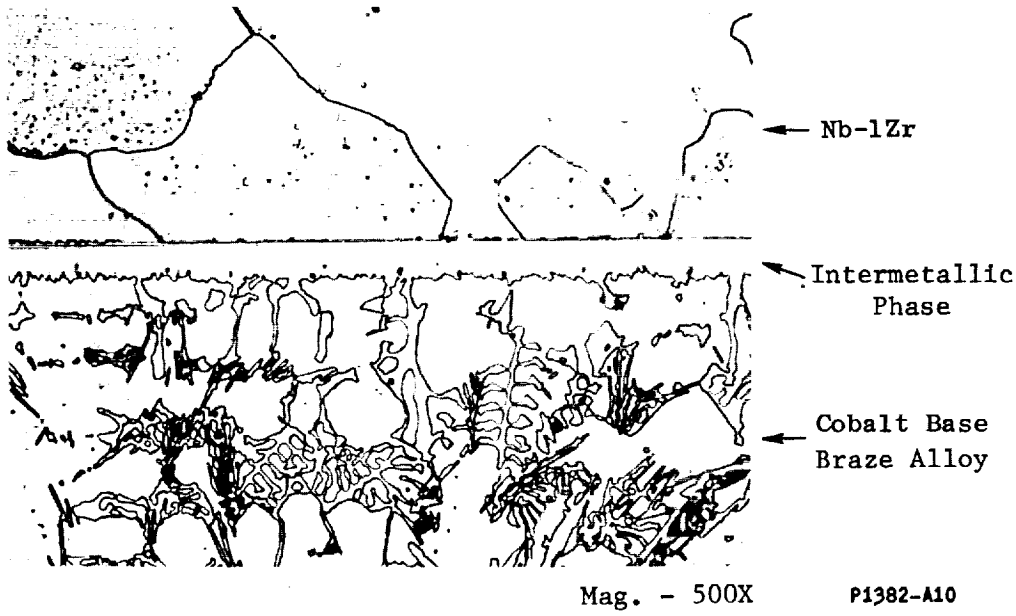

B. Enlarged View of Nb-1Zr Braze Interface

Figure 60. Microstructures of Nb-1Zr to Type 321 Stainless Steel Bi-Metallic "As Brazed" Trial Joint, at the Outside Section of the Tongue and Groove. (459-60)

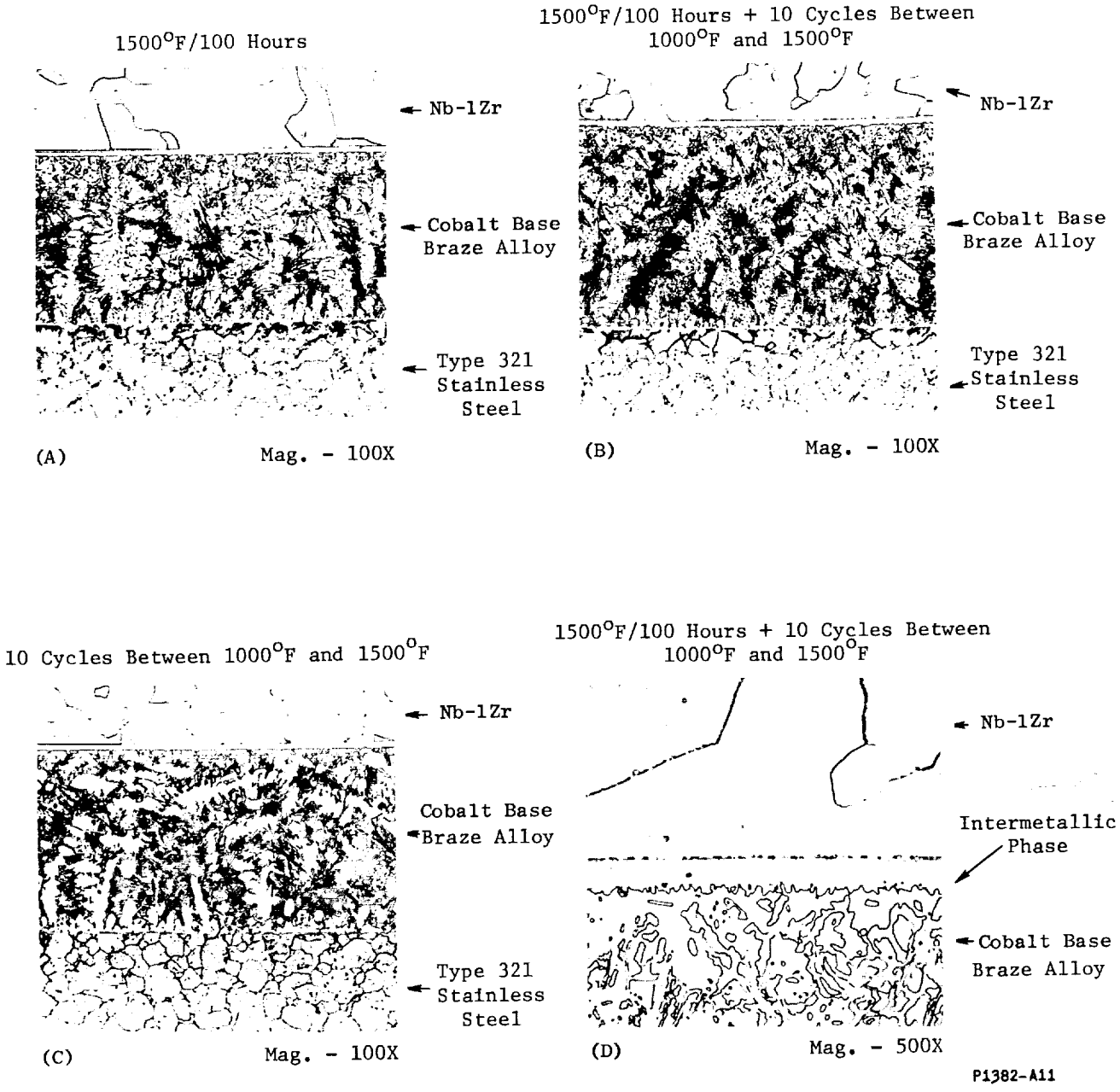

Figure 61. Representative Microstructures of Nb-1Zr to Type 321 Stainless Steel Bi-Metallic Joint, at the Outside Section of the Tongue and Groove, After Indicated Thermal Exposures and With an Enlarged View From (B) to Show the Inter-Metallic Phase (in D).

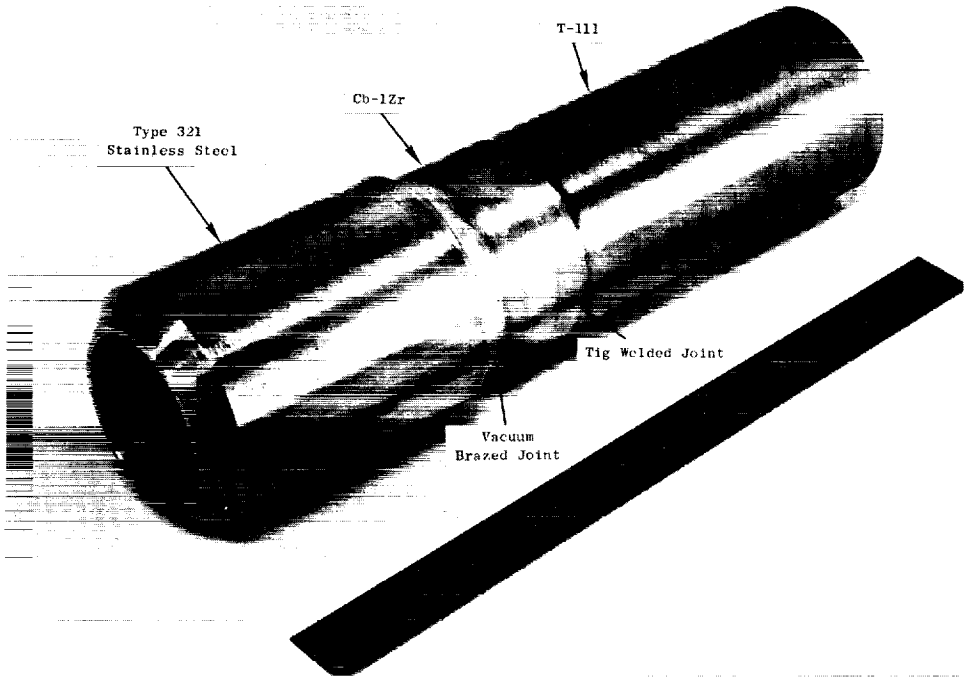

Figure 62. Pump Duct Inlet Pipe Transition (Bi-Metallic) Assembly for Connecting Between the T-111 Duct and the Test Loop Stainless Steel Piping.

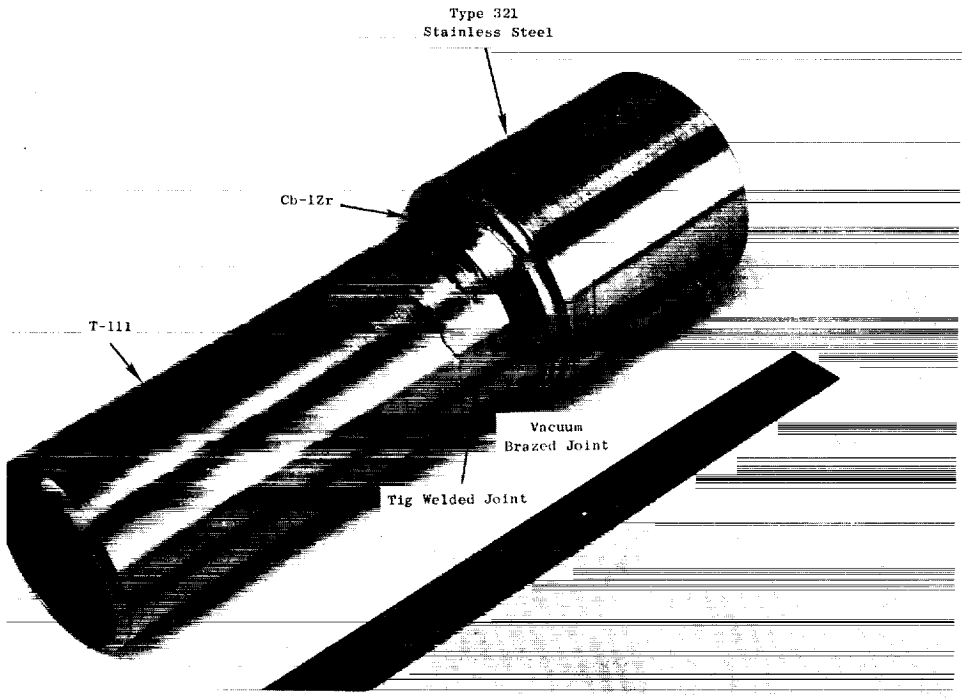

Figure 63. Pump Duct Outlet Pipe Transition (Bi-Metallic) Assembly for Connecting Between the T-111 Duct and the Test Loop Stainless Steel Piping.

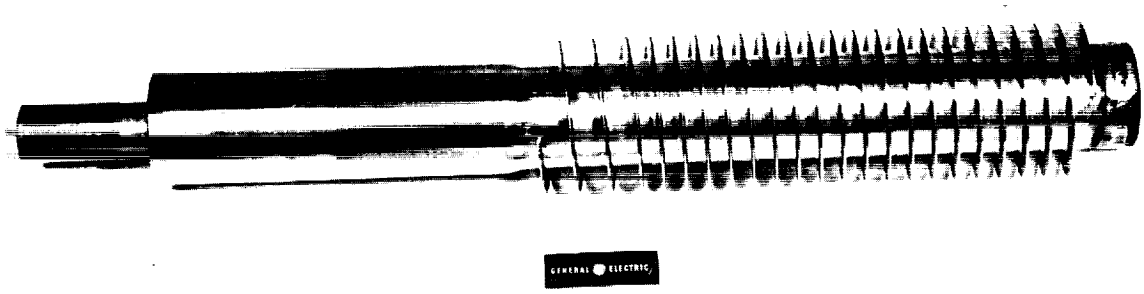

Figure 64. Welded Assembly of T-111 Helix, Helix Extension, and Center Return Pipe for EM Boiler Feed Pump.

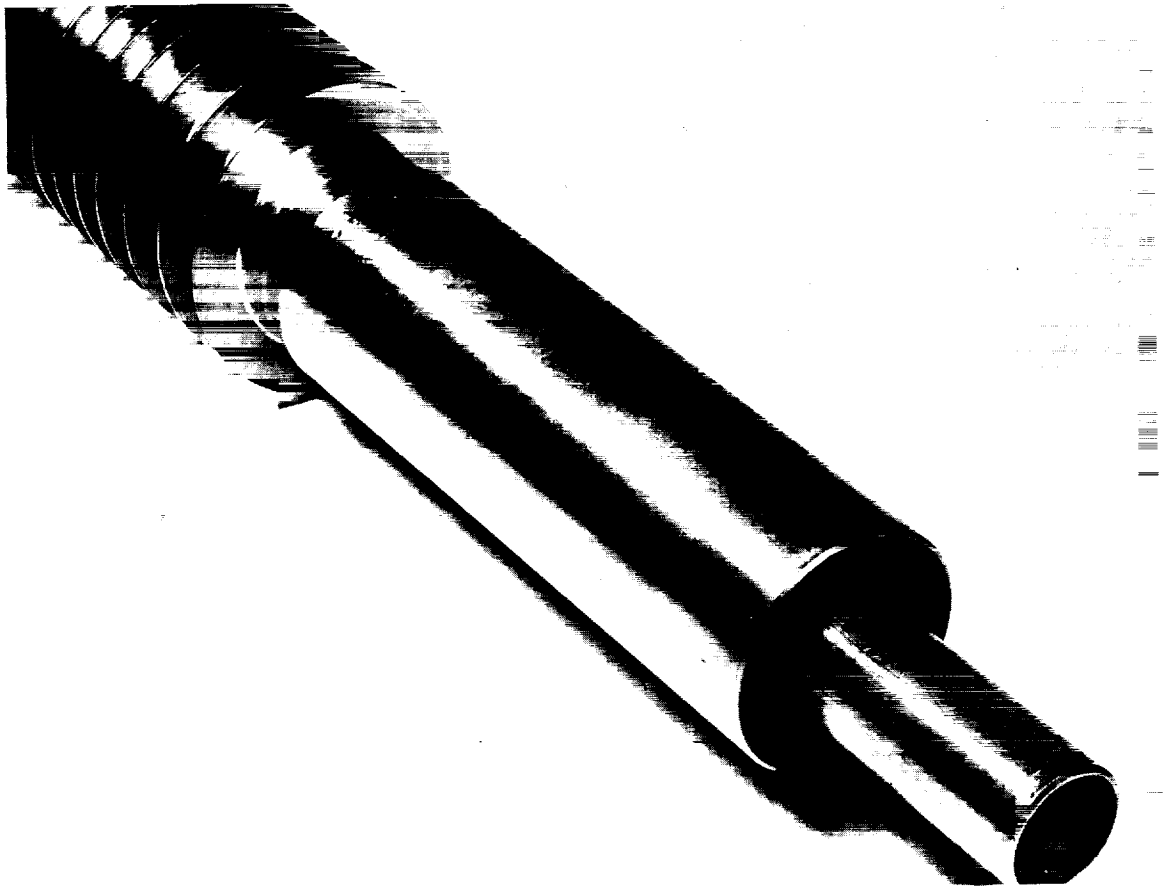

Figure 65. Close-up of T-111 Helix Extension and Center Return Pipe for EM Pump Duct.

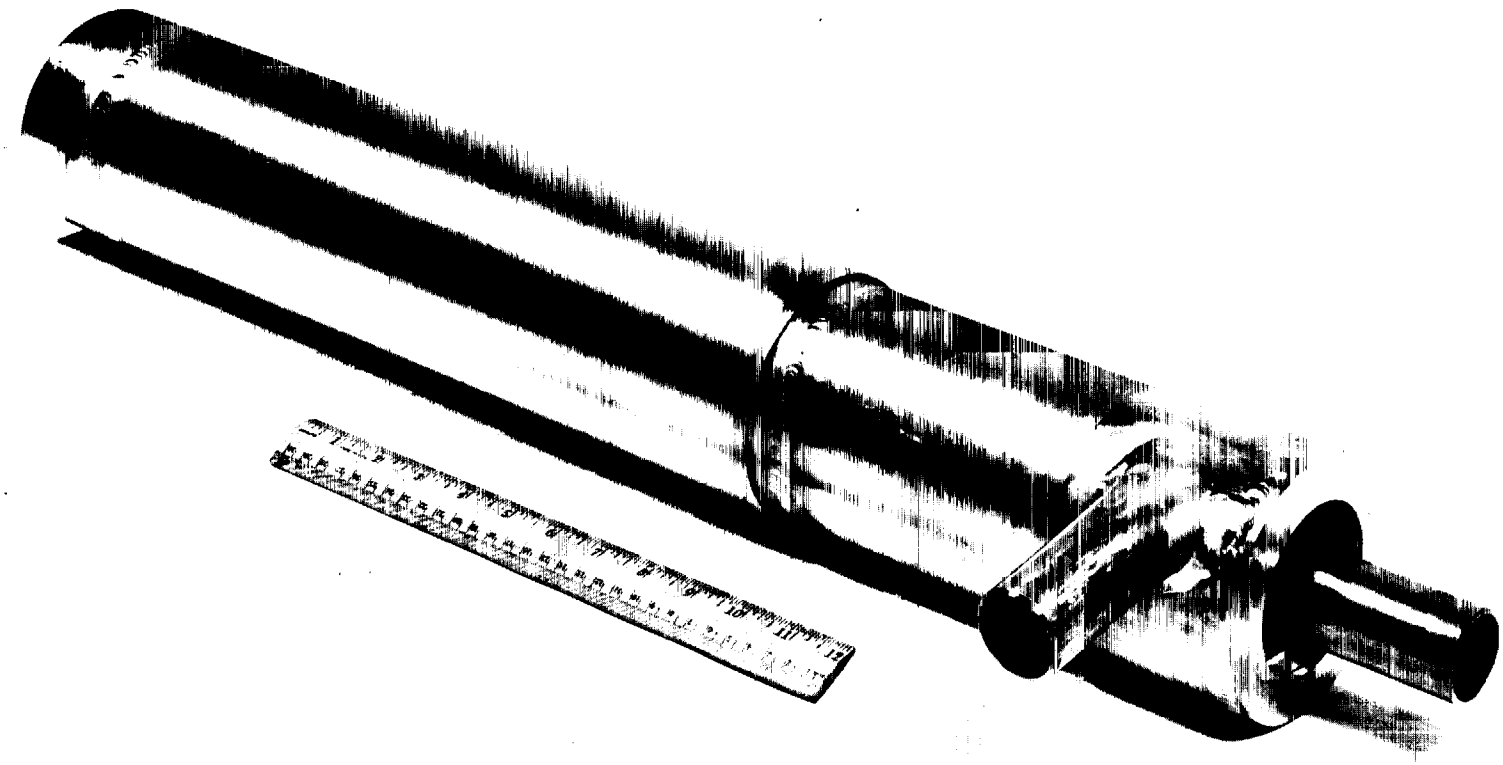

Figure 66. Assembled T-111 Duct for EM Pump (Without Bi-Metallic Transition Pipes) After Completion of Welding and Prior to Final Outside Machining.

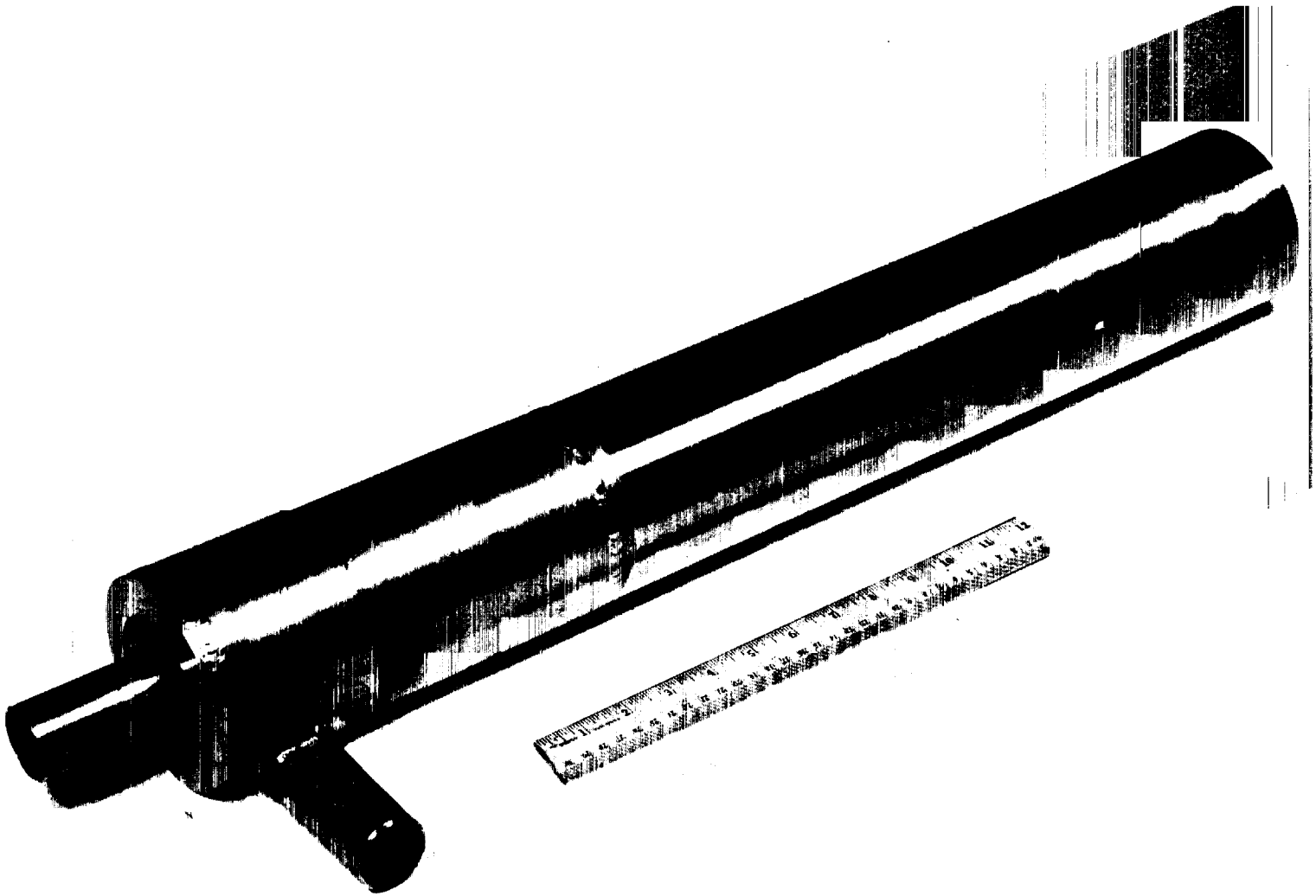

Figure 67. Assembled T-111 Duct After Machining of Outside (Wrapper and Extension) and Prior to Vacuum Annealing.

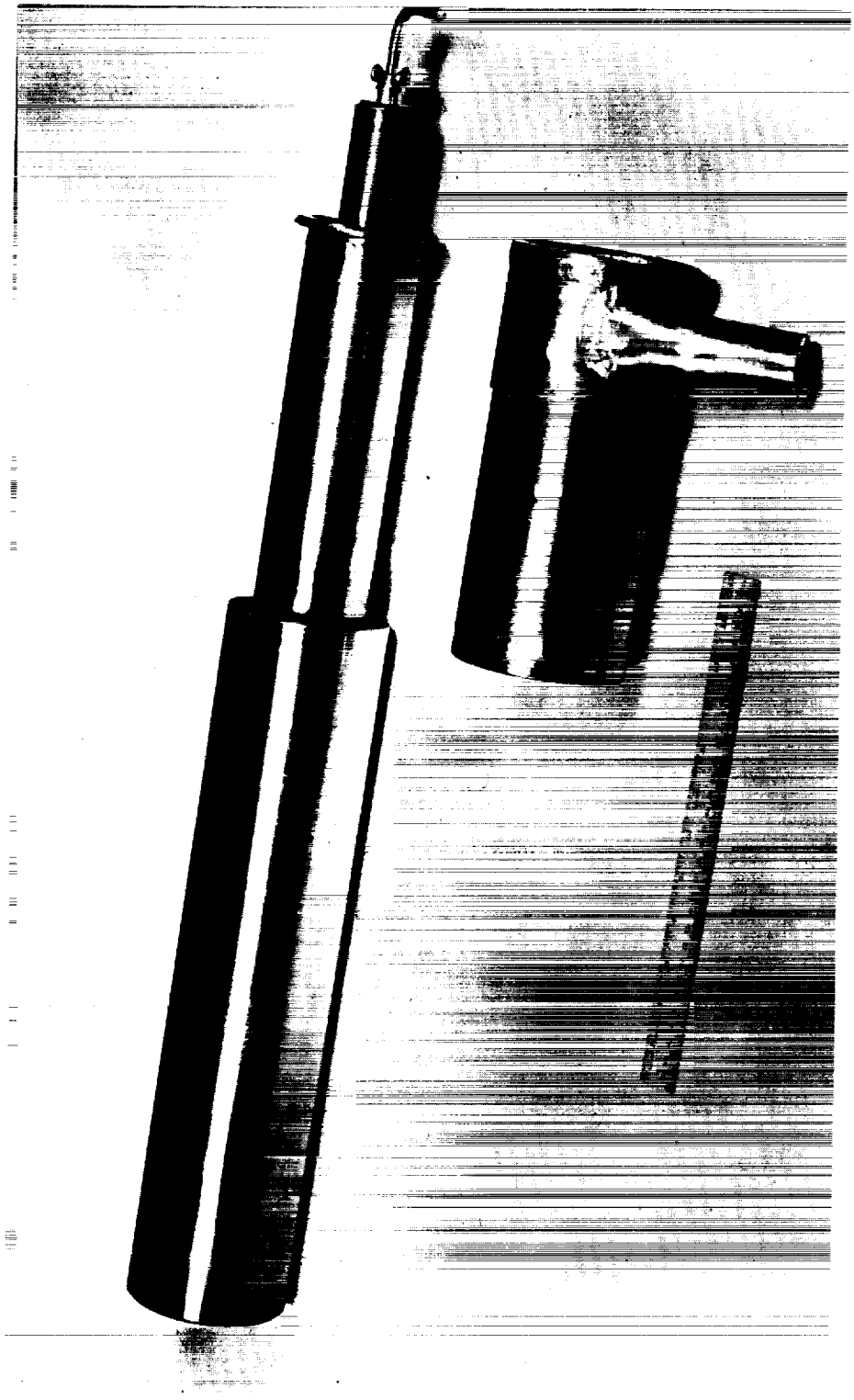

Figure 68. Pump Duct with Section of Wrapper Removed to Expose Area Where Small Leak was Detected.

Figure 69. Close-up of T-111 Duct Helix Extension Showing Spot (Outlined by Scribed Circle) Where Small Leak was Detected Near Weld.

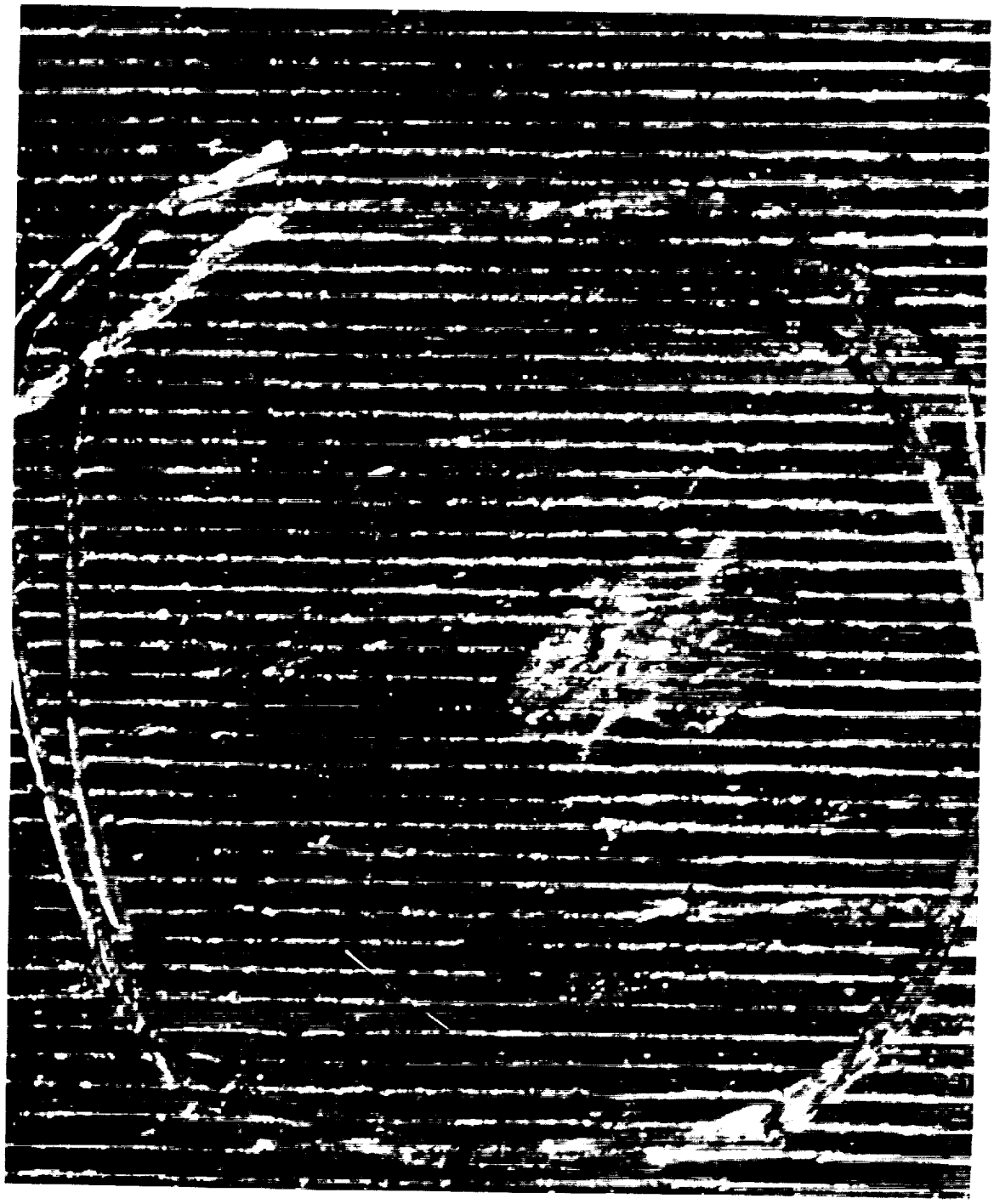

Figure 70. Enlargement (25X) View of Suspected Leak Area in T-111 Duct Helix Extension, Inside Scribed Circle.

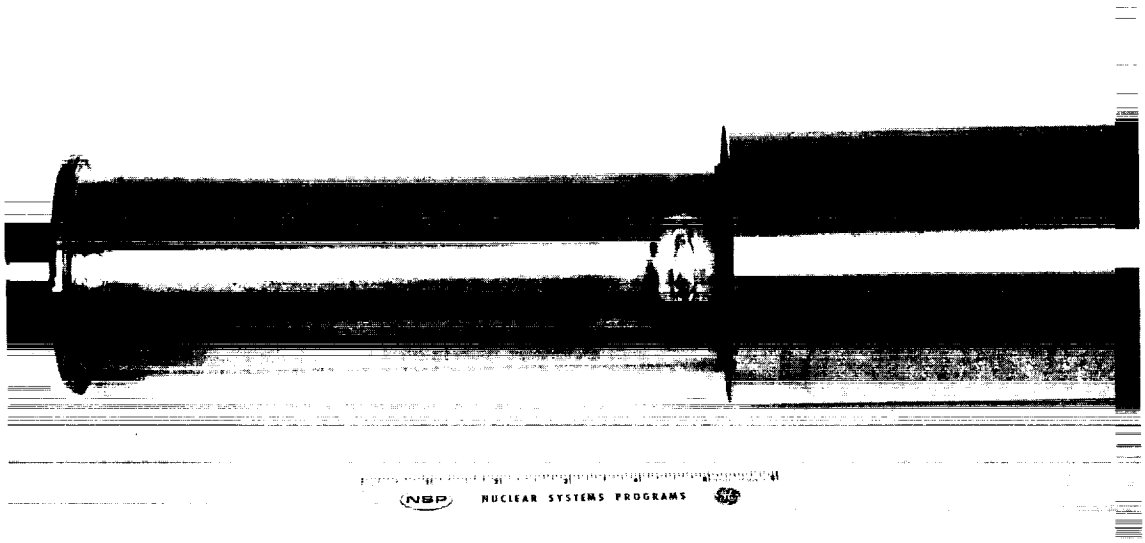

Figure 71. Pump Duct Assembly with Part of Outer Wrapper Removed and Leak Area in T-111 Helix Extension Repaired by Welding.

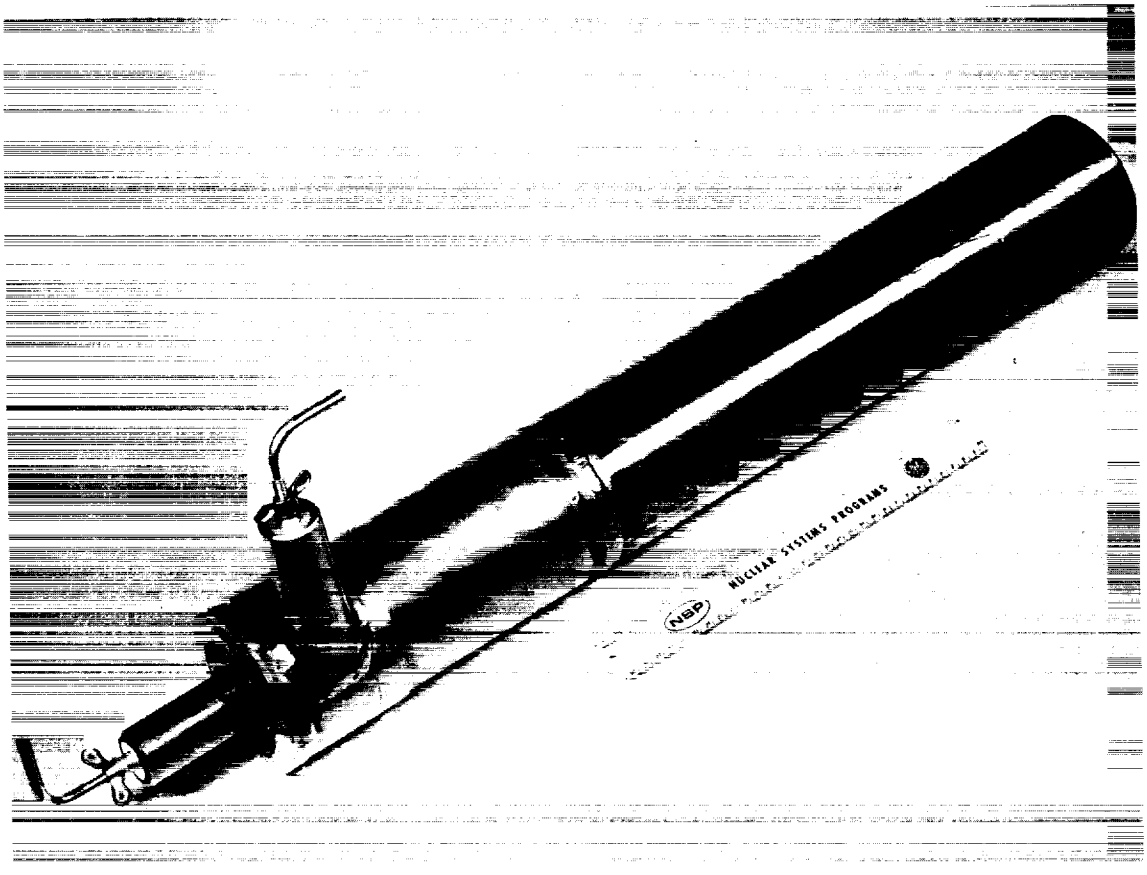

Figure 72. Pump Duct Assembly After Repair of Leak in Helix Extension and Replacement of Outer Wrapper Section which had been Removed.

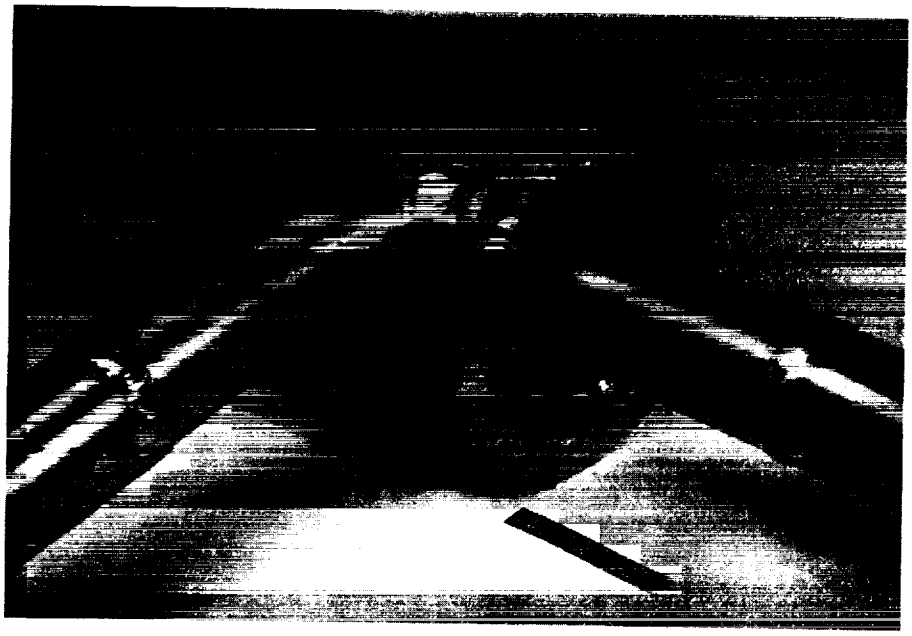

Figure 73. Pump Duct (T-111) Wrapper Section Which was Replaced After Repairing Leak in Helix Extension, Marked to Indicate Areas of Grain Boundary Separation in Welds (A&B) and Surface Checks (C) Requiring "Benching" and Polishing.

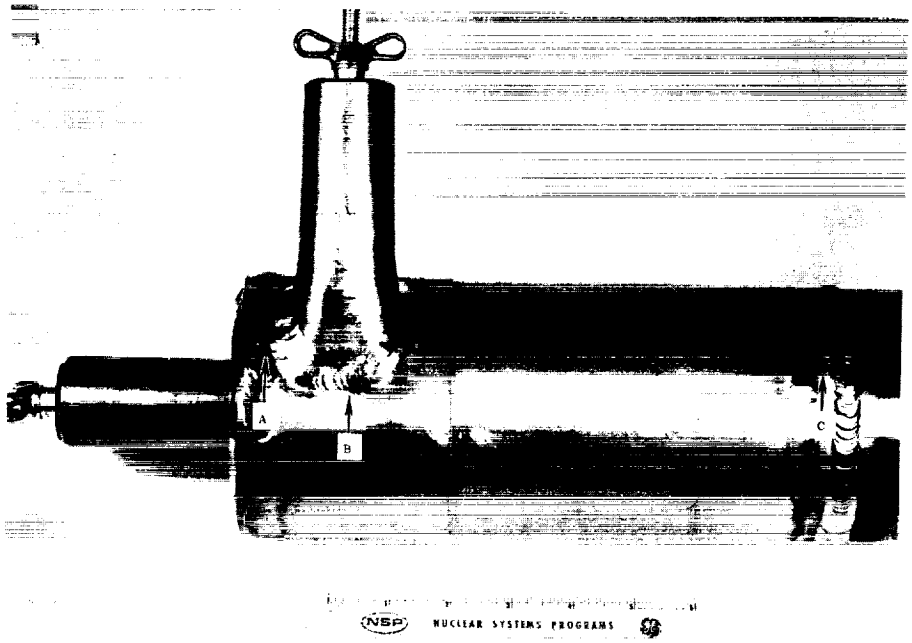

Figure 74. Inlet End of Assembled T-111 Pump Duct With Transition (Bi-Metal) Inlet and Outlet Pipes Attached, and the Snap Ring Holding the Duct Core, Spring Washers, and Retaining Sleeve in the Cavity Around the Center Pipe, Tacked in Place.

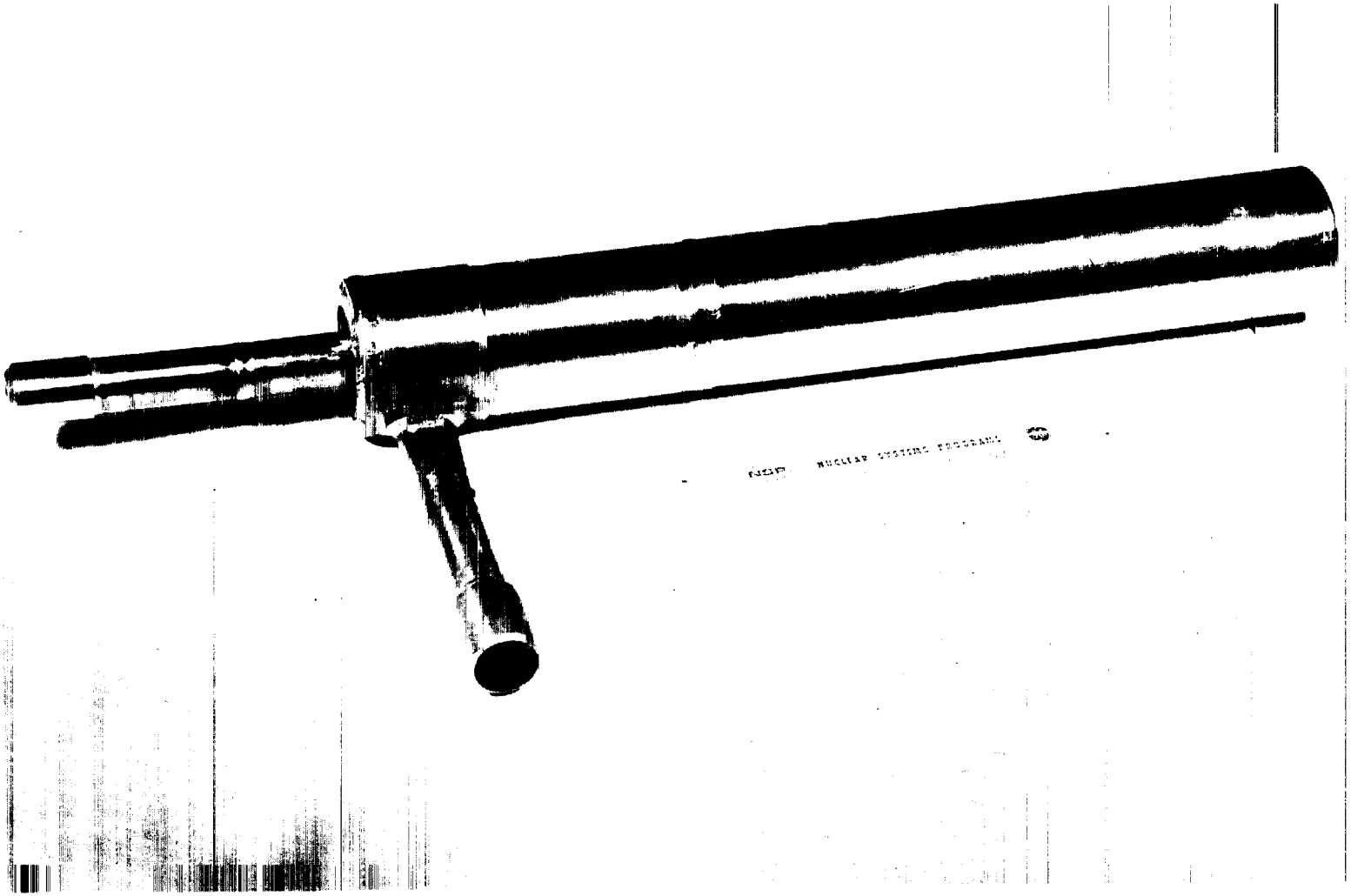

Figure 75. Completely Assembled and Leak Checked T-111 Duct for EM Boiler Feed Pump, Prior to Adding the Layers of Thermal Insulation.

Figure 76. Nb-1Zr Foil, 0.002 Inch Thick, Being Applied in Strips to the T-111 Pump Duct to Provide a Total of 10 Layers for Thermal Insulation.

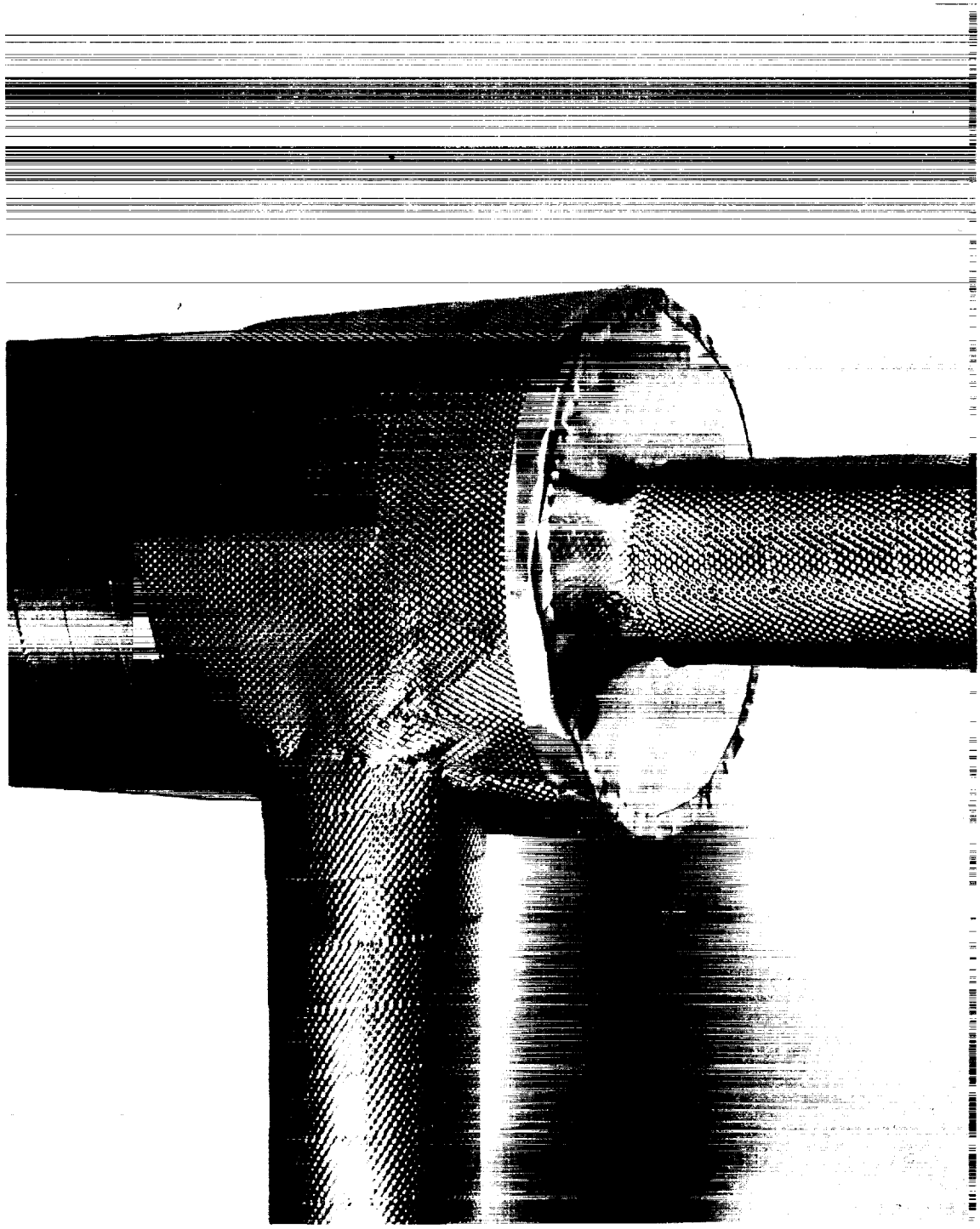

Figure 77. Inlet and Outlet Pipe Connection End of T-111 Pump Duct After Application of Nb-1Zr Foil for Thermal Insulation.

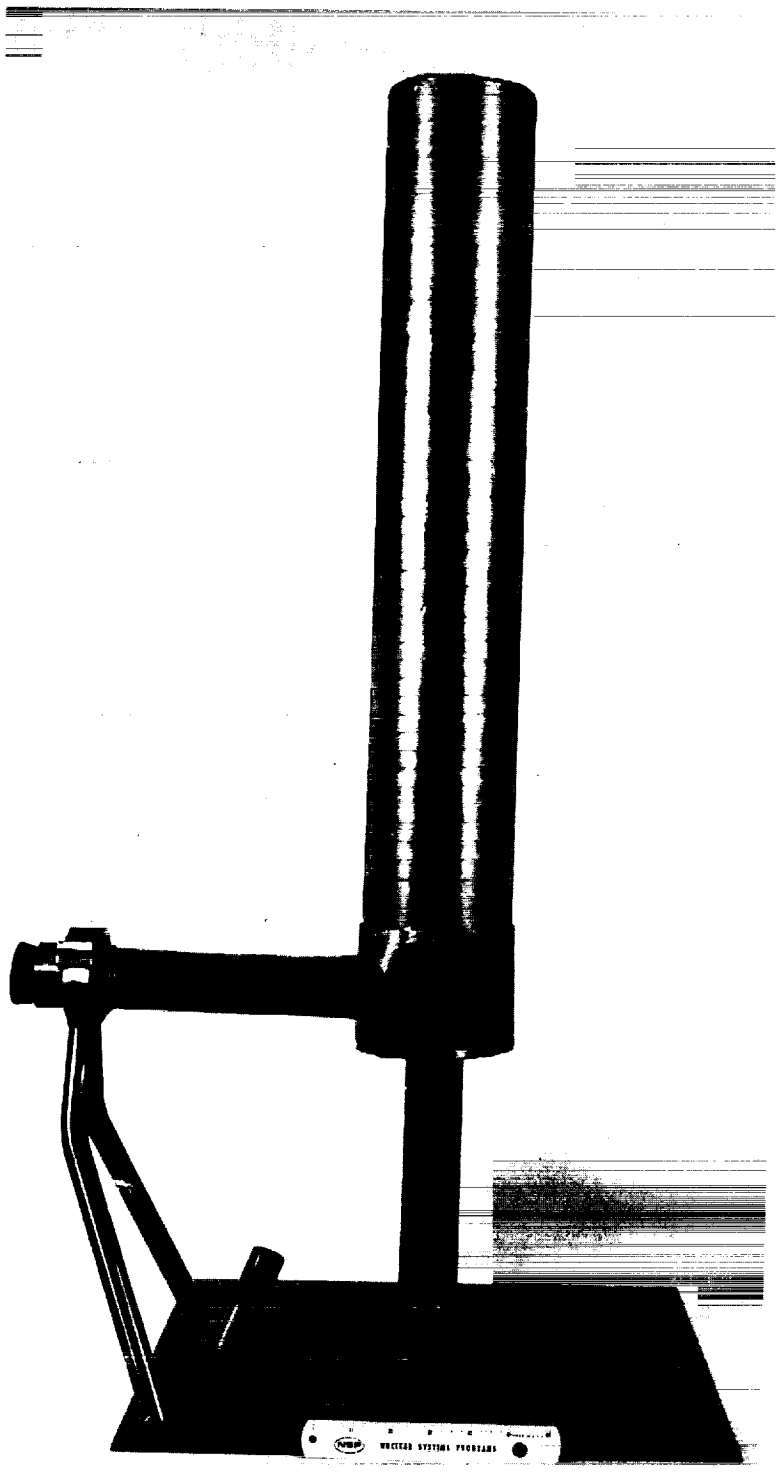

Figure 78. Overall View of Pump Duct with Nb-1Zr Thermal Insulation Completed, and the Assembly Ready for Insertion into the Stator.

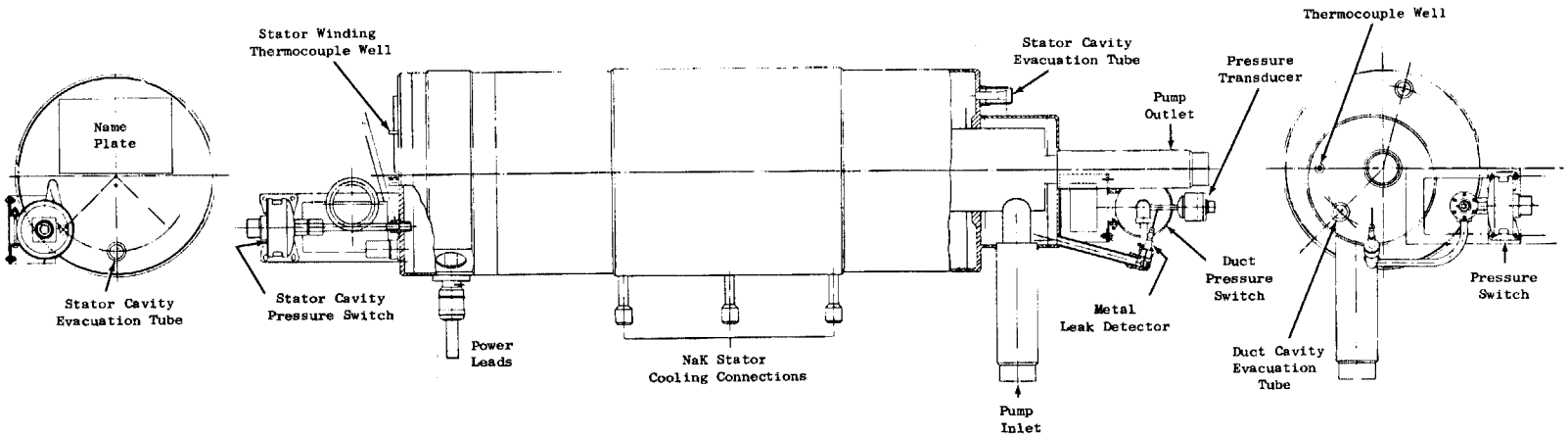

Figure 79. Layout Drawing of Assembled EM Boiler Feed Pump With Attached Instrumentation Items for Cavity Pressure and Metal Leak Measurements.

Figure 80. The "Trial" Mating of the Insulated Pump Duct into the Stator Bore Can to Check for Proper Clearance.

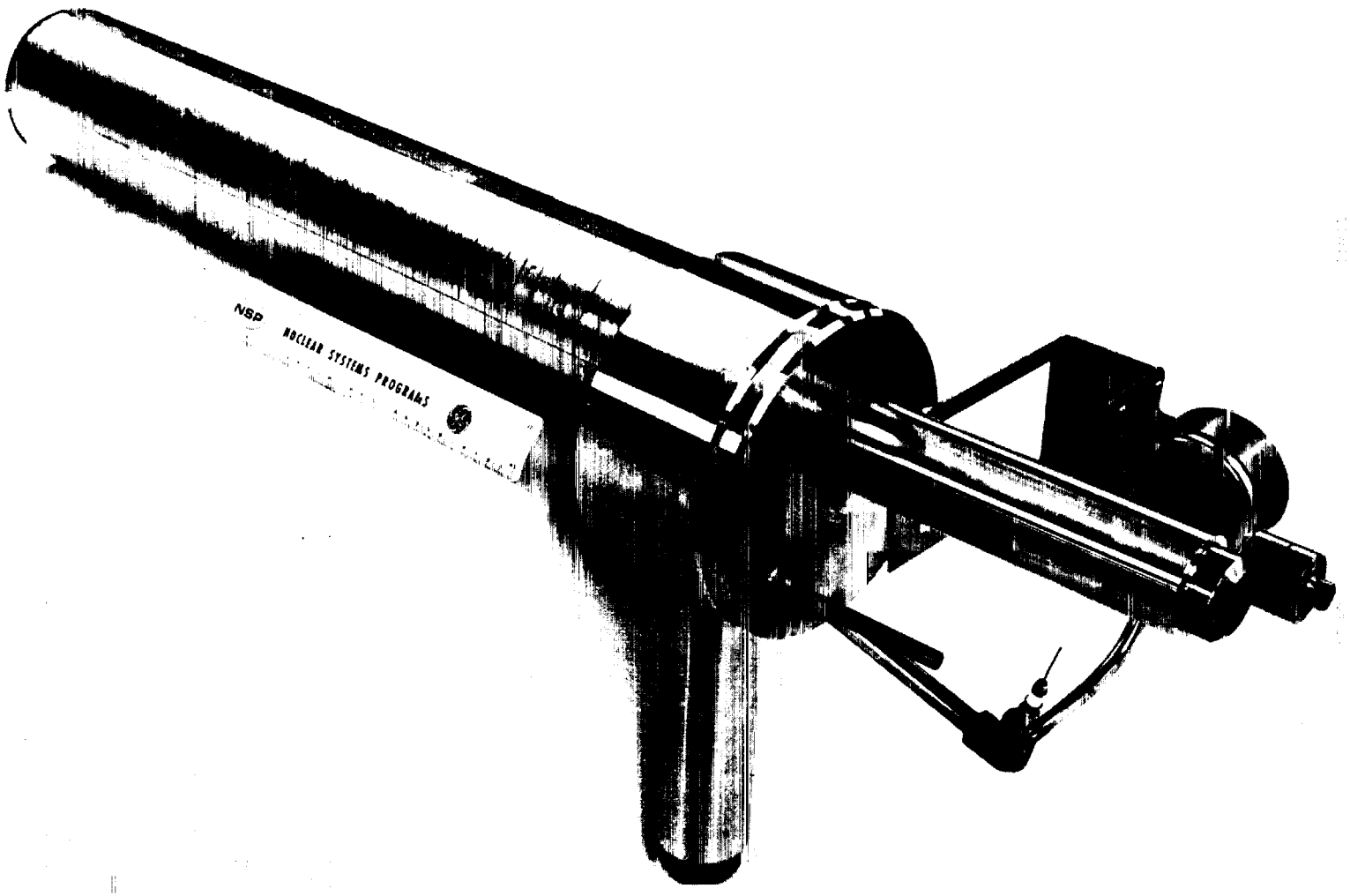

Figure 81. Insulated Pump Duct with Duct Shroud and Instrumentation, and Pipe Sleeves, Tacked in Place Ready for Final Welding.

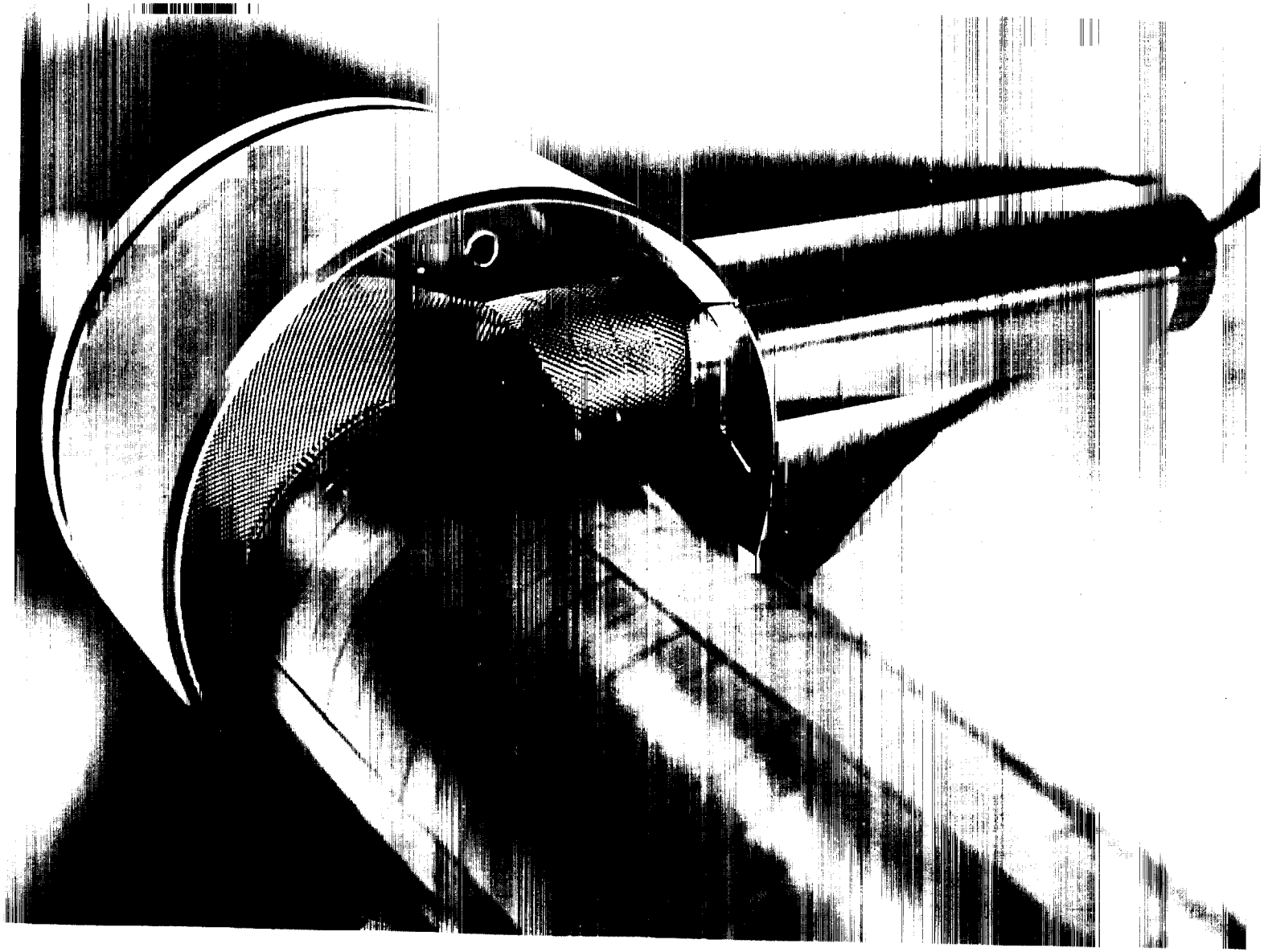

Figure 82. Close-up of Inside of Pump Duct Shroud and Sleeve Over Inlet Pipe, During Fit-up of the Parts.

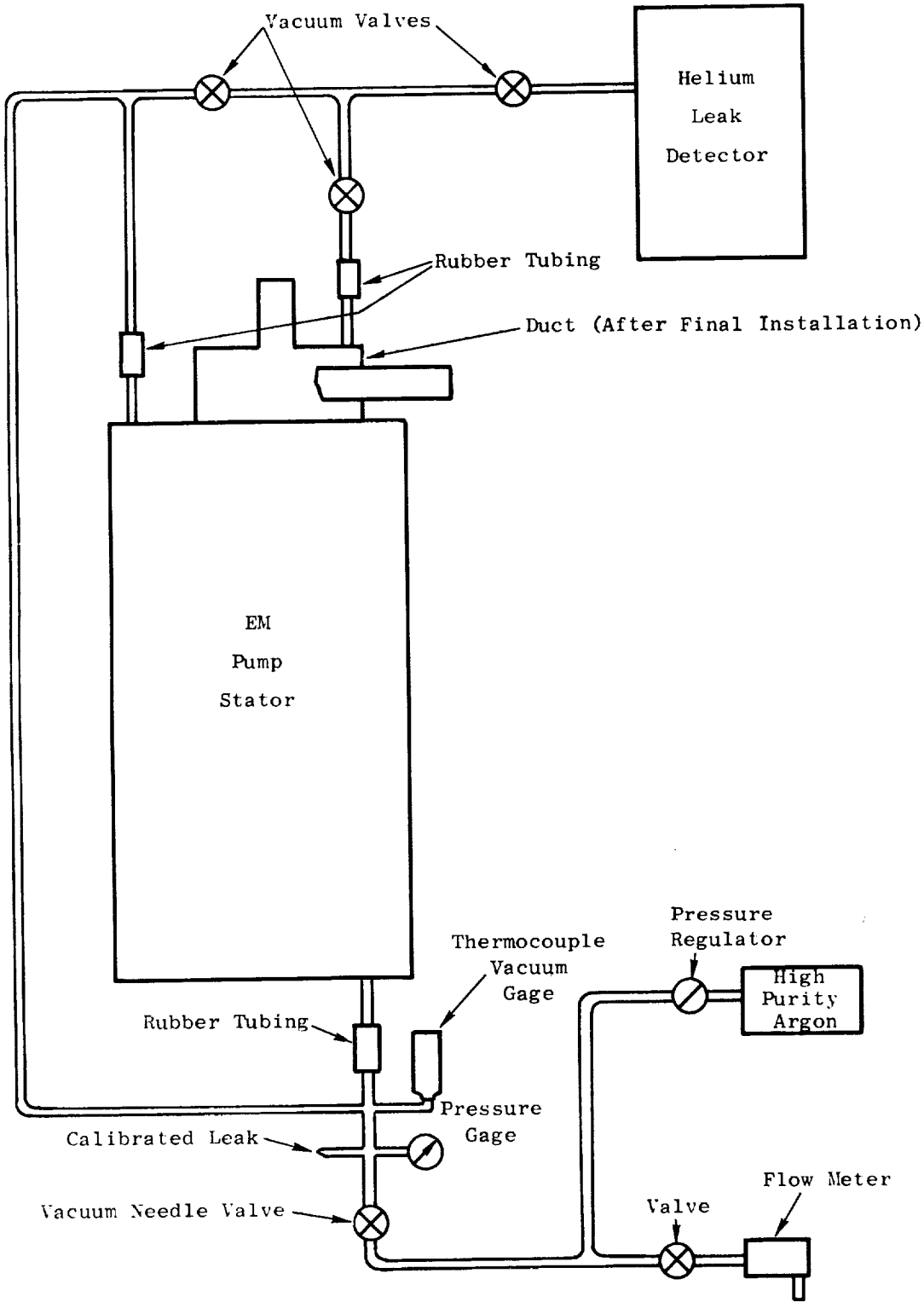

Figure 83. Schematic Diagram of Leak Detection and Argon Filling Arrangement for Duct and Stator Cavities of EM Pump.

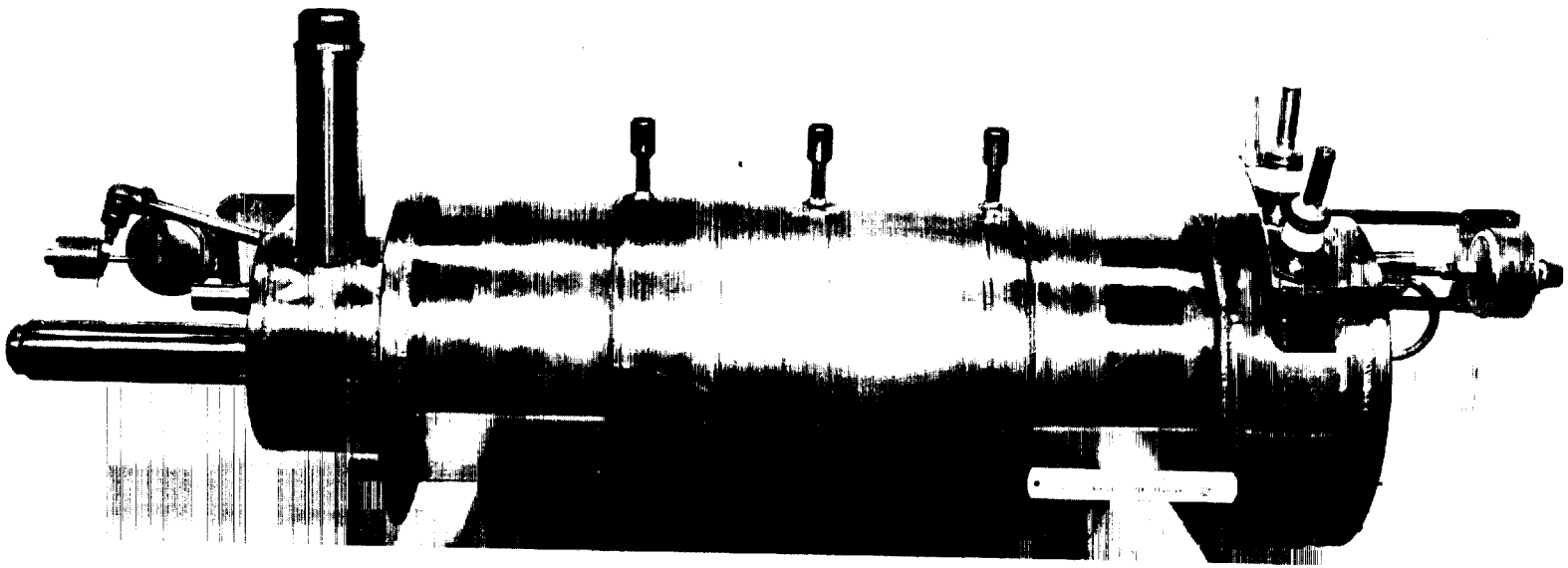

Figure 84. Overall View of Completely Assembled EM Boiler Feed Pump, with Cavities Filled with Argon and Instrumentation Attached, Ready for Installation in the Test Facility.

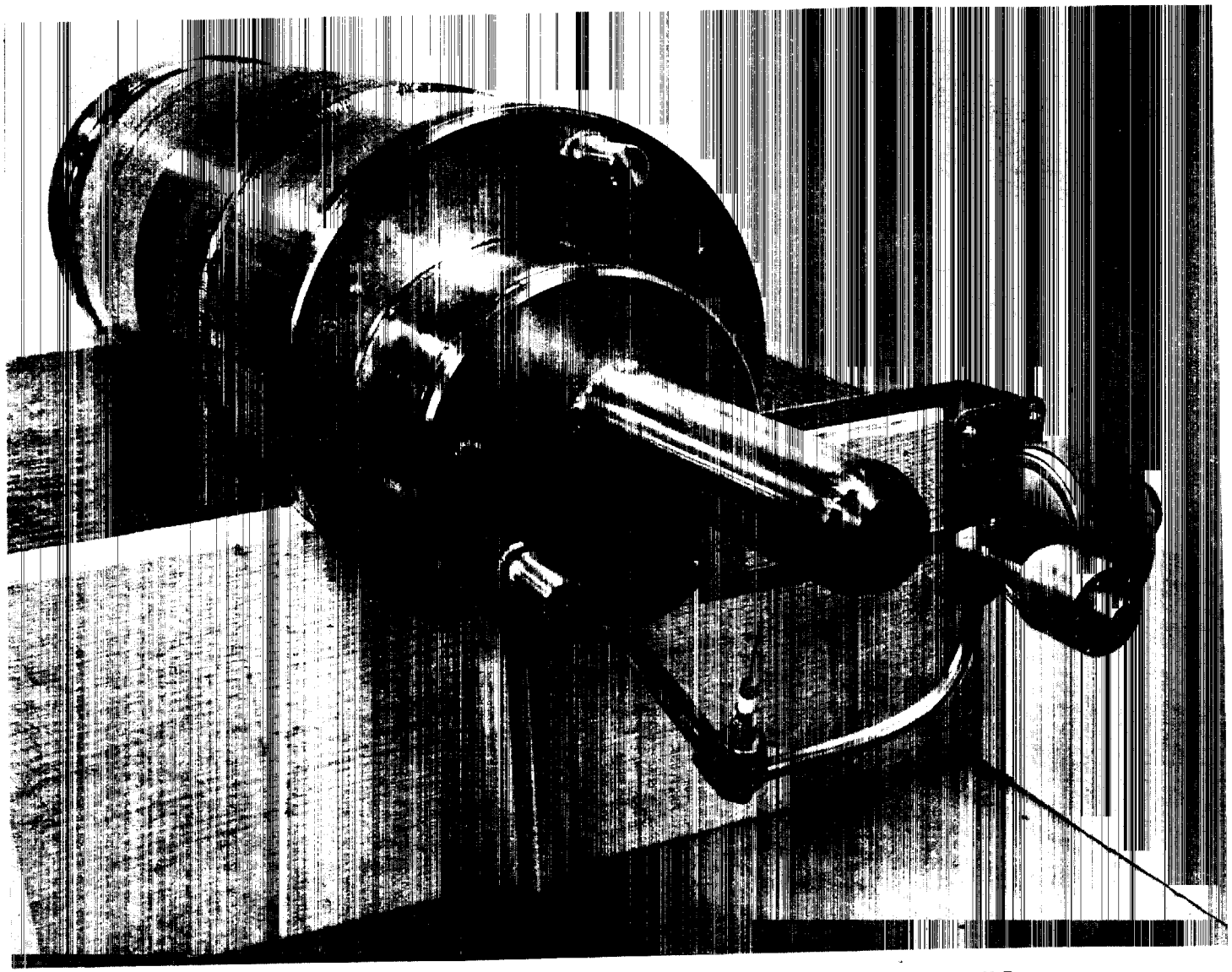

Figure 85. Duct Inlet and Outlet (Center) Pipe Connection End of Assembled EM Pump.

Figure 86. Power Lead Connection End of Assembled EM Boiler Feed Pump, with Stator Cavity Pressure Switch and T/C Wells in End Shield.

TABLE 1

BASIC PERFORMANCE CHARACTERISTICS

CALCULATED VALUES AT DESIGN POINT

Fluid Pumped	Potassium
Fluid Temperature (°F)	1000
Flow Rate (GPM)	32.8
Flow Rate (lb/sec)	3.25
Developed Pressure (psi)	240
Power Output (kW)	3.42
Power Input (kW)	19
Efficiency (%)	18
Input (kva)	39
Power Factor (%)	48
Weight (lbs)	400
Winding Temperature Rise - Hot Spot (°F) (Above coolant average temperature)	325
Winding Temperature Rise - Average (°F) (Above coolant average temperature)	210
Heat Exchanger Requirements	
- Flow Rate (lb/sec NaK)	0.7
- Pressure Drop (psi)	12
- Total Heat Load (kW)	7
- Coolant Inlet Temperature (°F)	800
- Coolant Temperature Rise (°F)	50

TABLE 2

DETAILED ELECTRICAL DESIGN CHARACTERISTICS

CALCULATED VALUES AT DESIGN POINT

(3.25 lb/sec, 240 psi, 1000°F Potassium)

Line Current (amps)	165
Line Voltage (volts)	135
Power Factor (%)	48
Efficiency (%)	18
Losses and Power Requirements	
- Stator Windings I^2R (kW)	4.7
- Iron Loss (kW)	1.5
- Stator Can Loss (kW)	0.31
- Duct Loss (kW)	3.8
- Hydraulic Loss (kW)	0.64
- Fluid (Slip) Loss (kW)	4.6
- Total Losses (kW)	15.55
- Output (kW)	3.42
- Input (kW)	19
- Input (kVA)	39
Slip	0.46
Winding Current Density (A/in^2)	2600
Tooth Peak Flux Density (kilogauss)	8.5
Yoke Peak Flux Density (kilogauss)	11.3
Center Iron Peak Flux Density (kilogauss)	8.8
Gap Peak Flux Density (kilogauss)	2.5

TABLE 3

DETAILED HYDRAULIC DESIGN CHARACTERISTICS

CALCULATED VALUES AT DESIGN POINT

(3.25 lb/sec, 240 psi, 1000°F Potassium)

Velocity of Fluid in Duct (ft/sec)	
- First turn of helix	20.2
- Second turn of helix (average)	25.7
- Remaining turns of helix	31.1
Velocity Head of Fluid in Duct (psi)	
- First turn of helix	1.96
- Second turn of helix (average)	3.18
- Remaining turns of helix	4.65
Total Hydraulic Loss thru Duct (psi)	44.2

TABLE 4

DETAILED THERMAL DESIGN CHARACTERISTICS

CALCULATED VALUES AT DESIGN POINT

(3.25 lb/sec; 240 psi, 1000°F Potassium)

Winding Hot Spot Temperature Rise (°F)	325
Winding Average Temperature Rise (°F)	210
Heat Load from Duct Through Thermal Insulation (kW)	0.1
Total Heat Load to Coolant (kW)	7
Coolant (NaK) Flow Required (lb/sec)	0.7
Coolant (NaK) Inlet Temperature (°F)	800
Coolant (NaK) Temperature Rise (°F)	50
Coolant (NaK) Pressure Drop (psi)	12
Heat Generated in Duct and Fluid (kW)	9
Fluid (Potassium) Temperature Rise (°F)	14.5

TABLE 5

CALCULATED NPSH REQUIREMENTS

AT

DESIGN TEMPERATURE, 1000°F POTASSIUM

NPSH (psi)	Maximum Recommended Flow
3	2.8 lb/sec
4	3.25 lb/sec
5	3.6 lb/sec
6	3.95 lb/sec
7	4.25 lb/sec

TABLE 6

NICKEL PLATED SAMPLE STRANDS S1-S11

Conductor Sample No.	Plating Procedure[1]	Outgassing	Heating Cycle	Remarks
S1	Glass bead blast Electrolytic alkaline clean HNO_3 activation with current Cu strike Nickel plate ends and 1/2 inch up sides at 1.0 volt - 2 hrs. Strand in plating solution for 3/4 inch.	375°F in air for 3 hrs.	1725°F for 3 minutes, using 450 Kc induction unit with hairpin coil argon environment.	Plating blistered on sides and bulged on end. Samples made from development wire.
S2	Same as #S1	Same as #S1	1800°F for 3 minutes with 450 Kc induction unit and hairpin coil.	Same as #S1; also Ag melted and ran out, indicating bond and seal not adequate to contain molten Ag. Development wire used.
S3	Same as #S1	Same as #S1	1725°F for 3 minutes in vacuum furnace, slower heating than with induction.	Same as #S1; Vacuum furnace heating showed no significant difference. Development wire used.
S4	Same as #S1 except no strike	Same as #S1	Same as #S1 (with surge to 1825°F).	Many blisters. Very poor.
S5	Glass bead blast; Electrolytic alkaline clean H_2SO_4 (50% concentration) activation - no current. Cu strike H_2SO_4 (50%) reactivation with no current Nickel strike Ni plate ends and 1/2" up sides at 20 A/ft^2 - 2 hrs.	None	Same as #S1	Plating blistered on sides; end bulged. Development wire used.

(Continued)

TABLE 6

NICKEL PLATED SAMPLE STRANDS S1-S11

(Cont'd)

Conductor Sample No.	Plating Procedure[1]	Outgassing	Heating Cycle	Remarks
S6	Same as #S5	None	1725°F for 4 min. using 450 Kc induction unit and hairpin coil.	Same as #S5. Vacuum annealed wire used.
S7	Same as #S5	375°F in air for 12 hrs.	Same as #S1	Same as #S5. Development wire.
S8	Same as #S5	375°F in air for 14 hrs.	Same as #S1	Blistering on one only; other side had no blisters; best so far. Vacuum annealed wire used.
S9	Vapor blast (1200 grit Al_2O_3) Ni strike - 100 A/ft^2/2 min. Au plate - 5A/ft^2/3 min. Ni strike - 100 A/ft^2/2 min. Ni plate - 20 A/ft^2/ 1 hour - 0.001" plate on side	600°F, 30 minutes in vacuum.	One sample, same as #S1 second sample slow	Both samples blistered on sides and ends bulged. Development wire used.
S10	Vapor blast Chemical clean - HCl - H_2O (50 - 50 by vol)/1 min Ni strike - 100 A/ft^2/2 min. Au plate - 5 A/ft^2/ 5 min. Ni strike - 100 A/ft^2/5 min. Ni plate - 50 A/ft^2/ 75 min.	Same as #S9	Same as #S9	Similar to #S9 samples, although smaller blisters. Development wire used.

(Continued)

TABLE 6

NICKEL PLATED SAMPLE STRANDS S1-S11

(Cont'd)

Conductor Sample No.	Plating Procedure[1]	Outgassing	Heating Cycle	Remarks
S11	Vapor blast Cathodic treat - HCL - H_2O (50-50 by vol.)/1 min. Ni strike - 100 A/ft^2/2 min. Au plate - 10 A/ft^2/ 5 min. Ni strike - 100 A/ft^2/2 min. Ni plate - 30 A/ft^2/3 hours.	Same as #S9	Same as #S9	Same as #S9 samples. Development wire used.

[1] All plating in Sulfamate bath, timed to provide 0.003 inch to 0.005 inch thick nickel with exception of S-9 samples.

TABLE 7

NICKEL PLATED SAMPLE STRANDS S12-S21

Sample	Basic Plating Method	Nickel Strike	Outgas	Heating Cycle	Remarks
S-12	Ultrasonic clean; electropolish; file bevel, ultrasonic; H_2SO_4 activation w/o power; plate in Sulfamate.	No	No	1725°F for 3 min	1 raised area (blister or bulge) 0.07" x 0.06" near end; otherwise pretty good.
S 13	(Same as S-12)	No	Vac-1400°F 6 hr rise 2 hr hold	1725/3 min	Several small blisters after outgassing; no additional blisters after heating.
S-14	(Same as S-12)	No	375-3 hrs in air	1725/3 min	No blisters or bulging; plating intact; no Ag melt. Very good.
S-15	(Same as S-12)	No	Vac-1300°F 6 hr rise 1 hr hold	1725/3 min (surge to 1780°F)	3 blisters after heating; Ag melted and came out TC attachment welds.
S-16	Same as S-12 except H_2SO_4 activation with power; nickel strike; then plate.	Yes	375-3 hrs	1725/1-1/2 min (surge to 1950)	No blisters or bulging; Ag melted - came out TC attachment. Plating good and still intact - partial crack through plate.
S-17	(Same as S-16)	Yes	(Same as S-15)	1725/3 min (surge to 1780°F)	Large blister (1/8 x 3/32) on side; crack in blister; Ag melted - came out end through crack.
S-18	Cathodic alkaline clean anodic etch; nickel plate.	No	Vac-600°F 1/2 hr rise 1/2 hr hold	1725/3 min	Few tiny blisters on plate termination - otherwise good.
S-19	(Same as S-18)	No	375-3 hrs	1725/3 min (surge to 1760)	No blisters or bulging; Ag melted - came out; crack in plating - otherwise good.
S-20	(Same as S-12)	No	No	1725/3 min (surge to 1780)	No blisters; Ag melted - came out TC attachment welds.
S-21	(Same as S-16)	Yes	No	1725/3 min	No blisters; plate cracked on end, trace of Ag came out.

TABLE 8

NICKEL PLATED SAMPLE STRANDS S22-S33

Sample	Nickel Strike	Outgas 375°F/3 hrs	Rhenium Overplate	Heating Cycle	Remarks
S-22	No	No	No	1725°F/3 min (surge to 1760°F)	Tiny blisters at plate termination. Otherwise good; Ag melted, came through crack at bottom.
S-23	No	No	No	1725/3 min	5 blisters; spot of Ag on end.
S-24	No	Yes	No	1625/3 min	Several blisters.
S-25	No	Yes	No	1725-1750/3 min	(Same as S-22).
S-26	Yes	No	No	1625/3 min	1 blister at plate termination. Otherwise good.
				Reheated to 1725° (surge to 2000)	No additional blisters but Ag melted and ran out. Section showed plate cracked.
S-27	Yes	No	No	1625/3 min	No blisters - very good.
				Reheated to 1725° (surge to 2000)	No blisters, but Ag melted and ran out. Section showed plate cracked.
S-28	Yes	Yes	No	1725°F	3 blisters at plate termination. Otherwise good, but Ag melted and came out through TC spot welds.
S-29	Yes	Yes	No	1725/3 min	6 blisters at plate termination. Otherwise good. Section showed plate cracked.
S-30	Yes	No	Yes (wet)	Sectioned only	Rhenium looks good but very thin; 0.1 mil; should be thicker.
S-31	Yes	No	Yes (dry)	Sectioned only	(Same as S-30).
S-32	Yes	No	Yes (wet)	1725/3 min	Few tiny blisters - no concern. Otherwise good; Ag melted and came out TC weld.
S-33	Yes	No	Yes (wet)	1725/3 min (surge to 1740)	No blisters; no Ag melting. Very good.
				Reheated to 1800	No blisters; no Ag out; very good.

TABLE 9

BRAZED JOINT SAMPLES (#1 through #13)

(Nicoro-80 Powder Preloaded in Nickel Cup)

Sample No.	Seal Type	Seal Welding	Cleaning After Welding	Nicoro 80 Braze Alloy	Inspection	Remarks
1	Nickel Plugs	TIG	Wiped	0.045 diam. wire	Visual X-ray	Poor; X-ray showed voids
2	Nickel plugs	TIG	Wiped	0.045 diam. wire	Visual X-ray	Looked good; slight void at bottom
3	Nickel plugs	TIG	Wiped	0.045 diam. wire	Visual, X-ray Metallographic	Resistance using double bridge--OK--looked promising, some voids in section
4	Nickel plugs	TIG	Clean with glass beads	0.045 diam. wire	Visual	Poor; brazing alloy did not flow
5	Nickel plugs	TIG	Clean with glass beads	0.045 diam. wire	Visual	Poor; need cleaner sample or better argon atmosphere
6	Nickel plugs	TIG	H_2 reduced	1/16 diam. wire	Visual X-ray	Fair; need improvement; voids in bottom
7	Palladium Bundle of 12	Single layer TIG	H_2 reduced	1/16 diam. wire	Visual X-ray	Fair; some dissolving or melting of Pd seal
8	Nickel plugs	TIG	H_2 reduced	1/16 diam. wire	Visual X-ray	Fair; need improvement; voids in bottom
9	Nickel plugs	TIG in dry box	Mech brushed	1/16 diam. wire	Visual Metallographic	Some dissolving of plugs and cup by braze - Ag attacked nickel plugs during brazing; dry box no help
10	Nickel plugs	TIG	Mech brushed	1/16 diam. wire	Visual Metallographic	Visually looked good - Braze alloy flowed freely but some dissolving of nickel by Au
11	Palladium 2 bundles of 6	2 layer TIG	Mech brushed	1/16 diam. wire	Visual Metallographic	TC's on sample during brazing; dissolving of Palladium where exposed to Ag
12	Palladium 2 bundles of 6	1 layer TIG	Mech brushed	1/16 diam. wire	Visual	TC's on sample during brazing; some dissolving of Pd seal
13	Palladium bundle of 12	2 layer TIG	Mech brushed	1/16 diam. wire	Visual Metallographic	Some dissolving of Palladium at ends exposed to Ag

TABLE 10

BRAZED JOINT SAMPLES (#14 through #18)

(Nickel Ferrule Used to Hold the Wires Together)

Sample No.	Seal	Braze Alloy	Inspection	Remarks
14	Nickel plugs TIG weld to ferrule	Nicoro-80 1/16" dia. wire	Visual X-ray Metallographic	Good sample; some braze alloy attack on nickel and some Au went thru cladding.
15	Nickel plugs TIG weld to ferrule	Nicoro-80 1/16" dia. wire	Visual X-ray Metallographic	(Same comments as #14)
16	Nickel plugs TIG weld to ferrule	80/20 Au/Cu 0.015 wire	Visual X-ray Metallographic	Very good sample; no apparent attack by alloy; no Au went thru nickel cladding.
17	Nickel plugs TIG weld to ferrule	Nicoro-80 1/16" dia. wire	Visual Measured resistance	Looked excellent visually; resistance measurement checked good.
18	Nickel plugs TIG weld to ferrule	80/20 Au/Cu 0.045" dia. wire	Visual Metallographic	Looked excellent; a little Au went thru cladding - temp. may have been slightly high.

Note: All samples cleaned by mechanical brushing.

TABLE 11

REPRESENTATIVE BRAZED JOINT SAMPLES (#F1 through #F8)

(With Au-Cu Braze Alloy)

Sample No.	Seal	Braze Alloy	Inspection	Remarks
F1	Nickel plugs and ferrule - TIG weld	80/20 Au/Cu 0.045" dia. wire	Visual	Looked very good.
F2	Nickel plugs and ferrule - TIG weld	80/20 Au/Cu 0.045" dia. wire	Visual Longitudinal Sections & photos	
F3	Nickel plugs and ferrule - TIG weld	80/20 Au/Cu 0.045" dia. wire	Visual Transverse Sections & photos	Visually these looked very good. Metallographic examination indicated nickel sheath erosion in the brazed joint.
F4	Nickel plugs and ferrule - TIG weld	80/20 Au/Cu 0.045" dia. wire	(Same as #F2)	
F5	Nickel plugs and ferrule - TIG weld	80/20 Au/Cu 0.045" dia. wire	(Same as #F3)	
F6	Nickel plugs and ferrule - TIG weld	80/20 Au/Cu 0.045" dia. wire	Visual	Visually looked very good.
F7	Nickel plugs and ferrule - TIG weld	80/20 Au/Cu 0.045" dia. wire	Visual	Looked good.
F8	Nickel plugs and ferrule - TIG weld	80/20 Au/Cu 0.045" dia. wire	Visual	Looked good.

TABLE 12

BRAZED JOINT SAMPLES (#F11 through #F17)

(With Au-Ni-Ge or In Braze Alloy)

Sample Number	Braze Alloy Composition	Braze Cycle	Remarks
F11	Au-17.4 Ni-3.2 Ge	1750°F/3 m.	Temperature was at high limit - braze flowed easily. Sections showed considerable erosion, some Ag melted, Au in 4 conductors.
F12	Au-17 Ni-7 In	1800°F/5 m.	Joint heated excessively. Erosion under ferrule and wire wrap. Good braze penetration. Au in several conductors.
F13	Au-17 Ni-7 In	1660°F/2.5 m. 1700°F/1 m.	Carefully controlled heat and maximum temp. Some voids - silver not melted. Gold in two conductors.
F14	-	-	Not brazed; examined for plug - seal welding only.
F15	Au-17 Ni-7 In	1450°F/5 m. 1700°F/4 m.	Preplaced braze alloy. Not good flow, poor fill between conductors. Considerable oxidation of surfaces.
F16	Au-17 Ni-7 In	1600°F/3.5 m. 1700°F/5 m.	Braze flowed sluggishly but strands finally filled at least 1/2 in. above ferrule. Large "blob" of braze where fed. Some oxidation.
F17	Au-17 Ni-7 In	1500°F/10 m. 1700°F/5 m.	Braze flowed poorly - strands not filled above ferrule. Temperature went to 1780°F for 10-15 seconds. Considerable oxidation of surfaces.

TABLE 13

BRAZED JOINT TEST SAMPLES (#F19 through #F25)

(With Au-Ni-In and Ge Braze Alloy)

Sample Number	Braze Alloy[1] Braze Cycle	Remarks
F19	1700°F/3 m 1400°F/3 m 1720°F/1.2 m	Tried brazing with the Ge alloy at 1700°F - no melt. Lowered temp. Then raised to 1720°F and brazed O.K. with In alloy. No Ag melt - Au in several strands - slight erosion.
F20	1740-1760°F/2 m	Heated to 1750°F - again tried Ge alloy but no melt. Then used In alloy with quick melting. Good appearance to joint. Slight Ag melt - no Au in strands - very slight erosion.
F21	1780-1790°F/4.2 m	Germanium braze flowed when applied. Ag melted in some strands - some erosion and Au in strands - some voids.
F22	1710-1750°F/2 m	Middle strands slow in coming to temp. Braze flowed smoothly after 30 sec. No Ag melted, but slight erosion and Au in strands.
F23	1700-1760°F/1.7 m	No conductor ends sealed. Slight melting of Ag in 2 strands. Good braze flow and overall joint.
F24[2]	2000°F initial, 1750°F/1 m	Joint heated rapidly. Braze flowed well. Ag melted in some strands. Au in one or two. Good filling. No erosion.
F25[2]	1720-1750°F/1 m	Joint heated rapidly, and looked good. Braze flowed well, except between some strands. No Ag melt, no Au in strands, no erosion.

(1) Au-17.1Ni-5In alloy for all samples except F21 which was made with Au-17.4Ni-3.2Ge braze alloy.

(2) Samples F24 and F25 made with peripheral type coil at 450 Kc. Samples F19 to F23 made with face type focusing coil at 3 Kc.

TABLE 14

RESULTS OF Au-Ni & Cu BRAZE ALLOY EROSION

ON NICKEL FOIL (0.002" THICK)

(Tests Made in Vacuum)

Sample No.	Braze Alloy	Test Temp. °F	Time at Temp.	Remarks
1	Au-18Ni	1800	1 Min.	No erosion (Initial Melt - 1780*)
6	Au-18Ni	1875	15 Min.	No erosion
4	Au-18Ni	1900	5 Min.	Slight erosion
7a	Au-20Cu	1750	5 Min.	No erosion (Initial Melt - 1720*)
10	Au-20Cu	1775	1 Min.	Slight erosion
9	Au-20Cu	1800	1 Min.	Complete erosion
14	Au-16.5Cu-2Ni	1760	1 Min.	No erosion (Initial Melt - 1730*)
16	Au-16.5Cu-2Ni	1755	1 Min.	Slight erosion
15	Au-16.5Cu-2Ni	1800	1 Min.	Complete erosion
17	Au-16.5Cu-2Ni	1750	5 Min.	No erosion

*Published Values on Braze Alloys Are:

Au-18Ni	1742°F Solidus,	1742°F Liquidus
Au-20Cu	1632°F Solidus,	1632°F Liquidus
Au-16.5Cu-2Ni	1670°F Solidus,	1697°F Liquidus

TABLE 15

CRITICAL TEMPERATURES FOR Au-Ni BRAZE ALLOYS CONTAINING INDIUM AND GERMANIUM

Allov Composition (%)	Solidus Temperature[1] (°F)	Liquidus Temperature[1] (°F)
Au-17.5Ni-3In	1690	1720
Au-17.1Ni-5In	1605	1650
Au-16.2Ni-10In	1350	1550
Au-19Cu-5In	1550	>1660
Au-17.7Ni-1.6Ge	1720	1740
Au-17.4Ni-3.2Ge	1690	1720

(1) Data was obtained by testing in a vacuum furnace with thermocouple attached to foil next to sample alloy.

TABLE 16

EROSION TEST RESULTS FOR BASIC Au-Ni BRAZE ALLOY WITH In OR Ge MELTING POINT DEPRESSANT ADDITIONS

Sample Number	Alloy Composition	Heating Cycle	Remarks
1	Au-17.1 Ni-5 In	1650°F/5 m.	Initial melting at 1605°F; approximately 90% molten at 1650°F, indicating approximately 50-60°F melting range. No erosion detected.
2	Au-17.1 Ni-5 In	1700°F/5 m.	Good flow, complete melting. No visible erosion.
3	Au-17.1 Ni-5 In	1630°F/15 m. 1750°F/5 m.	Simulated braze cycle to observe possible segregation. Complete liquation noted at 1630°F after 15 m. No visible "through" erosion after indicated cycle.
4	Au-17.1 Ni-5 In	1750°F/30 m.	No visible erosion. Higher temperature may be ok, but silver melts.
5	Au-16.2 Ni-10 In	1650°F/30 m.	Initial melting at 1350°F, molten at 1525-1550°F, excellent wetting at indicated braze temperature. No visible "through" erosion. Low solidus temp. is negative factor.
6	Au-17.7 Ni-1.6 Ge	1760°F/15 m.	Initial melting at 1710-1720°F, completely fluid at 1740°F; excellent wetting observed. No visible "through" erosion.
7	Au-17.4 Ni-3.2 Ge	1700°F/15 m.	Initial melting at 1670°F; complete flow at 1690°F; sample cooled to 1630°F to check solidification temp. after thermal cycle. As sample reheated to 1700°F the 1670-1690°F melting temp. was again noted. No visible "through" erosion after cycle.
8	Au-17.4 Ni-3.2 Ge	1710-1720°F/ 30 m.	Initial melting at 1680-1690°F; complete flow at 1705°F. No visible erosion noted after indicated cycle.

TABLE 17

INITIAL JOINT BRAZING

SAMPLES WITH CONDUCTOR ENDS NICKEL PLATED

Sample Number	Braze Cycle[1]	Remarks
P1	1750°F (Briefly) Held 1680-1720°F/3 m	Nickel on ends and exposed sides. Braze flow somewhat sluggish with no fillet on back side. No Ag melt, no erosion. Au in 2 strands where thin Ni plate loosened.
P2	1800°F (Briefly) Held 1720-1750°F/3 m	Nickel plate on ends only. Good braze flow and acceptable fillets. No Ag melt, no erosion. Au in one strand where thin Ni was pulled loose at one corner.

(1) Brazed with Au-17.1Ni-5In alloy, using a two-turn peripheral coil and 450 k Hz induction equipment.

TABLE 18

BRAZED SAMPLE ASSEMBLIES

WITH VARIOUS PLATING METHODS

Braze Sample #	Plating Procedure[1]	Remarks
P3 & P3A	Glass bead blast Electrolytic clean in caustic HNO_3 activation with current 6 strands Cu strike 6 strands Au strike Nickel plate ends only at 1.0 V. 2 hours in bundles of 6 strands (mask-off between strands) Outgas at 375°F in air for 3 hours.	Plating bridged across some strands, but overall looked good prior to brazing. Metallographic examination after brazing showed bond questionable; plate not intact on some ends, came loose or bulged on strand bottom; no erosion of sheath; some shrinkage voids in braze alloy; Cu strike appears better than Au.
P4 & P4A	Same as #P3 except strands, in bundles of 6, separated slightly to prevent bridging during plating.	Similar to #P3. Bond still not good enough; Cu strike better than Au, but plating "ends only" does not provide adequate surface area for good bond; bulging or looseness of plate still occurred; a little Ag melted due to localized hot spot in corners during brazing cycle with hairpin coil.
P5	Same as #P3 except all 12 strands had Cu strike and plating was on ends and up sides of each strand for about 1/2 inch; no masking; strands immersed in plating solution approximately 3/4 inch.	Plating looked good prior to brazing. Metallographic examination after brazing showed some localized Ag melting, blistering of plating on strand sides, and bulging of plating on bottom of strands; plating damaged and fractured in places.

[1] All nickel plating is in Sulfamate bath, with current and time to provide 0.003 inches to 0.005 inches thick nickel.

TABLE 19

BRAZED SAMPLE JOINT ASSEMBLIES

WIRES PLATED IN BUNDLES OF SIX STRANDS,

TWO BUNDLES BRAZED TOGETHER

Sample	Rhenium	Alloy	Heating Cycle	Remarks
P-6	No	Au/Ni/In	1690-1720/3 min (surge to 1740)	Plating is excellent; partial erosion on 1 strand - good capillaries except 2 on back side. Appears satisfactory - mechanically and electrically. No voids in strands.
P-7	No	Au/Cu	1725-1760/6 min	Flowed well; good capillaries - electrically and mechanically. Very poor in section - general mixture of Au and Ag and considerable erosion, Ni plate ruptured.
P 8	Yes	Au/Cu	1700-1725°F	Visually looked adequate except for 1 hole in strand at top of cup; section looks poor - void in capillaries - too cold a joint; some erosion. Some Ag and Au interchange due to Ag melting - plate cracked.
P-9	No	Au/Ni/In	1680-1700°F 1710-1725 10 min total	No visible evidence of Ag or exposed surface erosion; appears adequate electrically and mechanically, but joint made too cold; capillaries not quite as good as P-6; alloy buildup on feed side; section showed some voids in capillaries; plate good.
P-10	Yes (doubled time to increase thickness)	Au/Cu	1710-1740°F (TC loose; chart shows as high as 1800) 9 min	Joint still appears to be made too cold; alloy eroded through some strands and some Ag melting; section shows poor joint; considerable erosion; rhenium loose and not attached; Au and Ag intermixed.
P-11	No	Au/Ni/In	1680-1725/3 min (1740 initially - reheated to braze back side)	Capillaries are good; no visible evidence of Ag melting; some excess alloy build-up, braze too cold but good joint visually.

TABLE 20

REFRACTORY MATERIALS FOR EM PUMP DUCT

Item	Application	Outside Diameter (Inches)	Inside Diameter (Inches)	Wall Thickness (Inches)	Length Required (Inches)	Approx. Wt. of Required Quantity (Pounds)	G.E.-NSP Material Specification Number
		T-111 Alloy Items - Group I					
Tube	Wrapper	4.313	3.807	0.253	17	33	01-0035-01-D
Tube	Wrapper Extension	4.313	3.807	0.253	10	19	01-0035-01-D
Tube	Helix	4.111	2.561	0.775	17	84	01-0035-01-D
Tube	Helix Extension	2.937	2.561	0.188	10	10	01-0035-01-D
Bar	End Pieces	4.625	--	--	4.5	40	01-0015-01-D
					Total	186	
		T-111 Alloy Items - Group II					
Tube	Center Return Pipe	1.500	1.300	0.100	27 5/8	8	01-0035-01-D
Tube	Inlet Trans. Pipe	1.500	1.300	0.100	5 3/4	1.8	01-0035-01-D
Tube	Bimetal Joint	1.500	1.300	0.100	7 1/4	2	01-0035-01-D
		Nb-1Zr Foil - Group III					
		Thickness (Inches)	Width (Inches)				
Foil	Heat Treat Wrap and Insulation	0.002	5.00	--	125	4	01-0054-00-C
Foil	Thermal Insulation	0.002	0.5	--	500 ft.	18	01-0054-00-C

TABLE 21

EFFECT OF PERCENT REDUCTION ON T-111 GRAIN SIZE

Forged Diameter (Inches)	Total Percent Reduction %	ASTM Grain Size No. at Various Radial Locations				
		Edge	1/2"	1"	1 1/2"	2"
5 1/2	32	6.0	4.0	3.5	2.0	2.0
4 1/2	55	5.5	5.0	4.5	5.5	5.0
4	63	6.0	5.0	4.0	4.5	5.0
3 1/2	71	6.7	6.5	6.5	6.1	NA(1)
3 1/4	75	7.0	6.3	5.5	6.5	NA
2 1/2	80	7.3	6.5	6.5	NA	NA

(1) NA = Not Applicable

TABLE 22

LIST OF QUALITY ASSURANCE TESTS FOR
T-111 ALLOY MILL PRODUCTS

1. Item, Nominal Size
2. Lot Number
3. Heat Number
4. Ingot Vendor
5. Processing Vendor
6. Control Number
7. Weight (100%)
8. Dimension (100%)
   - Length
   - Outside Diameter
   - Wall Thickness
   - Straightness
   - Flatness
9. Surface Condition (100%)
10. Fluorescent Penetrant (100%)
11. Ultrasonic Inspection (100%)
12. Flare, Tube (2 each lot or ingot)
13. Hardness (2 each lot or ingot)
14. Grain Size/Microstructure (2 each lot or ingot)
15. Room Temperature Tensile Properites (2 each lot or ingot)
16. 2400°F Stress-Rupture Properties (Chemical Analysis of Specimen) (2 each lot or ingot)
17. Chemistry
    - Ingot (4 each ingot)
    - Final Product, C, O, H, N, (1 each lot or ingot)

TABLE 23

CHEMICAL COMPOSITION OF T-111 ALLOY INGOTS

Heat #	Application	Location of Ingot Sample	ppm O	H	N	C[a]	Co	Cr	Fe	Mo	Nb	V	Zr	W	Hf
7327	Wrapper Extension	Top Outside Radius	15	2	17	51	<5	<1	25	20	100	2	990	7.7 %	2.0 %
		Top Middle Radius	7	2	16	46	<5	<1	25	15	70	2	795	7.55%	1.95%
		Top Center	11	2	15	35	<5	<1	3	25	100	2	1110[b]	7.46%	1.92%
		Bottom Center	10	2	17	38	<5	<1	10	20	90	2	990	7.62%	1.92%
7325	Helix	Top Outside Radius	21	1	25	31	<5	<1	30	20	200	2	930	7.88%	1.98%
		Top Middle Radius	5	1	25	49	<5	<1	30	20	280	2	1440[b]	7.55%	1.94%
		Top Center	8	1	24	35	<5	<1	10	15	200	2	1110[b]	7.55%	2.55%[c]
		Bottom Center	7	1	18	39	<5	<1	10	20	100	2	645	7.62%	2.72%[c]
7236	Helix Extension	Top Outside Radius	15	1	33	31	<1	<1	10	30	250	<1	200	7.6 %	2.1 %
		Top Middle Radius	<10	1	37	40	<1	<1	5	30	250	<1	200	7.6 %	2.3 %
		Top Center	11	1	31	48	<1	<1	5	30	250	<1	175	7.6 %	2.2 %
		Bottom Center	13	1	50	28	<1	<1	5	50	250	<1	200	7.7 %	2.1 %
7665	Wrapper	Top Outside Radius	27	3	33	24	<5	<1	1	10	<25	2	300	7.48%	1.92%
		Top Middle Radius	17	2	30	21	<5	<1	10	25	<25	2	400	7.32%	1.92%
		Top Center	17	1	39	21	<5	<1	8	10	<25	2	300	7.48%	1.86%
		Bottom Center	13	2	29	18	<5	<1	10	10	<25	2	400	7.62%	2.05%
8098	Center Pipe		78	1	12	29	<5	2	20	5	450	2	500	7.95%	2.28%
NSP Tubing Specification Values			100	10	50	40	50	200	50	1000	1000	20	1000	7-9	1.8-2.4

[a] Some of the carbon contents measured in the ingot exceeded the 40 ppm allowed by the specifications. Permission to use the ingots was given because the average deviation was small and vendor was confident that final products chemistry would be within specification.

[b] The average Zr content for this ingot was 1030 ppm which was considered a small nondeleterious deviation from the specifications.

[c] Two of the four ingot analysis for Hf were high (2.4% Hf maximum permitted by specification) but the material was accepted because the average of the four ingot analysis was within specification.

TABLE 24

MECHANICAL PROPERTIES OF T-111 ITEMS

Application	Sample	0.2% Offset Yield Stress, psi	Ultimate Tensile Stress, psi	Percent[a] Elongation	Min. Rupture Life, at Least 20 Hours at 2400°F[b]
Wrapper Extension	B	78,500	93,500	20	Yes
	C	77,400	93,200	20	Yes
Helix	B	77,000	93,500	28	Yes
	C	78,200	94,500	24	Yes
Helix Extension	A	77,000	93,500	26	Yes
	B	76,400	92,000	24	Yes
End Pieces	A	77,000	93,500	26	Yes
	B	76,400	92,000	24	Yes
Wrapper	A	72,000	88,300	34	Yes
	B	72,000	87,500	28	Yes
Center Pipe			89,300	25	Yes
			90,000	24	Yes
NSP Specification		65,000 - 100,000	80,000 - 110,000	20	Yes

[a]Percent tensile elongation in 2-inch gage length.

[b]Stress during test was 19,000 psi as required by the specifications.

TABLE 25

QUALITY ASSURANCE RESULTS ON T-111 ITEMS

Application	Interstitial Analysis, ppm C*	O	N	H	ASTM Grain Size No. Trans.	Long.	Average Hardness DPH	% Recrystallization
Wrapper Extension	56	25	18	4	2-4**	3-4	249	100
Helix	13	12	16	1	4	3	226	100
Helix Extension	36	11	34	1	4	4	239	100
End Pieces	30	24	22	2	2-4**	2-4**	230	100
Wrapper	52	33	23	4	3	3	-	100
Center Pipe	61	15	14	1	6	6	-	100
NSP Specification	50	150	75	10	3	3	NA	90

*Some of the carbon contents measured in the final product exceed the 50 ppm allowed by the specification. These mill products were accepted and used because the deviations were small and considered non-deleterious for the intended application.

**Minimum ASTM Number permitted by the T-111 alloy specification is ASTM 3. Only a few isolated areas had grain size of ASTM 2 and the piece was considered acceptable.

TABLE 26

QUALITY ASSURANCE RESULTS Cb-1Zr FOIL ITEMS

Application	Interstitial Analyses, ppm C	O	N	H	ASTM Grain Size No. Trans.	Long.	% Recrystallization
Heat Treat Wrapping	150	501*	47	1	7-8	7-8	100
Thermal** Insulation	213	2075	38	<1	-	-	
	153	721	50	3	-	-	
	157	1392	31	<1	7-8	7-8	100
Thermal Insulation	70	267	23	<1	-	-	100
	67	265	17	<1	-	-	100
	61	261	20	<1	-	-	100

*The oxygen content measured in the final product exceeded the 300 ppm allowed in the specification. However, this foil was used for the noncritical application of wrapping foil for heat treating.

**Because all the oxygen contents and some of the carbon contents measured in the final product exceeded the specification allowance (300 ppm for oxygen and 150 ppm for carbon), this foil was considered not adequate for the intended application and therefore was rejected.

* U. S. GOVERNMENT PRINTING OFFICE : 1972 735-026/1079